

Electronic Thesis and Dissertation Repository

5-6-2019 10:30 AM

Phenotypic and Metabolic Plasticity In Canine Cellular Reprogramming

Ian C. Tobias, *The University of Western Ontario*

Supervisor: Betts, Dean H., *The University of Western Ontario*

A thesis submitted in partial fulfillment of the requirements for the Doctor of Philosophy degree in Physiology and Pharmacology

© Ian C. Tobias 2019

Follow this and additional works at: <https://ir.lib.uwo.ca/etd>



Part of the [Developmental Biology Commons](#)

Recommended Citation

Tobias, Ian C., "Phenotypic and Metabolic Plasticity In Canine Cellular Reprogramming" (2019). *Electronic Thesis and Dissertation Repository*. 6224.

<https://ir.lib.uwo.ca/etd/6224>

This Dissertation/Thesis is brought to you for free and open access by Scholarship@Western. It has been accepted for inclusion in Electronic Thesis and Dissertation Repository by an authorized administrator of Scholarship@Western. For more information, please contact wlsadmin@uwo.ca.

Abstract

Embryonic stem cells (ESCs) and induced pluripotent stem cells (iPSCs) derived from large mammals reproduce few characteristics displayed by rodent or human counterparts. This is complicated by the inherent plasticity of mammalian ESC/iPSC cultures that resemble a variety of developmental stages including the naïve and primed pluripotent states. Defining the extrinsic signals that modulate the developmental identity of canine ESC/iPSC (i.e. primed versus naïve) will improve knowledge integration with more sophisticated rodent and primate research. In this thesis, I sought to determine if manipulation of the culture environment can promote nuclear and metabolic reprogramming of canine cell lines towards a more primitive state of pluripotency. Using growth factors and kinase inhibitors to modulate pluripotency of canine ESCs (cESCs), I demonstrated that cESCs exhibit the plasticity to adopt multiple developmental identities. I observed that lineage-specific differentiation of cESCs is influenced by pluripotent state modulation, coincident with changes to colony architecture, transcriptional and epigenetic markers of developmental maturity. I found that primed- and naïve-like cESCs exhibit pluripotent-state specific mitochondrial structure and function, including differential reliance on glucose oxidation pathways for steady-state proliferation *in vitro*. Lastly, using comparative sequence analysis and biochemical assays, I observed that evolutionary differences in genomic CpG density at pluripotency-associated promoters correlate with functionally relevant cytosine modifications to the induction and maintenance of pluripotency. I showed the utility of physiological metabolites that regulate 5-methylcytosine oxidation in promoting cellular and transcriptional features associated with early nuclear reprogramming of canine fibroblasts (e.g. mesenchymal-to-epithelial transition). Taken together, my work establishes a binary cESC model of primed- and naïve-pluripotent states, providing insight into shared and divergent features of pluripotency progression and acquisition in placental mammals.

Keywords

Embryonic Stem Cell, Induced Pluripotent Stem Cell, Canine, Pluripotency, Naïve Pluripotent State, Metabolism, Mitochondria, DNA Methylation, TET Dioxygenase

Co-Authorship Statement

Chapter 2

Tobias, I.C., Brooks, C.R., Teichroeb, J.H., Villagómez, D.A, Hess, D.A., Séguin, C.A., and Betts, D.H. (2016). *Small-molecule induction of canine embryonic stem cells toward naive pluripotency*. *Stem Cells and Development* 25 (16), 1208-1222. Text and figures are reproduced here with permission from Mary Ann Liebert, Inc. (Appendix B), and modified for relevance to the thesis. IC Tobias designed all experiments with the assistance of Drs. Cheryle A. Séguin, David A. Hess and Dean H. Betts. All data was generated by IC Tobias in the laboratory of DH Betts. All figures were prepared by IC Tobias. The manuscript was written by IC Tobias with the assistance of DH Betts.

Chapter 3

Tobias, I.C., Isaac, R.R., Dierolf, J.G., Khazaei, R., Cumming, RC, and Betts, D.H. (2018). *Metabolic plasticity during transition to naïve-like pluripotency in canine embryo-derived stem cells*. *Stem Cell Research* 30, 22-33. Text and figures are reproduced here with permission from Elsevier publishers (Appendix B) and modified for relevance to the thesis. IC Tobias designed all experiments with the assistance of RC Cumming and DH Betts. IC Tobias generated all data and prepared all figures. The manuscript was written by IC Tobias with the assistance of RC Cumming and DH Betts.

Chapter 4

Chapter four is entitled “*L-ascorbic acid and retinoic acid promote 5-hydroxymethylcytosine accumulation and epithelialization in early canine reprogramming*”. Courtney R Brooks performed emGFP control Sendai virus transduction. Courtney R Brooks performed flow cytometry data collection of emGFP cells with assistance from IC Tobias. Custom oligonucleotide design, culture of canine fibroblasts, RT-qPCR analysis of TET expression was performed by IC Tobias with the assistance of Mian Mian C Kao. IC Tobias designed all experiments with the assistance of DH Betts. IC Tobias generated all data and prepared all figures. The manuscript was written by IC Tobias with the assistance of DH Betts.

Acknowledgments

Thank you to all the past and current members of the Betts lab for your friendship, guidance and insightful discussion. The laboratory and office were always lively and collegial spaces to work. A special thank you to Courtney Brooks, who provided technical assistance and instruction in cell culture and clonal line derivation, and to Hailey Hunter who provided efficient and friendly laboratory management. I would like to extend thanks to Dr. Jonathan Teichroeb, who offered mentorship and guidance when I first began research in the Betts lab.

I would also like to thank previous and current members of the Watson, Regnault and Hardy labs for exemplifying the spirit of collaboration and creating a supportive environment. Particularly, Dr. Lin Zhao and Dr. Christina Vanderpoor, who did a wonderful job maintaining a safe and productive laboratory. I would also like to thank my colleagues in the Departments of Physiology & Pharmacology and the Department of Biology for their feedback and advice.

Thank you to Dr. Richard Gardner, Karen Nygard and Reza Khazaei of the Integrated Microscopy division of the Biotron for their technical expertise and assistance with transmission electron microscopy. I would also like to thank Dr. Robert Cumming for lending his help, reagents and live-cell imaging equipment.

A special thanks to my thesis advisory committee members – Drs. Cheryle Séguin, John DiGuglielmo, Timothy Regnault and Lina Dagnino – for offering their guidance and scholarly critique throughout my graduate studies.

Thank you to my family for being so understanding about my commitment to graduate studies. I would also like to thank Laura for being the most supportive partner I could ask for.

Lastly, thank you to my supervisor, Dr. Dean Betts. I am extremely grateful to have worked with you and I have become a better scientist with your guidance. Thank you for all your support.

Table of Contents

Abstract	i
Keywords	ii
Co-Authorship Statement.....	iii
Acknowledgments.....	iv
Table of Contents	v
List of Tables	xi
List of Figures	xii
List of Appendices	xvi
List of Abbreviations	xvii
Chapter 1	1
1 Introduction	1
1.1 Overview.....	1
1.1.1 Stem Cells, Fate Decisions and Cellular Plasticity.....	1
1.2 Mammalian Development and Embryo-derived Pluripotent Stem Cells	3
1.2.1 Overview of Early Mammalian Development	3
1.2.2 Mouse Pluripotent Stem Cells from Peri-implantation Embryos	5
1.2.3 Naïve and Primed Pluripotent States	7
1.2.4 Generation of Transient Embryonic States <i>in vitro</i>	9
1.3 Characteristics of Mammalian Pluripotent Stem Cells	10
1.3.1 Techniques to Study Self-Renewal and Differentiation	10
1.3.2 Gene Regulatory Networks in Pluripotency	11
1.3.3 Transcriptional and Epigenetic Crosstalk at Developmentally-Regulated Genes.....	12
1.3.4 Hyperdynamic and Poised Features of the Pluripotent Regulatory Epigenome	14

1.3.5	Dynamic Heterogeneity and Epigenetic Barriers to Pluripotent State Transitions.....	15
1.4	Metabolism in Pluripotent Stem Cells	19
1.4.1	Overview of Cell Metabolism.....	19
1.4.2	Metabolic Regulation of Self-Renewal and Differentiation	20
1.4.3	Metabolic Reprogramming in Pluripotent State Transitions	21
1.5	Induced Pluripotent Stem Cells	23
1.5.1	Overview of Induced Pluripotent Stem Cell Generation	23
1.5.2	Phase-Dependent Obstacles to Somatic Cell Reprogramming	25
1.5.3	Modifiers of DNA Methylation to Facilitate Reprogramming	26
1.6	Pluripotent Stem Cells from Domesticated Large Mammals	30
1.6.1	Livestock and Companion Animals in Regenerative Medicine	30
1.6.2	Regulative Implications of Evolutionary Variation to Pluripotency	32
1.6.3	Canine Embryogenesis and Embryonic Stem Cells.....	33
1.6.4	Canine Induced Pluripotent Stem Cells	35
1.7	Rationale and Study Aims	36
1.8	References.....	38
Chapter 2.....		72
2	Manipulation of developmental signaling pathways alters the pluripotency characteristics of canine embryonic stem cells	72
2.1	Introduction.....	73
2.2	Materials and Methods.....	74
2.2.1	Feeder layer and Embryonic Stem Cell Culture	74
2.2.2	Metaphase Spread Preparation and Karyotyping.....	75
2.2.3	Reverse Transcription and Quantitative PCR.....	76
2.2.4	Indirect Immunofluorescence Microscopy	77
2.2.5	Protein Extraction, SDS-PAGE and Western Blotting.....	79

2.2.6	Embryoid Body Formation and Directed Differentiation of Outgrowths.	79
2.2.7	Neural Progenitor Cell Formation Assay.....	80
2.2.8	Manipulation of TGF β Signaling.....	80
2.2.9	Single-cell Cloning Efficiency Assay.....	81
2.2.10	Cell Counting and Population Doubling Time Calculation.....	81
2.2.11	5-methylcytosine Enzyme-linked Immunosorbent Assay (ELISA)	81
2.2.12	Immunodeficient Mouse Xenograft Assay	82
2.2.13	Statistical Analysis.....	82
2.3	Results.....	82
2.3.1	PD0325901, CHIR99021 and LIF (2iL) induce compact cESC colony morphology	82
2.3.2	2iL cESCs are pluripotent and up-regulate transcript markers of an earlier developmental identity.....	83
2.3.3	STAT3 phosphorylation but not SMAD2/3 signaling are influenced by 2iL culture	87
2.3.4	L/F cESCs exhibit a greater lineage-specific bias for neurectoderm and mesoderm differentiation	92
2.3.5	DNA methylation and H3K27me3 modifications are depleted in 2iL cESCs.....	96
2.3.6	Enhanced colony-forming efficiency but not tumorigenicity of 2iL cESCs	99
2.4	Discussion.....	102
2.5	References.....	106
Chapter 3.....		112
3	Pluripotent state influences metabolic activity and mitochondrial structure in canine embryonic stem cells.....	112
3.1	Introduction.....	113
3.2	Materials and Methods.....	115
3.2.1	Feeder Layer and Embryonic Stem Cell Culture.....	115

3.2.2	Oxygen Consumption Rate and Extracellular Acidification Rate	115
3.2.3	Protein Extraction, SDS-PAGE and Western Blotting	116
3.2.4	Flow Cytometric Analysis of cESC-MEF Co-cultures.....	117
3.2.5	Chemifluorescence and Flow Cytometry.....	117
3.2.6	Chemifluorescence and Live Cell Imaging.....	118
3.2.7	Mitochondrial and Genomic DNA Isolation and Quantitative PCR	119
3.2.8	Sample Preparation for Transmission Electron Microscopy	119
3.2.9	Mitochondrial Morphometric Image Analysis.....	120
3.2.10	Metabolic Inhibitor Treatment and Cell Counting.....	121
3.2.11	Cellular ATP Detection Assay.....	121
3.2.12	Cell Death and Apoptosis Assay.....	121
3.2.13	Statistical Analysis.....	122
3.3	Results.....	122
3.3.1	Enhanced glucose oxidation and respiratory capacity in 2iL cESC	122
3.3.2	Altered mitochondrial ultrastructure but not mitochondrial biomass in 2iL cESC	125
3.3.3	Increased mitochondrial membrane potential and ATP level in 2iL cESC	129
3.3.4	Differentiation regulation of pyruvate metabolizing enzymes is associated with altered lipid accumulation.....	133
3.3.5	HXK2 level and glycolytic capacity are correlated among mammalian ESC lines.....	137
3.3.6	Bioenergetic pathway inhibition differentially affects L/F and 2iL cESCs	141
3.4	Discussion.....	141
3.5	References.....	148
	Chapter 4.....	156
4	Bioactive metabolite supplementation promotes mesenchymal-to-epithelial transition in early canine reprogramming	156

4.1	Introduction.....	156
4.2	Materials and Methods.....	158
4.2.1	Genomic Sequence Retrieval and Processing.....	158
4.2.2	Identification of CpG Islands and Calculation of CpG Sequence Metrics	159
4.2.3	Sequence Alignment and Motif Discovery.....	160
4.2.4	Primary Cell Culture.....	160
4.2.5	Somatic Cell Reprogramming.....	160
4.2.6	Reverse Transcription and Quantitative PCR.....	161
4.2.7	Targeted Bisulfite PCR.....	162
4.2.8	Clone Sequencing and Methylation Analysis.....	163
4.2.9	DNA Enzyme-linked Immunosorbant Assay (ELISA).....	164
4.2.10	RT ² Profiler PCR Array Analysis.....	164
4.2.11	Statistical Analysis.....	165
4.3	Results.....	165
4.3.1	A subset of reprogramming-associated orthologues is CpG-rich in the canine genome assembly.....	165
4.3.2	OCT4 and NANOG promoters are methylated in canine fibroblasts and partially reprogrammed cells.....	169
4.3.3	5-hmC level varies among species and cell type.....	172
4.3.4	Identification of L-ascorbic acid and retinoic acid concentrations that increase TET activity.....	172
4.3.5	Physiological oxygen changes the influence of metabolites on TET activity.....	174
4.3.6	L-ascorbic acid and retinoic acid promote focal epithelialization during early canine reprogramming.....	177
4.4	Discussion.....	184
4.5	References.....	188
	Chapter 5.....	197

5	General Discussion and Conclusions	197
5.1	Discussion and Significance of Research	197
5.1.1	Pluripotent state-specific signaling and metabolic pathways support cESC maintenance	200
5.1.2	Intracellular signaling pathways may link bioenergetics to self-renewal and tumorigenicity of cESCs	202
5.2	Future Studies: Purification and analysis of canine reprogramming intermediate cells	205
5.3	Summary	210
5.4	References	210
	Appendix A: Materials and Methods for cell surface marker validation.....	216
	Immunolabeling for Fluorescence Microscopy	216
	Immunolabeling for Flow Cytometry	216
	Appendix B: Copyright Approval.....	218
	Appendix C: Animal Use Protocol Approval	220
	Appendix D: Curriculum Vitae.....	221

List of Tables

Table 2-1. Custom oligonucleotide primer sequences	76
Table 2-2. Primary antibody information	78
Table 3-1. Primary antibody information	116
Table 3-2. Custom oligonucleotide primer sequences.....	119
Table 4-1. Summary of conserved reprogramming-associated gene products.....	159
Table 4-2. Custom oligonucleotide primer sequences.....	162
Table 4-3. NANOG and OCT4 primer sequences for bisulfite PCR.....	163
Table 0-1. Primary antibody information for flow cytometry.....	216

List of Figures

Figure 1-1. Conserved features of naïve and primed pluripotency in placental mammals.....	18
Figure 1-2. Metabolic regulation of self-renewal and pluripotency.	22
Figure 1-3. Cellular, transcriptional and epigenetic characteristics of each phase of cellular reprogramming.....	27
Figure 2-1. PD0325901, CHIR99021 and LIF (2iL) induce compact cESC colony morphology.....	84
Figure 2-2. 2iL cESCs are dependent on the 2i molecules for compact morphology.	85
Figure 2-3. Establishment of 2iL cultures in the IO3 cESC line and preliminary characterization by stage-specific embryonic antigen 4 (SSEA4) staining.....	86
Figure 2-4. 2iL cESCs express SOX2 and OCT4 with nuclear localization.	88
Figure 2-5. 2iL cESCs accumulate NANOG and down-regulate OTX2 compared to L/F cESCs.....	89
Figure 2-6. Canine ESCs expanded in 2iL retain tri-lineage differentiation capacity <i>in vitro</i>	90
Figure 2-7. 2iL cESCs up-regulate several known naïve pluripotency-associated transcripts but not primed pluripotency-related markers.....	91
Figure 2-8. Enhanced STAT3 phosphorylation in 2iL-enriched cESCs.....	93
Figure 2-9. Steady-state L/F cESCs exhibit cytosolic phospho-SMAD2 and tolerate acute inhibition Activin-like kinase (ALK) activity.....	94
Figure 2-10. L/F cESCs exhibit a greater sensitivity for spontaneous neural differentiation and BMP4-induced mesendoderm differentiation.	95
Figure 2-11. DNA methylation and H3K27me3 modifications are depleted in 2iL cESCs...	97

Figure 2-12. Decreased nuclear condensations of H3K27me3 antibody stain are observed in 2iL cESCs.	98
Figure 2-13. Altered growth kinetics and colony-forming efficiency between L/F and 2iL cESCs.....	100
Figure 2-14. <i>In vivo</i> tumorigenicity and differentiation potential of typical human ESC line is not recapitulated by either L/F or 2iL cESCs.	101
Figure 3-1. Culture in 2iL enhances glucose oxidation and respiratory capacity of BE5 cESCs.....	123
Figure 3-2. 2iL-induced respiration is reproducible in IO3 cESC line.....	124
Figure 3-3. 2iL cESCs show lower MitoTracker Green FM accumulation independent of cell size.	126
Figure 3-4. 2iL cESCs exhibit a selective decrease in the inner mitochondrial membrane protein MIC60.....	127
Figure 3-5. L/F and 2iL cESCs harbor structurally distinct mitochondria but do not differ in mitochondrial biomass.....	128
Figure 3-6. Remodeling of mitochondrial ultrastructure in 2iL cESC.	130
Figure 3-7. Dynamic redistribution but not static accumulation of mitochondrial polarization-sensitive dyes correlates with respiratory activity in cESCs.	131
Figure 3-8. Selective decrease in mitochondrial but not cytosolic staining with FCCP treatment.	132
Figure 3-9. Altered respiratory chain complex subunit abundances between L/F and 2iL cESCs.....	134
Figure 3-10. 2iL cESCs display elevated ATP content and AMPK signaling.	135

Figure 3-11. Differential regulation of pyruvate metabolizing enzymes between L/F and 2iL cESCs.....	136
Figure 3-12. Altered lipogenic properties between L/F and 2iL cESCs.....	138
Figure 3-13. Both L/F and 2iL cESC exhibit lower glycolytic capacities than human or mouse ESC.....	139
Figure 3-14. Both L/F and 2iL cESCs exhibit lower HXK2 abundance compared to human or murine ESC.....	140
Figure 3-15. Different chemical inhibitors of bioenergetics influence the acute expansion of L/F or 2iL cESCs.	142
Figure 3-16. Selective metabolic pathway inhibition affects ATP level of 2iL cESCs but not L/F cESCs.	143
Figure 3-17. Titrated metabolic pathway inhibitors do not increase apoptotic or dead cESCs.	144
Figure 4-1. Class assignments and CpG-rich sequence score among promoters of genes associated with somatic cell reprogramming.....	167
Figure 4-2. A subset of promoters associated with reprogramming is exclusively CpG-rich in the canine genome.....	168
Figure 4-3. Canine dermal fibroblasts exposed transiently to 5-azacytidine (5-AzaC) generate partially reprogrammed cell lines.	170
Figure 4-4. Incomplete demethylation of the NANOG promoter in canine partially reprogrammed cells.....	171
Figure 4-5. 5-hydroxymethylcytosine level varies with species and cell type.	173
Figure 4-6. L-ascorbic acid and retinoic acid modulates 5-hmC level at concentrations without detectable changes in TET paralogs expression.....	175

Figure 4-7. L-ascorbic acid suppresses hypoxia-mediated induction of cTET1 and cTET3.	176
Figure 4-8. Optimization of multiplicity of infection (MOI) in canine fibroblast using Sendai emGFP control vector.	178
Figure 4-9. L-ascorbic acid and retinoic acid promote focal epithelialization and primary colony formation in early canine reprogramming.	179
Figure 4-10. L-ascorbic acid and retinoic acid enhance a transcriptional response resembling mesenchymal-to-epithelial transition.	180
Figure 4-11. Validation of differentially abundant mesenchymal and epithelial transcripts using custom oligonucleotide primers.	182
Figure 4-12. Presumptive canine iPSCs are temporarily supported in media containing fetal bovine serum and LIF supplementation.	183
Figure 5-1. Conserved and divergent features of pluripotent state progression in canines. .	199
Figure 5-2. Different metabolic pathway activities support proliferation of canine ESCs approximating primed and naïve pluripotency.	201
Figure 5-3. Strategy to investigate conserved and divergent reprogramming mechanisms in the dog.	208
Figure 5-4. Validation of canine-reactive surface markers to discriminate mesenchymal or epithelial canine cells.	209

List of Appendices

Appendix A: Materials and Methods for cell surface marker validation.....	216
Appendix B: Copyright Approval.....	218
Appendix C: Animal Use Protocol Approval	220
Appendix D: Curriculum Vitae.....	221

List of Abbreviations

AA	L-ascorbic acid
ACC	Acetyl-coenzyme A carboxylase
ACVR	Activin receptor
A/F	Activin A and fibroblast growth factor
ALK	Activin receptor like kinase
AMPK	Adenosine monophosphate activated protein kinase
ANOVA	Analysis of variance
BMP	Bone morphogenetic protein
BRA	Brachyury
CDH	Cadherin
CDX	Caudal homeobox
cDNA	Complementary deoxyribonucleic acid
cESC	Canine embryonic stem cell
CGI	Cytosine-phosphate-guanine island
CoA	Coenzyme A
CpG	Cytosine-phosphate-guanine dinucleotide
CRM	Cis-regulatory module
DAPI	4',6-diamidino-2-phenylindole
DNMT	DNA methyltransferase

EB	Embryoid body
ECAR	Extracellular acidification rate
ECM	Extracellular matrix
EMT	Epithelial-to-mesenchymal transition
EOMES	Eomesodermin
ESC	Embryonic stem cell
ESRR	Estrogen receptor related
ETC	Electron transport chain
FASN	Fatty acid synthase
FBS	Fetal bovine serum
FCCP	Carbonyl cyanide-4-(trifluoromethoxy)phenylhydrazone
FGF	Fibroblast growth factor
FITC	Fluorescein isothiocyanate
FSC	Forward light scatter
GATA	GATA binding protein
gBGC	GC biased gene conversion
GBX	Gastrulation brain homeobox
gDNA	Genomic deoxyribonucleic acid
GLUT	Glucose transporter
GRN	Gene regulatory network

GSK	Glycogen synthase kinase
hESC	Human embryonic stem cell
HIF	Hypoxia inducible factor
HXK	Hexokinase
H3Ac	Histone H3 acetylated
H3K4me1/3	Histone H3 lysine 4 mono/trimethylated
H3K9me2/3	Histone H3 lysine 9 di/trimethylated
H3K27me3	Histone H3 lysine 27 trimethylated
ICM	Inner cell mass
IGF	Insulin like growth factor
iPSC	Induced pluripotent stem cells
JAK	Janus kinase
KLF	Krüppel-like factor
LDH	Lactate dehydrogenase
LIF	Leukemia inhibitory factor
MAPK	Mitogen activated protein kinase
MDCK	Madin Darby canine kidney cell line
MEF	Mouse embryonic fibroblast
MEK	Mitogen activated protein kinase kinase
mEpiLC	Mouse epiblast like cells

mEpiSC	Mouse epiblast stem cells
mESC	Mouse embryonic stem cells
MET	Mesenchymal-to-epithelial transition
MIC	Mitochondrial contact site subunit
MOI	Multiplicity of infection
mRNA	Messenger ribonucleic acid
mtDNA	Mitochondrial deoxyribonucleic acid
mTOR	Mechanistic target of rapamycin
MYC	Myelocytomatosis viral oncogene homolog
NAD	Nicotinamide adenine dinucleotide
NANOG	NANOG homeobox
OCR	Oxygen consumption rate
OCT	Octamer binding transcription factor
OTX	Orthodenticle homeobox
OXPHOS	Oxidative phosphorylation
PBS	Phosphate buffered saline
PCR	Polymerase chain reaction
PDH	Pyruvate dehydrogenase
PE	Primitive endoderm
PGC	Primordial germ cell

PKM	Pyruvate kinase muscle
PRDM	PR domain
PSC	Pluripotent stem cell
PTM	Post-translational modification
qPCR	Quantitative polymerase chain reaction
RA	All-trans retinoic acid
RIPA	Radioimmunoprecipitation assay
ROS	Reactive oxygen species
RPS	Ribosomal protein S
SAM	S-adenosylmethionine
SDH	Succinate dehydrogenase
SEM	Standard error of the mean
SeV	Sendai virus
S/L	Serum and leukemia inhibitory factor
SMAD	Mothers against decapentaplegic homolog
SOX	Sex determining region Y box
SSEA	Stage specific embryonic antigen
STAT	Signal transducer and activator of transcription
TBP	TATA binding protein
TBX	T-box

TCA	Tricarboxylic acid
TDG	Thymidine DNA glycosylase
TE	Trophectoderm
TEM	Transmission electron microscopy
TET	Ten eleven translocation
TF	Transcription factor
TGF	Transforming growth factor
TMRM	Tetramethylrhodamine, methyl ester
TOMM	Translocase of outer mitochondrial membrane
WNT	Wingless integrated
XIST	X-inactive specific transcript
ZIC	Zinc finger protein of the cerebellum
ZFP	Zinc finger protein
2DG	2-deoxy-D-glucose
2i	Two inhibitor (CHIR99021 and PD0325901)
5azaC	5-azacytidine
5-mC	5-methylcytosine
5-hmC	5-hydroxymethylcytosine
7AAD	7-aminoactinomycin D

Chapter 1

1 Introduction

1.1 Overview

1.1.1 Stem Cells, Fate Decisions and Cellular Plasticity

Ontogenesis broadly refers to the formation of an entire multicellular organism, which includes a vast increase in cell number by means of replication and spatially patterned differentiation into functionally mature cell types (Longo et al., 2015). A population of undifferentiated cells, referred to as stem cells, exist at many developmental stages and are defined by two fundamental cellular processes: self-renewal and differentiation (Evans and Kaufman, 1981; Till and McCulloch, 1961). Self-renewal describes the replication of undifferentiated cells without age-related deterioration or transformation, thereby maintaining the stem cell reserve (Zeng and Rao, 2007). Whereas differentiation describes the commitment to a more specialized cell type by the coordinated expression of gene products critical for that lineage (Bruno et al., 2004). These observable traits comprise the stem cell phenotype, however stem cells are further classified by the niche they reside in and their latent capacity to derive one or more lineages (Barker et al., 2010; De Los Angeles et al., 2015). The *ex vivo* culture of a variety of stem cells and knowledge of external stimuli that regulate self-renewal and differentiation, hold exciting promise in regenerative medicine and drug discovery (Hanna et al., 2007; Kondo et al., 2013).

Cell fate decisions are partially determined by the range of commitment opportunities available to a cell (i.e. potency) (Mitalipov and Wolf, 2009). Pluripotent stem cells (PSCs) can differentiate into all cell types found in postnatal tissues (Nagy et al., 1993) and are conventionally derived from the inner cell mass or epiblast of mammalian preimplantation embryos (Martin, 1981; Thomson et al., 1998). Embryonic stem cells (ESCs) are authenticated by prolonged self-renewal *in vitro* and differentiation into progenitor cells from all three primary lineages (i.e. endoderm, mesoderm, ectoderm) (Huang et al., 2011). Cell potency is subject to varying degrees of restriction or

broadening (i.e. plasticity) in response to environmental and experimental perturbations (Lakshmi and Verfaillie, 2005). This notion that cell fate is progressively and irreversibly restricted was famously conceptualized as an epigenetic landscape by Conrad Waddington (Waddington, 1957). It is now understood that epigenetic modification of chromatin regulates the developmental competence of PSCs to respond to environmental cues and enables the maintenance of acquired information in their derivatives (Mohn and Schübeler, 2009). However, persistent disruption of signal transduction pathways or gene regulatory networks can ectopically induce or prevent the formation of a lineage (Ladewig et al., 2013).

The extent of cellular plasticity is exemplified by direct reprogramming of somatic cells to an ESC-like phenotype, known as induced pluripotent stem cells (iPSCs) (Takahashi and Yamanaka, 2006). These reprogramming technologies progressively reconfigure the cytoskeleton, organelles, active signaling pathways and modifications to chromatin to attain a self-perpetuating pluripotency gene regulatory network (Jaenisch and Young, 2008; Sakurai et al., 2014). Interestingly, cellular reprogramming to a pluripotent state is associated with changes in cellular metabolism (Folmes et al., 2011; Panopoulos et al., 2012). Functional studies interrogating metabolic pathway activity and metabolite availability perceive metabolism as a determinant in cellular reprogramming and differentiation (Moussaieff et al., 2015; Sone et al., 2017). In this metabolic-epigenomic axis, metabolites regulate cell fate by functioning as rate-limiting reactants or cofactors for post-translational modifying enzymes that target chromatin (Carey et al., 2014; Sperber et al., 2015).

The variation among developmental gene expression and range of differentiation potentials exhibited by different PSC lines and their embryonic correlates *in vivo* (Beddington and Robertson, 1989; Gardner et al., 1985; Huang et al., 2012) are currently observed and modeled as pluripotency comprising multiple discrete phases rather than a unitary state (Ghimire et al., 2018; Yachie-Kinoshita et al., 2018). Developmental progression through pluripotency may be conditionally paused or reversed by modulating activities of protein kinases through cytokines, growth factors and selective inhibitors (Morgani et al., 2017; Weinberger et al., 2016). Alterations to mitochondrial dynamics or

the metabolites produced and/or consumed by mitochondria appear to regulate these pluripotent state transitions (Bahat et al., 2018; Tischler et al., 2019). Present findings support the notion that pluripotency progression is conserved in placental mammals (Bernardo et al., 2018). However, identifying the species-specific requirements for culture, molecular and functional attributes remains an ongoing challenge (Roberts et al., 2016).

1.2 Mammalian Development and Embryo-derived Pluripotent Stem Cells

1.2.1 Overview of Early Mammalian Development

Embryonic development begins with the fertilization of the oocyte and later continues as fetal development during gestation. Progression through mammalian embryonic development is best understood in murine embryogenesis, where lineage-tracing and transplantation studies have resolved the spatiotemporal variations of embryonic cell potency (Lokken and Ralston, 2016). Fertilization of the oocyte initiates a series of fixed mitotic divisions (i.e. cleavage) followed by a gradual strengthening of basolateral cell-cell interactions resulting in compaction of blastomeres (White et al., 2016). Successful completion of cleavage is dependent on activation of zygotic transcriptional programs by maternal factors that decondense chromatin and erase much of the epigenetic modifications to the genome (Evsikov et al., 2006; Svoboda et al., 2015). The zygote and blastomeres of two-to-eight cell murine embryos are generally considered totipotent with the capacity to contribute to either embryonic or extra-embryonic lineages and develop into viable offspring under appropriate conditions (Cockburn and Rossant, 2010). Totipotency is lost in the sixteen-cell embryo, known as the morulae, as the apical-basal polarity established by compaction initiates positional and mechanical cues essential to the first lineage specification event (Leung et al., 2016; Suwińska et al., 2008; Tarkowski et al., 2010).

The innermost cells of morulae embryos give rise apolar cluster of pluripotent cells called the inner cell mass (ICM) enveloped by an epithelial layer known as trophectoderm (TE) (Rossant, 1987). The TE contains only the multipotent cells that derive placental tissues

for implantation, whereas the ICM will give rise to all embryonic tissues including some extraembryonic membranes (Rossant, 1987). Cell restriction to either lineage is mediated by signaling pathways and gene regulatory mechanisms that reinforce differential expression of transcription factors (TFs) associated with TE identity (e.g. CDX2, EOMES) versus ICM identity (e.g. POU5F1/OCT4, SOX2 and NANOG) (Strumpf et al., 2005; Wicklow et al., 2014). Formation of a fluid-filled space (i.e. blastocoele) after ICM-TE lineage segregation is an indication successful progression to the early blastocyst stage (Madan et al., 2007).

ICM proliferation and enhanced integrin-mediated interactions with the extracellular matrix (ECM) are associated with a second differentiation event that generates the early epiblast and primitive endoderm (Copp, 1978; Sakai et al., 2003). The early epiblast retains the pluripotent cell population, but transitions from spherical morphology to a radially symmetric monolayer (Beddington and Robertson, 1999). Epiblast morphogenesis creates a cylinder-like shape in rodents, as opposed to the disc-like morphology adopted by the primate epiblast (Bedzhov and Zernicka-Goetz, 2014). It is believed that probabilistic variation in fibroblast growth factor (FGF) ligand and receptor expression among ICM cells randomly restricts either NANOG or GATA6 to the epiblast or primitive endoderm (PE), respectively (Guo et al., 2010; Kang et al., 2017). Cells differentiating into PE upregulate several TFs (e.g. GATA4, SOX17), migrate towards the blastocoele-facing surface of the early epiblast and give rise to the extraembryonic endoderm portions of the yolk sac (Chazaud and Yamanaka, 2016; Gardner and Rossant, 1979).

At gastrulation, a subpopulation of the epiblast undergoes epithelial-to-mesenchymal transition (EMT), resulting in a loss of epithelial adhesive junctions and increased cell motility (Shook and Keller, 2003; Thiery et al., 2009). Migration of epiblast cells undergoing EMT through a dorsal structure known as the primitive streak establishes the definitive mesoderm (Ciruna and Rossant, 2001; Sun and Stathopoulos, 2018). Whereas the cells within the anterior third of the primitive streak form definitive endoderm (Ang et al., 1993). Continued cellular migration elongates the whole embryo and rearranges the late epiblast into an asymmetric structure known as the anterior to posterior epiblast

(Brennan et al., 2001; Lawson et al., 1991). Late epiblast cells continue to proliferate and expand, becoming spatially restricted, yet remaining pluripotent until the onset of somitogenesis (DeVeale et al., 2013; Osorno et al., 2012). Epiblast-derived primordial germ cells (PGCs) are induced during gastrulation and actively migrate to genital ridge via the posterior endoderm (Ginsburg et al., 1990). PGCs represent a form of unipotent stem cell *in vivo* which do not continue specification into gametes until gonad development (Ginsburg et al., 1990). Migrating PGCs undergo programmed epigenetic erasure and may be isolated and expanded *in vitro* with defined extracellular factors as pluripotent embryonic germ cells (Resnick et al., 1992; Stewart et al., 1994). Marked differences in the timing of transcriptional events, the wiring of regulatory circuits, and epiblast morphogenesis are observed when embryonic development of the mouse is compared to other mammals (Rossant and Tam, 2017). However, the functional relevance of these evolutionarily divergent features to the establishment or resolution of embryonic pluripotency remains less clear.

1.2.2 Mouse Pluripotent Stem Cells from Peri-implantation Embryos

Although pluripotent cells exist only transiently *in vivo*, it is possible to research stem cell lines that are paused in a stable pluripotent identity within a defined milieu. Pluripotent stem cells (PSCs) maintain the ability to differentiate into the all somatic and germline cell types of the ectoderm, mesoderm and endoderm (Doetschman et al., 1985; Leahy et al., 1999). In contrast to pluripotent cells within early embryos, PSCs in culture acquire the distinct ability to undergo prolonged self-renewal (Evans and Kaufman, 1981; Thomson et al., 1998). The precise molecular alterations that conditionally adapt embryonic cells to an *ex vivo* environment remain unclear (Buehr et al., 2003). Mouse embryonic stem cells (mESCs) are routinely established from the epiblast outgrowths of preimplantation embryos explanted on a mouse embryonic fibroblast (MEF) layer (Brook and Gardner, 1997; Evans and Kaufman, 1981; Martin, 1981). When embryos retrieved at an earlier developmental time point, embryos progress to the blastocyst stage under derivation conditions before mESCs arise (Boroviak et al., 2014).

Among the supportive factors secreted by MEFs or present in serum, leukemia inhibitory factor (LIF) was identified as the component with anti-differentiation activity (Smith et al., 1988). Exogenous LIF preparations have enabled the feeder-free propagation of mESCs (Makino et al., 2004). Supplementation with LIF promotes mESC self-renewal and expression of pluripotency-associated TFs through the LIF receptor-gp130 complex and activation of Janus kinase (JAK)-signal transducer and activator of transcription 3 (STAT3) signaling (Matsuda et al., 1999; Niwa et al., 1998). LIF-STAT3 signaling can synergize with the bone morphogenetic protein 4 (BMP4)-SMAD1 signaling to support the maintenance of undifferentiated mESC (Ying et al., 2003a). The observation that BMP4 bioactivity is partly mediated by repression of mitogen-activated protein kinase (MAPK) pathways was followed by the identification of two kinase inhibitors (2i) that negate pro-differentiation stimuli in mESCs and established a minimal input so-called ground state of pluripotency (Qi et al., 2004; Ying et al., 2008).

Cell lines equivalent to mESC cannot be derived from the murine post-implantation epiblast in serum and LIF (S/L) conditions. However, culture with Activin A and FGF2 (A/F) mimics the signaling within the peri-gastrulation niche and enables the establishment of cell lines known as mouse epiblast stem cells (mEpiSC) (Brons et al., 2007; Tesar et al., 2007). mEpiSC meet the self-renewal and tri-lineage differentiation criteria of a PSC population (Brons et al., 2007; Tesar et al., 2007). In contrast to mESC, mEpiSC cannot autonomously produce the ECM components needed to maintain their undifferentiated state, and therefore are propagated on a layer of MEFs or synthetic ECM (Hunt et al., 2012; Veluscek et al., 2016). Activin A supports mEpiSC pluripotency via SMAD2/3 transactivation of NANOG expression, which operates in a negative feedback loop to repress SMAD2/3. In this delicately balanced mechanism, Activin A signaling opposes neuroectoderm differentiation by maintaining NANOG, while NANOG prevents mesendoderm cell fate by limiting the transcriptional activity of SMAD2/3 (Vallier et al., 2009). FGF2-MAPK kinase (MEK) signaling does not appear to directly promote pluripotency-associated TFs, but rather dually suppresses regulators of neuroectoderm fate and krüppel-like factor 2 (KLF2) (Greber et al., 2010).

1.2.3 Naïve and Primed Pluripotent States

Given that pluripotent cells can be isolated from different compartments of developing embryos with different requirements for self-renewal, it was proposed that mESC and mEpiSC represent different temporal iterations of pluripotency *in vitro* (Tesar et al., 2007). Importantly, the divergent features of mESC and mEpiSC were not explained by the mouse strain of origin (Brons et al., 2007). The observation that mEpiSC exhibit transcriptional signatures and signaling requirements similar to human ESC (hESC) suggests that PSC subtypes are conserved in mammals (Rossant, 2008; Tesar et al., 2007). A combination of evolutionary variation among pluripotency regulatory mechanisms and developmental maturity of human blastocysts donated from fertility clinics to derive conventional hESCs, likely contribute to their homology to mEpiSCs (Hanna et al., 2010, 2009a). The generic terminology naïve or primed pluripotent state were adopted to describe the pan-mammalian existence of two discrete phases of pluripotency exemplified by mESC (S/L and 2i conditions) or mEpiSC and hESC, respectively (Nichols and Smith, 2009).

Primed and naïve PSC exhibit similar ultrastructural features including a large nucleus, scant cytoplasm, perinuclear mitochondria and intercellular junctional complexes (i.e. desmosomes) (Baharvand and Matthaei, 2003; Sathanathan et al., 2002). A notable exception is the mitochondria of mESC are oval in shape, whereas tubular mitochondria are observed in mEpiSC and hESC (Zhou et al., 2012). Obvious differences exist in the morphological appearance of multicellular colonies formed by naïve or primed PSC. mESCs proliferate in multi-layer, hemispherical colonies of compacted cells which are difficult to distinguish by light microscopy (Baharvand and Matthaei, 2003). In contrast, mEpiSC/hESC form planar, disc-shaped colonies with compacted interior cells with a “cobblestone” appearance, surrounded by distended columnar cells at the margins (Sathanathan et al., 2002). The colony-forming ability (i.e. clonogenicity) of PSC is influenced by the pluripotent state, which impacts culture protocols and the efficiency of cell selection. mESC are routinely passaged by enzymatic dissociation into single cells. However, primed PSC are intrinsically hypersensitive to apoptotic stimuli and mechanical fragmentation often improves viability and self-renewal of mEpiSC or hESC

(Hartung et al., 2010; Pernaute et al., 2014). Clonogenicity of hESC can be improved with Rho-associated kinase (ROCK) inhibition or epithelial-type cadherin (CDH1) overexpression, suggesting that cytoskeletal and cell adhesion dynamics regulate PSC clonality (L. Li et al., 2010; Watanabe et al., 2007).

Mouse naïve or primed PSC contribute to chimeric embryos within a defined range of development following orthotopic transplantation, suggesting that intrinsic properties to either pluripotent state influences differentiation capabilities *in vivo*. Whereas mESCs readily differentiate to somatic tissues and the germ line upon reintroduction into the preimplantation blastocyst, mEpiSC do not contribute to the embryo proper at this developmental time point (Bradley et al., 1984; Guo et al., 2009; Tesar et al., 2007). Identification of the variables that influence cellular competence for embryonic integration have greatly improved the efficiency and reproducibility of chimeric embryo generation including matched developmental timing, reducing competition with host cells or dampening cell responsiveness to pro-apoptotic stimuli (Masaki and Nakauchi, 2017; Wu et al., 2016). The *in vivo* pluripotency of mEpiSC was demonstrated by functional engraftment into the anterior-mid primitive streak of post-implantation host embryos (Huang et al., 2012; Kojima et al., 2014; Tsakiridis et al., 2014). The use of chimeric blastocyst functional assays to unambiguously dichotomize PSC as naïve or primed, generally excludes primate PSC lines in many jurisdictions for technical, legal and ethical reasons (Streiffer, 2007). However, the conceptual barriers to interspecies embryonic chimerism are receding with improved cell fate-mapping, developmental stage-matching and a softening international stance on procedures which include early termination policies (Mascetti and Pedersen, 2016; Wu et al., 2016). The development of teratomas upon PSC engraftment into somatic tissues of immune-deficient mice is a shared feature among mESC, mEpiSC or hESC (Brons et al., 2007; Reubinoff et al., 2000; Tesar et al., 2007). Therefore, teratoma formation assays are not useful in discriminating between naïve or primed PSC.

Collections of molecular genome annotations and transcriptional output associated with those regions have generated integrated global signatures of any given cell type (Roadmap Epigenomics Consortium et al., 2015). Transcriptional profiling studies

indicate that mESC transcriptomes resemble the ICM or preimplantation epiblast, depending on the culture conditions (Boroviak et al., 2014; Martin Gonzalez et al., 2016; Tang et al., 2010). Debate and imprecision with regards to the precise developmental correlate of mESC likely stem from variables that influence the transcriptome such as the inclusion of serum, application of 2i, use of MEF feeders or different substratum (Kolodziejczyk et al., 2015; Marks et al., 2012). Conversely, mEpiSC exhibit transcriptomic features of primitive streak cells found within gastrulating embryos rather than the post-implantation epiblast from which they are derived (Kojima et al., 2014; Tsakiridis et al., 2014). Therefore, mESC and mEpiSC exhibit both molecular and functional equivalence to temporally distinct stages of embryonic development (Morgani et al., 2017). Both pluripotent states represent generalizable phenotypes among PSC derived from mice, humans and likely other mammals (Theunissen et al., 2016; Weinberger et al., 2016). Recently, ectopic stabilization of naïve pluripotency in developing mouse and human embryos was shown to disrupt amniotic cavity formation, thereby demonstrating a conserved physiological relevance of pluripotent state progression in tissue morphogenesis (Shahbazi et al., 2017).

1.2.4 Generation of Transient Embryonic States *in vitro*

Cells resembling mEpiSC can be generated from mESC in A/F conditions, but this appears to be a prolonged and inefficient transition that features a strong negative selection (Turco et al., 2012). This suggests that the naïve-to-primed pluripotent state transition is not a single-step, but rather a dynamical process that is poorly recapitulated *in vitro* (Kalkan and Smith, 2014). Access and characterization of this embryonic stage has not been possible due to the methodological difficulty of isolating these transient cells in mouse preimplantation development (Bedzhov et al., 2014). These mouse epiblast-like cells (mEpiLC) can generate PGCs in response to BMP4, recapitulating the developmental potential exhibited by a subpopulation of the native epiblast *in vivo* (Hayashi et al., 2011; Lawson et al., 1999). If an intermediate PSC population were to be purified, a theoretical “formative” pluripotent state is proposed to relinquish aspects of naïve pluripotency before upregulating gastrulation-stage lineage markers observed in the primed pluripotent state (Smith, 2017). Because mEpiLC are a heterogeneous mixture,

moderate expression levels of both naïve and primed pluripotency markers are not considered to be strong evidence of formative pluripotency.

1.3 Characteristics of Mammalian Pluripotent Stem Cells

1.3.1 Techniques to Study Self-Renewal and Differentiation

The clonogenicity, self-renewal, broad differentiation abilities of PSC lines make feasible large-scale functional genomics and high-throughput screening approaches, compared to embryo models where limitations cell numbers and embryo availability exist (Boiani and Schöler, 2005; Desbordes and Studer, 2013). Despite the existence of cell culture-related artifacts, both naïve and primed PSC are viewed as complementary *in vitro* systems to animal models of preimplantation development to dissect the molecular basis of pluripotency and lineage specification (Niwa, 2010). PSCs are typically studied under self-renewing conditions *in vitro* (i.e. steady-state) and static comparisons may be made to an independent culture of differentiated PSC progeny (Reubinoff et al., 2000). When higher temporal resolution is desirable, reporter genes (e.g. fluorescent proteins) are introduced under the genetic control of either pluripotency or differentiation affiliated regulatory elements to dynamically track changes in gene expression (Gossler et al., 1989).

In the absence of essential self-renewal factors (i.e. S/L or 2i for mESC, A/F for mEpiSC/hESC), PSCs will spontaneously differentiate into an assortment of stem or progenitor cell types from the ectoderm, mesoderm and endoderm lineages (Spencer et al., 2011). Spontaneous differentiation of PSC in low adherence conditions yields spherical aggregates of committed progeny (i.e. embryoid bodies), which crudely mimics postimplantation development to achieve an even distribution of the primary embryonic lineages compared to adherent culture (Doetschman et al., 1985; Martin and Evans, 1975). A basic understanding of the soluble or matrix-dependent signals for lineage specification, permits the use of selective differentiation protocols, which can be advantageous for PSC lines with skewed lineage bias (Murry and Keller, 2008). Stepwise application of specific differentiation stimuli to differentiating PSC over multiple weeks can guide the maturation of cell types formed later in gestation (Ying et al., 2003b).

1.3.2 Gene Regulatory Networks in Pluripotency

Gene regulatory networks (GRNs) are critical for the integrity of pluripotent states and for stable commitment to a given lineage upon differentiation. The architecture of GRNs include few “master” TFs, many “collaborating” TFs, regulatory non-coding RNA and chromatin modifying enzymes, which act in auto- and cross-regulatory circuits to exert combinatorial control on *cis*-regulatory modules (CRMs) of target genes (Hackett et al., 2014; Peter and Davidson, 2016). GRNs frequently act upstream of pluripotency and lineage related genes such that cell fate decisions are executed only when pre-existing cell state and differentiation stimulus is appropriate (Martín et al., 2016). The transcription factors OCT4, SOX2 and NANOG (O-S-N) are central to naïve mouse pluripotency GRNs both *in vivo* and *in vitro* (Mitsui et al., 2003; Nichols et al., 1998). Strong imbalances in O-S-N expression leads to extraembryonic or germ lineage differentiation, rather than reinforcing a stable pluripotent state (Niwa et al., 2000; Thomson et al., 2011). However, minute fluctuations in the core GRN factors are effectively buffered by dense regulatory interconnectivity and redundant CRM occupancy with collaborating TFs (MacArthur et al., 2009). Under steady-state conditions the pluripotency GRN collectively antagonizes lineage-specific GRNs, while simultaneously remaining sensitive to differentiation cues (Jaenisch and Young, 2008). In this model, variations in pluripotency GRN membership (i.e. TFs expressed) and wiring/topology (i.e. available CRMs in genome) would account for the different properties of spatiotemporal or evolutionary iterations of PSCs (Li and Belmonte, 2017).

Input from several developmentally regulated signaling pathways can be finely tuned to either support or destabilize the pluripotency GRN. In many cases, small molecule inhibition of protein kinases or knockdown of epigenetic modifiers are titrated to levels of partial antagonism or depletion (Cheloufi et al., 2015; Mor et al., 2018). Dual inhibition of glycogen synthase kinase 3 β (GSK3 β) and MEK in the 2i condition synergistically reinforces the naïve pluripotency GRN in mice (Ying et al., 2008). Stimulation of WNT signaling induces nuclear localization of β -catenin, which de-represses OCT4-SOX2 targeted genes (Cole et al., 2008; Qiu et al., 2015; Wray et al., 2011). Partial blockade of FGF–ERK signaling elevates KLF2/4 and NANOG

accumulation by transcriptional and post-translational mechanisms (Kim et al., 2014; Yeo et al., 2014). Beyond the direct impact on NANOG and KLF2, several collaborating TFs associated with naïve pluripotency are reinforced by 2i such as TBX3, ZFP42/REX1, GBX2 or ESRRB (De Los Angeles et al., 2015). By these mechanisms, the 2i condition is proposed to reduce spontaneous differentiation and increase mESC derivation efficiency from refractory strains by optimally stabilizing the naïve pluripotency GRN (Hanna et al., 2009a; Wray et al., 2011).

Whereas hESCs also exhibit an O-S-N centric GRN, mEpiSCs operate with Zic family member 2 (ZIC2) and orthodenticle homeobox 2 (OTX2) in place of NANOG (Boyer et al., 2005; Iwafuchi-Doi et al., 2012; Matsuda et al., 2017). NANOG is required for acquisition of naïve pluripotency during ICM development *in vivo* but is dispensable for transactivation of target pluripotency genes and overall mESC maintenance (Chambers et al., 2007; Silva and Smith, 2008). Several collaborative TFs associated with naïve pluripotency are direct targets of NANOG and downregulated in mEpiSCs (Festuccia et al., 2012; Osorno and Chambers, 2011). Therefore, primed PSC appear to possess a less densely interconnected GRN owing to fewer collaborating TFs that directly support the undifferentiated state (Iwafuchi-Doi et al., 2012). Rather, hESC/mEpiSCs exhibit sporadic expression of early lineage specification genes from each germ layer including FGF5, SOX17 and brachyury (T/BRA) (Tsakiridis et al., 2014). The combination of variably co-expressed lineage-specific genes and a less insulated GRN may explain the considerable heterogeneity and propensity for spontaneous differentiation in the primed pluripotent state (Ghimire et al., 2018; Hough et al., 2009).

1.3.3 Transcriptional and Epigenetic Crosstalk at Developmentally-Regulated Genes

The basic unit of genomic DNA (gDNA) organization is the nucleosome, an octamer of histone proteins each surrounded by roughly 147 bp of the gDNA string (Kaplan et al., 2009). CRMs contained within nucleosomal gDNA are generally inaccessible to TFs and RNA polymerase (Lee et al., 2004; Lorch et al., 1987). The active (i.e. euchromatin) and inactive (i.e. heterochromatin) portions of the genome are physically segregated through interactions with architectural chromatin proteins to presumably facilitate chromosomal

interactions pertinent to cell identity (Novo and Rugg-Gunn, 2016). Euchromatin domains are enriched for interactions with the transcriptional coactivators, whereas heterochromatin is associated with laminin B that tethers transcriptionally inert regions to the inner nuclear membrane (Handoko et al., 2011). TFs, RNA polymerase and architectural proteins compete with histones for occupancy of CRMs in order liberate segments of gDNA from the nucleosome (Gilchrist et al., 2010; Krebs et al., 2017). Epigenetic modifications affecting local chromatin accessibility regulate the influence of pluripotency or lineage GRNs by modulating the ability of TFs to physically engage with target CRMs (John et al., 2011; Mao et al., 2011).

Targeted and reversible covalent modifications on gDNA or histones control the accessibility of a given CRM by changing the steric properties of the chromatin interface and alter the affinity of DNA or chromatin binding proteins (Keshet et al., 1986; Yin et al., 2017). DNA methylation involves transfer of a methyl group to the 5-position of cytosine base (5-mC), which occurs predominantly in the context of cytosine-phosphate-guanine (CpG) dinucleotides (Gruenbaum et al., 1982). Whereas, histone proteins can undergo a variety of post-translational modifications (PTM) at the histone tail domain that protrudes from the nucleosome (Jenuwein and Allis, 2001). Specific histone tail modifications may be either correlated or anti-correlated with overlapping DNA methylation, implying extensive crosstalk between these enzyme families.

The variety of distinct PTM and/or DNA methylation patterns introduces different levels of epigenetic resistance and non-uniform regulatory control over transcriptional activity dependent on the genomic context (Cedar and Bergman, 2009). Constitutive heterochromatin is marked by co-occurrence DNA methylation and histone H3 lysine 9 di/tri-methylation (H3K9me_{2/3}), which is believed to encourage chromatin compaction and a non-permissive transcriptionally state (Sarraf and Stancheva, 2004; Smallwood et al., 2007). Large repressive domains of constitutive heterochromatin are characteristic of repetitive sequences, mobile elements and subsets lineage-specific genes needed for stable differentiated cell fates (Becker et al., 2016; Saksouk et al., 2015). Conversely, facultative heterochromatin involves H3 lysine 27 trimethylation (H3K27me₃) and the absence of DNA methylation, that promotes transcriptional repression yet maintains

accessibility to general transcriptional machinery (Dellino et al., 2004; Jermann et al., 2014; Reddington et al., 2013). H3K27me3 offers a reversible mode of silencing for CRMs of lineage-associated genes that are dynamically expressed during development (Margueron and Reinberg, 2011; Trojer and Reinberg, 2007).

Several mechanisms exist to grant certain TFs access to gDNA within a fully constituted nucleosome and initiate local epigenome remodeling. Certain TFs have affinity for partial binding sites in nucleosomal gDNA or histone proteins themselves, granting these TFs “pioneer activity” to engage previously inaccessible chromatin (Cirillo et al., 2002; Sekiya et al., 2009). Pioneer TFs can provide a platform for sequence-independent recruitment of histone modifying and/or chromatin remodeling enzymes, which can destabilize, reposition or remove histones to generate nucleosome depleted regions (Klemm et al., 2019). Transcriptionally active CRMs are associated with acetylation of histone H3 and H4 proteins, which is proposed to accumulate in regions with frequent nucleosome destabilization (Henikoff, 2008; Müller and Leutz, 2001).

1.3.4 Hyperdynamic and Poised Features of the Pluripotent Regulatory Epigenome

The nuclei of PSC contain smaller, more diffuse H3K9me3 domains that is suggestive of a lower prevalence of heterochromatin genome-wide, compared to lineage restricted cells (Ahmed et al., 2010; Fussner et al., 2011; Park et al., 2004). PSCs also exhibit hyperdynamic chromatin compared to committed progenitor cells, which is exemplified by rapid turnover of architectural chromatin proteins (Meshorer et al., 2006). As a likely consequence of a permissive chromatin state, PSCs are transcriptionally hyperactive and feature greater histone acetylation levels (Efroni et al., 2008; Meshorer et al., 2006). Chromatin plasticity in PSCs manifests as frequent non-specific chromosomal interactions and less prominent insulator boundaries (i.e. topologically associating domains) (De Wit et al., 2013; Pękowska et al., 2018). Differentiation of PSCs is associated with greater chromosomal interaction specificity and enhanced compartmentalization of the genome by chromatin architectural proteins (Melcer et al., 2012; Pękowska et al., 2018).

One mechanism employed by PSCs to transcriptionally repress the euchromatic portions of the genome, while remaining poised for lineage specifying cues is the maintenance of bivalent chromatin (Azuara et al., 2006; Bernstein et al., 2006; Mikkelsen et al., 2007). Bivalent domains are characterized by the co-occurrence of H3K27me3 at H3K4me3-marked promoters on different histone tail domains within the same nucleosome (Shema et al., 2016). Resolution of bivalent domains to single activating or silencing marks could be theoretically mediated by the selective recruitment of the appropriate lysine demethylase enzyme (Pasini et al., 2008). However, bivalent domain partitioning is representative of only a minority of developmentally-regulated promoters and epigenetic remodeling during differentiation occurs principally at distal CRMs bearing the enhancer-associated H3 lysine 4 monomethylation (H3K4me1) mark (Hawkins et al., 2011). Distal CRMs marked solely by H3K4me1 are considered poised enhancers, which are discriminated from actively-used enhancers with H3K4me1 and acetylated histone H3 (H3Ac) (Creyghton et al., 2010). Core pluripotency GRN TFs preferentially interact with poised enhancers, which is believed to maintain or bookmark a repertoire of distal CRMs available to be activated when a lineage is specified (Creyghton et al., 2010; Hawkins et al., 2011).

1.3.5 Dynamic Heterogeneity and Epigenetic Barriers to Pluripotent State Transitions

The permissive chromatin landscape of PSCs allows dynamic fluctuations between closely-related pluripotency GRNs and introduces variation among individual cells, known as dynamic heterogeneity (Rompolas et al., 2013; Singer et al., 2014). Initially, single-cell analyses demonstrated at least two molecularly and functionally distinct sub-populations exist interchangeably among S/L mESCs (Hayashi et al., 2008). Promoting hyper-acetylation of nucleosomes can skew the sub-populations in dynamic equilibrium, therefore highlighting the contribution of epigenetic plasticity to this phenomenon (Hayashi et al., 2008). External input from the microenvironment, such as paracrine signals or exogenously supplemented molecules, stabilize different cell identities without differentiation so long that perturbations do not exceed the buffering capacity of pluripotency GRNs (Davey and Zandstra, 2006; Yachie-Kinoshita et al., 2018). The

notion that extrinsic signals dictate the predominant phenotype adopted among available cell identities is loosely referred to as metastability (Hanna et al., 2009a). Cell intrinsic sources of variation also contribute to dynamic heterogeneity of pluripotent cell populations both *in vitro* and *in vivo* such as transcriptional noise and cell cycle stage (Navarro et al., 2012; Singh et al., 2013).

Changes in cell fate that follow a developmental progression are relatively efficient by making use of epigenomic plasticity and poised GRNs. In contrast, experimental manipulations that force the rejuvenation of a mature nuclear environment (i.e. nuclear reprogramming) must overcome epigenetic barriers established during development leading to inefficiency (Morgani et al., 2017; Weinberger et al., 2016). Switching the mESC media containing S/L to a composition with F/A will promote a naïve-to-primed transition and generate mEpiSCs (Guo et al., 2009; Onishi et al., 2012). Overexpression of NANOG in mESC resists naïve-to-primed transition despite prolonged exposure to F/A conditions (Osorno and Chambers, 2011). The mESC-to-mEpiSC conversion is dependent on FGF2-mediated induction of OTX2, which is co-expressed in low NANOG expressing cells among the originating S/L mESC population (Acampora et al., 2012). Naïve-to-primed transition involves the decommissioning of naïve-specific enhancers through gains in DNA methylation (Buecker et al., 2014; Factor et al., 2014).

The reversion of mEpiSC to mESC is infrequent yet reproducibly observed when F/A conditions are replaced with S/L media (Bao et al., 2009). Forced expression of NANOG, KLF2/4, ESRRB or STAT3 can induce nuclear reprogramming of mEpiSC to reset mESCs when F/A is replaced with S/L (Guo et al., 2009; Hall et al., 2009; Silva et al., 2009; Yang et al., 2010). mEpiSC are also considered to be in dynamic equilibrium with sub-states exhibiting low levels of naïve pluripotency TF expression (Han et al., 2010). The mEpiSC subpopulation that is poised to transition towards naïve pluripotency can spontaneously transition to the mESC phenotype with greater (~15-fold) efficiency (Han et al., 2010). The addition of 2i to either growth factor or transgene mediated reprogramming of mEpiSC to mESC promotes NANOG expression and reactivation of naïve pluripotency-specific enhancers (Adachi et al., 2018). Reset mESC exhibit transcriptomic, epigenomic and morphological similarity to steady state mESC as well as

competency to repopulate the germline in chimeras (Bao et al., 2009; Lai and Bu, 2016; Zhang et al., 2016b). These outcomes suggest that a subset of mEpiSCs are poised to adopt a naïve pluripotency GRN and overcome the epigenetic barriers established during lineage priming in a LIF/STAT3 signaling environment, which can be augmented by reintroduction of naïve pluripotency TFs (Fig. 1-1).

Global comparisons of DNA methylation show that S/L mESC have a less methylated genome compared to mEpiSC (Habibi et al., 2013; von Meyenn et al., 2016). Moreover, 2i mESC display even greater DNA hypomethylation, in part by repression of DNA methyltransferase expression (DNMT) (Hackett et al., 2013; Leitch et al., 2013; Yagi et al., 2017). Additionally, mEpiSCs show more frequent facultative heterochromatin indicated by greater numbers of H3K27me3 domains, whereas gains in H3K9me3 heterochromatin are disputed as cell culture artifacts (Joshi et al., 2015; Marks et al., 2012). Genetically female mEpiSCs exhibit inactivation of one X-chromosome, a form of dosage compensation that occurs late in embryogenesis, that is mediated by the non-coding RNA Xist and H3K27me3 deposition (Augui et al., 2011; Plath et al., 2003). Erasure of genome-wide DNA methylation and reactivation of the silent X-chromosome are both reproducible features of steady state and reset mESC (Bao et al., 2009; Guo et al., 2009). DNA methylation exhibits a strong correspondence with restricted developmental potential and is associated with stronger interactions between histones and nucleosomal DNA (Choy et al., 2010; Smith and Meissner, 2013). Accordingly, the chromatin of primed PSC is comparatively less hyperdynamic than naïve mESCs but remain more plastic than differentiated cells (Pękowska et al., 2018). In addition to nuclear determinants of pluripotency, nutrient-sensing and mitochondrial crosstalk pathways are emerging as coordinators self-renewal and cell fate decisions in embryos and PSCs.

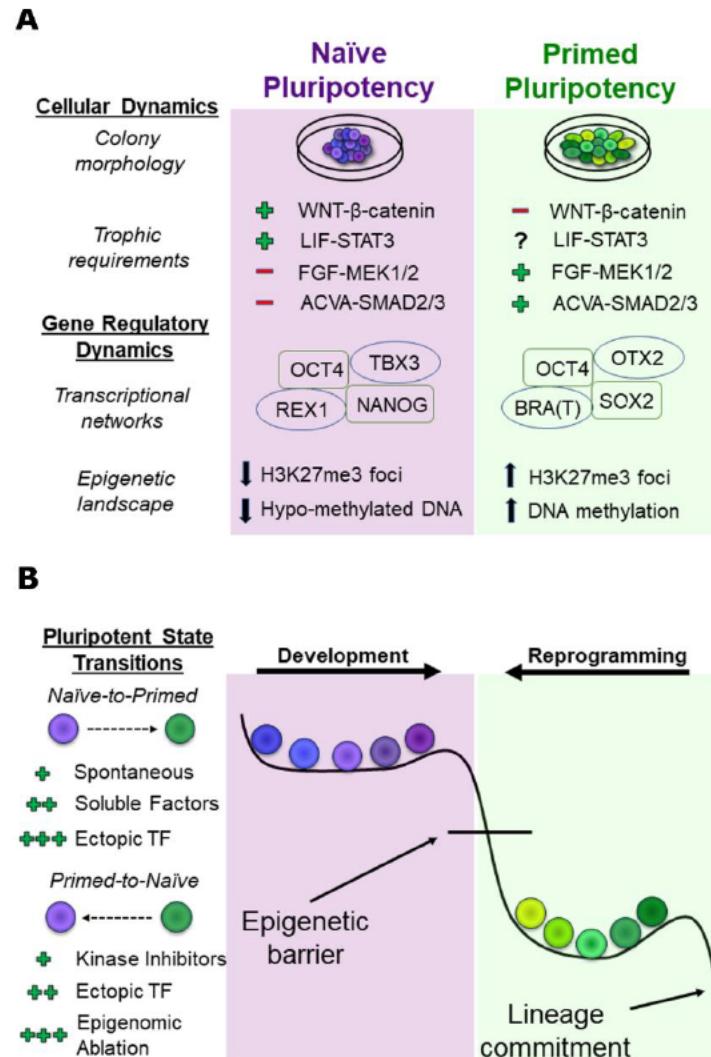


Figure 1-1. Conserved features of naïve and primed pluripotency in placental mammals.

(A) Discriminatory morphological features and extrinsic requirements of naïve and primed pluripotent stem cell populations. Different gene regulatory network components are reinforced by distinct epigenetic landscapes with an enrichment of repressive marks and early lineage regulators in primed pluripotency. (B) Plateau model of pluripotent states accommodates cell-cell variation within epigenomic constraints. Naïve-to-primed pluripotency transition follows endogenous developmental programming that can be funneled by extrinsic or intrinsic determinants of primed pluripotency. Whereas primed-to-naïve pluripotency transition must overcome epigenetic barriers at decommissioned naïve-specific elements to reactivate the naïve pluripotency gene regulatory networks.

1.4 Metabolism in Pluripotent Stem Cells

1.4.1 Overview of Cell Metabolism

Metabolism broadly describes the collection of enzyme-catalyzed reactions organized parallel and sequential pathways that provide molecular energy, substrates or cofactors necessary for cell viability, division and function. Eukaryotic cells produce chemical energy in the form of adenosine triphosphate (ATP) molecules through the breakdown of carbohydrates, amino acids and lipids (i.e. catabolism). The major ATP-producing pathways are segregated into oxygen-independent cytosolic reactions (glycolysis) and oxygen-dependent mitochondrial processes, known as oxidative phosphorylation (OXPHOS). However, most molecules are never completely consumed by bioenergetic pathways, and instead diverted at a variety of branch points to alternative metabolic pathways (i.e. shunts) that produce essential substrates for biosynthetic reactions (i.e. anabolism) (Folmes et al., 2011). Otherwise, metabolic intermediates with cofactor or co-substrate functions can be made available to non-metabolic reactions through redirection to a different subcellular compartment such as the nucleus (DeBerardinis et al., 2008).

The relative activity of glycolysis, mitochondrial metabolism and intermediary metabolic pathways depends on the functional demands of a cell type and the physicochemical composition of the extracellular environment (Gardner, 1998). Glycolysis involves a series of phosphorylation, isomerization and oxidoreduction (redox) reactions that converts glucose to pyruvate. Metabolite turnover through glycolysis reactions (i.e. flux) regulates the availability of glycolytic intermediates to alternative biosynthetic pathways such as the pentose phosphate pathway or the hexosamine biosynthetic pathway (Reitzer et al., 1980; Wellen et al., 2010). Glycolysis-derived pyruvate is shunted away from mitochondrial metabolism in a metabolic configuration known as aerobic glycolysis. Lactate dehydrogenase (LDH) is central to this mode of metabolism by regenerating electron acceptor NAD^+ for the GAPDH enzyme, thereby sustaining glycolysis independent of OXPHOS (Brand and Hermfisse, 1997; Ochocki and Simon, 2013). Reduced electron transport chain (ETC) activity limits the efficiency of ATP synthesis by OXPHOS but offers a rapid source of anabolic substrates and decreases cell exposure to reactive oxygen species (ROS) produced by mitochondria (Lunt and Vander Heiden,

2011). Therefore, aerobic glycolysis may be selectively beneficial for cell types that rapidly proliferate or reside in hypoxic niches.

1.4.2 Metabolic Regulation of Self-Renewal and Differentiation

Mouse preimplantation embryos show elevated glucose consumption at the blastocyst stage, suggesting that pluripotent cells of the epiblast exhibit high glycolytic flux (Houghton et al., 1996; Leese and Barton, 2004). Indeed, mESCs display high glycolytic activity in self-renewing conditions but upregulate genes involved in mitochondrial biogenesis and OXPHOS upon differentiation into specialized lineages (Cho et al., 2006; Chung et al., 2007; Kondoh et al., 2007). The rapid pace of cell division set by glycolytic flux in PSC likely promotes self-renewal by desensitizing PSC to pro-differentiation stimuli. PSCs continuously transit through the cell cycle due to an abbreviated G1 checkpoint, spending most of the cell cycle in S-phase where PSCs are refractory to developmental cues (Becker et al., 2006; Neganova et al., 2009; Pauklin and Vallier, 2013). High glycolytic flux in mESC or hESC drives pentose phosphate pathway activity which is important to maintain the cytosolic NADPH pool and a reducing redox environment *in vitro* (Filosa et al., 2003; Zhang et al., 2016a). Manipulating the cellular redox state by the addition of pro-oxidative metabolites encourages germ layer differentiation from PSCs (Yanes et al., 2010). Endogenous levels of ROS appear to be regulated by multiple developmental stimuli and likely has signal transduction functionality to coordinate early lineage specification (Sharifpanah et al., 2008). The observation that OCT4 DNA-binding ability is negatively affected in oxidizing conditions suggests that the redox environment can induce functionally-relevant biochemical changes to pluripotency TFs (Marsboom et al., 2016).

Both mESC and hESC possess structurally immature mitochondria compared to differentiated cells and express several isoenzymes limiting the availability of pyruvate to oxidative metabolic pathways in the mitochondria (Prigione and Adjaye, 2010; Varum et al., 2011, 2009; Zhang et al., 2011). Coupling of glycolysis to reactions within the mitochondria offers efficient ATP generation for energy-consuming processes in specialized cells. Inhibition of the ETC does not impair PSC self-renewal, suggesting that glycolysis alone is sufficient to meet energy demands (Varum et al., 2009). Mitochondria

also produces a variety of metabolites such as tricarboxylic acid (TCA) cycle intermediates, which may be used in anabolism or participate in non-metabolic processes (Nagaraj et al., 2017; Wellen et al., 2009) (Fig. 1-2A). Beyond conventionally recognized retrograde signals (e.g. ROS, ATP), fluctuations in nucleo-cytosolic levels of metabolites are sensed by chromatin modifying enzymes (Shi and Tu, 2015).

Histone acetylation and chromatin remodeling in mammalian cells is regulated by the conversion of TCA intermediate citrate to acetyl-coenzyme A (CoA), the universal acetyl group donor, by the ATP citrate lyase enzyme (Wellen et al., 2009). Acetyl-CoA level is also dependent on the upstream provision of pyruvate by glycolysis. High glycolytic flux maintains histone acetylation and pluripotent gene expression signatures in naïve mESC, primed mEpiSC and hESC (Moussaieff et al., 2015). Depletion of cytosolic acetyl-CoA with mechanistically distinct pathway inhibitors promotes PSC differentiation, whereas acetate supplementation supports the undifferentiated state (Moussaieff et al., 2015). Similarly, histone and DNA methyltransferase enzymes primarily use the methyl donor S-adenosylmethionine (SAM), an intermediate of the one-carbon metabolism pathway (Finkelstein, 1990; Locasale, 2013). Physiological variations in threonine or methionine, the amino acids upstream of SAM synthesis in mice or humans respectively, have been shown to affect histone methylation patterns in mammalian cells (Mentch et al., 2015; Ulrey et al., 2005). Supplementation of threonine/methionine is necessary for the self-renewal of both mESCs and hESCs, whereas depletion of these respective molecules selectively decreases the promoter-associated H3K4me3 modification and augments differentiation (Shiraki et al., 2014; Shyh-Chang et al., 2013). These observations shed light on an emerging metabolo-epigenetic axis and suggest that the variations in the metabolic state of PSCs contribute to differentiation into a variety of lineages and cell types (Fig 1-2B).

1.4.3 Metabolic Reprogramming in Pluripotent State Transitions

Redistribution and local dynamics of certain epigenetic modifications (e.g. DNA methylation, H3K27me3) are recognized to facilitate stable naïve-to-primed transitions without complete exit from the pluripotent state (Joshi et al., 2015; Tosolini et al., 2018). LIF-STAT3 signaling in mESC synergistically promotes mitochondrial respiration

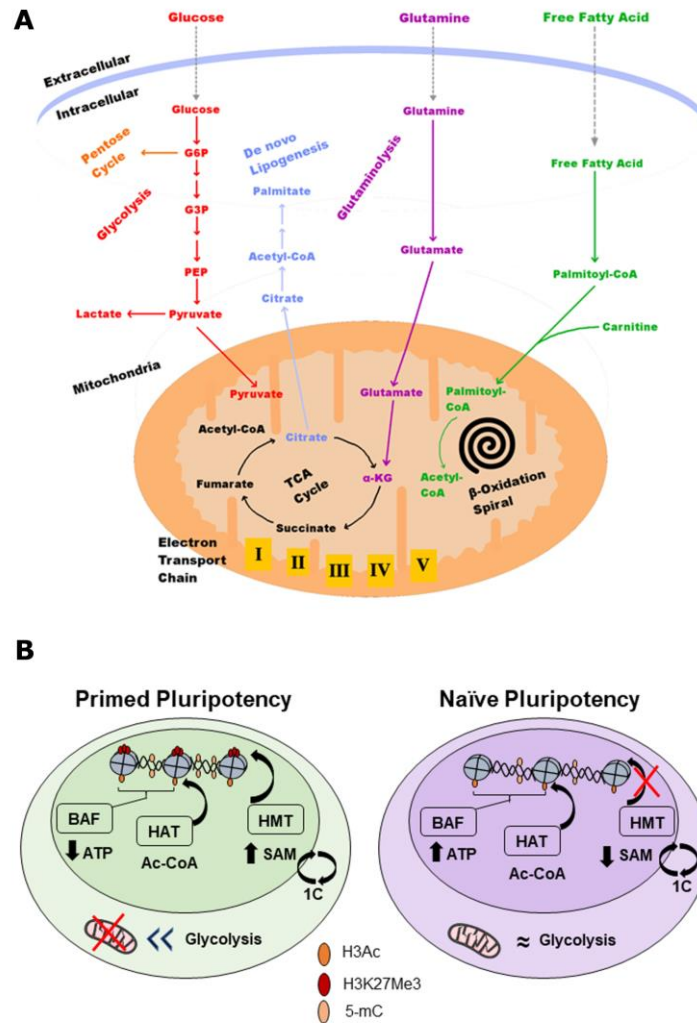


Figure 1-2. Metabolic regulation of self-renewal and pluripotency.

(A) Glucose uptake fuels the pentose cycle and provides substrates for intermediary metabolism. Glutamine metabolism replenishes the tricarboxylic acid (TCA) cycle at the level of alpha-ketoglutarate (α KG). Metabolic intermediates are diverted to anabolic pathways such as lipid synthesis. (B) The relative balance of glycolytic and mitochondrial metabolism and the one carbon cycle (1C) are implicated in regulating epigenetic cofactors acetyl-coenzyme A (Ac-CoA) and s-adenosylmethionine (SAM) to facilitate epigenetic events during pluripotent state transitions. Implicated epigenome modifiers are histone acetyltransferase (HAT), histone methyltransferase (HMT) and ATP-dependent chromatin remodellers (BAF).

alongside accessory naïve GRN members such as ESRRB (Carbognin et al., 2016; Sone et al., 2017). As a result, naïve mESC maintain greater steady-state ATP levels than primed mEpiSC or hESC through glucose and lipid oxidation (Sperber et al., 2015). Interestingly, mESC are metabolically flexible and tolerate pharmacological blockade of glycolysis or ETC activity without loss of pluripotency (Vlaski-Lafarge et al., 2019). The functional relevance of emphasizing ATP generation by oxidative phosphorylation is still unclear. However, it has recently been proposed that efficient ATP generation is necessary to maintain ATP-dependent chromatin remodeling, histone acetyltransferase activity and hyperdynamic chromatin characteristic of the naïve pluripotent state (Zhang et al., 2018).

Activation of SMAD2 signaling in F/A conditions used to maintain and derive primed mEpiSC or hESC suppresses the expression of cytochrome c oxidase subunits (Zhou et al., 2012). Hypoxia inducible factor 1 α (HIF1 α) is necessary for naïve-to-primed transition and reinforces the SMAD2-driven transcriptional program (Sperber et al., 2015). Although primed PSC display a relative suppression of ETC activity and glycolytic bias, they exhibit mature tubular-shaped mitochondria compared to naïve PSC (Zhou et al., 2012). Primed PSC contain mitochondria with an active, albeit truncated TCA cycle that siphons and replaces different intermediate metabolites found in the mitochondrial matrix (Tohyama et al., 2016). These studies posit that a switch from a balanced glycolysis/OXPHOS metabolic state to a preferentially glycolytic mode is reinforced by the extrinsic signals and GRNs associated with each pluripotent state. The knowledge that cell metabolism can influence both specific TF activity and higher levels of genome organization, has informed culture media preparations to enhance reprogramming from a relatively constrained somatic nuclear environment.

1.5 Induced Pluripotent Stem Cells

1.5.1 Overview of Induced Pluripotent Stem Cell Generation

Nuclear reprogramming of somatic cells directly to a pluripotent state with similar attributes to ESCs has been a widely adopted technique to study mechanisms in development, model a variety of diseases or establish a renewable cell source for

regenerative medicine (Robinton and Daley, 2012). The original induced pluripotent stem cell (iPSC) generation protocol involved the forced expression of exogenous TFs namely OCT4, KLF4, SOX2 and c-MYC (O-K-S-M) (Takahashi et al., 2007; Takahashi and Yamanaka, 2006). Ectopic expression of O-K-S-M can reprogram donor cells to either naïve or primed pluripotent state depending on the derivation environment (Han et al., 2011). Nucleic acid constructs encoding O-K-S-M are typically delivered to cells by integrative DNA, non-integrative DNA or RNA-based systems (Hussein and Nagy, 2012). Regardless of delivery method, O-K-S-M overabundance initiates widespread interactions between reprogramming factors with pioneer activity and somatic chromatin (Soufi et al., 2012). The selection of donor cell type affects the route to induced pluripotency, but most data are collected in dermal fibroblast to date (Nefzger et al., 2017). In a fraction of the reprogramming cell population, O-K-S factors outcompete the somatic GRN to allow *de novo* silencing of lineage-related CRMs antagonizing pluripotency induction (Hanna et al., 2008; Shao et al., 2016). Transfactors recruit endogenous transcriptional coactivators to previously silent CRMs to facilitate local epigenetic remodeling and reactivation of the endogenous pluripotency GRN (Ho et al., 2009; Singhal et al., 2010).

Somatic cell reprogramming is associated with a stepwise progression of few cells through intermediate cell states, which is reflected in measurable changes in cell phenotype over a period of days to weeks (Polo et al., 2012; Stadtfeld et al., 2008). The fluctuant latency involved in putative iPSCs emergence is partially attributed to experimental variables such as O-K-S-M stoichiometry, cell cycle stage or the existence of privileged cell subpopulations within a heterogeneous culture (Carey et al., 2011; Chen et al., 2012; Guo et al., 2014). However, even when the aforementioned variables are controlled, successful reprogramming remains inefficient (<1%) due to the ordered, probabilistic mechanisms associated with overcoming somatic epigenetic constraints and acquiring pluripotency (David and Polo, 2014). Complicating the study of reprogramming intermediates is that many observed changes to bulk reprogramming cells are not specific to those undergoing successful reprogramming (i.e. productive trajectory) compared to bulk intermediates that adopt alternative cell fates (Koche et al., 2011). Many O-K-S-M expressing cells undergo alternative trajectories (e.g. senescence,

apoptosis) because reprogramming factor binding is largely non-specific and capable of inadvertently activating antagonistic processes that restrict the frequency of pluripotency acquisition (Lujan et al., 2015; Polo et al., 2012).

1.5.2 Phase-Dependent Obstacles to Somatic Cell Reprogramming

Two major reconfiguration events of the transcriptome and proteome occur during reprogramming, which broadly segment reprogramming into early, mid and late phases (Hansson et al., 2012; Polo et al., 2012; Samavarchi-Tehrani et al., 2010). The early phase (i.e. initiation) occurs within the first few days of reprogramming and is characterized by a loss of somatic identity, acquisition of glycolytic metabolism and a hyperproliferative state (Hansson et al., 2012; Mikkelsen et al., 2008; Polo et al., 2012). Changes to cell phenotype in early reprogramming are dependent on persistent O-K-S-M expression and reprogramming factor engagement with pre-existing accessible regions on somatic chromatin (Chen et al., 2016; Smith et al., 2010; Stadtfeld et al., 2008). Immune and DNA damage responses to ectopic TF expression are barriers to early reprogramming by inducing cell cycle arrest and apoptosis (González et al., 2013; Kawamura et al., 2009; Li et al., 2009). Experimental manipulations that promote cell evasion of apoptosis, increase proliferation or high glycolytic flux reproducibly facilitate early reprogramming progression (Folmes et al., 2011; Hanna et al., 2009b). Repression of somatic identity genes by reprogramming factors elicits a variable response dependent on the donor cell population but manifests as mesenchymal-to-epithelial transition (MET) in reprogramming dermal fibroblasts (R. Li et al., 2010; Samavarchi-Tehrani et al., 2010).

The mid phase (i.e. maturation) occurs after the first week of reprogramming and involves gradual and probabilistic transactivation of a theoretical endogenous gene subset, called pluripotency-initiating or maturation factors (Chung et al., 2014). Expression of these early maturation markers is reversible, dependent on the exogenous transgenes and therefore does not guarantee complete reprogramming (Teshigawara et al., 2016). Maturation is characterized by a high rate of reprogramming failure, accounts for most of the latency in reprogramming and may be further subdivided at a single-cell resolution (Natarajan et al., 2017; Tanabe et al., 2013). Transcriptome analysis of

reprogramming intermediates showed the maturation phase exhibits the greatest transcriptional variability, likely due to a combination of clonal dominance of highly proliferative cells and activation of competing transcriptional responses (Kuno et al., 2018; Tanabe et al., 2013). Chromatin modifying complexes with negative rheostatic functions such as polycomb repressive complex 2 (PRC2) and nucleosome remodeling deacetylase (NuRD) are implicated in the maturation phase (Khazaie et al., 2016; Rais et al., 2013). PRC2 and NuRD are necessary for *de novo* silencing of lineage-related genes during maturation but may be inadvertently recruited to critical pluripotency regions and oppose reactivation (Dos Santos et al., 2014; Pereira et al., 2010; Rais et al., 2013). Integrated analysis of reprogramming factor binding, and epigenetic modifications show a gradual enrichment of TF binding at previously silent pluripotency enhancers during iPSC maturation. Subsequent epigenetic remodeling at targeted pluripotency loci is followed by promoter reactivation and pluripotency gene expression, marking the transition to the final phase of reprogramming (Chen et al., 2016).

The late phase (i.e. stabilization) occurs after two or three weeks and is characterized by transgene independent (through depletion or epigenetic silencing) self-renewal and stable expression of endogenous pluripotency GRN (David and Polo, 2014; Golipour et al., 2012). Concurrently, a small set of pluripotency-associated genes appear to elicit deterministic completion of reprogramming by a coordinated and hierarchical transcriptional program (Buganim et al., 2012). The factors at the top of the deterministic hierarchy are considered refractory to O-K-S-M binding because they are spanned by large constitutive heterochromatin domains (Soufi and Zaret, 2013). Provided that stabilized iPSC intermediates are in a permissive signaling environment for pluripotency GRN maintenance, they will adopt transcriptional and epigenetic signatures as well as differentiation capabilities equivalent to ESC (Hanna et al., 2008; Wang et al., 2018; Wernig et al., 2007) (Fig. 3-1).

1.5.3 Modifiers of DNA Methylation to Facilitate Reprogramming

Reprogramming progress is constrained by repressive chromatin modifications at pluripotency-specific CRMs, and a lack thereof at lineage-associated CRMs (Chen et al., 2013; Wang et al., 2011). Therefore, the extent of epigenetic remodeling that must occur

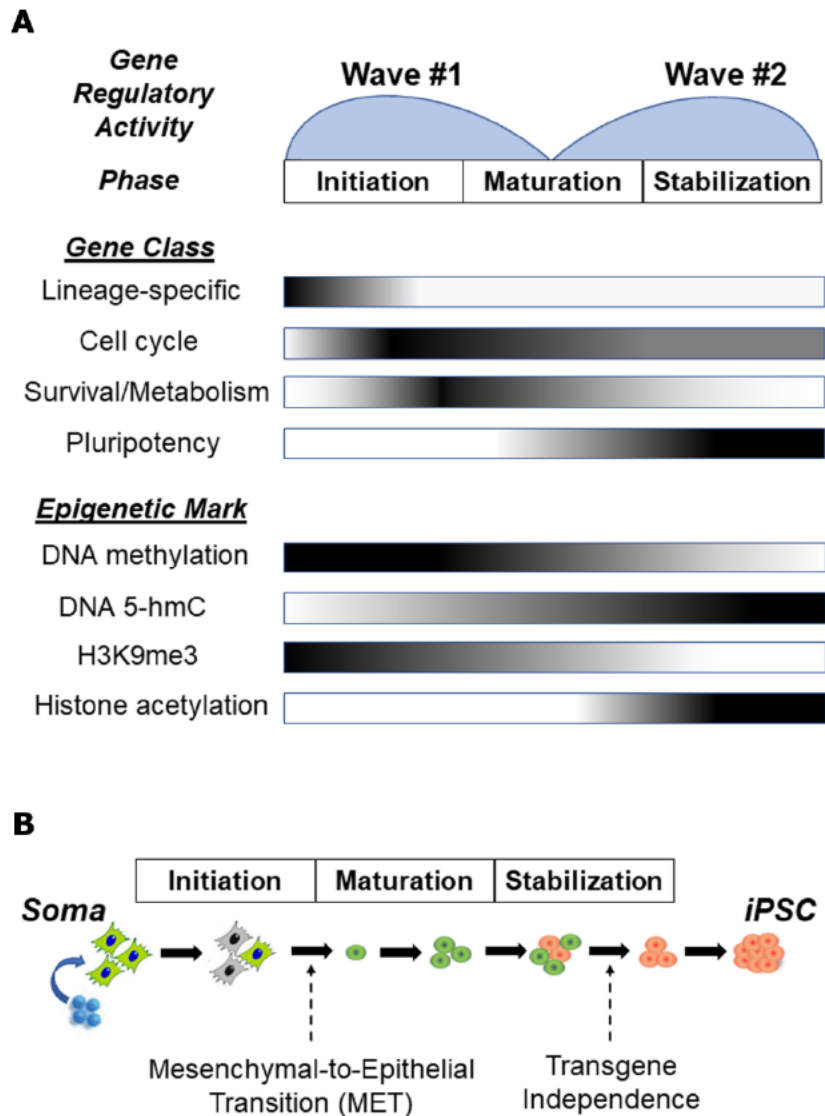


Figure 1-3. Cellular, transcriptional and epigenetic characteristics of each phase of cellular reprogramming.

(A) Two major waves in gene regulatory activity mediate the initiation-to-maturation and maturation-to-stabilization transitions in somatic cell reprogramming. Different classes of gene products and the epigenetic barriers associated with each gene subset differ within each phase of reprogramming. Stable reactivation of an endogenous pluripotency GRN is associated with global oxidation of methylated cytosine to 5-hydroxymethylation (5-hmC). (B) In fibroblast reprogramming, a mesenchymal-to-epithelial transition highlights the beginning of maturation for pre-iPSC. Stabilization bestows transgene-independent self-renewal to *bona fide* iPSC.

at both pluripotency and lineage-specific genes can play a role in the relative efficiency of reprogramming (i.e. colony yield) or reprogramming kinetics (i.e. time interval to iPSC establishment) (Chen et al., 2011). For instance, variations in reprogramming efficiency between somatic cell types shows a strong positive correspondence with the number shared hypermethylated CRMs for tissue-related genes that are shared with ESCs (Barrero et al., 2012). Furthermore, incomplete DNA methylation of lineage-related CRMs during reprogramming can propagate a transcriptional memory, which affects the differentiation potential of the resultant iPSC (Kim et al., 2011; Ohi et al., 2011). Understanding the network of proteins that evoke targeted remodeling of genome-wide methylation with desirable reprogramming outcomes are important to the development of experimental manipulations that improve reprogramming efficiency, kinetics and quality of iPSC lines.

Genes related to pluripotency or the germline tend to be regulated by CpG-rich promoter and/or enhancer sequences, which are stably silenced in differentiated cells by DNA methylation (Li et al., 2007; Smith and Meissner, 2013). Transfer of the methyl group from the co-substrate SAM to CpG dinucleotides are catalyzed by the DNMT family of enzymes (Robertson and Jones, 2000). The DNMT1 enzyme, known as the maintenance methyltransferase, has a distinguishable preference for hemi-methylated CpG palindromes established by semi-conservative DNA replication (Sharif et al., 2007; Yoder et al., 1997). Small molecule inhibitors of DNMTs, such as the cytidine analogue 5-azacytidine (5azaC), induce genome-wide demethylation largely by disrupting maintenance DNMT1 from re-establishing DNA methylation on the daughter strand leading to progressive dilution of methylated cytosine with each cell division (i.e. passive DNA demethylation) (Christman, 2002; Wu and Zhang, 2010). Non-specific DNMT inhibitors can modestly increase reprogramming efficiency, particularly when applied late in reprogramming such that lineage-related CRMs are appropriately silenced (Mikkelsen et al., 2008). 5azaC treatment has also been shown to promote the stabilization of partially reprogrammed cells (i.e. intermediates stuck in maturation phase) or erasing residual epigenomic memory (Bilic and Izpisua Belmonte, 2012; Mikkelsen et al., 2008). However, prolonged DNMT inhibition exposure is not desirable

due to elevated transposable element motility and loss of genomic imprints (Eden et al., 2003; Walsh et al., 1998).

The TET dioxygenase family of enzymes catalyze the iterative oxidation of 5-methylcytosine (5-mC) to 5-hydroxymethylcytosine (5-hmC) and less stable derivatives 5-formylcytosine and 5-carboxycytosine (Ito et al., 2011; Tahiliani et al., 2009). Subsequently, thymine DNA glycosylase (TDG) may excise of the oxidized derivatives and return the non-modified cytosine independent of cell replication (i.e. active demethylation) via the base-excision repair pathway. Therefore, TET catalyzes the rate-limiting step in the most widely-accepted and biochemically validated mechanism of DNA demethylation in mammals (Inoue et al., 2011; Zhang et al., 2012). TET family members (TET1-3) exhibit partial functional redundancy with regards to genomic affinities but differ in protein-protein interaction partners and substrate preferences (Putiri et al., 2014; Xu et al., 2011; Zhang et al., 2010). TET enzymes have catalysis-independent functions in protecting CpG-rich regions from *de novo* methylation, however these are poorly understood (Williams et al., 2011; Wu et al., 2011). Expression and activity of TET1 and TET2 are highly correlated with differential methylation, epigenetic remodeling and pluripotency factor expression (Di Stefano et al., 2014; Gao et al., 2013). The knockdown or deletion of either paralog negatively affects pluripotency TF binding and reprogramming success rates (Costa et al., 2013; Doege et al., 2012).

Somatic fibroblasts and early reprogramming intermediates (days 3-6) have similar genome-wide DNA methylation levels (Schwarz et al., 2018). After the initiation phase, roughly 25% of 5mC-enriched regions and 10% of 5hmC-enriched regions are redistributed compared to the initial somatic environment (Sardina et al., 2018). Gains in 5hmC negatively correlate with 5mC level dynamics, suggesting that active, rather than passive DNA demethylation occurs during early reprogramming (Sardina et al., 2018). The role of TET-mediated active DNA methylation is substantiated by the inability of TET triple knockout or thymidine DNA glycosylase knockout MEFs to reprogram (Hu et al., 2014). Hypomethylated CRMs are established in two distinct waves of demethylation during that correlate with the progression to maturation and stabilization phases (Schwarz et al., 2018). Reprogramming transactors with pioneer activity can bind nucleosomal

DNA and recruit TET enzymes for active demethylation (Koche et al., 2011; Sardina et al., 2018; Soufi et al., 2015). After focal DNA demethylation, TET enzymes can recruit histone modifying enzymes (e.g. SET1-COMPASS, EP300) to gene regulatory regions to create a more permissive environment for pluripotency TF occupancy (Chen et al., 2016; Deplus et al., 2013; Wei et al., 2015).

1.6 Pluripotent Stem Cells from Domesticated Large Mammals

1.6.1 Livestock and Companion Animals in Regenerative Medicine

The establishment of human ESCs and eventually iPSCs has spurred a new generation of cell-based therapies seeking to replace or repair human tissues (Tsuji et al., 2019).

Dozens of therapeutically desirable cell types can be differentiated from human ESC/iPSC, each with specific cell maturation and purification strategies (Rodrigues et al., 2015). Specialized cell types derived from human ESC/iPSC perform reasonably well in functional assays *in vitro* (Schwartzentruber et al., 2018). Xenotransplantation experiments have demonstrated proof-of-concept that therapeutic cells expanded and manipulated *ex vivo* are efficacious in a variety of rodent disease models (Nagamoto et al., 2016). First-in-human trials still pose considerable risk for volunteer participants because therapeutic cells derived from ESC/iPSC may elicit an immune reaction or harbor potentially tumorigenic cells (Heslop et al., 2015). Occasionally, mice carrying disease-relevant mutations do not recapitulate the pathogenic features observed in humans (Carvalho-Oliveira et al., 2007; Li and Li, 2012). PSCs derived from domesticated farm or companion animals would offer preclinical mammalian models of inherited or acquired disease to complement existing transgenic murine systems (Ezashi et al., 2015). Evidence from preclinical studies in mammals with greater longevity should affirm the safety, viability and functionality of *ex vivo* manufactured cell products for the anticipated duration of therapeutic efficacy *in vivo* (Trounson and DeWitt, 2016). Furthermore, the development of dosing and delivery procedures in domesticated mammals better emulates the organ size and immune system physiology encountered in human patients (Casal and Haskins, 2006; Harding et al., 2013).

In livestock species (e.g. porcine, bovine), embryological studies have yielded insights into evolutionarily conserved or divergent features of embryonic pluripotency (Liu et al., 2014). Data from both *in vivo* or *in vitro* matured preimplantation embryos provide a comparative reference to scrutinize the specificity of orthologous pluripotency-related gene products (Bernardo et al., 2018). Consequently, PSCs derived from farm species have performed more consistently in teratoma assays and have generated a larger repertoire of functional differentiated cell types (Ezashi et al., 2015). In contrast, challenges facing the procurement and culture of embryos from companion and work animals (e.g. canine, equine) have deferred similar embryo characterization studies causing uncertainty regarding molecular signature of embryonic pluripotency in these species (Paris et al., 2010; Wilcox et al., 2009).

Among companion animals, the domestic dog (*Canis lupus familiaris*) shares a variety of inherited diseases exhibiting complex genetic and environmental interactions including cancer, respiratory, endocrine, neurological and age-related disorders (Head et al., 2002; Schneider et al., 2008; Shearin and Ostrander, 2010). In this regard, exposure to common mutagenic agents throughout human-canine co-evolutionary history and high percentage (94%) of conserved ancestral DNA is proposed to favor analogous defects in gene products and similarity in disease presentation (Breen and Modiano, 2008). Given the high degree of genomic sequence similarity, the research community was initially optimistic that stem cells derived from dogs would be more representative of stem cell biology in humans than rodents (Tecirlioglu and Trounson, 2007). However, PSC from companion species do not maintain their pluripotency characteristics with prolonged culture (Roberts et al., 2016). The broad availability reprogramming vectors and well-conserved ability of O-K-S-M factors to promote ESC-like state indicates that derivation of iPSC from large mammals is attainable. Regardless of source, PSC derivation in domestic mammals will be hindered by an incomplete understanding of species-dependent variation in pluripotency GRN hierarchies and the unique signaling inputs needed to stabilize a self-sustaining pluripotent state.

1.6.2 Regulative Implications of Evolutionary Variation to Pluripotency

Our knowledge of the signaling pathways and GRNs involved in steady-state pluripotency, pluripotent state transitions, acquired pluripotency and early lineage restriction is derived from rodents and primates (Boyer et al., 2005; Loh et al., 2006). Core pluripotency TFs are well conserved in vertebrates with respect to protein structure and role in developmental plasticity (Dixon et al., 2010; Morrison, 2006). Comparisons of gene expression and core pluripotency TF binding sites among mammals has revealed extensive rewiring of the regulatory interactions (Kunarso et al., 2010; Xie et al., 2010). Regulatory variation between mammals appears to be driven by single base-pair mutations that create and destroy individual TF binding sites, or the insertion of entire CRMs by mobile elements that constitute approximately 40% of mammalian genomes (Waterston et al., 2002; Xie et al., 2010). Only about 5% of OCT4 and NANOG binding events occur in homologous sequences between mouse and human ESCs, with the remaining species-specific regulatory elements harbored in transposable sequences (Kunarso et al., 2010). Pluripotency TF binding sites within transposable sequence are co-opted as distal CRMs (Feschotte, 2008) and targeted by DNMT or TET to control transcriptional output by differential DNA methylation (de la Rica et al., 2016; Muramoto et al., 2010). The introduction of new TFs or alterations to hierarchical relationships between existing TFs have driven divergence in orthologous gene expression patterns and contribute to species-specific phenotypes in development and pluripotency (Barakat et al., 2018; Glinsky, 2015; Kojima et al., 2017).

CpG islands (CGIs) are regions of CpG dinucleotide overrepresentation spanning a region of 0.5-1 kilobase on average (Han and Zhao, 2009a). CGIs are hallmarks of regulatory elements that are silenced by DNA methylation and either situated adjacent to the 5' end (i.e. promoter) of a subset of mammalian genes or at distal CRMs (i.e. enhancer) (Antequera et al., 1990; Bell and Vertino, 2017; Mendizabal and Yi, 2016). Interestingly, CGI density is the highest in the canine assembly among completely sequenced placental mammals (2-3 fold greater than mouse or human), despite no marked difference in overall guanine and cytosine prevalence (Han et al., 2008). The

dramatic increase in CGI density in dogs is thought to be a consequence of a bias in meiotic recombination, rather than mobile elements/repeats or differential rates of cytosine deamination (Han and Zhao, 2009b).

Dogs and all ancestral canids sequenced to date carry a frameshift mutation in PR domain containing 9 (PRDM9) (Muñoz-Fuentes et al., 2011). PRDM9 is a H3K4 trimethylase that regulates the distribution of highly recombining regions during meiosis in mammals (Baudat et al., 2010). Mouse PRDM9 knockouts are infertile in both males and females (Oliver et al., 2009). It is proposed that meiotic recombination hotspots have remained the same in canines due to the loss of PRDM9, thereby increasing local CG content through GC-biased gene conversion (gBGC) (Axelsson et al., 2012). gBGC is a form of base substitution where AT/CG sites in heteroduplex DNA preferentially include the CG allele (Dreszer et al., 2007; Mugal et al., 2015). These features may have driven genome instability, chromosomal rearrangements, altered the local properties of distal CRMs and decreased the overall euchromatic portion of the dog genome throughout canid evolution (Auton et al., 2013; Berglund et al., 2015; Lindblad-Toh et al., 2005; Webber and Ponting, 2005).

1.6.3 Canine Embryogenesis and Embryonic Stem Cells

Embryogenesis in placental mammals is dependent on intricate intercellular communication mechanisms between the embryo proper and TE. Numerous differences exist between mammals during early embryogenesis, including divergent responses to trophic signals or pathway inhibitors (Kuijk et al., 2012; Roode et al., 2012), differences in the pattern of developmental gene expression (Petropoulos et al., 2015; Xie et al., 2010), and timing and mechanistic variation in epigenetic events (e.g. X-chromosome inactivation, zygotic genome activation) (Okamoto et al., 2011). The peculiarities of canine embryonic development begin at ovulation, where the oocyte is released at the germinal vesicle stage. Meiosis resumes after 48-72 hours in the oviduct becoming competent for fertilization soon afterward (Reynaud et al., 2005). Zygotic genome activation is believed to occur at the eight-cell stage (Hyttel et al., 2010). Canine morulae and blastocysts can be found in the uterine horn starting 8-10 days after ovulation (Bysted et al., 2001). Gastrulation and uterine attachment occur around 15-16 days after a period

of free-floating embryo migration (Renton et al., 1991; Reynaud et al., 2006). Canine blastocysts exhibit positive immunostaining for OCT4 within the ICM, but the existence of naïve or primed pluripotency signatures has not been investigated in the embryo (Wilcox et al., 2009).

Canines have a comparatively short gestation compared to similarly-sized mammals (Pretzer, 2008) and differ from rodents and primates by their placental architecture. Primate or rodent embryos invade the uterine epithelium, remaining completely encircled by TE and directly eroding maternal vasculature (i.e. discoid hemochorial placenta) (Carter and Enders, 2004). Whereas canine embryo implantation is distinguishable by the proliferation and invasion of only the middle third of trophoblast forming a single banded point of attachment which approximates but does not dissolve the maternal endothelial barrier (i.e. zonary endotheliochorial placenta) (Carter and Enders, 2004). The differences in both the duration preimplantation embryo migration and fetal membrane organization may have yet unknown consequences on the nutritional environment and metabolism of any remaining pluripotent cells within canine peri-implantation embryos.

Attempts to derive ESCs from canine blastocyst embryos have established heterogeneous cultures exhibiting some of the molecular hallmarks of PSCs from mice or humans. For instance, various cESC lines show reactivity to cell surface glycoprotein epitopes specific to mESC (Hatoya et al., 2006; Schneider et al., 2008) or hESC (Vaags et al., 2009; Wilcox et al., 2009). Loss of pluripotency marker expression and compact colony morphology upon LIF withdrawal, suggests that exogenous LIF is required for the self-renewal of cESC (Vaags et al., 2009; Wilcox et al., 2009). The co-supplementation of LIF and FGF (L/F) appears to promote longer-term maintenance of cESCs (Vaags et al., 2009; Wilcox et al., 2009). However, these canine ESCs (cESCs) cells tend to spontaneously differentiate and are tedious to maintain in prolonged culture despite intensive efforts (Gonçalves et al., 2014; Hayes et al., 2008). Only two groups attempted different derivation procedures from canine preimplantation embryos (Vaags et al., 2009; Wilcox et al., 2009), therefore the challenges facing long-term culture of cESCs could relate to the narrow subset of culture conditions investigated.

1.6.4 Canine Induced Pluripotent Stem Cells

A variety of donor cell populations from the mesodermal lineage have been used to produce canine iPSC (ciPSC) including embryonic and adult fibroblast, mesenchymal cells from testes or adipose tissue. Integrating viral vectors (i.e. retrovirus, lentivirus) have been the predominant strategy to deliver human O-K-S-M orthologs, with some exceptions (Menon et al., 2019). Co-transduction of O-K-S-M with LIN28 and NANOG also supports ciPSC generation (Whitworth et al., 2012), as does the delivery of murine O-K-S-M orthologs (Gonçalves et al., 2017; Koh et al., 2013). Similar to cESCs, ciPSCs form heterogeneous cultures and exhibit inherent variability in pluripotency-associated marker expression, which cannot be resolved with fluorescence activated cell sorting (FACS) (Koh et al., 2013; Luo et al., 2011). Incomplete silencing and maintained expression of exogenous O-K-S-M factors is a persistent issue and likely contributes to the heterogeneous features of ciPSC (Koh et al., 2013; Luo et al., 2011).

L/F conditions appear to be best suited for ciPSC derivation, but lines dependent solely on either LIF or FGF2 have been reported (Chow et al., 2017; Gonçalves et al., 2017; Koh et al., 2013; Luo et al., 2011; Nishimura et al., 2013; Whitworth et al., 2012). The requirement of L/F conditions is peculiar because these signaling pathways have opposing influences on murine pluripotency (Nichols and Smith, 2009). It is believed that LIF signaling is mediated by STAT3 similar to mESCs (Luo et al., 2011). Whereas, FGF signaling is believed to resemble the mechanisms characterized in hESCs, involving paracrine TGF β ligand secretion from MEF feeders and SMAD2 induction of NANOG in ciPSC (Luo and Cibelli, 2016).

The establishment of transgene-dependent, partially reprogrammed ciPSC clones appears to be reproducible in multiple labs and donor cell populations. However, there is diminishing value in continuing to characterize transgene-dependent cell populations stuck within an ill-defined alternative reprogramming trajectory. Recent efforts have navigated towards commercially available RNA-based sendai virus reprogramming vectors, which do not integrate into host genomes (Chow et al., 2017). Previous studies have stressed the importance of studying genomic stability and the epigenetic state of ciPSC, as aberrations in these attributes may confer selective growth advantages and lead

to genetic drift in cultures (Koh et al., 2013). Investigations focusing on the precise nature of signaling networks and GRNs associated with the induction and maintenance of pluripotency, should build the foundational knowledge required for reproducible derivation of stable cESC and ciPSC.

1.7 Rationale and Study Aims

PSC represent a tractable system to probe the molecular mechanisms underlying the acquisition, maintenance and loss of pluripotency (Morgani et al., 2017; Rossant and Tam, 2017). Once the regulative character and clonogenic attributes of PSC can be exploited with precision, PSC offer a scalable source of healthy cells for regenerative medicine or to assess the molecular basis and drug responsiveness of disease states (Ilic and Ogilvie, 2016; Robinton and Daley, 2012). Evolutionary rewiring of pluripotency associated regulatory elements and contrasting embryological features will likely drive the emergence of species-specific phenotypes and culture requirements among mammalian PSC (Greber et al., 2010; Xie et al., 2010). Although early mammalian embryos share morphological similarities, there is a lack of clarity regarding the defining molecular characteristics of pluripotent cells within canine peri-implantation blastocysts. The derivation and maintenance of PSC analogous to mESC or mEpiSC in canines would contribute to our understanding of the evolutionary variations in regulatory mechanisms impacting pluripotency induction or maintenance across mammals. A growing appreciation of the interdependent epigenetic, transcriptional and metabolic mechanisms in pluripotent state transitions and nuclear reprogramming, suggests that specific manipulations to the culture environment can influence the plasticity of mammalian cells.

For my thesis work, I used canine embryonic stem cells (cESCs) as a model system to evaluate discriminatory markers and functional assays to decipher the developmental approximate of cESCs in different microenvironments. Additionally, I used transcription factor-mediated de-differentiation of canine fibroblasts to study the early stages of nuclear reprogramming. cESC established from *in vivo*-derived blastocyst explants exhibit requirements of exogenous LIF and FGF2, clump passaging techniques and MEF co-culture, neural lineage default in minimal media that are indicative of the primed pluripotent state (Wilcox et al., 2011, 2009). Furthermore, partial antagonism of MEK1/2

and activation of WNT signaling in mouse or human PSC appears to have an essential role in stabilizing a naïve-like pluripotency stage (Weinberger et al., 2016).

Given these observations, I predict that direct manipulation of the culture conditions can facilitate nuclear reprogramming of canine cells. The overall hypothesis of my thesis is that *the culture environment can promote nuclear and metabolic reprogramming of canine cell lines towards a more primitive state of pluripotency*. First, I will determine if LIF-FGF2 cESCs exhibit molecular and functional characteristics of primed pluripotency typified by mEpiSCs, and if manipulation of FGF2-MEK and WNT signaling pathways can support a less mature state of pluripotency (Chapter Two). Secondly, I aim to determine the influence of cESC pluripotent state on mitochondrial structure and activity of relevant bioenergetic pathways to cell proliferation (Chapter Three). Lastly, I aim to determine if metabolites influencing DNA methylation can promote transcriptional responses associated with the initiation of canine reprogramming (Chapter Four). These studies further our understanding of conditions suitable for canine pluripotent stem cell expansion and establish a framework for cESCs as a model to assess the molecular events in canine developmental progression. Collectively, these investigations substantiate the role of extrinsic factors regulating pluripotent states and pose fundamental questions regarding evolutionarily conserved features of mammalian pluripotency.

1.8 References

- Acampora, D., Di Giovannantonio, L. G., & Simeone, A. (2012). Otx2 is an intrinsic determinant of the embryonic stem cell state and is required for transition to a stable epiblast stem cell condition. *Development*.
- Adachi, K., Kopp, W., Wu, G., Heising, S., Greber, B., Stehling, M., ... Schöler, H. R. (2018). Esrrb Unlocks Silenced Enhancers for Reprogramming to Naive Pluripotency. *Cell Stem Cell*.
- Ahmed, K., Dehghani, H., Rugg-Gunn, P., Fussner, E., Rossant, J., & Bazett-Jones, D. P. (2010). Global chromatin architecture reflects pluripotency and lineage commitment in the early mouse embryo. *PLoS ONE*.
- Ang, S. L., Wierda, A., Wong, D., Stevens, K. A., Cascio, S., Rossant, J., & Zaret, K. S. (1993). The formation and maintenance of the definitive endoderm lineage in the mouse: involvement of HNF3/forkhead proteins. *Development*.
- Antequera, F., Boyes, J., & Bird, A. (1990). High levels of De Novo methylation and altered chromatin structure at CpG islands in cell lines. *Cell*, 62(3), 503–514.
- Augui, S., Nora, E. P., & Heard, E. (2011). Regulation of X-chromosome inactivation by the X-inactivation centre. *Nature Reviews Genetics*.
- Auton, A., Rui Li, Y., Kidd, J., Oliveira, K., Nadel, J., Holloway, J. K., ... Boyko, A. R. (2013). Genetic Recombination Is Targeted towards Gene Promoter Regions in Dogs. *PLoS Genetics*.
- Axelsson, E., Webster, M. T., Ratnakumar, A., Ponting, C. P., & Lindblad-Toh, K. (2012). Death of PRDM9 coincides with stabilization of the recombination landscape in the dog genome. *Genome Research*, 22(1), 51–63.
- Azuara, V., Perry, P., Sauer, S., Spivakov, M., Jørgensen, H. F., John, R. M., ... Fisher, A. G. (2006). Chromatin signatures of pluripotent cell lines. *Nature Cell Biology*.
- Baharand, H., & Matthaiei, K. I. (2003). The ultrastructure of mouse embryonic stem cells. *Reproductive Biomedicine Online*, 7(3), 330–335.
- Bahat, A., Goldman, A., Zaltsman, Y., Khan, D. H., Halperin, C., Amzallag, E., ... Gross, A. (2018). MTCH2-mediated mitochondrial fusion drives exit from naïve pluripotency in embryonic stem cells. *Nature Communications*, 9(1), 51–59.
- Bao, S., Tang, F., Li, X., Hayashi, K., Gillich, A., Lao, K., & Surani, M. A. (2009). Epigenetic reversion of post-implantation epiblast to pluripotent embryonic stem cells. *Nature*, 461(7268), 1292–1295.

- Barakat, T. S., Halbritter, F., Zhang, M., Rendeiro, A. F., Perenthaler, E., Bock, C., & Chambers, I. (2018). Functional Dissection of the Enhancer Repertoire in Human Embryonic Stem Cells. *Cell Stem Cell*.
- Barker, N., Bartfeld, S., & Clevers, H. (2010). Tissue-resident adult stem cell populations of rapidly self-renewing organs. *Cell Stem Cell*.
- Barrero, M. J., Berdasco, M., Paramonov, I., Bilic, J., Vitaloni, M., Esteller, M., & Belmonte, J. C. I. (2012). DNA hypermethylation in somatic cells correlates with higher reprogramming efficiency. *Stem Cells*.
- Baudat, F., Buard, J., Grey, C., Fledel-Alon, A., Ober, C., Przeworski, M., ... De Massy, B. (2010). PRDM9 is a major determinant of meiotic recombination hotspots in humans and mice. *Science*, 327(5967), 836–40.
- Becker, J. S., Nicetto, D., & Zaret, K. S. (2016). H3K9me3-Dependent Heterochromatin: Barrier to Cell Fate Changes. *Trends in Genetics*.
- Becker, K. A., Ghule, P. N., Therrien, J. A., Lian, J. B., Stein, J. L., Van Wijnen, A. J., & Stein, G. S. (2006). Self-renewal of human embryonic stem cells is supported by a shortened G1 cell cycle phase. *Journal of Cellular Physiology*.
- Beddington, R. S., & Robertson, E. J. (1989). An assessment of the developmental potential of embryonic stem cells in the midgestation mouse embryo. *Development*.
- Beddington, R. S., & Robertson, E. J. (1999). Axis development and early asymmetry in mammals. *Cell*, 96(2), 195–209.
- Bedzhov, I., Graham, S. J. L., Leung, C. Y., & Zernicka-Goetz, M. (2014). Developmental plasticity, cell fate specification and morphogenesis in the early mouse embryo. *Philosophical Transactions of the Royal Society B: Biological Sciences*.
- Bedzhov, I., & Zernicka-Goetz, M. (2014). Self-organizing properties of mouse pluripotent cells initiate morphogenesis upon implantation. *Cell*.
- Bell, J. S. K., & Vertino, P. M. (2017). Orphan CpG islands define a novel class of highly active enhancers. *Epigenetics*, 12(6), 449–464.
- Berglund, J., Quilez, J., Arndt, P. F., & Webster, M. T. (2015). Germline methylation patterns determine the distribution of recombination events in the dog genome. *Genome Biology and Evolution*.
- Bernardo, A. S., Jouneau, A., Marks, H., Kensche, P., Kobolak, J., Freude, K., ... Dinnyes, A. (2018). Mammalian embryo comparison identifies novel pluripotency genes associated with the naïve or primed state. *Biology Open*.

- Bernstein, B. E., Mikkelsen, T. S., Xie, X., Kamal, M., Huebert, D. J., Cuff, J., ... Lander, E. S. (2006). A Bivalent Chromatin Structure Marks Key Developmental Genes in Embryonic Stem Cells. *Cell*.
- Bilic, J., & Izpisua Belmonte, J. C. (2012). Concise review: Induced pluripotent stem cells versus embryonic stem cells: Close enough or yet too far apart? *Stem Cells*.
- Boiani, M., & Schöler, H. R. (2005). Regulatory networks in embryo-derived pluripotent stem cells. *Nature Reviews Molecular Cell Biology*.
- Boroviak, T., Loos, R., Bertone, P., Smith, A., & Nichols, J. (2014). The ability of inner-cell-mass cells to self-renew as embryonic stem cells is acquired following epiblast specification. *Nature Cell Biology*.
- Boyer, L. A., Tong, I. L., Cole, M. F., Johnstone, S. E., Levine, S. S., Zucker, J. P., ... Young, R. A. (2005). Core transcriptional regulatory circuitry in human embryonic stem cells. *Cell*.
- Bradley, A., Evans, M., Kaufman, M. H., & Robertson, E. (1984). Formation of germ-line chimaeras from embryo-derived teratocarcinoma cell lines. *Nature*.
- Brand, K. A., & Hermfisse, U. (1997). Aerobic glycolysis by proliferating cells: a protective strategy against reactive oxygen species. *The FASEB Journal*.
- Breen, M., & Modiano, J. F. (2008). Evolutionarily conserved cytogenetic changes in hematological malignancies of dogs and humans - Man and his best friend share more than companionship. *Chromosome Research*.
- Brennan, J., Lu, C. C., Norris, D. P., Rodriguez, T. A., Beddington, R. S. P., & Robertson, E. J. (2001). Nodal signalling in the epiblast patterns the early mouse embryo. *Nature*.
- Brons, I. G. M., Smithers, L. E., Trotter, M. W. B., Rugg-Gunn, P., Sun, B., Chuva de Sousa Lopes, S. M., ... Vallier, L. (2007). Derivation of pluripotent epiblast stem cells from mammalian embryos. *Nature*, 448(7150), 191–195.
- Brook, F. A., & Gardner, R. L. (1997). The origin and efficient derivation of embryonic stem cells in the mouse. *Proceedings of the National Academy of Sciences*.
- Bruno, L., Hoffmann, R., McBlane, F., Brown, J., Gupta, R., Joshi, C., ... Enver, T. (2004). Molecular Signatures of Self-Renewal, Differentiation, and Lineage Choice in Multipotential Hemopoietic Progenitor Cells In Vitro. *Molecular and Cellular Biology*.
- Buecker, C., Srinivasan, R., Wu, Z., Calo, E., Acampora, D., Faial, T., ... Wysocka, J. (2014). Reorganization of enhancer patterns in transition from naive to primed pluripotency. *Cell Stem Cell*.

- Buehr, M., Smith, A., Camus, A., Merry, C., & Kumar, P. M. (2003). Genesis of embryonic stem cells. *Philosophical Transactions of the Royal Society B: Biological Sciences*.
- Buganim, Y., Faddah, D. A., Cheng, A. W., Itskovich, E., Markoulaki, S., Ganz, K., ... Jaenisch, R. (2012). Single-cell expression analyses during cellular reprogramming reveal an early stochastic and a late hierarchic phase. *Cell*.
- Bysted, B. V., Dieleman, S. J., Hyttel, P., & Greve, T. (2001). Embryonic developmental stages in relation to the LH peak in dogs. *J Reprod Fertil Suppl*.
- Carbognin, E., Betto, R. M., Soriano, M. E., Smith, A. G., & Martello, G. (2016). Stat3 promotes mitochondrial transcription and oxidative respiration during maintenance and induction of naive pluripotency. *The EMBO Journal*, 35(6), 618–34.
- Carey, B. W., Finley, L. W. S., Cross, J. R., Allis, C. D., & Thompson, C. B. (2014). Intracellular α -ketoglutarate maintains the pluripotency of embryonic stem cells. *Nature*, 518(7539), 413–416.
- Carey, B. W., Markoulaki, S., Hanna, J. H., Faddah, D. A., Buganim, Y., Kim, J., ... Jaenisch, R. (2011). Reprogramming factor stoichiometry influences the epigenetic state and biological properties of induced pluripotent stem cells. *Cell Stem Cell*.
- Carter, A. M., & Enders, A. C. (2004). Comparative aspects of trophoblast development and placentation. *Reproductive Biology and Endocrinology*.
- Carvalho-Oliveira, I., Scholte, B. J., & Penque, D. (2007). What have we learned from mouse models for cystic fibrosis? *Expert Review of Molecular Diagnostics*.
- Casal, M., & Haskins, M. (2006). Large animal models and gene therapy. *European Journal of Human Genetics*.
- Cedar, H., & Bergman, Y. (2009). Linking DNA methylation and histone modification: Patterns and paradigms. *Nature Reviews Genetics*.
- Chambers, I., Silva, J., Colby, D., Nichols, J., Nijmeijer, B., Robertson, M., ... Smith, A. (2007). Nanog safeguards pluripotency and mediates germline development. *Nature*.
- Chazaud, C., & Yamanaka, Y. (2016). Lineage specification in the mouse preimplantation embryo. *Development*.
- Cheloufi, S., Elling, U., Hopfgartner, B., Jung, Y. L., Murn, J., Ninova, M., ... Hochedlinger, K. (2015). The histone chaperone CAF-1 safeguards somatic cell identity. *Nature*.

- Chen, J., Chen, X., Li, M., Liu, X., Gao, Y., Kou, X., ... Gao, S. (2016). Hierarchical Oct4 Binding in Concert with Primed Epigenetic Rearrangements during Somatic Cell Reprogramming. *Cell Reports*.
- Chen, J., Guo, L., Zhang, L., Wu, H., Yang, J., Liu, H., ... Pei, D. (2013). Vitamin C modulates TET1 function during somatic cell reprogramming. *Nature Genetics*, 45(12), 1504–1509.
- Chen, J., Liu, J., Chen, Y., Yang, J., Chen, J., Liu, H., ... Pei, D. (2011). Rational optimization of reprogramming culture conditions for the generation of induced pluripotent stem cells with ultra-high efficiency and fast kinetics. *Cell Research*.
- Chen, M., Huang, J., Yang, X., Liu, B., Zhang, W., Huang, L., ... Ge, J. (2012). Serum starvation induced cell cycle synchronization facilitates human somatic cells reprogramming. *PLoS ONE*.
- Cho, Y. M., Kwon, S., Pak, Y. K., Seol, H. W., Choi, Y. M., Park, D. J., ... Lee, H. K. (2006). Dynamic changes in mitochondrial biogenesis and antioxidant enzymes during the spontaneous differentiation of human embryonic stem cells. *Biochemical and Biophysical Research Communications*, 348(4), 1472–1478.
- Chow, L., Johnson, V., Regan, D., Wheat, W., Webb, S., Koch, P., & Dow, S. (2017). Safety and immune regulatory properties of canine induced pluripotent stem cell-derived mesenchymal stem cells. *Stem Cell Research*, 25, 221–232.
- Choy, J. S., Wei, S., Lee, J. Y., Tan, S., Chu, S., & Lee, T. H. (2010). DNA methylation increases nucleosome compaction and rigidity. *Journal of the American Chemical Society*.
- Christman, J. K. (2002). 5-Azacytidine and 5-aza-2'-deoxycytidine as inhibitors of DNA methylation: Mechanistic studies and their implications for cancer therapy. *Oncogene*.
- Chung, K. M., Kolling, F. W., Gajdosik, M. D., Burger, S., Russell, A. C., & Nelson, C. E. (2014). Single cell analysis reveals the stochastic phase of reprogramming to pluripotency is an ordered probabilistic process. *PLoS ONE*.
- Chung, S., Dzeja, P. P., Faustino, R. S., Perez-Terzic, C., Behfar, A., & Terzic, A. (2007). Mitochondrial oxidative metabolism is required for the cardiac differentiation of stem cells. *Nature Clinical Practice Cardiovascular Medicine*, 4, S60–S67.
- Cirillo, L. A., Lin, F. R., Cuesta, I., Friedman, D., Jarnik, M., & Zaret, K. S. (2002). Opening of compacted chromatin by early developmental transcription factors HNF3 (FoxA) and GATA-4. *Molecular Cell*.

- Ciruna, B., & Rossant, J. (2001). FGF Signaling Regulates Mesoderm Cell Fate Specification and Morphogenetic Movement at the Primitive Streak. *Developmental Cell*.
- Cockburn, K., & Rossant, J. (2010). Making the blastocyst: Lessons from the mouse. *Journal of Clinical Investigation*.
- Cole, M. F., Johnstone, S. E., Newman, J. J., Kagey, M. H., & Young, R. A. (2008). Tcf3 is an integral component of the core regulatory circuitry of embryonic stem cells. *Genes and Development*.
- Copp, A. J. (1978). Interaction between inner cell mass and trophectoderm of the mouse blastocyst. I. A study of cellular proliferation. *Journal of Embryology and Experimental Morphology*.
- Costa, Y., Ding, J., Theunissen, T. W., Faiola, F., Hore, T. A., Shliaha, P. V., ... Wang, J. (2013). NANOG-dependent function of TET1 and TET2 in establishment of pluripotency. *Nature*, 495(7441), 370–374.
- Creyghton, M. P., Cheng, A. W., Welstead, G. G., Kooistra, T., Carey, B. W., Steine, E. J., ... Jaenisch, R. (2010). Histone H3K27ac separates active from poised enhancers and predicts developmental state. *Proceedings of the National Academy of Sciences*.
- Davey, R. E., & Zandstra, P. W. (2006). Spatial Organization of Embryonic Stem Cell Responsiveness to Autocrine Gp130 Ligands Reveals an Autoregulatory Stem Cell Niche. *Stem Cells*.
- David, L., & Polo, J. M. (2014). Phases of reprogramming. *Stem Cell Research*.
- de la Rica, L., Deniz, Ö., Cheng, K. C. L., Todd, C. D., Cruz, C., Houseley, J., & Branco, M. R. (2016). TET-dependent regulation of retrotransposable elements in mouse embryonic stem cells. *Genome Biology*.
- De Los Angeles, A., Ferrari, F., Xi, R., Fujiwara, Y., Benvenisty, N., Deng, H., ... Daley, G. Q. (2015). Hallmarks of pluripotency. *Nature*.
- De Wit, E., Bouwman, B. A. M., Zhu, Y., Klous, P., Splinter, E., Verstegen, M. J. A. M., ... De Laat, W. (2013). The pluripotent genome in three dimensions is shaped around pluripotency factors. *Nature*.
- DeBerardinis, R. J., Lum, J. J., Hatzivassiliou, G., & Thompson, C. B. The Biology of Cancer: Metabolic Reprogramming Fuels Cell Growth and Proliferation, *Cell Metabolism* 11–20 (2008).
- Dellino, G. I., Schwartz, Y. B., Farkas, G., McCabe, D., Elgin, S. C. R., & Pirrotta, V. (2004). Polycomb silencing blocks transcription initiation. *Molecular Cell*.

- Deplus, R., Delatte, B., Schwinn, M. K., Defrance, M., Méndez, J., Murphy, N., ... Fuks, F. (2013). TET2 and TET3 regulate GlcNAcylation and H3K4 methylation through OGT and SET1/COMPASS. *EMBO Journal*.
- Desbordes, S. C., & Studer, L. (2013). Adapting human pluripotent stem cells to high-throughput and high-content screening. *Nature Protocols*.
- DeVeale, B., Brokhman, I., Mohseni, P., Babak, T., Yoon, C., Lin, A., ... van der Kooy, D. (2013). Oct4 Is Required ~E7.5 for Proliferation in the Primitive Streak. *PLoS Genetics*.
- Di Stefano, B., Sardina, J. L., Van Oevelen, C., Collombet, S., Kallin, E. M., Vicent, G. P., ... Graf, T. (2014). C/EBP α poises B cells for rapid reprogramming into induced pluripotent stem cells. *Nature*.
- Dixon, J. E., Allegrucci, C., Bian, Y., Voss, S. R., Alberio, R., Sottile, V., ... Johnson, A. D. (2010). Axolotl Nanog activity in mouse embryonic stem cells demonstrates that ground state pluripotency is conserved from urodele amphibians to mammals. *Development*.
- Doege, C. A., Inoue, K., Yamashita, T., Rhee, D. B., Travis, S., Fujita, R., ... Abeliovich, A. (2012). Early-stage epigenetic modification during somatic cell reprogramming by Parp1 and Tet2. *Nature*.
- Doetschman, T. C., Eistetter, H., Katz, M., Schmidt, W., & Kemler, R. (1985). The in vitro development of blastocyst-derived embryonic stem cell lines: formation of visceral yolk sac, blood islands and myocardium. *Journal of Embryology and Experimental Morphology*.
- Dos Santos, R. L., Tosti, L., Radzsheuskaya, A., Caballero, I. M., Kaji, K., Hendrich, B., & Silva, J. C. R. (2014). MBD3/NuRD facilitates induction of pluripotency in a context-dependent manner. *Cell Stem Cell*.
- Dreszer, T. R., Wall, G. D., Haussler, D., & Pollard, K. S. (2007). Biased clustered substitutions in the human genome: The footprints of male-driven biased gene conversion. *Genome Research*.
- Eden, A., Gaudet, F., Waghmare, A., & Jaenisch, R. (2003). Chromosomal instability and tumors promoted by DNA hypomethylation. *Science*.
- Efroni, S., Duttagupta, R., Cheng, J., Dehghani, H., Hoepfner, D. J., Dash, C., ... Meshorer, E. (2008). Global Transcription in Pluripotent Embryonic Stem Cells. *Cell Stem Cell*.
- Evans, M. J., & Kaufman, M. H. (1981). Establishment in culture of pluripotential cells from mouse embryos. *Nature*.

- Evsikov, A. V., Graber, J. H., Brockman, J. M., Hampl, A., Holbrook, A. E., Singh, P., ... Knowles, B. B. (2006). Cracking the egg: Molecular dynamics and evolutionary aspects of the transition from the fully grown oocyte to embryo. *Genes and Development*.
- Ezashi, T., Yuan, Y., & Roberts, R. M. (2015). Pluripotent Stem Cells from Domesticated Mammals. *Annual Review of Animal Biosciences*.
- Factor, D. C., Corradin, O., Zentner, G. E., Saiakhova, A., Song, L., Chenoweth, J. G., ... Tesar, P. J. (2014). Epigenomic comparison reveals activation of “seed” enhancers during transition from naive to primed pluripotency. *Cell Stem Cell*.
- Feschotte, C. (2008). Transposable elements and the evolution of regulatory networks. *Nature Reviews Genetics*.
- Festuccia, N., Osorno, R., Halbritter, F., Karwacki-Neisius, V., Navarro, P., Colby, D., ... Chambers, I. (2012). Esrrb is a direct Nanog target gene that can substitute for Nanog function in pluripotent cells. *Cell Stem Cell*.
- Filosa, S., Fico, A., Paglialunga, F., Balestrieri, M., Crooke, A., Verde, P., ... Martini, G. (2003). Failure to increase glucose consumption through the pentose-phosphate pathway results in the death of glucose-6-phosphate dehydrogenase gene-deleted mouse embryonic stem cells subjected to oxidative stress. *Biochemical Journal*.
- Finkelstein, J. D. (1990). Methionine metabolism in mammals. *The Journal of Nutritional Biochemistry*.
- Folmes, C. D. L., Nelson, T. J., Martinez-Fernandez, A., Arrell, D. K., Lindor, J. Z., Dzeja, P. P., ... Terzic, A. (2011). Somatic Oxidative Bioenergetics Transitions into Pluripotency-Dependent Glycolysis to Facilitate Nuclear Reprogramming. *Cell Metabolism* (Vol. 14).
- Fussner, E., Djuric, U., Strauss, M., Hotta, A., Perez-Iratxeta, C., Lanner, F., ... Bazett-Jones, D. P. (2011). Constitutive heterochromatin reorganization during somatic cell reprogramming. *EMBO Journal*.
- Gao, Y., Chen, J., Li, K., Wu, T., Huang, B., Liu, W., ... Gao, S. (2013). Replacement of Oct4 by Tet1 during iPSC induction reveals an important role of DNA methylation and hydroxymethylation in reprogramming. *Cell Stem Cell*, 12(4), 453–469.
- Gardner, D. K. (1998). Changes in requirements and utilization of nutrients during mammalian preimplantation embryo development and their significance in embryo culture. In *Theriogenology*.
- Gardner, R. L., Lyon, M. F., Evans, E. P., & Burtenshaw, M. D. (1985). Clonal analysis of X-chromosome inactivation and the origin of the germ line in the mouse embryo. *J Embryol Exp Morphol*.

- Gardner, R. L., & Rossant, J. (1979). Investigation of the fate of 4-5 day post-coitum mouse inner cell mass cells by blastocyst injection. *Journal of Embryology and Experimental Morphology*, 52, 141–52.
- Ghimire, S., Van Der Jeught, M., Neupane, J., Roost, M. S., Anckaert, J., Popovic, M., ... Heindryckx, B. (2018). Comparative analysis of naive, primed and ground state pluripotency in mouse embryonic stem cells originating from the same genetic background. *Scientific Reports*.
- Gilchrist, D. A., Dos Santos, G., Fargo, D. C., Xie, B., Gao, Y., Li, L., & Adelman, K. (2010). Pausing of RNA polymerase II disrupts DNA-specified nucleosome organization to enable precise gene regulation.
- Ginsburg, M., Snow, M. H., & McLaren, A. (1990). Primordial germ cells in the mouse embryo during gastrulation. *Development*.
- Glinisky, G. V. (2015). Transposable elements and DNA methylation create in embryonic stem cells human-specific regulatory sequences associated with distal enhancers and noncoding RNAs. *Genome Biology and Evolution*.
<http://doi.org/10.1093/gbe/evv081>
- Golipour, A., David, L., Liu, Y., Jayakumaran, G., Hirsch, C. L., Trcka, D., & Wrana, J. L. (2012). A late transition in somatic cell reprogramming requires regulators distinct from the pluripotency network. *Cell Stem Cell*.
- Gonçalves, N., Ambrósio, C., & Piedrahita, J. (2014). Stem Cells and Regenerative Medicine in Domestic and Companion Animals: A Multispecies Perspective. *Reproduction in Domestic Animals*.
- Gonçalves, N. J. N., Bressan, F. F., Roballo, K. C. S., Meirelles, F. V., Xavier, P. L. P., Fukumasu, H., ... Ambrósio, C. E. (2017). Generation of LIF-independent induced pluripotent stem cells from canine fetal fibroblasts. *Theriogenology*.
- González, F., Georgieva, D., Vanoli, F., Shi, Z. D., Stadtfeld, M., Ludwig, T., ... Huangfu, D. (2013). Homologous Recombination DNA Repair Genes Play a Critical Role in Reprogramming to a Pluripotent State. *Cell Reports*.
- Gossler, A., Joyner, A. L., Rossant, J., & Skarnes, W. C. (1989). Mouse embryonic stem cells and reporter constructs to detect developmentally regulated genes. *Science*.
- Greber, B., Wu, G., Bernemann, C., Joo, J. Y., Han, D. W., Ko, K., ... Schöler, H. R. (2010). Conserved and Divergent Roles of FGF Signaling in Mouse Epiblast Stem Cells and Human Embryonic Stem Cells. *Cell Stem Cell*.
- Gruenbaum, Y., Cedar, H., & Razin, A. (1982). Substrate and sequence specificity of a eukaryotic DNA methylase. *Nature*.

- Guo, G. G., Yang, J., Nichols, J., Hall, J. S., Eyres, I., Mansfield, W., ... Mansfield, W. (2009). Klf4 reverts developmentally programmed restriction of ground state pluripotency. *Development*, 136(7), 1063–9.
- Guo, G., Huss, M., Tong, G. Q., Wang, C., Li Sun, L., Clarke, N. D., & Robson, P. (2010). Resolution of Cell Fate Decisions Revealed by Single-Cell Gene Expression Analysis from Zygote to Blastocyst. *Developmental Cell*.
- Guo, S., Zi, X., Schulz, V. P., Cheng, J., Zhong, M., Koochaki, S. H. J., ... Lu, J. (2014). Nonstochastic reprogramming from a privileged somatic cell state. *Cell*.
- Habibi, E., Brinkman, A. B., Arand, J., Kroeze, L. I., Kerstens, H. H. D., Matarese, F., ... Stunnenberg, H. G. (2013). Whole-genome bisulfite sequencing of two distinct interconvertible DNA methylomes of mouse embryonic stem cells. *Cell Stem Cell*.
- Hackett, J. A. A., Azim Surani, M., & Surani, M. A. Regulatory principles of pluripotency: From the ground state up, 15 *Cell Stem Cell* 416–430 (2014).
- Hackett, J. A., Dietmann, S., Murakami, K., Down, T. A., Leitch, H. G., & Surani, M. A. (2013). Synergistic mechanisms of DNA demethylation during transition to ground-state pluripotency. *Stem Cell Reports*, 1(6), 518–531.
- Hall, J., Guo, G., Wray, J., Eyres, I., Nichols, J., Grotewold, L., ... Smith, A. (2009). Oct4 and LIF/Stat3 Additively Induce Krüppel Factors to Sustain Embryonic Stem Cell Self-Renewal. *Cell Stem Cell*.
- Han, D. W., Greber, B., Wu, G., Tapia, N., Araúzo-Bravo, M. J., Ko, K., ... Schöler, H. R. (2011). Direct reprogramming of fibroblasts into epiblast stem cells. *Nature Cell Biology*.
- Han, D. W., Tapia, N., Joo, J. Y., Greber, B., Araúzo-Bravo, M. J., Bernemann, C., ... Schöler, H. R. (2010). Epiblast stem cell subpopulations represent mouse embryos of distinct pregastrulation stages. *Cell*.
- Han, L., Su, B., Li, W. H., & Zhao, Z. (2008). CpG island density and its correlations with genomic features in mammalian genomes. *Genome Biology*, 9(5).
- Han, L., & Zhao, Z. (2009a). Contrast features of CpG islands in the promoter and other regions in the dog genome. *Genomics*, 94(2), 117–124.
- Han, L., & Zhao, Z. (2009b). CpG islands or CpG clusters: How to identify functional GC-rich regions in a genome? *BMC Bioinformatics*, 10.
- Handoko, L., Xu, H., Li, G., Ngan, C. Y., Chew, E., Schnapp, M., ... Wei, C. L. (2011). CTCF-mediated functional chromatin interactome in pluripotent cells. In *Nature Genetics*.

- Hanna, J., Cheng, A. W., Saha, K., Kim, J., Lengner, C. J., Soldner, F., ... Jaenisch, R. (2010). Human embryonic stem cells with biological and epigenetic characteristics similar to those of mouse ESCs. *Proceedings of the National Academy of Sciences*.
- Hanna, J., Markoulaki, S., Mitalipova, M., Cheng, A. W., Cassady, J. P., Staerk, J., ... Jaenisch, R. (2009). Metastable Pluripotent States in NOD-Mouse-Derived ESCs. *Cell Stem Cell*.
- Hanna, J., Markoulaki, S., Schorderet, P., Carey, B. W., Beard, C., Wernig, M., ... Jaenisch, R. (2008). Direct Reprogramming of Terminally Differentiated Mature B Lymphocytes to Pluripotency. *Cell*.
- Hanna, J., Saha, K., Pando, B., Van Zon, J., Lengner, C. J., Creighton, M. P., ... Jaenisch, R. (2009). Direct cell reprogramming is a stochastic process amenable to acceleration. *Nature*.
- Hanna, J., Wernig, M., Markoulaki, S., Sun, C. W., Meissner, A., Cassady, J. P., ... Jaenisch, R. (2007). Treatment of sickle cell anemia mouse model with iPS cells generated from autologous skin. *Science*.
- Hansson, J., Rafiee, M. R., Reiland, S., Polo, J. M., Gehring, J., Okawa, S., ... Krijgsveld, J. (2012). Highly Coordinated Proteome Dynamics during Reprogramming of Somatic Cells to Pluripotency. *Cell Reports*.
- Harding, J., Roberts, R. M., & Mirochnitchenko, O. (2013). Large animal models for stem cell therapy. *Stem Cell Research and Therapy*.
- Hartung, O., Huo, H., Daley, G. Q., & Schlaeger, T. M. (2010). Clump passaging and expansion of human embryonic and induced pluripotent stem cells on mouse embryonic fibroblast feeder cells. *Current Protocols in Stem Cell Biology*.
- Hatoya, S., Torii, R., Kondo, Y., Okuno, T., Kobayashi, K., Wijewardana, V., ... Inaba, T. (2006). Isolation and characterization of embryonic stem-like cells from canine blastocysts. *Molecular Reproduction and Development*, 73(3), 298–305.
- Hawkins, R. D., Hon, G. C., Yang, C., Antosiewicz-Bourget, J. E., Lee, L. K., Ngo, Q. M., ... Ren, B. (2011). Dynamic chromatin states in human ES cells reveal potential regulatory sequences and genes involved in pluripotency. *Cell Research*.
- Hayashi, K., Lopes, S. M. C. de S., Tang, F., & Surani, M. A. (2008). Dynamic Equilibrium and Heterogeneity of Mouse Pluripotent Stem Cells with Distinct Functional and Epigenetic States. *Cell Stem Cell*.
- Hayashi, K., Ohta, H., Kurimoto, K., Aramaki, S., & Saitou, M. (2011). Reconstitution of the mouse germ cell specification pathway in culture by pluripotent stem cells. *Cell*.

- Hayes, B., Fagerlie, S. R., Ramakrishnan, A., Baran, S., Harkey, M., Graf, L., ... Torok-Storb, B. (2008). Derivation, Characterization, and In Vitro Differentiation of Canine Embryonic Stem Cells. *Stem Cells*, 26(2), 465–473.
- Head, E., Liu, J., Hagen, T. M., Muggenburg, B. A., Milgram, N. W., Ames, B. N., & Cotman, C. W. (2002). Oxidative damage increases with age in a canine model of human brain aging. *Journal of Neurochemistry*.
- Henikoff, S. (2008). Nucleosome destabilization in the epigenetic regulation of gene expression. *Nature Reviews Genetics*.
- Heslop, J. A., Hammond, T. G., Santeramo, I., Tort Piella, A., Hopp, I., Zhou, J., ... Park, B. K. (2015). Concise Review: Workshop Review: Understanding and Assessing the Risks of Stem Cell-Based Therapies. *STEM CELLS Translational Medicine*.
- Ho, L., Jothi, R., Ronan, J. L., Crabtree, G. R., Zhao, K., & Cui, K. (2009). An embryonic stem cell chromatin remodeling complex, esBAF, is an essential component of the core pluripotency transcriptional network. *Proceedings of the National Academy of Sciences*.
- Hough, S. R., Laslett, A. L., Grimmond, S. B., Kolle, G., & Pera, M. F. (2009). A continuum of cell states spans pluripotency and lineage commitment in human embryonic stem cells. *PLoS ONE*.
- Houghton, F. D., Thompson, J. G., Kennedy, C. J., & Leese, H. J. (1996). Oxygen consumption and energy metabolism of the early mouse embryo. *Molecular Reproduction and Development*.
- Hu, X., Zhang, L., Mao, S. Q., Li, Z., Chen, J., Zhang, R. R., ... Xu, G. L. (2014). Tet and TDG mediate DNA demethylation essential for mesenchymal-to-epithelial transition in somatic cell reprogramming. *Cell Stem Cell*, 14(4), 512–522.
- Huang, J., Wang, F., Okuka, M., Liu, N., Ji, G., Ye, X., ... Liu, L. (2011). Association of telomere length with authentic pluripotency of ES/iPS cells. *Cell Research*.
- Huang, Y., Osorno, R., Tsakiridis, A., & Wilson, V. (2012). In Vivo Differentiation Potential of Epiblast Stem Cells Revealed by Chimeric Embryo Formation. *Cell Reports*.
- Hunt, G. C., Singh, P., & Schwarzbauer, J. E. (2012). Endogenous production of fibronectin is required for self-renewal of cultured mouse embryonic stem cells. *Experimental Cell Research*.
- Hussein, S. M. I., & Nagy, A. A. (2012). Progress made in the reprogramming field: New factors, new strategies and a new outlook. *Current Opinion in Genetics and Development*.

- Hyttel, P., Sinowatz, F., & Vejlsted, M. (2010). *Essentials of domestic animals embryology*. Saunders Elsevier.
- Ilic, D., & Ogilvie, C. (2016). Human Embryonic Stem Cells - What Have We Done? What Are We Doing? Where Are We Going? *Stem Cells*, 35(1), 17–25.
- Inoue, A., Shen, L., Dai, Q., He, C., & Zhang, Y. (2011). Generation and replication-dependent dilution of 5fC and 5caC during mouse preimplantation development. *Cell Research*.
- Ito, S., Shen, L., Dai, Q., Wu, S. C., Collins, L. B., Swenberg, J. A., ... Zhang, Y. (2011). Tet proteins can convert 5-methylcytosine to 5-formylcytosine and 5-carboxylcytosine. *Science*, 333(6047), 1300–1303.
- Iwafuchi-Doi, M., Matsuo, I., Tesar, P. J., Murakami, K., Niwa, H., Aruga, J., ... Kondoh, H. (2012). Transcriptional regulatory networks in epiblast cells and during anterior neural plate development as modeled in epiblast stem cells. *Development*.
- Jaenisch, R., & Young, R. (2008). *Stem Cells, the Molecular Circuitry of Pluripotency and Nuclear Reprogramming*. Cell.
- Jenuwein, T., & Allis, C. D. (2001). Translating the histone code. *Science*.
- Jermann, P., Hoerner, L., Burger, L., & Schubeler, D. (2014). Short sequences can efficiently recruit histone H3 lysine 27 trimethylation in the absence of enhancer activity and DNA methylation. *Proceedings of the National Academy of Sciences*.
- John, S., Sabo, P. J., Thurman, R. E., Sung, M. H., Biddie, S. C., Johnson, T. A., ... Stamatoyannopoulos, J. A. (2011). Chromatin accessibility pre-determines glucocorticoid receptor binding patterns. *Nature Genetics*.
- Joshi, O., Wang, S. Y., Kuznetsova, T., Atlasi, Y., Peng, T., Fabre, P. J., ... Stunnenberg, H. G. (2015). Dynamic Reorganization of Extremely Long-Range Promoter-Promoter Interactions between Two States of Pluripotency. *Cell Stem Cell*.
- Kalkan, T., & Smith, A. (2014). Mapping the route from naive pluripotency to lineage specification. *Philosophical Transactions of the Royal Society B: Biological Sciences*.
- Kang, M., Garg, V., & Hadjantonakis, A. K. (2017). Lineage Establishment and Progression within the Inner Cell Mass of the Mouse Blastocyst Requires FGFR1 and FGFR2. *Developmental Cell*.
- Kaplan, N., Moore, I. K., Fondufe-Mittendorf, Y., Gossett, A. J., Tillo, D., Field, Y., ... Segal, E. (2009). The DNA-encoded nucleosome organization of a eukaryotic genome. *Nature*.

- Kawamura, T., Suzuki, J., Wang, Y. V., Menendez, S., Morera, L. B., Raya, A., ... Belmonte, J. C. I. (2009). Linking the p53 tumour suppressor pathway to somatic cell reprogramming. *Nature*.
- Keshet, I., Lieman-Hurwitz, J., & Cedar, H. (1986). DNA methylation affects the formation of active chromatin. *Cell*.
- Khazaie, N., Massumi, M., Wee, P., Salimi, M., Mohammadnia, A., & Yaqubi, M. (2016). Involvement of Polycomb Repressive Complex 2 in Maturation of Induced Pluripotent Stem Cells during Reprogramming of Mouse and Human Fibroblasts. *PLoS ONE*.
- Kim, K., Zhao, R., Doi, A., Ng, K., Unternaehrer, J., Cahan, P., ... Daley, G. Q. (2011). Donor cell type can influence the epigenome and differentiation potential of human induced pluripotent stem cells. *Nature Biotechnology*.
- Kim, S. H., Kim, M. O., Cho, Y. Y., Yao, K., Kim, D. J., Jeong, C. H., ... Dong, Z. (2014). ERK1 phosphorylates Nanog to regulate protein stability and stem cell self-renewal. *Stem Cell Research*.
- Klemm, S. L., Shipony, Z., & Greenleaf, W. J. (2019). Chromatin accessibility and the regulatory epigenome. *Nature Reviews Genetics*.
- Koche, R. P., Smith, Z. D., Adli, M., Gu, H., Ku, M., Gnirke, A., ... Meissner, A. (2011). Reprogramming factor expression initiates widespread targeted chromatin remodeling. *Cell Stem Cell*.
- Koh, S., Thomas, R., Tsai, S., Bischoff, S., Lim, J.-H., Breen, M., ... Piedrahita, J. A. (2013). Growth Requirements and Chromosomal Instability of Induced Pluripotent Stem Cells Generated from Adult Canine Fibroblasts. *Stem Cells and Development*.
- Kojima, Y., Kaufman-Francis, K., Studdert, J. B., Steiner, K. A., Power, M. D., Loebel, D. A. F., ... Tam, P. P. L. (2014). The transcriptional and functional properties of mouse epiblast stem cells resemble the anterior primitive streak. *Cell Stem Cell*.
- Kojima, Y., Sasaki, K., Yokobayashi, S., Sakai, Y., Nakamura, T., Yabuta, Y., ... Saitou, M. (2017). Evolutionarily Distinctive Transcriptional and Signaling Programs Drive Human Germ Cell Lineage Specification from Pluripotent Stem Cells. *Cell Stem Cell*.
- Kolodziejczyk, A. A., Kim, J. K., Tsang, J. C. H., Ilicic, T., Henriksson, J., Natarajan, K. N., ... Teichmann, S. A. (2015). Single Cell RNA-Sequencing of Pluripotent States Unlocks Modular Transcriptional Variation. *Cell Stem Cell*.
- Kondo, T., Asai, M., Tsukita, K., Kutoku, Y., Ohsawa, Y., Sunada, Y., ... Inoue, H. (2013). Modeling Alzheimer's disease with iPSCs reveals stress phenotypes

associated with intracellular A β and differential drug responsiveness. *Cell Stem Cell*.

- Kondoh, H., Leonart, M. E., Nakashima, Y., Yokode, M., Tanaka, M., Bernard, D., ... Beach, D. (2007). A high glycolytic flux supports the proliferative potential of murine embryonic stem cells. *Antioxidants & Redox Signaling*, 9(3), 293–299.
- Krebs, A. R., Imanci, D., Hoerner, L., Gaidatzis, D., Burger, L., & Schübeler, D. (2017). Genome-wide Single-Molecule Footprinting Reveals High RNA Polymerase II Turnover at Paused Promoters. *Molecular Cell*, 67(3), 411–422.
- Kuijk, E. W., Van de Velde, H., van Tol, L. T. A., Roelen, B. A. J., Geijsen, N., Welling, M., & Wubbolts, R. (2012). The roles of FGF and MAP kinase signaling in the segregation of the epiblast and hypoblast cell lineages in bovine and human embryos. *Development*.
- Kunarso, G., Chia, N. Y., Jeyakani, J., Hwang, C., Lu, X., Chan, Y. S., ... Bourque, G. (2010). Transposable elements have rewired the core regulatory network of human embryonic stem cells. *Nature Genetics*.
- Kuno, A., Nishimura, K., & Takahashi, S. (2018). Time-course transcriptome analysis of human cellular reprogramming from multiple cell types reveals the drastic change occurs between the mid phase and the late phase. *BMC Genomics*.
- Ladewig, J., Koch, P., & Brüstle, O. (2013). Leveling Waddington: The emergence of direct programming and the loss of cell fate hierarchies. *Nature Reviews Molecular Cell Biology*.
- Lai, D., & Bu, S. (2016). Comparison of the Ultrastructures of Primed and Naïve Mouse Embryonic Stem Cells. *Cellular Reprogramming*, 18(1), 48–53.
- Lakshmipathy, U., & Verfaillie, C. (2005). Stem cell plasticity. *Blood Reviews*.
- Lawson, K. A., Dunn, N. R., Roelen, B. A. J., Zeinstra, L. M., Davis, A. M., Wright, C. V. E., ... Hogan, B. L. M. (1999). Bmp4 is required for the generation of primordial germ cells in the mouse embryo. *Genes and Development*.
- Lawson, K. A., Meneses, J. J., & Pedersen, R. A. (1991). Clonal analysis of epiblast fate during germ layer formation in the mouse embryo. *Development*
- Leahy, A., Weixiong, J., Kuhnert, F., & Stuhlmann, H. (1999). Use of developmental marker genes to define temporal and spatial patterns of differentiation during embryoid body formation. *Journal of Experimental Zoology*.
- Lee, C. K., Shibata, Y., Rao, B., Strahl, B. D., & Lieb, J. D. (2004). Evidence for nucleosome depletion at active regulatory regions genome-wide. *Nature Genetics*.

- Leese, H. J., & Barton, A. M. (2004). Pyruvate and glucose uptake by mouse ova and preimplantation embryos. *Reproduction*.
- Leitch, H. G., McEwen, K. R., Turp, A., Encheva, V., Carroll, T., Grabole, N., ... Hajkova, P. (2013). Naive pluripotency is associated with global DNA hypomethylation. *Nature Structural & Molecular Biology*, 20(3), 311–316.
- Leung, C. Y., Zhu, M., & Zernicka-Goetz, M. (2016). Polarity in Cell-Fate Acquisition in the Early Mouse Embryo. In *Current Topics in Developmental Biology*.
- Li, H., Collado, M., Villasante, A., Strati, K., Ortega, S., Cãmerno, M., ... Serrano, M. (2009). The Ink4/Arf locus is a barrier for iPS cell reprogramming. *Nature*.
- Li, J.-Y., Pu, M.-T., Hirasawa, R., Li, B.-Z., Huang, Y.-N., Zeng, R., ... Xu, G.-L. (2007). Synergistic Function of DNA Methyltransferases Dnmt3a and Dnmt3b in the Methylation of Oct4 and Nanog. *Molecular and Cellular Biology*.
- Li, L., Wang, B. H., Wang, S., Moalim-Nour, L., Mohib, K., Lohnes, D., & Wang, L. (2010). Individual cell movement, asymmetric colony expansion, Rho-associated kinase, and E-cadherin impact the clonogenicity of human embryonic stem cells. *Biophysical Journal*.
- Li, M., & Belmonte, J. C. I. (2017). Ground rules of the pluripotency gene regulatory network. *Nature Reviews Genetics*.
- Li, R., Liang, J., Ni, S., Zhou, T., Qing, X., Li, H., ... Pei, D. (2010). A mesenchymal-to-Epithelial transition initiates and is required for the nuclear reprogramming of mouse fibroblasts. *Cell Stem Cell*.
- Li, X. J., & Li, S. (2012). Influence of Species Differences on the Neuropathology of Transgenic Huntington's Disease Animal Models. *Journal of Genetics and Genomics*.
- Lindblad-Toh, K., Wade, C. M., Mikkelsen, T. S., Karlsson, E. K., Jaffe, D. B., Kamal, M., ... Lander, E. S. (2005). Genome sequence, comparative analysis and haplotype structure of the domestic dog. *Nature*, 438(7069), 803–819.
- Liu, Y., Ma, Y., Yang, J. Y., Cheng, D., Liu, X., Ma, X., ... Wang, H. (2014). Comparative Gene Expression Signature of Pig, Human and Mouse Induced Pluripotent Stem Cell Lines Reveals Insight into Pig Pluripotency Gene Networks. *Stem Cell Reviews and Reports*.
- Locasale, J. W. (2013). Serine, glycine and one-carbon units: Cancer metabolism in full circle. *Nature Reviews Cancer*.
- Loh, Y. H., Wu, Q., Chew, J. L., Vega, V. B., Zhang, W., Chen, X., ... Ng, H. H. (2006). The Oct4 and Nanog transcription network regulates pluripotency in mouse embryonic stem cells. *Nature Genetics*.

- Lokken, A. A., & Ralston, A. (2016). The Genetic Regulation of Cell Fate During Preimplantation Mouse Development. In *Current Topics in Developmental Biology*.
- Longo, G., Montévil, M., Sonnenschein, C., Soto, A. M., Montevil, M., Sonnenschein, C., ... Soto, A. M. (2015). In search of principles for a Theory of Organisms. *Journal of Biosciences*, 40(5), 955–68.
- Lorch, Y., LaPointe, J. W., & Kornberg, R. D. (1987). Nucleosomes inhibit the initiation of transcription but allow chain elongation with the displacement of histones. *Cell*.
- Lujan, E., Zunder, E. R., Ng, Y. H., Goronzy, I. N., Nolan, G. P., & Wernig, M. (2015). Early reprogramming regulators identified by prospective isolation and mass cytometry. *Nature*.
- Lunt, S. Y., & Vander Heiden, M. G. (2011). Aerobic Glycolysis: Meeting the Metabolic Requirements of Cell Proliferation. *Annual Review of Cell and Developmental Biology*, 27(1), 441–464.
- Luo, J., & Cibelli, J. B. (2016). Conserved Role of bFGF and a Divergent Role of LIF for Pluripotency Maintenance and Survival in Canine Pluripotent Stem Cells. *Stem Cells and Development*, 25(21), 1670–1680.
- Luo, J., Suhr, S. T. S. T., Chang, E. A. E. A., Wang, K., Ross, P. J. P. J., Nelson, L. L. L., ... Cibelli, J. B. J. B. (2011). Generation of leukemia inhibitory factor and basic fibroblast growth factor-dependent induced pluripotent stem cells from canine adult somatic cells. *Stem Cells and Development*, 20(10), 1669–1678.
- MacArthur, B. D., Maayan, A., & Lemischka, I. R. (2009). Systems biology of stem cell fate and cellular reprogramming. *Nature Reviews Molecular Cell Biology*.
- Madan, P., Rose, K., & Watson, A. J. (2007). Na/K-ATPase β 1 subunit expression is required for blastocyst formation and normal assembly of trophectoderm tight junction-associated proteins. *Journal of Biological Chemistry*.
- Makino, H., Hasuda, H., & Ito, Y. (2004). Immobilization of leukemia inhibitory factor (LIF) to culture murine embryonic stem cells. *Journal of Bioscience and Bioengineering*, 98(5), 374–379.
- Mao, C., Brown, C. R., Griesenbeck, J., & Boeger, H. (2011). Occlusion of regulatory sequences by promoter nucleosomes In Vivo. *PLoS ONE*.
- Margueron, R., & Reinberg, D. (2011). The Polycomb complex PRC2 and its mark in life. *Nature*.

- Marks, H., Kalkan, T., Menafrá, R., Denissov, S., Jones, K., Hofemeister, H., ... Stunnenberg, H. G. (2012). The transcriptional and epigenomic foundations of ground state pluripotency. *Cell*.
- Marsboom, G., Zhang, G. F., Pohl-Avila, N., Zhang, Y., Yuan, Y., Kang, H., ... Rehman, J. (2016). Glutamine Metabolism Regulates the Pluripotency Transcription Factor OCT4. *Cell Reports*.
- Martin, G. R. (1981). Isolation of a pluripotent cell line from early mouse embryos cultured in medium conditioned by teratocarcinoma stem cells. *Developmental Biology*.
- Martin, G. R., & Evans, M. J. (1975). Differentiation of clonal lines of teratocarcinoma cells: formation of embryoid bodies in vitro. *Proceedings of the National Academy of Sciences*.
- Martin Gonzalez, J., Morgani, S. M., Bone, R. A., Bonderup, K., Abelchian, S., Brakebusch, C., & Brickman, J. M. (2016). Embryonic Stem Cell Culture Conditions Support Distinct States Associated with Different Developmental Stages and Potency. *Stem Cell Reports*.
- Martín, M., Organista, M. F., & de Celis, J. F. (2016). Structure of developmental gene regulatory networks from the perspective of cell fate-determining genes. *Transcription*, 7(1), 32–37.
- Masaki, H., & Nakauchi, H. (2017). Interspecies chimeras for human stem cell research. *Development*.
- Mascetti, V. L., & Pedersen, R. A. (2016). Human-Mouse Chimerism Validates Human Stem Cell Pluripotency. *Cell Stem Cell*.
- Matsuda, K., Andrabi, M., Oki, S., Kondoh, H., Yamaguchi, K., Shigenobu, S., ... Mikami, T. (2017). ChIP-seq analysis of genomic binding regions of five major transcription factors highlights a central role for ZIC2 in the mouse epiblast stem cell gene regulatory network. *Development*.
- Matsuda, T., Nakamura, T., Nakao, K., Arai, T., Katsuki, M., Heike, T., & Yokota, T. (1999). STAT3 activation is sufficient to maintain an undifferentiated state of mouse embryonic stem cells. *EMBO Journal*.
- Melcer, S., Hezroni, H., Rand, E., Nissim-Rafinia, M., Skoultchi, A., Stewart, C. L., ... Meshorer, E. (2012). Histone modifications and lamin A regulate chromatin protein dynamics in early embryonic stem cell differentiation. *Nature Communications*.
- Mendizabal, I., & Yi, S. V. (2016). Whole-genome bisulfite sequencing maps from multiple human tissues reveal novel CpG islands associated with tissue-specific regulation. *Human Molecular Genetics*, 25(1), 69–82.

- Menon, D. V., Patel, D., Joshi, C. G., & Kumar, A. (2019). The road less travelled: The efficacy of canine pluripotent stem cells. *Experimental Cell Research*.
- Mentch, S. J., Mehrmohamadi, M., Huang, L., Liu, X., Gupta, D., Mattocks, D., ... Locasale, J. W. (2015). Histone Methylation Dynamics and Gene Regulation Occur through the Sensing of One-Carbon Metabolism. *Cell Metabolism*.
- Meshorer, E., Yellajoshula, D., George, E., Scambler, P. J., Brown, D. T., & Misteli, T. (2006). Hyperdynamic plasticity of chromatin proteins in pluripotent embryonic stem cells. *Developmental Cell*.
- Mikkelsen, T. S., Hanna, J., Zhang, X., Ku, M., Wernig, M., Schorderet, P., ... Meissner, A. (2008). Dissecting direct reprogramming through integrative genomic analysis. *Nature*.
- Mikkelsen, T. S., Ku, M., Jaffe, D. B., Issac, B., Lieberman, E., Giannoukos, G., ... Bernstein, B. E. (2007). Genome-wide maps of chromatin state in pluripotent and lineage-committed cells. *Nature*.
- Mitalipov, S., & Wolf, D. (2009). Totipotency, pluripotency and nuclear reprogramming. *Advances in Biochemical Engineering/Biotechnology*.
- Mitsui, K., Tokuzawa, Y., Itoh, H., Segawa, K., Murakami, M., Takahashi, K., ... Yamanaka, S. (2003). The homeoprotein nanog is required for maintenance of pluripotency in mouse epiblast and ES cells. *Cell*.
- Mohn, F., & Schübeler, D. (2009). Genetics and epigenetics: stability and plasticity during cellular differentiation. *Trends in Genetics*.
- Mor, N., Rais, Y., Sheban, D., Peles, S., Aguilera-Castrejon, A., Zviran, A., ... Hanna, J. H. (2018). Neutralizing Gatad2a-Chd4-Mbd3/NuRD Complex Facilitates Deterministic Induction of Naive Pluripotency. *Cell Stem Cell*.
- Morgani, S., Nichols, J., & Hadjantonakis, A. K. (2017). The many faces of Pluripotency: In vitro adaptations of a continuum of in vivo states. *BMC Developmental Biology*.
- Morrison, G. M. (2006). Conserved roles for Oct4 homologues in maintaining multipotency during early vertebrate development. *Development*.
- Moussaieff, A., Rouleau, M., Kitsberg, D., Cohen, M., Levy, G., Barasch, D., ... Nahmias, Y. (2015). Glycolysis-mediated changes in acetyl-CoA and histone acetylation control the early differentiation of embryonic stem cells. *Cell Metabolism*, 21(3), 392–402.
- Mugal, C. F., Weber, C. C., & Ellegren, H. (2015). GC-biased gene conversion links the recombination landscape and demography to genomic base composition: GC-

biased gene conversion drives genomic base composition across a wide range of species. *BioEssays*.

- Müller, C., & Leutz, A. (2001). Chromatin remodeling in development and differentiation. *Current Opinion in Genetics and Development*.
- Muñoz-Fuentes, V., Rienzo, A., & Vilà, C. (2011). Prdm9, a major determinant of meiotic recombination hotspots, is not functional in dogs and their wild relatives, wolves and coyotes. *PLoS ONE*, 6(11).
- Muramoto, H., Yagi, S., Hirabayashi, K., Sato, S., Ohgane, J., Tanaka, S., & Shiota, K. (2010). Enrichment of short interspersed transposable elements to embryonic stem cell-specific hypomethylated gene regions. *Genes to Cells*.
- Murry, C. E., & Keller, G. (2008). Differentiation of Embryonic Stem Cells to Clinically Relevant Populations: Lessons from Embryonic Development. *Cell*.
- Nagamoto, Y., Takayama, K., Ohashi, K., Okamoto, R., Sakurai, F., Tachibana, M., ... Mizuguchi, H. (2016). Transplantation of a human iPSC-derived hepatocyte sheet increases survival in mice with acute liver failure. *Journal of Hepatology*.
- Nagaraj, R., Sharpley, M. S., Chi, F., Braas, D., Zhou, Y., Kim, R., ... Banerjee, U. (2017). Nuclear Localization of Mitochondrial TCA Cycle Enzymes as a Critical Step in Mammalian Zygotic Genome Activation. *Cell*.
- Nagy, A., Rossant, J., Nagy, R., Abramow-Newerly, W., & Roder, J. C. (1993). Derivation of completely cell culture-derived mice from early-passage embryonic stem cells. *Proceedings of the National Academy of Sciences*, 90(18), 8424–8.
- Natarajan, K. N., Teichmann, S. A., & Kolodziejczyk, A. A. (2017). Single cell transcriptomics of pluripotent stem cells: reprogramming and differentiation. *Current Opinion in Genetics and Development*.
- Navarro, P., Festuccia, N., Colby, D., Gagliardi, A., Mullin, N. P., Zhang, W., ... Chambers, I. (2012). OCT4/SOX2-independent Nanog autorepression modulates heterogeneous Nanog gene expression in mouse ES cells. *EMBO Journal*.
- Nefzger, C. M., Rossello, F. J., Chen, J., Liu, X., Knaupp, A. S., Firas, J., ... Polo, J. M. (2017). Cell Type of Origin Dictates the Route to Pluripotency. *Cell Reports*.
- Neganova, I., Zhang, X., Atkinson, S., & Lako, M. (2009). Expression and functional analysis of G1 to S regulatory components reveals an important role for CDK2 in cell cycle regulation in human embryonic stem cells. *Oncogene*.
- Nichols, J., & Smith, A. (2009). Naive and Primed Pluripotent States. *Cell Stem Cell*, 4(6), 487–492.

- Nichols, J., Zevnik, B., Anastassiadis, K., Niwa, H., Klewe-Nebenius, D., Chambers, I., ... Smith, A. (1998). Formation of pluripotent stem cells in the mammalian embryo depends on the POU transcription factor Oct4. *Cell*.
- Nishimura, T., Hatoya, S., Kanegi, R., Sugiura, K., Wijewardana, V., Kuwamura, M., ... Inaba, T. (2013). Generation of Functional Platelets from Canine Induced Pluripotent Stem Cells. *Stem Cells and Development*.
- Niwa, H. (2010). Mouse ES cell culture system as a model of development. *Development Growth and Differentiation*.
- Niwa, H., Burdon, T., Chambers, I., & Smith, A. (1998). Self-renewal of pluripotent embryonic stem cells is mediated via activation of STAT3. *Genes and Development*.
- Niwa, H., Miyazaki, J. I., & Smith, A. G. (2000). Quantitative expression of Oct-3/4 defines differentiation, dedifferentiation or self-renewal of ES cells. *Nature Genetics*.
- Novo, C. L., & Rugg-Gunn, P. J. (2016). Chromatin organization in pluripotent cells: Emerging approaches to study and disrupt function. *Briefings in Functional Genomics*.
- Ochocki, J. D., & Simon, M. C. (2013). Nutrient-sensing pathways and metabolic regulation in stem cells. *Journal of Cell Biology*.
- Ohi, Y., Qin, H., Hong, C., Blouin, L., Polo, J. M., Guo, T., ... Ramalho-Santos, M. (2011). Incomplete DNA methylation underlies a transcriptional memory of somatic cells in human iPS cells. *Nature Cell Biology*.
- Okamoto, I., Patrat, C., Thépot, D., Peynot, N., Fauque, P., Daniel, N., ... Heard, E. (2011). Eutherian mammals use diverse strategies to initiate X-chromosome inactivation during development. *Nature*.
- Oliver, P. L., Goodstadt, L., Bayes, J. J., Birtle, Z., Roach, K. C., Phadnis, N., ... Ponting, C. P. (2009). Accelerated evolution of the Prdm9 speciation gene across diverse metazoan taxa. *PLoS Genetics*, 5(12).
- Onishi, K., Tonge, P. D., Nagy, A., & Zandstra, P. W. (2012). Microenvironment-mediated reversion of epiblast stem cells by reactivation of repressed JAK-STAT signaling. *Integrative Biology*.
- Osorno, R., & Chambers, I. (2011). Transcription factor heterogeneity and epiblast pluripotency. *Philosophical Transactions of the Royal Society B: Biological Sciences*.

- Osorno, R., Economou, C., Scotting, P. J., Wilkie, R., Wong, F., Blin, G., ... Wilson, V. (2012). The developmental dismantling of pluripotency is reversed by ectopic Oct4 expression. *Journal of Cell Science*.
- Panopoulos, A. D., Yanes, O., Ruiz, S., Kida, Y. S., Diep, D., Tautenhahn, R., ... Belmonte, J. C. I. (2012). The metabolome of induced pluripotent stem cells reveals metabolic changes occurring in somatic cell reprogramming. *Cell Research*, 22(1), 168–177.
- Paris, D., Kuijk, E., Roelen, B., & Stout, T. (2010). Stage specific changes in expression of OCT4, CDX2, NANOG and GATA6 mRNA during blastocyst formation in the horse. *Animal Reproduction Science*, (121), 291–292.
- Park, S. H., Park, S. H., Kook, M. C., Kim, E. Y., Park, S., & Lim, J. H. (2004). Ultrastructure of human embryonic stem cells and spontaneous and retinoic acid-induced differentiating cells. *Ultrastructural Pathology*.
- Pasini, D., Hansen, K. H., Christensen, J., Agger, K., Cloos, P. A. C., & Helin, K. (2008). Coordinated regulation of transcriptional repression by the RBP2 H3K4 demethylase and Polycomb-Repressive Complex 2. *Genes and Development*.
- Pauklin, S., & Vallier, L. (2013). XThe cell-cycle state of stem cells determines cell fate propensity. *Cell*, 155(1), 135–147.
- Pękowska, A., Klaus, B., Xiang, W., Severino, J., Daigle, N., Klein, F. A., ... Huber, W. (2018). Gain of CTCF-Anchored Chromatin Loops Marks the Exit from Naive Pluripotency. *Cell Systems*.
- Pereira, C. F., Piccolo, F. M., Tsubouchi, T., Sauer, S., Ryan, N. K., Bruno, L., ... Fisher, A. G. (2010). ESCs require PRC2 to direct the successful reprogramming of differentiated cells toward pluripotency. *Cell Stem Cell*.
- Pernaute, B., Spruce, T., Smith, K. M., Sánchez-Nieto, J. M., Manzanares, M., Cobb, B., & Rodríguez, T. A. (2014). MicroRNAs control the apoptotic threshold in primed pluripotent stem cells through regulation of BIM. *Genes and Development*.
- Peter, I. S., & Davidson, E. H. (2016). Implications of Developmental Gene Regulatory Networks Inside and Outside Developmental Biology. In *Current Topics in Developmental Biology*.
- Petropoulos, S., Edsgard, D., Reinius, B., Deng, Q., Panula, S. P., Codeluppi, S., ... Lanner, F. (2015). Single-Cell RNA-Seq Reveals Lineage and X Chromosome Dynamics in Human Preimplantation Embryos. *Cell*.
- Plath, K., Fang, J., Mlynarczyk-Evans, S. K., Cao, R., Worringer, K. A., Wang, H., ... Zhang, Y. (2003). Role of histone H3 lysine 27 methylation in X inactivation. *Science*.

- Polo, J. M., Anderssen, E., Walsh, R. M., Schwarz, B. A., Nefzger, C. M., Lim, S. M., ... Hochedlinger, K. (2012). A molecular roadmap of reprogramming somatic cells into iPS cells. *Cell*, 151(7), 1617–1632.
- Pretzer, S. D. (2008). Canine embryonic and fetal development: A review. *Theriogenology*.
- Prigione, A., & Adjaye, J. (2010). Modulation of mitochondrial biogenesis and bioenergetic metabolism upon in vitro and in vivo differentiation of human ES and iPS cells. *The International Journal of Developmental Biology*, 54(11–12), 1729–41.
- Putiri, E. L., Tiedemann, R. L., Thompson, J. J., Liu, C., Ho, T., Choi, J. H., & Robertson, K. D. (2014). Distinct and overlapping control of 5-methylcytosine and 5-hydroxymethylcytosine by the TET proteins in human cancer cells. *Genome Biology*.
- Qi, X., Li, T.-G., Mishina, Y., Hu, J., Miura, S., Wang, J., ... Hao, J. (2004). BMP4 supports self-renewal of embryonic stem cells by inhibiting mitogen-activated protein kinase pathways. *Proceedings of the National Academy of Sciences*.
- Qiu, D., Ye, S., Ruiz, B., Zhou, X., Liu, D., Zhang, Q., & Ying, Q. L. (2015). Klf2 and Tfcp2l1, Two Wnt/ β -Catenin Targets, Act Synergistically to Induce and Maintain Naive Pluripotency. *Stem Cell Reports*.
- Rais, Y., Zviran, A., Geula, S., Gafni, O., Chomsky, E., Viukov, S., ... Hanna, J. H. (2013). Deterministic direct reprogramming of somatic cells to pluripotency. *Nature*.
- Reddington, J. P., Perricone, S. M., Nestor, C. E., Reichmann, J., Youngson, N. A., Suzuki, M., ... Meehan, R. R. (2013). Redistribution of H3K27me3 upon DNA hypomethylation results in de-repression of Polycomb target genes. *Genome Biology*.
- Reitzer, L. J., Wice, B. M., & Kennell, D. (1980). The pentose cycle. Control and essential function in HeLa cell nucleic acid synthesis. *Journal of Biological Chemistry*.
- Renton, J. P., Boyd, J. S., Eckersall, P. D., Ferguson, J. M., Harvey, M. J., Mullaney, J., & Perry, B. (1991). Ovulation, fertilization and early embryonic development in the bitch (*Canis familiaris*). *Journal of Reproduction and Fertility*, 93(1), 221–31.
- Resnick, J. L., Bixler, L. S., Cheng, L., & Donovan, P. J. (1992). Long-term proliferation of mouse primordial germ cells in culture. *Nature*.
- Reubinoff, B. E., Pera, M. F., Fong, C.-Y. Y., Trounson, A., Bongso, A., Reubinoff, B. E., ... Bongso, A. (2000). Embryonic stem cell lines from human blastocysts: Somatic differentiation in vitro. *Nature Biotechnology*, 18(4), 399–404.

- Reynaud, K., Fontbonne, A., Marseloo, N., Thoumire, S., Chebrou, M., Viaris de Lesegno, C., & Chastant-Maillard, S. (2005). In vivo meiotic resumption, fertilization and early embryonic development in the bitch. *Reproduction*.
- Reynaud, K., Fontbonne, A., Marseloo, N., Viaris de Lesegno, C., Saint-Dizier, M., & Chastant-Maillard, S. (2006). In vivo canine oocyte maturation, fertilization and early embryogenesis: A review. *Theriogenology*.
- Roadmap Epigenomics Consortium. (2015). Integrative analysis of 111 reference human epigenomes. *Nature*.
- Roberts, R. M., Yuan, Y., & Ezashi, T. (2016). Exploring early differentiation and pluripotency in domestic animals. *Reproduction, Fertility, and Development*, 29(1), 101–107.
- Robertson, K. D., & Jones, P. A. (2000). DNA methylation: Past, present and future directions. *Carcinogenesis*.
- Robinton, D. A., & Daley, G. Q. (2012). The promise of induced pluripotent stem cells in research and therapy. *Nature*.
- Rodrigues, G. M. C., Rodrigues, C. A. V., Fernandes, T. G., Diogo, M. M., & Cabral, J. M. S. (2015). Clinical-scale purification of pluripotent stem cell derivatives for cell-based therapies. *Biotechnology Journal*.
- Rompolas, P., Mesa, K. R., & Greco, V. (2013). Spatial organization within a niche as a determinant of stem-cell fate. *Nature*.
- Roode, M., Blair, K., Snell, P., Elder, K., Marchant, S., Smith, A., & Nichols, J. (2012). Human hypoblast formation is not dependent on FGF signalling. *Developmental Biology*.
- Rossant, J. (1987). Cell lineage analysis in mammalian embryogenesis. *Current Topics in Developmental Biology*, 23, 115–46.
- Rossant, J. (2008). *Stem Cells and Early Lineage Development*. Cell.
- Rossant, J., & Tam, P. P. L. (2017). *New Insights into Early Human Development: Lessons for Stem Cell Derivation and Differentiation*. Cell Stem Cell.
- Sakai, T., Li, S., Docheva, D., Grashoff, C., Sakai, K., Kostka, G., ... Fässler, R. (2003). Integrin-linked kinase (ILK) is required for polarizing the epiblast, cell adhesion, and controlling actin accumulation. *Genes and Development*.
- Saksouk, N., Simboeck, E., & Déjardin, J. (2015). Constitutive heterochromatin formation and transcription in mammals. *Epigenetics and Chromatin*.

- Sakurai, K., Talukdar, I., Patil, V. S., Dang, J., Li, Z., Chang, K. Y., ... Rana, T. M. (2014). Kinome-wide functional analysis highlights the role of cytoskeletal remodeling in somatic cell reprogramming. *Cell Stem Cell*.
- Samavarchi-Tehrani, P., Golipour, A., David, L., Sung, H. K., Beyer, T. A., Datti, A., ... Wrana, J. L. (2010). Functional genomics reveals a BMP-Driven mesenchymal-to-Epithelial transition in the initiation of somatic cell reprogramming. *Cell Stem Cell*.
- Sardina, J. L., Collombet, S., Tian, T. V., Gómez, A., Di Stefano, B., Berenguer, C., ... Graf, T. (2018). Transcription Factors Drive Tet2-Mediated Enhancer Demethylation to Reprogram Cell Fate. *Cell Stem Cell*.
- Sarraf, S. A., & Stancheva, I. (2004). Methyl-CpG binding protein MBD1 couples histone H3 methylation at lysine 9 by SETDB1 to DNA replication and chromatin assembly. *Molecular Cell*.
- Sathananthan, H., Pera, M., & Trounson, A. (2002). The fine structure of human embryonic stem cells. *Reproductive Biomedicine Online*, 4(1), 56–61.
- Schneider, M. R., Wolf, E., Braun, J., Kolb, H. J., & Adler, H. (2008). Canine embryo-derived stem cells and models for human diseases. *Human Molecular Genetics*.
- Schwartzentruber, J., Foskolou, S., Kilpinen, H., Rodrigues, J., Alasoo, K., Knights, A. J., ... Gaffney, D. J. (2018). Molecular and functional variation in iPSC-derived sensory neurons. *Nature Genetics*.
- Schwarz, B. A., Cetinbas, M., Clement, K., Walsh, R. M., Cheloufi, S., Gu, H., ... Hochedlinger, K. (2018). Prospective Isolation of Poised iPSC Intermediates Reveals Principles of Cellular Reprogramming. *Cell Stem Cell*.
- Sekiya, T., Muthurajan, U. M., Luger, K., Tulin, A. V., & Zaret, K. S. (2009). Nucleosome-binding affinity as a primary determinant of the nuclear mobility of the pioneer transcription factor FoxA. *Genes and Development*.
- Shahbazi, M. N., Scialdone, A., Skorupska, N., Weberling, A., Recher, G., Zhu, M., ... Zernicka-Goetz, M. (2017). Pluripotent state transitions coordinate morphogenesis in mouse and human embryos. *Nature*.
- Sharifpana, F., Wartenberg, M., Hannig, M., Piper, H.M., & Sauer, H. (2008). Peroxisome proliferator-activated receptor alpha agonists enhance cardiomyogenesis of mouse ES cells by utilization of a reactive oxygen species-dependent mechanism. *Stem Cells*.
- Shao, Z., Yao, C., Khodadadi-Jamayran, A., Xu, W., Townes, T. M., Crowley, M. R., & Hu, K. (2016). Reprogramming by De-bookmarking the Somatic Transcriptional Program through Targeting of BET Bromodomains. *Cell Reports*.

- Sharif, J., Muto, M., Takebayashi, S. I., Suetake, I., Iwamatsu, A., Endo, T. A., ... Koseki, H. (2007). The SRA protein Np95 mediates epigenetic inheritance by recruiting Dnmt1 to methylated DNA. *Nature*.
- Shearin, A. L., & Ostrander, E. A. (2010). Leading the way: canine models of genomics and disease. *Disease Models & Mechanisms*.
- Shema, E., Jones, D., Shores, N., Donohue, L., Ram, O., & Bernstein, B. E. (2016). Single-molecule decoding of combinatorially modified nucleosomes. *Science*.
- Shi, L., & Tu, B. P. (2015). Acetyl-CoA and the regulation of metabolism: Mechanisms and consequences. *Current Opinion in Cell Biology*.
- Shiraki, N., Shiraki, Y., Tsuyama, T., Obata, F., Miura, M., Nagae, G., ... Kume, S. (2014). Methionine Metabolism Regulates Maintenance and Differentiation of Human Pluripotent Stem Cells. *Cell Metabolism*, 19(5), 780–794.
- Shook, D., & Keller, R. (2003). Mechanisms, mechanics and function of epithelial-mesenchymal transitions in early development. *Mechanisms of Development*.
- Shyh-Chang, N., Locasale, J. W., Lyssiotis, C. A., Zheng, Y., Teo, R. Y., Ratanasirintrao, S., ... Daley, G. Q. (2013). Influence of threonine metabolism on S-adenosylmethionine and histone methylation. *Science*, 339(6116), 222–6.
- Silva, J., Nichols, J., Theunissen, T. W., Guo, G., van Oosten, A. L., Barrandon, O., ... Smith, A. (2009). Nanog Is the Gateway to the Pluripotent Ground State. *Cell*.
- Silva, J., & Smith, A. (2008). Capturing Pluripotency. *Cell*.
- Singer, Z. S., Yong, J., Tischler, J., Hackett, J. A., Altinok, A., Surani, M. A., ... Elowitz, M. B. (2014). Dynamic Heterogeneity and DNA Methylation in Embryonic Stem Cells. *Molecular Cell*.
- Singh, A. M., Chappell, J., Trost, R., Lin, L., Wang, T., Tang, J., ... Dalton, S. (2013). Cell-cycle control of developmentally regulated transcription factors accounts for heterogeneity in human pluripotent cells. *Stem Cell Reports*.
- Singhal, N., Graumann, J., Wu, G., Araúzo-Bravo, M. J., Han, D. W., Greber, B., ... Schöler, H. R. (2010). Chromatin-remodeling components of the baf complex facilitate reprogramming. *Cell*.
- Smallwood, A., Estève, P. O., Pradhan, S., & Carey, M. (2007). Functional cooperation between HP1 and DNMT1 mediates gene silencing. *Genes and Development*.
- Smith, A. (2017). Formative pluripotency: the executive phase in a developmental continuum. *Development*.

- Smith, A. G., Heath, J. K., Donaldson, D. D., Wong, G. G., Moreau, J., Stahl, M., & Rogers, D. (1988). Inhibition of pluripotential embryonic stem cell differentiation by purified polypeptides. *Nature*.
- Smith, Z. D., & Meissner, A. (2013). DNA methylation: Roles in mammalian development. *Nature Reviews Genetics*.
- Smith, Z. D., Nachman, I., Regev, A., & Meissner, A. (2010). Dynamic single-cell imaging of direct reprogramming reveals an early specifying event. *Nature Biotechnology*.
- Sone, M., Morone, N., Nakamura, T., Tanaka, A., Okita, K., Woltjen, K., ... Yamamoto, T. (2017). Hybrid Cellular Metabolism Coordinated by *Zic3* and *Esrrb* Synergistically Enhances Induction of Naive Pluripotency. *Cell Metabolism*.
- Soufi, A., Donahue, G., & Zaret, K. S. (2012). Facilitators and impediments of the pluripotency reprogramming factors' initial engagement with the genome. *Cell*.
- Soufi, A., Garcia, M. F., Jaroszewicz, A., Osman, N., Pellegrini, M., & Zaret, K. S. (2015). Pioneer transcription factors target partial DNA motifs on nucleosomes to initiate reprogramming. *Cell*.
- Soufi, A., & Zaret, K. S. (2013). Understanding impediments to cellular conversion to pluripotency by assessing the earliest events in ectopic transcription factor binding to the genome. *Cell Cycle*.
- Spencer, H., Keramari, M., & Ward, C. M. (2011). Using cadherin expression to assess spontaneous differentiation of embryonic stem cells. *Methods in Molecular Biology*, 690, 81–94.
- Sperber, H., Mathieu, J., Wang, Y., Ferreccio, A., Hesson, J., Xu, Z., ... Ruohola-Baker, H. (2015). The metabolome regulates the epigenetic landscape during naive-to-primed human embryonic stem cell transition. *Nature Cell Biology*, 17(12), 1523–1535.
- Stadtfield, M., Maherali, N., Breault, D. T., & Hochedlinger, K. (2008). Defining Molecular Cornerstones during Fibroblast to iPS Cell Reprogramming in Mouse. *Cell Stem Cell*.
- Stewart, C. L., Gadi, I., & Bhatt, H. (1994). Stem cells from primordial germ cells can reenter the germ line. *Developmental Biology*.
- Streiffer, R. (2007). At the Edge of Humanity. *Journal of Philosophical Research*, 32, 63–83.
- Strumpf, D., Mao, C.-A., Yamanaka, Y., Ralston, A., Chawengsaksophak, K., Beck, F., & Rossant, J. (2005). *Cdx2* is required for correct cell fate specification and

- differentiation of trophectoderm in the mouse blastocyst. *Development*, 132(9), 2093–2102.
- Sun, J., & Stathopoulos, A. (2018). FGF controls epithelial-mesenchymal transitions during gastrulation by regulating cell division and apicobasal polarity. *Development*.
- Suwińska, A., Czołowska, R., Ozdzeński, W., & Tarkowski, A. K. (2008). Blastomeres of the mouse embryo lose totipotency after the fifth cleavage division: Expression of Cdx2 and Oct4 and developmental potential of inner and outer blastomeres of 16- and 32-cell embryos. *Developmental Biology*.
- Svoboda, P., Franke, V., & Schultz, R. M. (2015). Sculpting the Transcriptome During the Oocyte-to-Embryo Transition in Mouse. In *Current Topics in Developmental Biology*.
- Tahiliani, M., Koh, K. P., Shen, Y., Pastor, W. A., Bandukwala, H., Brudno, Y., ... Rao, A. (2009). Conversion of 5-methylcytosine to 5-hydroxymethylcytosine in mammalian DNA by MLL partner TET1. *Science*.
- Takahashi, K., Tanabe, K., Ohnuki, M., Narita, M., Ichisaka, T., Tomoda, K., & Yamanaka, S. (2007). Induction of Pluripotent Stem Cells from Adult Human Fibroblasts by Defined Factors. *Cell*.
- Takahashi, K., & Yamanaka, S. (2006). Induction of Pluripotent Stem Cells from Mouse Embryonic and Adult Fibroblast Cultures by Defined Factors. *Cell*, 126(4), 663–676.
- Tanabe, K., Yamanaka, S., Narita, M., Takahashi, K., & Nakamura, M. (2013). Maturation, not initiation, is the major roadblock during reprogramming toward pluripotency from human fibroblasts. *Proceedings of the National Academy of Sciences*.
- Tang, F., Barbacioru, C., Bao, S., Lee, C., Nordman, E., Wang, X., ... Surani, M. A. (2010). Tracing the derivation of embryonic stem cells from the inner cell mass by single-cell RNA-seq analysis. *Cell Stem Cell*.
- Tarkowski, A. K., Suwińska, A., Czołowska, R., & Ozdzeński, W. (2010). Individual blastomeres of 16- and 32-cell mouse embryos are able to develop into foetuses and mice. *Developmental Biology*.
- Tecirlioglu, R. T., & Trounson, A. O. (2007). Embryonic stem cells in companion animals (horses, dogs and cats): present status and future prospects. *Reproduction, Fertility, and Development*, 19(6), 740–7.
- Tesar, P. J., Chenoweth, J. G., Brook, F. A., Davies, T. J., Evans, E. P., Mack, D. L., ... McKay, R. D. G. (2007). New cell lines from mouse epiblast share defining features with human embryonic stem cells. *Nature*, 448(7150), 196–199.

- Teshigawara, R., Hirano, K., Nagata, S., Ainscough, J., & Tada, T. (2016). OCT4 activity during conversion of human intermediately reprogrammed stem cells to iPSCs through mesenchymal-epithelial transition. *Development*.
- Theunissen, T. W., Friedli, M., He, Y., Planet, E., O'Neil, R. C., Markoulaki, S., ... Jaenisch, R. (2016). Molecular Criteria for Defining the Naive Human Pluripotent State. *Cell Stem Cell*.
- Thiery, J. P., Acloque, H., Huang, R. Y. J., & Nieto, M. A. (2009). Epithelial-Mesenchymal Transitions in Development and Disease. *Cell*.
- Thomson, J. A., Itskovitz-Eldor, J., Shapiro, S. S., Waknitz, M. A., Swiergiel, J. J., Marshall, V. S., & Jones, J. M. (1998). Embryonic stem cell lines derived from human blastocysts. *Science (New York, N.Y.)*, 282(5391), 1145–7.
- Thomson, M., Liu, S. J., Zou, L. N., Smith, Z., Meissner, A., & Ramanathan, S. (2011). Pluripotency factors in embryonic stem cells regulate differentiation into germ layers. *Cell*.
- Till, J. E., & McCulloch, E. A. (1961). A Direct Measurement of the Radiation Sensitivity of Normal Mouse Bone Marrow Cells. *Radiation Research*.
- Tischler, J., Gruhn, W. H., Reid, J., Allgeyer, E., Buettner, F., Marr, C., ... Surani, M. A. (2019). Metabolic regulation of pluripotency and germ cell fate through α -ketoglutarate. *The EMBO Journal*, 38(1).
- Tohyama, S., Fujita, J., Hishiki, T., Matsuura, T., Hattori, F., Ohno, R., ... Fukuda, K. (2016). Glutamine Oxidation Is Indispensable for Survival of Human Pluripotent Stem Cells. *Cell Metabolism*, 23(4), 663–674.
- Tosolini, M., Brochard, V., Adenot, P., Chebrou, M., Grillo, G., Navia, V., ... Jouneau, A. (2018). Contrasting epigenetic states of heterochromatin in the different types of mouse pluripotent stem cells. *Scientific Reports*.
- Trojer, P., & Reinberg, D. (2007). Facultative Heterochromatin: Is There a Distinctive Molecular Signature? *Molecular Cell*.
- Trounson, A., & DeWitt, N. D. (2016). Pluripotent stem cells progressing to the clinic. *Nature Reviews Molecular Cell Biology*.
- Tsakiridis, A., Huang, Y., Blin, G., Skylaki, S., Wymeersch, F. J., Osorno, R. R., ... Wilson, V. (2014). Distinct Wnt-driven primitive streak-like populations reflect in vivo lineage precursors. *Development*.
- Tsuji, O., Sugai, K., Yamaguchi, R., Tashiro, S., Nagoshi, N., Kohyama, J., ... Okano, H. (2019). Concise Review: Laying the Groundwork for a First-In-Human Study of an Induced Pluripotent Stem Cell-Based Intervention for Spinal Cord Injury. *Stem Cells*.

- Turco, M. Y., Furia, L., Dietze, A., Diaz, L. F., Ronzoni, S., Sciullo, A., ... Lanfrancone, L. (2012). Cellular heterogeneity during embryonic stem cell differentiation to epiblast stem cells is revealed by the ShcD/RaLP adaptor protein. *Stem Cells*.
- Ulrey, C. L., Liu, L., Andrews, L. G., & Tollefsbol, T. O. (2005). The impact of metabolism on DNA methylation. *Human Molecular Genetics*.
- Vaags, A. K., Rosic-Kablar, S., Gartley, C. J., Zheng, Y. Z., Chesney, A., Villagómez, D. A. F., ... Hough, M. R. (2009). Derivation and Characterization of Canine Embryonic Stem Cell Lines with In Vitro and In Vivo Differentiation Potential. *Stem Cells*, 27(2), 329–340.
- Vallier, L., Mendjan, S., Brown, S., Chng, Z., Teo, A., Smithers, L. E., ... Pedersen, R. A. (2009). Activin/Nodal signalling maintains pluripotency by controlling Nanog expression. *Development*.
- Varum, S., Momčilović, O., Castro, C., Ben-Yehudah, A., Ramalho-Santos, J., & Navara, C. S. (2009). Enhancement of human embryonic stem cell pluripotency through inhibition of the mitochondrial respiratory chain. *Stem Cell Research*, 3(2), 142–156.
- Varum, S., Rodrigues, A. S., Moura, M. B., Momcilovic, O., Easley, C. A., Ramalho-Santos, J., ... Schatten, G. (2011). Energy Metabolism in Human Pluripotent Stem Cells and Their Differentiated Counterparts. *PLoS ONE*, 6(6), e20914.
- Veluscek, G., Li, Y., Yang, S. H., & Sharrocks, A. D. (2016). Jun-Mediated Changes in Cell Adhesion Contribute to Mouse Embryonic Stem Cell Exit from Ground State Pluripotency. *Stem Cells*.
- Vlaski-Lafarge, M., Loncaric, D., Perez, L., Labat, V., Debeissat, C., Brunet de la Grange, P., ... Bœuf, H. (2019). Bioenergetic Changes Underline Plasticity of Murine Embryonic Stem Cells. *Stem Cells*.
- von Meyenn, F., Iurlaro, M., Habibi, E., Liu, N. Q., Salehzadeh-Yazdi, A., Santos, F., ... Stunnenberg, H. G. (2016). Impairment of DNA Methylation Maintenance Is the Main Cause of Global Demethylation in Naive Embryonic Stem Cells. *Molecular Cell*.
- Waddington, C. H. (1957). The strategy of the genes. A discussion of some aspects of theoretical biology. With an appendix by H. Kacser. *The Strategy of the Genes A Discussion of Some ...*
- Walsh, C. P., Chaillet, J. R., & Bestor, T. H. (1998). Transcription of IAP endogenous retroviruses is constrained by cytosine methylation. *Nature Genetics*.
- Wang, L., Jiang, Z., Huang, D., Duan, J., Huang, C., Sullivan, S., ... Tang, Y. (2018). JAK/STAT3 regulated global gene expression dynamics during late-stage reprogramming process. *BMC Genomics*.

- Wang, T., Chen, K., Zeng, X., Yang, J., Wu, Y., Shi, X., ... Pei, D. (2011). The histone demethylases Jhdm1a/1b enhance somatic cell reprogramming in a vitamin-C-dependent manner. *Cell Stem Cell*, 9(6), 575–587.
- Watanabe, K., Ueno, M., Kamiya, D., Nishiyama, A., Matsumura, M., Wataya, T., ... Sasai, Y. (2007). A ROCK inhibitor permits survival of dissociated human embryonic stem cells. *Nature Biotechnology*.
- Waterston, R. H., Lindblad-Toh, K., Birney, E., Rogers, J., Abril, J. F., Agarwal, P., ... Lander, E. S. (2002). Initial sequencing and comparative analysis of the mouse genome. *Nature*.
- Webber, C., & Ponting, C. P. (2005). Hotspots of mutation and breakage in dog and human chromosomes. *Genome Research*.
- Wei, T., Chen, W., Wang, X., Zhang, M., Chen, J., Zhu, S., ... Kang, J. (2015). An HDAC2-TET1 switch at distinct chromatin regions significantly promotes the maturation of pre-iPS to iPS cells. *Nucleic Acids Research*.
- Weinberger, L., Ayyash, M., Novershtern, N., & Hanna, J. H. (2016). Dynamic stem cell states: naive to primed pluripotency in rodents and humans. *Nature Reviews Molecular Cell Biology*, 17(3), 155–169.
- Wellen, K. E., Hatzivassiliou, G., Sachdeva, U. M., Bui, T. V., Cross, J. R., & Thompson, C. B. (2009). ATP-citrate lyase links cellular metabolism to histone acetylation. *Science*.
- Wellen, K. E., Lu, C., Mancuso, A., Lemons, J. M. S., Ryczko, M., Dennis, J. W., ... Thompson, C. B. (2010). The hexosamine biosynthetic pathway couples growth factor-induced glutamine uptake to glucose metabolism. *Genes and Development*.
- Wernig, M., Meissner, A., Foreman, R., Brambrink, T., Ku, M., Hochedlinger, K., ... Jaenisch, R. (2007). In vitro reprogramming of fibroblasts into a pluripotent ES-cell-like state. *Nature*.
- White, M. D., Bissiere, S., Alvarez, Y. D., & Plachta, N. (2016). Mouse Embryo Compaction. In *Current Topics in Developmental Biology*.
- Whitworth, D. J., Ovchinnikov, D. A., & Wolvetang, E. J. (2012). Generation and Characterization of LIF-dependent Canine Induced Pluripotent Stem Cells from Adult Dermal Fibroblasts. *Stem Cells and Development*, 21(12), 2288–2297.
- Wicklow, E., Blij, S., Frum, T., Hirate, Y., Lang, R. A., Sasaki, H., & Ralston, A. (2014). HIPPO Pathway Members Restrict SOX2 to the Inner Cell Mass Where It Promotes ICM Fates in the Mouse Blastocyst. *PLoS Genetics*.

- Wilcox, J. T., Lai, J., Semple, E., Brisson, B. A., Gartley, C., Armstrong, J. N., & Betts, D. H. (2011). Synaptically-competent neurons derived from canine embryonic stem cells by lineage selection with EGF and noggin. *PLoS ONE*, 6(5), e19768.
- Wilcox, J. T., Semple, E., Gartley, C., Brisson, B. A., Perrault, S. D., Villagómez, D. A. F., ... Betts, D. H. (2009). Characterization of Canine Embryonic Stem Cell Lines Derived From Different Niche Microenvironments. *Stem Cells and Development*, 18(8), 1167–1178.
- Williams, K., Christensen, J., Pedersen, M. T., Johansen, J. V., Cloos, P. A. C., Rappsilber, J., & Helin, K. (2011). TET1 and hydroxymethylcytosine in transcription and DNA methylation fidelity. *Nature*.
- Wray, J., Kalkan, T., Gomez-Lopez, S., Eckardt, D., Cook, A., Kemler, R., & Smith, A. (2011). Inhibition of glycogen synthase kinase-3 alleviates Tcf3 repression of the pluripotency network and increases embryonic stem cell resistance to differentiation. *Nature Cell Biology*, 13(7), 838–845.
- Wu, H., D'Alessio, A. C., Ito, S., Xia, K., Wang, Z., Cui, K., ... Zhang, Y. (2011). Dual functions of Tet1 in transcriptional regulation in mouse embryonic stem cells. *Nature*.
- Wu, J., Greely, H. T., Jaenisch, R., Nakauchi, H., Rossant, J., & Belmonte, J. C. I. (2016). Stem cells and interspecies chimaeras. *Nature*.
- Wu, S. C., & Zhang, Y. (2010). Active DNA demethylation: Many roads lead to Rome. *Nature Reviews Molecular Cell Biology*.
- Xie, D., Chen, C. C., Ptaszek, L. M., Xiao, S., Cao, X., Fang, F., ... Zhong, S. (2010). Rewirable gene regulatory networks in the preimplantation embryonic development of three mammalian species. *Genome Research*.
- Xu, Y., Wu, F., Tan, L., Kong, L., Xiong, L., Deng, J., ... Shi, Y. G. (2011). Genome-wide Regulation of 5hmC, 5mC, and Gene Expression by Tet1 Hydroxylase in Mouse Embryonic Stem Cells. *Molecular Cell*.
- Yachie-Kinoshita, A., Onishi, K., Ostblom, J., Langley, M. A., Posfai, E., Rossant, J., & Zandstra, P. W. (2018). Modeling signaling-dependent pluripotency with Boolean logic to predict cell fate transitions. *Molecular Systems Biology*, 14(1).
- Yagi, M., Kishigami, S., Tanaka, A., Semi, K., Mizutani, E., Wakayama, S., ... Yamada, Y. (2017). Derivation of ground-state female ES cells maintaining gamete-derived DNA methylation. *Nature*.
- Yanes, O., Clark, J., Wong, D.M., Patti, G.J., Sanchez-Ruiz, A., Benton, H.P., ... Siuzdak, G. (2010). Metabolic oxidation regulates embryonic stem cell differentiation. *Nat Chem Biol*.

- Yang, J., Van Oosten, A. L., Theunissen, T. W., Guo, G., Silva, J. C. R., & Smith, A. (2010). Stat3 activation is limiting for reprogramming to ground state pluripotency. *Cell Stem Cell*.
- Yeo, J. C., Jiang, J., Tan, Z. Y., Yim, G. R., Ng, J. H., Göke, J., ... Ng, H. H. (2014). Klf2 is an essential factor that sustains ground state pluripotency. *Cell Stem Cell*.
- Yin, Y., Morgunova, E., Jolma, A., Kaasinen, E., Sahu, B., Khund-Sayeed, S., ... Taipale, J. (2017). Impact of cytosine methylation on DNA binding specificities of human transcription factors. *Science*.
- Ying, Q.-L., Wray, J., Nichols, J., Batlle-Morera, L., Doble, B., Woodgett, J., ... Smith, A. (2008). The ground state of embryonic stem cell self-renewal. *Nature*, 453(7194), 519–523.
- Ying, Q. L., Nichols, J., Chambers, I., & Smith, A. (2003). BMP induction of Id proteins suppresses differentiation and sustains embryonic stem cell self-renewal in collaboration with STAT3. *Cell*.
- Ying, Q. L., Stavridis, M., Griffiths, D., Li, M., & Smith, A. (2003). Conversion of embryonic stem cells into neuroectodermal precursors in adherent monoculture. *Nature Biotechnology*.
- Yoder, J. A., Soman, N. S., Verdine, G. L., & Bestor, T. H. (1997). DNA (cytosine-5)-methyltransferases in mouse cells and tissues. Studies with a mechanism-based probe. *Journal of Molecular Biology*.
- Zeng, X., & Rao, M. S. (2007). Human embryonic stem cells: Long term stability, absence of senescence and a potential cell source for neural replacement. *Neuroscience*.
- Zhang, H., Badur, M. G., Divakaruni, A. S., Parker, S. J., Jäger, C., Hiller, K., ... Metallo, C. M. (2016). Distinct Metabolic States Can Support Self-Renewal and Lipogenesis in Human Pluripotent Stem Cells under Different Culture Conditions. *Cell Reports*, 16(6), 1536–47.
- Zhang, H., Gayen, S., Xiong, J., Zhou, B., Shanmugam, A. K., Sun, Y., ... Dou, Y. (2016). MLL1 Inhibition Reprograms Epiblast Stem Cells to Naive Pluripotency. *Cell Stem Cell*.
- Zhang, H., Zhang, X., Clark, E., Mulcahey, M., Huang, S., & Shi, Y. G. (2010). TET1 is a DNA-binding protein that modulates DNA methylation and gene transcription via hydroxylation of 5-methylcytosine. *Cell Research*.
- Zhang, J., Khvorostov, I., Hong, J. S., Oktay, Y., Vergnes, L., Nuebel, E., ... Teitell, M. A. (2011). UCP2 regulates energy metabolism and differentiation potential of human pluripotent stem cells. *The EMBO Journal*, 30(24), 4860–4873.

- Zhang, L., Lu, X., Lu, J., Liang, H., Dai, Q., Xu, G. L., ... He, C. (2012). Thymine DNA glycosylase specifically recognizes 5-carboxylcytosine-modified DNA. *Nature Chemical Biology*.
- Zhang, Y., Cui, P., Li, Y., Feng, G., Tong, M., Guo, L., ... Zhou, Q. (2018). Mitochondrially produced ATP affects stem cell pluripotency via Act16a-mediated histone acetylation. *FASEB Journal*.
- Zhou, W., Choi, M., Margineantu, D., Margaretha, L., Hesson, J., Cavanaugh, C., ... Ruohola-Baker, H. (2012). HIF1 α induced switch from bivalent to exclusively glycolytic metabolism during ESC-to-EpiSC/hESC transition. *The EMBO Journal*, 31(9), 2103–2116.

Chapter 2

2 Manipulation of developmental signaling pathways alters the pluripotency characteristics of canine embryonic stem cells

A version of this chapter has been published:

Tobias, I.C., Brooks, C.R., Teichroeb, J.H., Villagómez, D.A, Hess, D.A., Séguin, C.A., and Betts, D.H. (2016). *Small-molecule induction of canine embryonic stem cells toward naive pluripotency*. *Stem Cells and Development* 25 (16), 1208-1222.

Reproduced here with permission from Mary Ann Liebert, Inc., New Rochelle, NY (Appendix B).

2.1 Introduction

Canine reproduction and early embryonic development exhibit peculiar features that have limited the progress of assisted reproduction technologies and embryo maturation protocols in this species (Nagashima et al., 2015; Van Soom et al., 2014). Briefly, canids release oocytes at the immature germinal vesicle-stage and trophoectoderm differentiation does not occur until ten days post-ovulation (Renton et al., 1991; Reynaud et al., 2006). *In vivo* matured canine blastocyst embryos have been collected from the reproductive tracts of artificially inseminated dams after slightly less than two weeks after ovulation (Reynaud et al., 2006). A number of canine embryonic stem cell (cESC) have been established from the outgrowths of spontaneously or mechanically hatched blastocysts (Hatoya et al., 2006; Hayes et al., 2008; Schneider et al., 2007; Vaags et al., 2009). However, there is no clear consensus regarding the appropriate embryonic stage for cESC derivation or which extrinsic signals are required for self-renewal of cESCs (Betts and Tobias, 2015). As such, most presumptive cESCs rapidly lose *in vitro* characteristics of pluripotency before detailed molecular characterizations can be performed (Koh and Piedrahita, 2014).

We have previously shown that cESCs exhibiting core pluripotency TF expression (e.g. OCT4, SOX2) and hESC-like cell surface epitopes (e.g. SSEA4, TRA-1-81) can be reproducibly derived on mouse embryonic fibroblast (MEF) feeders when cultured in media containing both LIF and FGF (L/F) (Wilcox et al., 2009). Whereas LIF supports the naïve pluripotent state in mice, primed mEpiSC or hESCs depend on FGF2 and Activin A-SMAD2/3 signaling (Brons et al., 2007; Dahéron et al., 2004; Tesar et al., 2007; Vallier et al., 2009). The dual requirement of L/F indicate that cESCs may reflect a mixture of naïve or primed pluripotency characteristics. Canine iPSCs have been shown to quickly re-establish variable surface marker abundances after fluorescence-activated cell sorting (FACS), indicating that the canine pluripotent state is metastable (Hayashi et al., 2008; Koh et al., 2013).

Similar to primed mEpiSCs, explant-derived cESCs in L/F undergo apoptosis unless propagated with clump passaging techniques and exhibit a neural lineage default in minimal media (Greber et al., 2010; Wilcox et al., 2011). These observations indicate that

L/F cESCs may represent the canine-equivalent of primed pluripotency, despite the requirement of LIF for prolonged self-renewal. The application of two inhibitors (i.e. PD0325901 and CHIR99021, known as 2i) that partially suppress MEK and GSK3 β kinase activity maintains mESCs in a naïve pluripotent state (Qi et al., 2004; Ying et al., 2008). 2i and LIF (2iL) has been shown to overcome intrinsic determinants that promote an unstable pluripotent state in mouse strains that were previously considered refractory (Hanna et al., 2009). Supplementation with 2iL also appears to be important to stabilizing a naïve pluripotent state in primates, although several additional kinase inhibitors are usually included (Gafni et al., 2013; Hanna et al., 2010; Theunissen et al., 2014). We and others have reported considerable morphological heterogeneity among the outgrowths of canine blastocysts in the early derivation process, but there is no direct molecular evidence that multiple pluripotent states can be adopted by cESC (Vaags et al., 2009; Wilcox et al., 2009).

Given the partially conserved role of 2iL molecules to stabilize rodent and primate ESCs in a naïve-like pluripotent state in the absence of ectopic transgene expression, we explored the possibility that altering the culture conditions may induce an earlier development state in cESCs. We report the induction of a distinct state of canine pluripotency through modulation of environmental cues and intracellular signal transduction using 2iL. Our results demonstrate that the 2iL-enriched canine pluripotent state correlates with increased expression of genes associated with the preimplantation mammalian blastocyst, augmented STAT3 signaling, improved clonogenic potential, and decreased global repressive epigenetic modifications.

2.2 Materials and Methods

2.2.1 Feeder layer and Embryonic Stem Cell Culture

DR4 strain MEF feeders were mitotically arrested with γ -irradiation (8,000 rad) and maintained in Dulbecco's modified Eagle's medium (DMEM) supplemented with 10% fetal bovine serum (FBS) and 1X GlutaMAX. For co-cultures with cESCs, MEFs were seeded at a density of 2×10^4 cells/cm² and allowed to adhere overnight in MEF medium. cESCs were derived at the Ontario Veterinary College (OVC, University of Guelph,

Ontario) from explanted blastocysts (OVC.EX) and characterized in an earlier report (Wilcox et al., 2009). cESCs were seeded onto growth-arrested MEFs and cultured in basal media: KnockOut DMEM/Ham's F12, 15% KnockOut Serum Replacement (KOSR), 1X GlutaMAX, 1X nonessential amino acids, 10 ng/mL recombinant insulin-like growth factor (R₃IGF1; Sigma-Aldrich), and 0.1 mM 2-mercaptoethanol. Basal medium was supplemented with 10 ng/mL human recombinant LIF and 4 ng/mL recombinant human FGF2 (L/F) for maintenance of control cESCs; or 10 ng/mL human recombinant LIF, 0.5 μM MEK inhibitor PD0325901 (Selleck Chemicals), and 3 μM GSK3β inhibitor CHIR99021 (BioVision) for establishment and culture of 2iL cESCs. LIF-FGF2 cESC colonies were mechanically isolated, dissected into small clumps, and transferred onto fresh MEFs every 4–6 days. 2iL cESC colonies were picked from culture, dissociated enzymatically with TrypLE Express, and split onto new feeder layers. For feeder-free cESC cultures, dishes were covered in dilute Geltrex (1:100) solution and incubated at 37 °C for one or more hours. cESCs transferred to Geltrex-coated dishes were cultured with 70% MEF-conditioned medium balanced with nonconditioned basal media. Culture medium was exchanged daily and incubators were maintained at 37 °C, 5% CO₂, and ambient oxygen tensions. Unless otherwise stated, all reagents for cell culture were from Thermo Fisher Scientific.

2.2.2 Metaphase Spread Preparation and Karyotyping

Cells were seeded into Geltrex-coated T75 flasks and grown to 60% confluency before metaphase spread preparation. Approximately 16 hours before spread preparations, dividing cells were synchronized with 100 nM Methotrexate in fresh media. Cells were released from replication block with 10 mM thymidine and incubated for 3 hours at 37 °C. Cells were treated with 1.25 mM Ethidium Bromide for 50 minutes to prevent excessive chromosome compaction and 10 μg/mL Colcemid for 30 minutes to induce metaphase arrest. Cells were then dissociated, suspended in hypotonic solution (75 mM Potassium Chloride), and incubated at 37 °C for 15 minutes. A few drops of ice-cold Carnoy's fixative (3:1 methanol: acetic acid) were added and mixed by gentle agitation. The cells were pelleted and resuspended in the fixative twice before dropping the cells onto fixative-soaked microscope slides to prepare metaphase spreads. At least 30

metaphase cells were examined for each treatment group. Karyotypes were assembled according to ideograms using SmartType (Digital Scientific UK Ltd).

2.2.3 Reverse Transcription and Quantitative PCR

Cells were rinsed once with PBS and harvested directly into TRIzol Reagent. After phenol-chloroform extraction, the RNA was purified using the PureLinkTotal RNA Purification Kit. Quality and quantity of RNA samples were determined through spectrometry using a NanoDrop ND-2000. Genomic DNA was removed using RQ1 RNase-free DNase (Promega). Approximately 300 ng of total RNA was reverse transcribed using the SuperScript III First Strand cDNA synthesis kit (Thermo Fisher Scientific) with a random hexamer and oligo (dT)₁₅ primers (Promega). Primer pairs for each target gene were designed using NCBI Primer BLAST software, spanning an exon-exon junction where possible. Specificity of each primer set was determined if a single amplicon of the correct size was detected on a 2% agarose gel following electrophoresis. For primer sequences and amplicon sizes, see Table 2-1. Quantitative polymerase chain reaction (qPCR) was performed using the CFX384 detection system (BIO-RAD Technologies). To each reaction 5 μ L Power SYBR Green, 1 μ L custom oligonucleotide primers (250 nM final), 1 μ L water and 3 μ L template cDNA were added. Thermocycling conditions are as follows: 95 °C for 10 minutes, followed by 40 cycles of 95 °C for 20 seconds and 60 °C for 45 seconds. Relative transcript levels were normalized to internal reference gene TATA binding protein (TBP) using the $2^{-\Delta\Delta C_t}$ method and are expressed as relative ratios to L/F cESC samples.

Table 2-1. Custom oligonucleotide primer sequences

Gene Identifier	Sequence (5' to 3')	Amplicon Size (bp)
STAT3	F - CTGGGCATCAATCCTGTGGT R - CTCAGTCCTCGCTTTGTGGT	144
KLF4	F - CCATGGGGCCAACTACCCAC R - TGGGGTCAACACCATTCCGT	154
REX1	F - CGCCGACACCGTCCTCATCG R - GTTCCGCAGGGAGCGGCGGGC	161
GBX2	F - GCCTCTCCCGAGCGGTCTA R - AGACGAAATGGCCGGGGCTG	140
TBX3	F - AGACAGCCCTGCTACGGGGG R - CCCCTGCCACGTTGCGTGAT	133

PECAM1	F - GCACCCCCAGCCAACTTCACC R - TCCCCTGTCCGTCGCAGAGG	94
LIN28	F - GGCGGTGGAGTTCACCTTTA R - CCTTTGATCTGCGCTTCTGC	134
T/BRA	F - TGCAGTACCGAGTGGACACCT R - GCCGTTCTTGGTCACGATCATC	167
CER1	F - ACCTGGGACCCATGCCCTCAC R - GATCGTCTGGCCGAAGGGCAC	196
FGF5	F - AGCCACCTGATCCTCAGCGCC R - CGGGTCCGGGTTGCCCTTTG	70
OTX2	F - CTGCGAAGCAGTAAACCAGC R - GAACCCAGCCAGAAGGTCTC	129
SOCS3	F - CCCGCTTCGACTGCGTGCTC R - GAAGGCGGCTGCTCCGACAC	115
ACVR2B	F - TTCTGGATGTACCGCATCG R - TCATGAGCTGTGCCTTCCAG	163
LAMB1	F - ATGGTTCACGGACACTGCAT R - ATGTCGAAGTGGCACGAACT	167
GATA6	F - AGTGCGTGAAGTGCAGGCTCC R - ACGCGCTTCTGCGGCTTGAT	136
SNAI1	F - GTTTACCTTCCAGCAGCCCT R - AGAGAGTCCCAGATGAGCGT	108
ELF5	F - CTCCAGTCACCACACGTCG R - CCTGGGTTAGCAAGGCC	132
HAND1	F - AGCTGCAACAACACACTTGG R - AAGCATAGGGGCTTCGAAAT	218
FLK1	F - GTTGGGAGAGGAGAGAGGGT R - CAGTGCACCACAAAGACACG	112
TBP	F - GAGCTCTGGGATCGTGCCGC R - TCAGTGCAGTGGTTCGGGGC	169

2.2.4 Indirect Immunofluorescence Microscopy

Cells in multiwell dishes or Lab-Tek Chamber Slides (Thermo Fisher Scientific) formats were rinsed with PBS and fixed with 4% formaldehyde for 15 minutes. Cells were permeabilized with 0.1% Triton X-100 for 20 minutes. Epitope blocking was performed with 10% normal goat, donkey, or rabbit serum (Sigma-Aldrich) for 1 hour. The following primary antibodies were diluted to the indicated concentrations and incubated overnight at 4 °C: anti-OCT4, anti-OTX2, anti-GATA2, anti-GATA4, anti-TUJ1, anti-NES, anti-H3H27Me3 and anti-pSMAD2. For information regarding primary antibodies,

see Table 2-2. AlexaFluor 488 and/or AlexaFluor 547 secondary antibodies were diluted 1:250 in 5% serum and incubated at room temperature for 1 hour. Cells were counterstained with NucBlue specialized DAPI formulation. Cells were imaged on a Leica DMI 6000B with Orca Flash digital camera (Hamamatsu Photonics) using Leica Application Suite Advanced Fluorescence software (Leica Microsystems). H3K27me3-immunolabeled cells were observed with a Zeiss LSM 510 Duo Vario confocal microscope (Zeiss Canada, Inc.). Serial optical sections were taken in a total depth of 50–80 μ M. More than 30 images were assessed per treatment in three independent experiments. Nuclei were categorized based on the presence of well-delineated H3K27Me3 foci throughout the input stack. For representative images, extended depth of field composites was generated using ZProjector on ImageJ (National Institutes of Health). The primary antibody was replaced with diluent and incubated with the AlexaFluor secondary antibody to control for antibody specificity. Light or laser settings were unchanged when detecting the same primary antibody across samples. Brightness or contrast was set using secondary-only control and equivalent imaging parameters were applied to all other images.

Table 2-2. Primary antibody information

Target Protein	Isotype Species	Application (Dilution)	Supplier (Catalog)
OCT4	Mouse	WB (1:1000); IF (1:150)	Santa Cruz (sc-5729)
SOX2	Rabbit	WB (1:1000)	Cell Signaling (3579)
NANOG	Rabbit	WB (1:500)	Santa Cruz (sc-33759)
OTX2	Rabbit	WB (1:1000); IF (1:200)	Millipore (AB9566)
GATA2	Rabbit	IF (1:200)	Santa Cruz (sc-9008)
GATA4	Rabbit	IF (1:200)	Abcam (AB84593)
TUJ1	Mouse	IF (1:300)	BioLegend (MMS-435P)
NESTIN	Rat	IF (1:150)	DSHB (Rat-401)
STAT3	Rabbit	WB (1:1000)	Santa Cruz (sc-482)
p-STAT3 (T705)	Rabbit	WB (1:1500)	Santa Cruz (sc-7993-R)
ERK1/2	Rabbit	WB (1:2000)	Cell Signaling (4695)
p-ERK1/2 (T202/204)	Rabbit	WB (1:2000)	Cell Signaling (4377)
SMAD2/3	Rabbit	WB (1:1000)	Cell Signaling (3102)
p-SMAD2 (S465/467)	Rabbit	WB (1:1000); IF (1:150)	Cell Signaling (3101)

SMAD4	Rabbit	WB (1:1000)	Santa Cruz (sc-7154)
Histone H3	Rabbit	WB (1:1000)	Cell Signaling (9715)
Histone H3Ac	Rabbit	WB (1:1000)	Millipore (06-599)
H3K27me3	Rabbit	WB (1:1000); IF (1:250)	Millipore (07-449)
β -actin	Mouse	WB (1:30000)	Sigma (A3854)

2.2.5 Protein Extraction, SDS-PAGE and Western Blotting

Cells were rinsed in ice-cold PBS, scraped from 60 mm culture dishes and lysed in 200 μ L RIPA buffer (150 mM sodium chloride, 1% NP-40, 0.5% sodium deoxycholate, 0.1% sodium dodecyl sulfate, 50 mM Tris pH 8.0) with a protease and phosphatase inhibitor cocktail (EMD Millipore). Total protein concentration was determined by DC Protein Assay (BIO-RAD Technologies). Protein lysates were resolved on 4%–12% SDS-PAGE gels and transferred onto Immobilon polyvinylidene difluoride membranes. Epitope blocking was achieved by incubation with 5% skim milk powder/TBS/0.1% Tween-20 for 1 hour. The following primary antibodies at the indicated dilution were used: anti-OCT4, anti-SOX2, anti-NANOG, anti-OTX2, anti-pSTAT3, anti-STAT3, anti-pERK1/2, anti-ERK1/2, anti-pSmad2, anti-Smad2/3, anti-Smad4, anti-histone H3 lysine 27 trimethylated, anti-histone H3 acetylated, anti-histone H3, and β -actin horseradish peroxidase (HRP) conjugate. After 16 hours of primary antibody incubation, membranes were washed with TBS/0.1% Tween-20. Horseradish peroxidase (HRP)-coupled secondary anti-rabbit or anti-mouse IgG antibodies (Jackson Laboratories) were diluted in TBS/0.1% Tween-20 and applied to membranes for 1 hour at room temperature. Immune reactive protein epitopes were visualized by chemiluminescence on Molecular Imager VersaDoc System (BIO-RAD) and Quantity One software (BIO-RAD Technologies). Densitometry was performed using ImageLab 3.0 software (BIO-RAD Technologies).

2.2.6 Embryoid Body Formation and Directed Differentiation of Outgrowths

Cells were mechanically isolated and briefly triturated in basal culture media lacking 2iL. Disaggregated cESCs were transferred to suspension culture in non-adherent dishes to

form embryoid bodies (EBs). Basal media were exchanged daily for 7 days by allowing EBs to settle at the bottom of a conical tube and aspirating the supernatant. To promote neuroectoderm differentiation, 2iL-derived embryoid aggregates were gently dissociated and seeded onto laminin- and poly-L-ornithine-coated dishes in the presence of Activin/NODAL signaling antagonist 1 μ M SB431542 (SB431542) and 20 ng/mL Noggin (Sigma-Aldrich). Mesodermal fate was induced using 10 ng/mL BMP4 and 10 ng/mL FGF2 on a gelatin substratum. Endoderm differentiation was induced by chemical stimulation of WNT signaling using 1 μ M CHIR99021 and co-supplemented with 20 ng/mL Activin A on Geltrex-coated dishes. After 7 days under differentiation conditions, each experimental group were fixed with formaldehyde for immunocytochemistry.

2.2.7 Neural Progenitor Cell Formation Assay

Cells were mechanically isolated and disaggregated into small clumps by gentle pipetting. Cells were resuspended in basal culture medium lacking self-renewal supplements (e.g. LIF and FGF2, 2i and LIF) and transferred to suspension culture in non-adherent dishes to form EBs. Basal media were exchanged every other day for 5 days. The resultant EBs from L/F or 2iL cESCs were gently dissociated by pipetting and allowed to adhere to multiwell dishes coated with laminin and poly-L-ornithine. EB outgrowths were allowed to differentiate in basal media (i.e. spontaneous differentiation) or in basal media supplemented with 20 ng/mL Noggin (i.e. directed differentiation). After four days under adherent differentiation conditions, cells were fixed with 4% formaldehyde and prepared for indirect immunofluorescence microscopy. Primary and secondary antibody staining was performed with anti-NES antibody and AlexaFluor 488 secondary antibody. The number of EB outgrowths exhibiting positive NES staining were enumerated for each condition.

2.2.8 Manipulation of TGF β Signaling

For the BMP4 differentiation assay, LIF-FGF2 and 2iL cESCs were exposed to 20 ng/mL recombinant human BMP4 in addition to their standard culture media preparation for a period of 96 hours. Cells were harvested from multiwell dishes using TRIzol reagent for RNA isolation. RNA purification and first-strand cDNA synthesis were performed for

RT-qPCR. Transcript abundances indicative of mesoderm and extraembryonic lineages (e.g. CDX2, HAND1, GATA6, FLK1) were assessed. To examine LIF-FGF2 cESC responsiveness to SMAD2/3 signaling, cultures were supplemented with either 10 μ M activin receptor-like kinase (ALK) inhibitor SB431542 or 20 ng/mL Activin A for 96 hours before protein lysate harvest for western blotting.

2.2.9 Single-cell Cloning Efficiency Assay

To examine clonogenic potential, individual L/F or 2iL cESC colonies were mechanically isolated and incubated in 0.05% Trypsin to dissociate into single cells. Cells were resuspended in culture media containing LIF only, FGF2 only, L/F, or 2iL and passed through a 40- μ M cell strainer. Media with no growth factor or chemical inhibitor supplementation were applied for negative controls. Five hundred cells were seeded per well of a 24-well plate ($n = 6$). After 7 days, cells were washed in PBS and stained with AlexaFluor 488 anti-SSEA4 antibody (eBioscience) diluted 1:150 in cESC culture media. Following a 60 minutes incubation in a humidified incubator, cells were washed with PBS and direct immunofluorescence was visualized. Colony-forming efficiency was calculated as a percentage of SSEA4⁺ colonies per number of cells seeded.

2.2.10 Cell Counting and Population Doubling Time Calculation

For linear phase population doubling, 50,000 cESCs were seeded onto MEF-coated multiwell dishes in triplicate. Cells were detached at 96 and 144 hour timepoints using 0.05% trypsin to achieve a single-cell suspension. The total live cell number was determined using a hemocytometer. Population doubling time was calculated using the following formula: $PD = 48 X \left[\log 2 \div \log \left(\frac{\# \text{ cells day } 6}{\# \text{ cells day } 4} \right) \right]$.

2.2.11 5-methylcytosine Enzyme-linked Immunosorbent Assay (ELISA)

L/F or 2iL cESCs were dissected from culture dishes, pelleted by centrifugation and rinsed with PBS. Genomic DNA was purified using PureLink Genomic DNA kit. Global 5-methylcytosine (5-mC) levels were determined using the 5-mC DNA ELISA kit (Zymo Research Corp.) according to the manufacturer's instructions. A standard curve was

generated using *E. coli* control samples provided with the kit and raw data were calculated as percent 5-mC per 150 ng genomic DNA. Output values were corrected by the CpG density specific to canine genomic assembly and expressed as a relative ratio to L/F cESC samples.

2.2.12 Immunodeficient Mouse Xenograft Assay

1.2×10^6 LIF-FGF2 or 2iL cESCs ($n = 3$) were transplanted into Non-Obese Diabetic Severe Combined Immunodeficient (NOD/SCID) interleukin-2 receptor γ -chain null (IL2R $\gamma^{-/-}$) mice (Jackson Laboratory). HES2 hESC lines were injected as positive controls ($n = 2$). Cells were suspended in 50 mL Geltrex and kept on ice (<20 min) before intramuscular injection in rear hind leg. Injection sites were monitored every other day by palpation. Between 6 weeks and 10 weeks post-injection, mice were anesthetized with isoflurane and sacrificed by cervical dislocation, and the area of muscle around the injection site was excised. Samples were rinsed in PBS before overnight fixation in 4% paraformaldehyde. Fixed tissues were processed for embedding and sectioning. Hematoxylin and eosin staining were performed on sections. Animal experiments were approved by the Animal Use Subcommittee, AUP #2018-033 (Appendix C).

2.2.13 Statistical Analysis

Experiments were performed a minimum of three times with sample sizes indicated in figure legends. Data were analyzed using GraphPad Prism 6 by two-sample t-test or one-way analysis of variance (ANOVA) followed by Tukey's honestly squared difference multiple comparison method as appropriate. $P < 0.05$ was considered statistically significant. Data were visualized using GraphPad Prism 6 and presented as mean \pm standard error of the mean (SEM).

2.3 Results

2.3.1 PD0325901, CHIR99021 and LIF (2iL) induce compact cESC colony morphology

OVC.EX cESCs were expanded on MEFs by mechanical dissociation and expansion in LIF-FGF2 (L/F) medium. L/F cESCs were grown to high confluency (~80%) prior to

switching to 2iL supplemented medium due to strong negative selection associated with coercing pluripotent state transitions by kinase inhibitors (Fig. 2-1A). Consistent with earlier work on the same cESC lines (Wilcox et al., 2009), L/F cESCs exhibited planar morphology akin to hESCs/EpiSCs (Fig. 2-1B) and did not survive passaging regimens involving enzymatic dissociation reagents or mechanical dispersion to single-cells. 2iL culture was initially associated with observable cell death for a period of 72 hours. Within 4 to 5 days, three-dimensional cell clusters emerged from a proportion of cESC colonies. By 10 to 14 days, hemispherical colonies with compact borders were observed (Fig. 2-1B). Confocal microscopy and z-stack reconstruction of DAPI-stained colonies verified that 2iL treated cells formed multilayer stacks of cells, as opposed to L/F cESCs that invariably grew as monolayer colonies (Fig. 2-1C). Mature 2iL cESC colonies were maintained in the same medium applied for their induction and reproduced a canine 78 XY karyotype of the originating L/F cESC population (Fig. 2-2A).

When 2i is removed from the growth media, cESCs rapidly lose dome-like colony morphology (Fig. 2-2B). Before enzymatic dissociation could be employed, 2iL cESCs initially had to be enriched by sequential pick-passaging, to reduce the carry-over of neural progenitor-like cells that arose during the induction of 2iL cESCs (Fig 2-2C-D). As genetic background has been shown to influence the ability to derive naïve PSCs, the procedure was repeated in three independent OVC.EX cESC lines (Ohtsuka and Niwa, 2015; Wilcox et al., 2009) (OVC.EX.IO3, OVC.EX.IO7, and OVC.EX.BE5) with preliminary characterization of morphology and SSEA4 immunostaining (Fig. 2-3). OVC.EX.BE5 cESC that readily differentiate into each of the three germ layers *in vitro* (Wilcox et al., 2009) were selected for extended passaging and subsequent analysis in L/F and 2iL conditions. These findings suggest that removal of FGF2 and replacement with 2i permits the expansion of a scarce ESC-like population, which can be subsequently enriched based on compact colony architecture.

2.3.2 2iL cESCs are pluripotent and up-regulate transcript markers of an earlier developmental identity

To ensure 2iL-expanded canine cells retained pluripotent characteristics, we performed immunoblotting and immunofluorescence of pluripotency-associated transcription

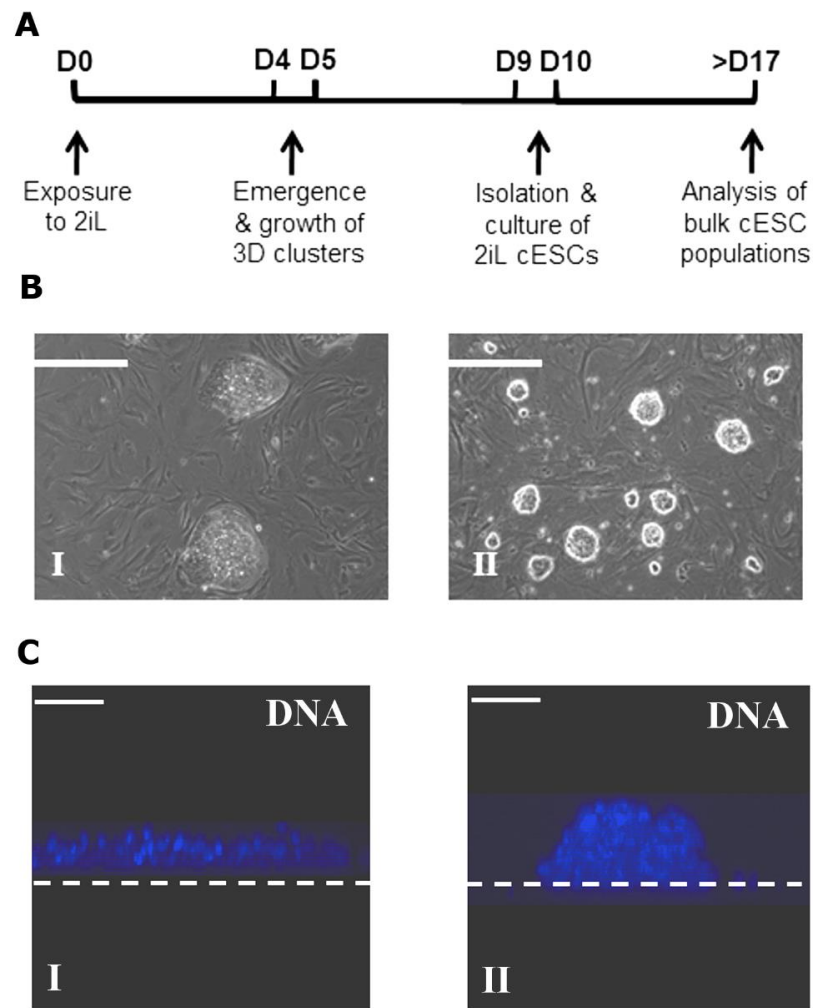


Figure 2-1. PD0325901, CHIR99021 and LIF (2iL) induce compact cESC colony morphology.

(A) Timeline schematic of induction, isolation and analysis of 2iL cESCs. (B) Representative phase-contrast micrographs of BE5 cESCs in (I) LIF and FGF2 (L/F) or (II) 2iL cESCs. Scale bar unit length is 200 μm . (C) Representative cross-section of reconstructed Z-stack image for DAPI-stained (I) L/F (monolayer) and (II) 2iL (multi-layer) cESC colonies. Dashed white line approximates the culture surface. Scale bar unit length is 50 μm .

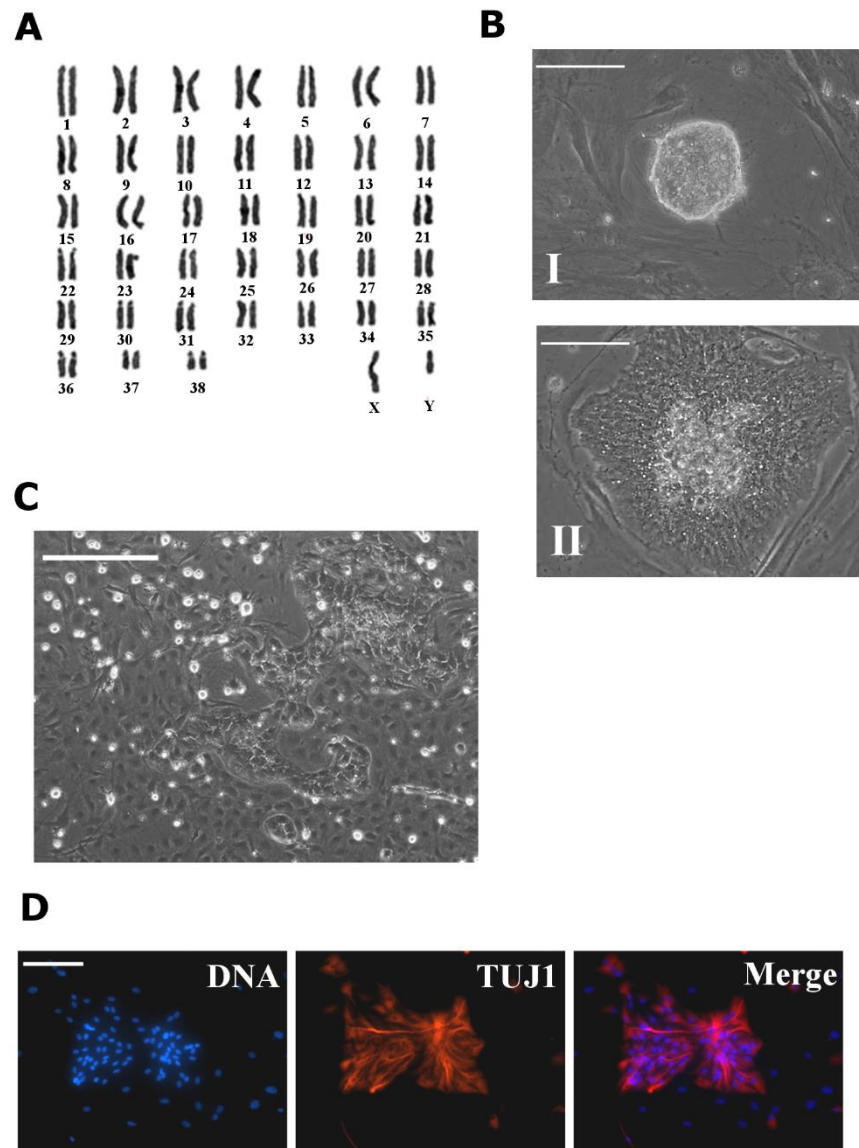


Figure 2-2. 2iL cESCs are dependent on the 2i molecules for compact morphology.

(A) Representative diploid karyotype ($2n = 78$ XY) from the BE5 2iL cESC line. (B) Representative phase-contrast micrograph of (I) steady-state 2iL cESC or (II) differentiating 2iL cESC colony 48 hours after 2i removal. Scale bar unit length is 100 μm . (C) Representative phase-contrast micrograph of neural progenitor-like cells derived from LIF-FGF2 (L/F) cESCs that proliferate in 2iL culture. Scale bar is 200 μm . (D) Indirect immunofluorescence image for class III neuronal beta-tubulin (TUJ1) antibody stain and DAPI nuclear counterstain. Scale bar unit length is 150 μm .

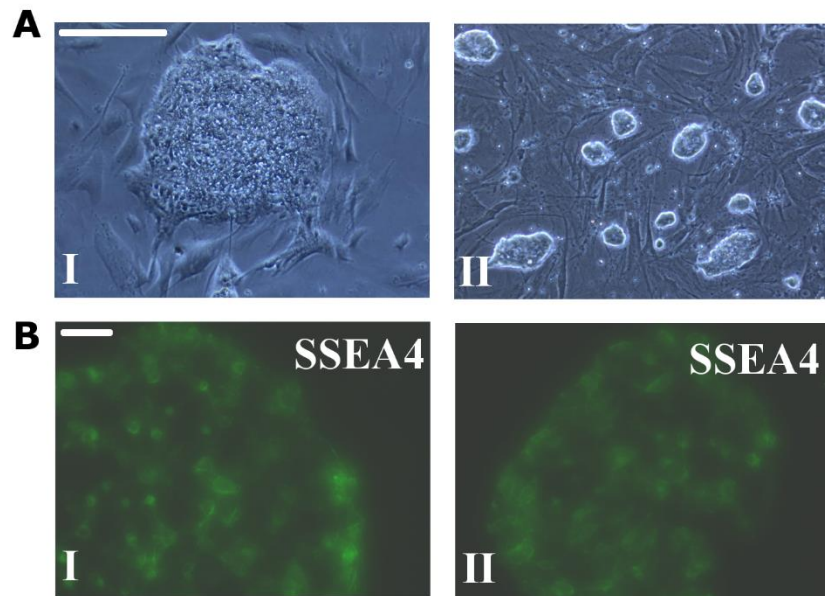


Figure 2-3. Establishment of 2iL cultures in the IO3 cESC line and preliminary characterization by stage-specific embryonic antigen 4 (SSEA4) staining.

(A) Representative phase-contrast micrographs of IO3 cESCs in (I) LIF and FGF2 (L/F) or (II) 2iL cESCs. Scale bar is 200 μm . (B) Direct immunofluorescence image for stage-specific embryonic antigen 4 (SSEA4) antibody stain. Scale bar unit length is 50 μm .

factors. There was no difference in OCT4 or SOX2 protein abundance between L/F and 2iL cESCs (Fig. 2-4A-B, $P = 0.76$ & $P = 0.36$). Both L/F and 2iL cESCs exhibited nuclear OCT4 staining (Fig. 2-4C). However, there was a significant induction of NANOG in 2iL cESC lysates compared to L/F cESC samples (Fig. 2-5A, $P = 9.0 \times 10^{-4}$). Further, OTX2 was significantly decreased in 2iL cESCs compared to L/F cESCs. (Fig. 2-5B, $P = 3.5 \times 10^{-3}$). OTX2 immunostaining was localized to the nucleus and perinuclear region of L/F cESC colonies, whereas specific intracellular OTX2 staining was not observed in 2iL cESCs (Fig. 2-5C). 2iL cESCs formed embryoid body (EB) aggregates in suspension culture to assess cESC pluripotency *in vitro* (Fig. 2-6A). 2iL cESCs formed EBs that could be directed to form putative early progenitors of endoderm, mesoderm, and ectoderm as assessed by fluorescent immunocytochemistry for expression of GATA4, GATA2, and neuronal beta-III tubulin (TUJ1), respectively (Fig. 2-6B-D).

We next investigated the gene expression signatures of several orthologous markers of naïve and primed pluripotency in L/F or 2iL cESCs to determine whether these cells bear transcriptional similarities to naïve mESC or primed mEpiSC/hESC. RT-qPCR analysis revealed that naïve-like cESCs stabilized in 2iL exhibit significant reductions in the relative transcript abundance of late epiblast markers, including FGF5, ACVR2B and OTX2 (Fig. 2-7A, $P < 0.039$). Conversely, a significant induction of naïve pluripotency markers REX1, TBX3, GBX2, PECAM1, and STAT3 (Fig. 2-7B, $P < 0.035$) was observed in 2iL cESCs. The relative abundance of KLF4 and LIN28 transcripts did not differ between L/F and 2iL cESCs (Fig. 2-7B). The down-regulation of naïve pluripotency-associated transcripts following 2i removal is consistent with destabilization of a naïve-like pluripotency program (Fig. 2-7B). These results suggest that 2iL promotes a pluripotent phenotype with altered transcriptional profile resembling the ICM/early epiblast, which is dependent on persistent repression of GSK3 β and MEK1/2 signaling.

2.3.3 STAT3 phosphorylation but not SMAD2/3 signaling are influenced by 2iL culture

To examine signaling pathways associated with maintenance of undifferentiated L/F and 2iL cESCs, we assessed the phosphorylation status of FGF-ERK, Activin-SMAD2/3, and LIF-STAT3 signal transduction proteins. The fraction of phosphorylated ERK1/2

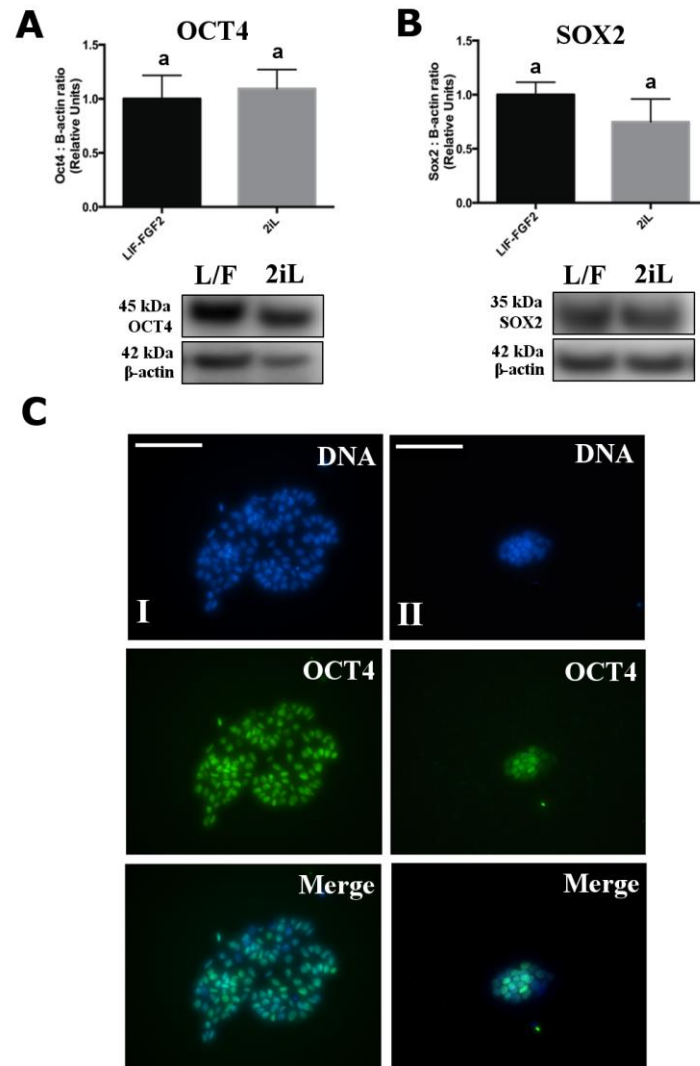


Figure 2-4. 2iL cESCs express SOX2 and OCT4 with nuclear localization.

Representative western blot images from whole cell lysates and quantification by densitometry for (A) OCT4 and (B) SOX2. Means are normalized to internal standard β -actin and expressed as a relative ratio to LIF-FGF2 (L/F) cESC samples. Bars represent standard error of the mean (SEM), $n = 3$. Means followed by the same letter are not significantly different, $P < 0.05$. (C) Representative indirect immunofluorescence image of OCT4 antibody stain and DAPI nuclear counterstain in (I) L/F cESCs and (II) 2iL cESC colonies. Scale bar unit length is $150 \mu\text{m}$.

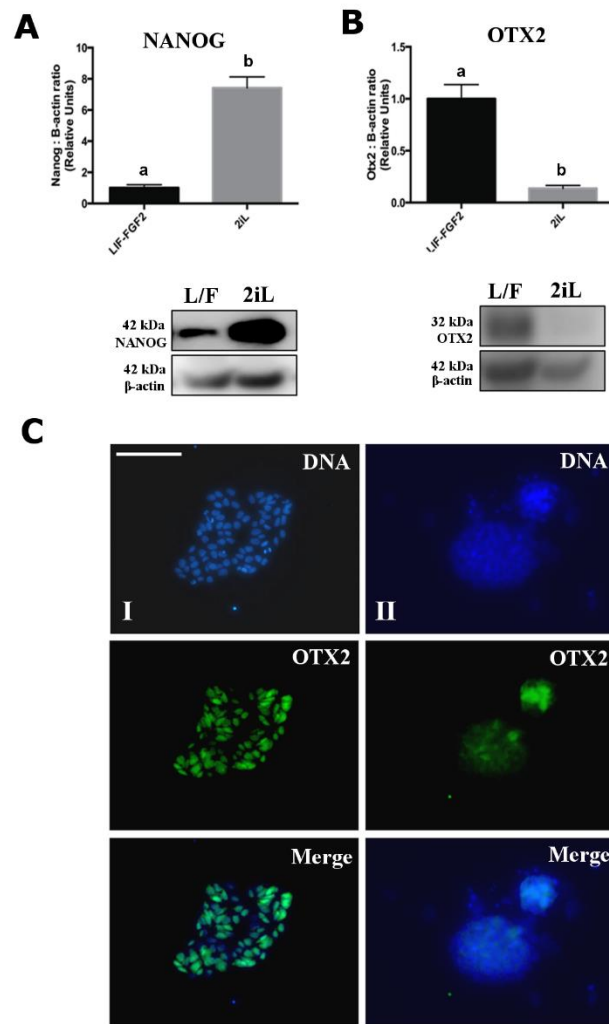


Figure 2-5. 2iL cESCs accumulate NANOG and down-regulate OTX2 compared to L/F cESCs.

(A). Representative western blot images from whole cell lysates and quantification by densitometry for (A) NANOG and (B) OTX2. Means are normalized to internal standard β -actin and expressed as a relative ratio to L/F cESC samples. Bars represent standard error of the mean (SEM), $n = 3$. Means followed by the same letter are not significantly different $P < 0.05$. (C) Representative indirect immunofluorescence image of OTX2 antibody stain and DAPI nuclear counterstain in (I) L/F cESCs and (II) 2iL cESC colonies. Scale bar unit length is 150 μ m.

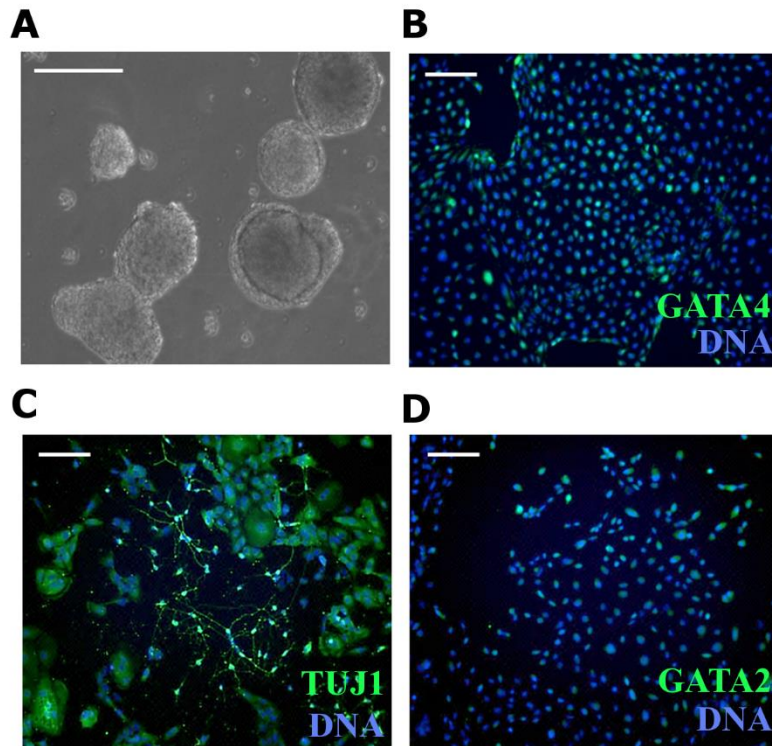


Figure 2-6. Canine ESCs expanded in 2iL retain tri-lineage differentiation capacity *in vitro*.

(A) Isolated 2iL cESCs form embryoid bodies (EBs) in suspension culture. EB outgrowths undergo directed differentiation to embryonic lineages in the presence of specific chemical inhibitors and growth factors. Scale bar unit length is 300 μm . (B) GATA4-positive cells form in the presence of Activin A and GSK3 β inhibitor CHIR. (C) Neuronal β III tubulin (TUJ1)-positive cells form in the presence of BMP inhibitor Noggin and ALK inhibitor SB431542. (D) GATA2-positive cells form in the presence of FGF2 and BMP4. Scale bar unit length is 75 μm and applies to panels B, C and D.

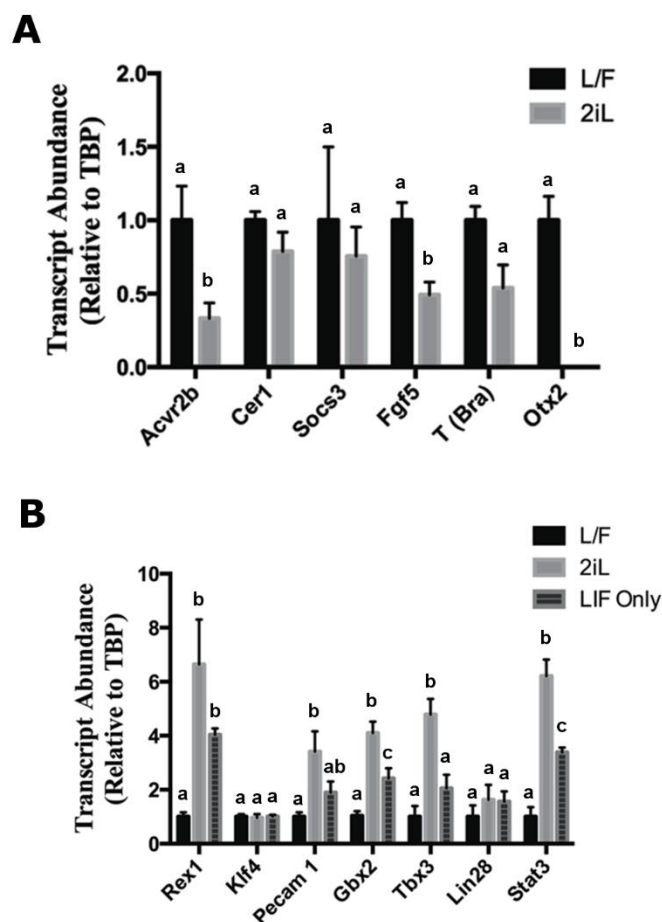


Figure 2-7. 2iL cESCs up-regulate several known naïve pluripotency-associated transcripts but not primed pluripotency-related markers.

(A) Abundance of discriminatory transcripts of mammalian primed pluripotency within L/F cESCs and cESCs cultured in 2iL. (B) Abundance of discriminatory transcripts of mammalian naïve pluripotency in L/F cESCs, 2iL cESCs and the cell population formed 96 hours after 2i removal (LIF Only). Means are normalized to internal standard TATA-binding protein (TBP) and expressed as relative ratios to L/F cESC samples. Bars represent standard error of the mean (SEM), $n=3$. Means followed by the same letter are not significantly different, $P < 0.05$.

(T202/204) was not significantly different between L/F and 2iL cESCs (Fig. 2-8A, $P = 0.20$). However, there was a significant increase in the ratio of phospho-STAT3 (Y705) to total STAT3 in 2iL cESC lysates compared to L/F cESCs (Fig. 2-8B, $P = 1.2 \times 10^{-3}$). Whereas the ratio of phospho-SMAD2 (S465/467) to total SMAD2/3 was unchanged between cESCs populations (Fig. 2-8C, $P = 0.74$). Fluorescence immunocytochemistry revealed no obvious difference in phospho-SMAD2 staining intensity, but unexpectedly revealed a clear pattern of nuclear exclusion under both conditions (Fig. 2-9A-B).

We further assessed the integrity of the SMAD2/3 signaling pathway in L/F cESCs, as well as the acute dependence on this pathway in steady-state culture. We quantified the relative abundance of phospho-SMAD2 and SMAD4 in the presence of exogenous Activin A or ALK inhibitor (SB431542). L/F cESCs were responsive to Activin A supplementation, inferred from elevated SMAD2 phosphorylation after 96 hours of treatment (Fig. 2-9C, $P = 1.8 \times 10^{-3}$). However, L/F cESCs also tolerated 10 μ M SB431542 with no overt differentiation over the same time course. Furthermore, SB431542 treatment did not significantly alter the ratio of phospho-SMAD2 to total SMAD2/3 protein levels compared to steady-state L/F cESCs (Fig. 2-9C, $P = 0.17$). Collectively these results suggest that 2iL cESCs have more pronounced STAT3 signaling with no change in SMAD2 phosphorylation. Furthermore, L/F cESCs have intact Activin-SMAD2/3 signal transduction machinery and need only low basal levels of SMAD2/3 phosphorylation for proliferation *in vitro*.

2.3.4 L/F cESCs exhibit a greater lineage-specific bias for neurectoderm and mesoderm differentiation

To investigate whether 2iL culture alters the inherent neural lineage bias of L/F cESCs, the ability of either cESC population to form NESTIN (NES) positive neural stem/progenitor cells under spontaneous and directed differentiation conditions were compared. Intriguingly, 2iL cESCs exhibited a lower efficiency of neural differentiation under spontaneous differentiation conditions ($P = 2.7 \times 10^{-3}$), but not under directed differentiation culture ($P = 0.402$), compared with L/F cESCs (Fig. 2-10A-B). Given the context-dependent role of BMP4 signaling in promoting mESC maintenance or inducing non-ectodermal differentiation of mEpiSC (Bernardo et al., 2011; Ying et al., 2003),

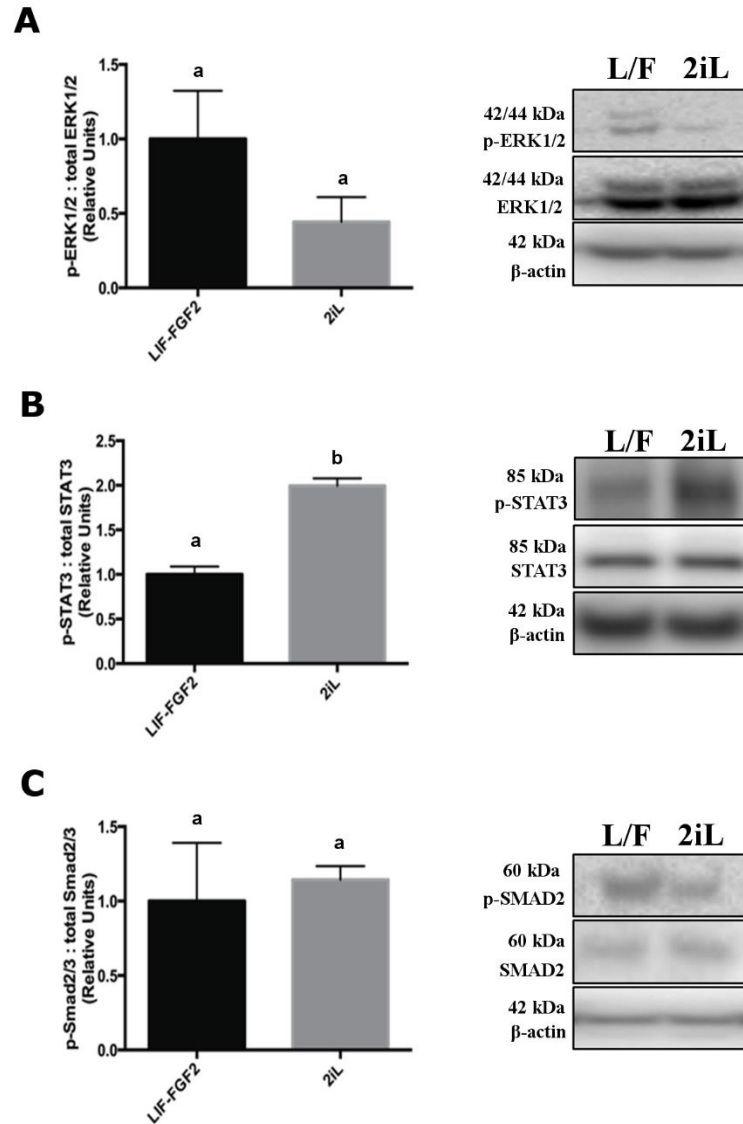


Figure 2-8. Enhanced STAT3 phosphorylation in 2iL-enriched cESCs.

Representative western blot membrane images and quantification by densitometry for phosphorylated (p) and total (A) ERK1/2, (B) STAT3 and (C) SMAD2. Means are normalized to internal standard β -actin and expressed as relative ratios to L/F cESC samples. Bars represent standard error of the mean (SEM), $n = 3$. Means followed by the same letter are not significantly different $P < 0.05$.

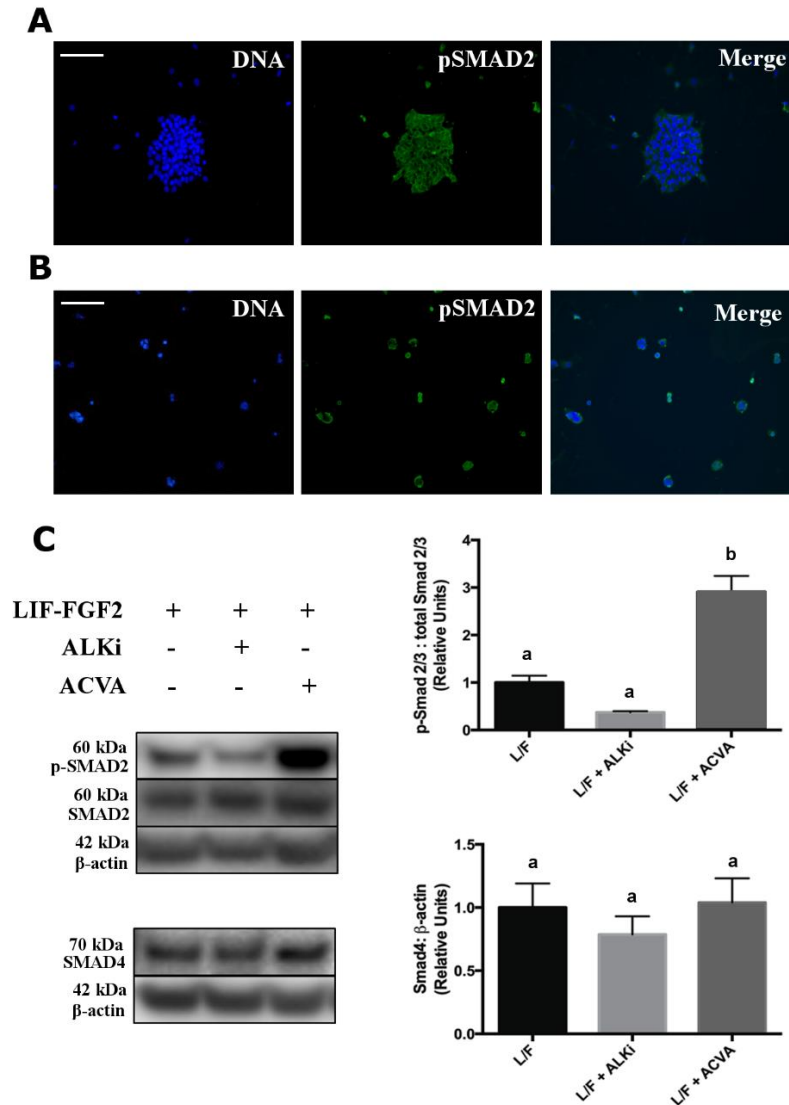


Figure 2-9. Steady-state L/F cESCs exhibit cytosolic phospho-SMAD2 and tolerate acute inhibition Activin-like kinase (ALK) activity.

Representative indirect immunofluorescence image for phosphorylated SMAD2 (pSMAD2) in (A) LIF-FGF2 cESCs and (B) 2iL cESCs. Nuclei were counterstained DAPI and the scale bar unit length is 200 μ m. (C) Representative immunoblot and densitometric quantification of phosphorylated and total SMAD2 as well as SMAD4 in L/F cESCs treated with 10 μ m SB431542 (ALKi) or 20 ng/mL Activin A (AcvA) for 96 hours. Bars represent standard error of the mean (SEM), $n = 3$. Means followed by the same letter are not significantly different, $P < 0.05$.

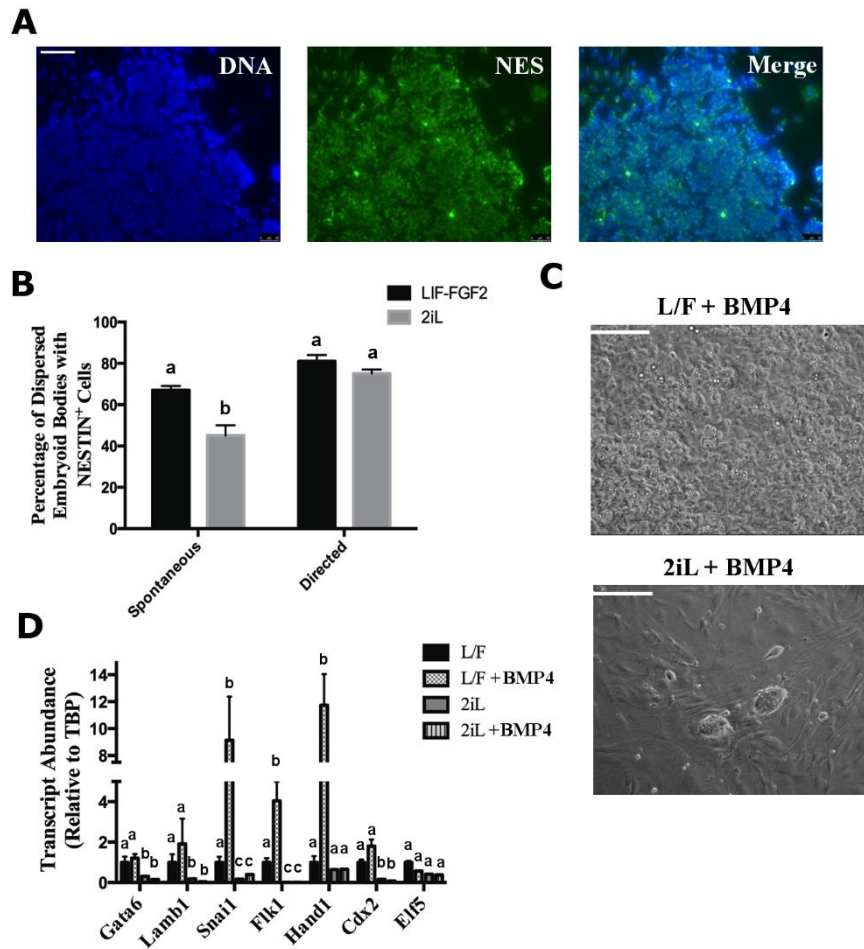


Figure 2-10. L/F cESCs exhibit a greater sensitivity for spontaneous neural differentiation and BMP4-induced mesendoderm differentiation.

(A) Representative indirect immunofluorescence image of neural intermediate filament protein Nestin (NES) antibody stain and DAPI nuclear counterstain. Scale bar unit length is 150 μ m. (B) Enumeration of NES⁺ embryoid body outgrowths L/F cESCs or 2iL cESCs in the presence of minimal media (spontaneous), or Noggin and SB431542 (directed). (C) Representative phase-contrast micrographs resultant L/F cESC or 2iL cESC cultures following 20 ng/mL BMP4 treatment for 96 hours. Scale bar unit length is 150 μ m. (D) Relative quantity of early differentiation transcripts associated with non-ectodermal lineages in L/F and 2iL cESC cultures in the presence and absence of 20 ng/mL BMP4. Bars represent standard error of the mean (SEM), n=3. Means followed by the same letter are not significantly different, $P < 0.05$.

we assessed the sensitivity of 2iL and L/F cESCs to differentiation in the presence of BMP4. L/F cESCs supplemented with 20 ng/mL BMP4 for 96 hours lost planar epithelium-like morphology and formed a heterogeneous mixture of narrow fibroblastic and broader vacuolated derivatives (Fig. 2-10C). In contrast, 2iL cESCs exhibited no observable morphological differentiation in a parallel BMP4 treatment (Fig. 2-10C). The expression of mesodermal markers Snail family transcriptional repressor (SNAIL), fetal liver kinase 1 (FLK1) and heat and neural crest derivatives expressed 1 (HAND1) were significantly upregulated following BMP4 addition to L/F cESCs ($P < 0.032$), but not for 2iL cESCs (Fig. 2-10D). Transcripts for pan-endodermal markers (SOX17, FOXA2) and visceral endoderm marker hepatocyte nuclear factor 4A (HNF4A) were not detected in BMP4-treated cESCs by RT-qPCR. In summary, 2iL cESCs exhibit a lesser intrinsic neural differentiation bias and a lower sensitivity to BMP-induced mesodermal differentiation. These results indicate that 2iL cESCs exhibit different regulative characteristics than L/F cESCs.

2.3.5 DNA methylation and H3K27me3 modifications are depleted in 2iL cESCs

To investigate whether 2iL enriched cESCs contain a lower abundance epigenetic modifications associated with development, we probed genomic DNA and protein samples from cESCs using antibodies that selectively recognize epitopes containing these covalent modifications. Culture of cESCs in 2iL induced a significant decrease in relative genome-wide DNA methylation compared with L/F cESCs (Fig. 2-11A, $P = 0.048$). In addition, the ratio of H3K27me3 to total histone H3 was increased in L/F cESCs compared to 2iL cESCs (Fig. 2-11B-C, $P = 0.031$). Pan histone H3 acetylation (H3Ac) did not significantly differ between L/F and 2iL cESCs (Fig. 2-11D, $P = 0.92$). Subtle differences in the pattern of nuclear H3K27me3 localization was also observed between cESC populations. L/F cESCs displayed non-uniform condensations of H3K27me3, whereas H3K27me3 immunofluorescence showed diffuse patterns in 2iL cESCs (Fig. 2-12A-C, $P < 6.5 \times 10^{-3}$). Collectively, our results suggest that epigenetic modifications associated with developmental gene silencing are less prominent in 2iL cESCs.

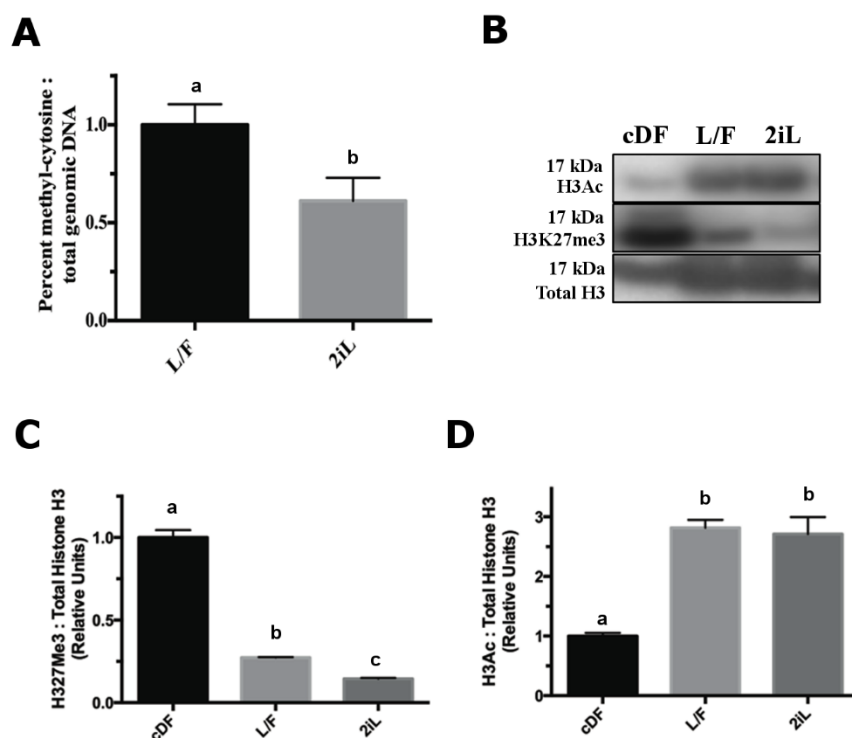


Figure 2-11. DNA methylation and H3K27me3 modifications are depleted in 2iL cESCs.

(A) Percent of 5-methylcytosine (5-mC) per 100 ng of purified genomic DNA, quantified in L/F cESCs and 2iL cESCs by 5-mC DNA ELISA. (B) Representative western blot images for total acetylated histone H3 (H3Ac), histone H3 lysine 27 trimethylation (H3K27Me3) and total histone H3. Densitometric quantification of (C) H3Ac and (D) H3K27Me3 normalized to total histone H3. Mean are expressed as relative ratios to canine dermal fibroblasts (cDFs) samples. Bars represent standard error of the mean (SEM), n=3. Means followed by the same letter are not significantly different, $P < 0.05$.

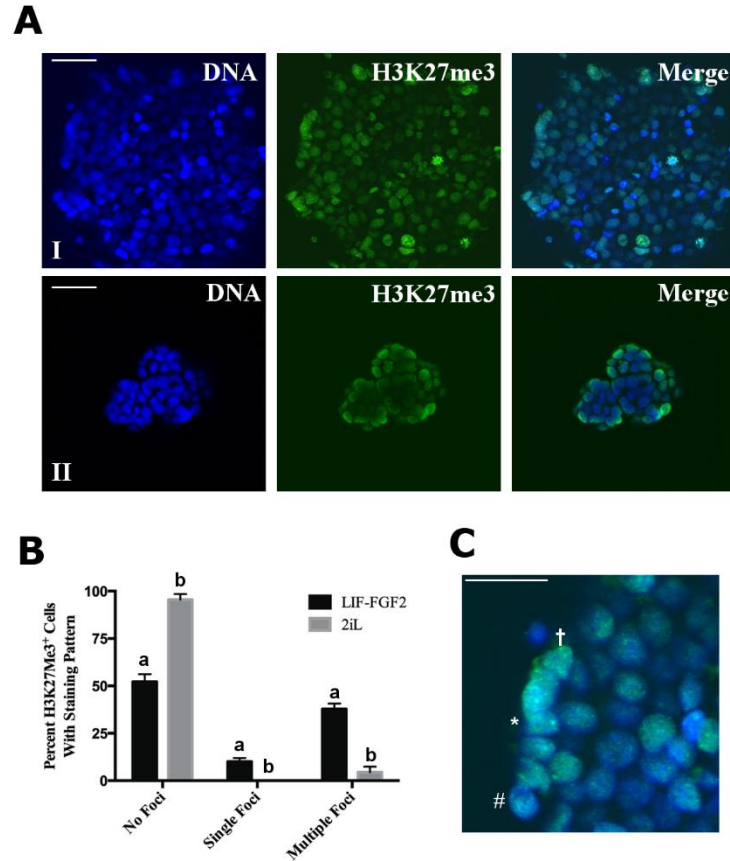


Figure 2-12. Decreased nuclear condensations of H3K27me3 antibody stain are observed in 2iL cESCs.

(A) Representative indirect immunofluorescence image of H3K27Me3 antibody staining in (I) L/F cESCs and (II) 2iL cESC colonies. The scale bar unit length is 100 μm (B) Barplot depicting the percentage of H3K27Me3⁺ nuclei that meet staining pattern criteria. Bars represent standard error of the mean, n=4. Means followed by the same letter are not significantly different, $P < 0.05$. (C) Digital zoom of merged image of L/F cESC in panel A with a scale bar unit length of 25 μm . The asterisks symbol (*) denotes a nucleus with a single focus, the dagger symbol (†) represents a nucleus with multiple H3K27Me3 clouds and the hash symbol (#) indicates a nucleus without observable condensations.

2.3.6 Enhanced colony-forming efficiency but not tumorigenicity of 2iL cESCs

Population doubling time and colony-forming efficiency were quantified to compare growth kinetics of cESCs populations, which is relevant for gene-targeting applications. Culture with 2iL significantly prolonged the calculated linear-phase population doubling time from approximately 33 hours in L/F cESCs to 52 hours in 2iL cESC cultures (Fig. 2-13A, $P = 3.0 \times 10^{-3}$). Moreover, the population doubling interval of both L/F and 2iL cESCs were significantly greater than that of conventional mESC and hESC lines (Fig. 2-13A, $P < 0.035$). Upon single-cell dissociation, the ability of L/F cESCs to re-establish pluripotent SSEA4⁺ colonies (~ 0.03% efficiency) was not significantly different from control media lacking LIF and/or FGF2 (Fig. 2-13B-C). In contrast, singularized 2iL cESCs re-seeded into 2i medium without LIF formed SSEA4⁺ colonies at a significantly lower efficiency (0.25%) compared with 2iL cESCs (3.18%) (Fig. 2-13D, $P < 0.0001$). The cloning efficiency achieved with 2i alone was significantly greater than medium containing only LIF or control basal medium (Fig. 2-13D, $P = 0.045$). Individualized 2iL cESCs have greater viability in single-cell suspensions compared to L/F cESCs following enzymatic dissociation (Fig. 2-13E, $P = 0.039$). Our findings suggest that 2iL culture compromises the rate of cESC proliferation but improves the ability of cESCs to form clonal populations, in part by reducing cell death when colonies are disaggregated.

Intramuscular xenograft assays were performed in NOD/SCID/IL2R $\gamma^{-/-}$ immune deficient mice to examine whether 2iL and L/F cESCs differ in their capacity for proliferation and differentiation *in vivo*. Control mice injected with hESCs (n = 2/2) generated well-formed teratomas by 6 weeks (Fig. 2-14A), composed of mature derivatives of mesoderm (hyaline cartilage), endoderm (villus epithelium), and ectoderm (melanocytes). However, no overt tumor growth was observed 10 weeks following transplantation of either L/F (n = 0/3) or 2iL (n = 0/3) cESCs.

Prolonged culture of independent 2iL cESC derivations (>20 passages) revealed that cESCs in 2iL media have a limited replication capacity in the undifferentiated state. It remains possible that karyotypically abnormal cells accumulate within extended cESC

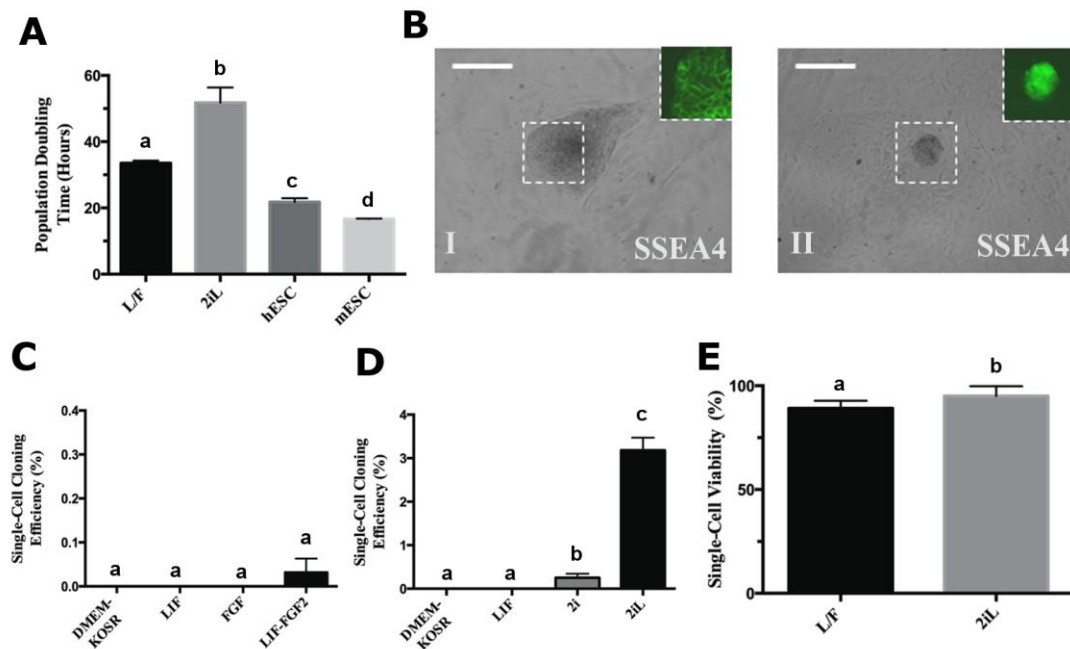


Figure 2-13. Altered growth kinetics and colony-forming efficiency between L/F and 2iL cESCs.

(A) Calculated population doubling time (hours) from cell counts in steady-state growth conditions for L/F cESCs, 2iL cESCs, human ESC line HES2 and mouse ESC line R1. (B) Representative images of SSEA4⁺ colonies from (I) L/F cESC or (II) 2iL cESC cultures, five-days post dissociation and seeding at clonal density. Scale bar unit length is 150 μ m. SSEA4⁺ colonies from (C) L/F cESC or (D) 2iL cESC cultures were counted, and single-cell cloning efficiency was calculated as a percentage of cells seeded. (E) Percentage of viability cESCs following enzymatic dissociation to single-cells of individual cESCs was identified by Trypan Blue exclusion. Bars represent standard error of the mean, n=3-6. Means followed by the same letter are not significantly different, $P < 0.05$.

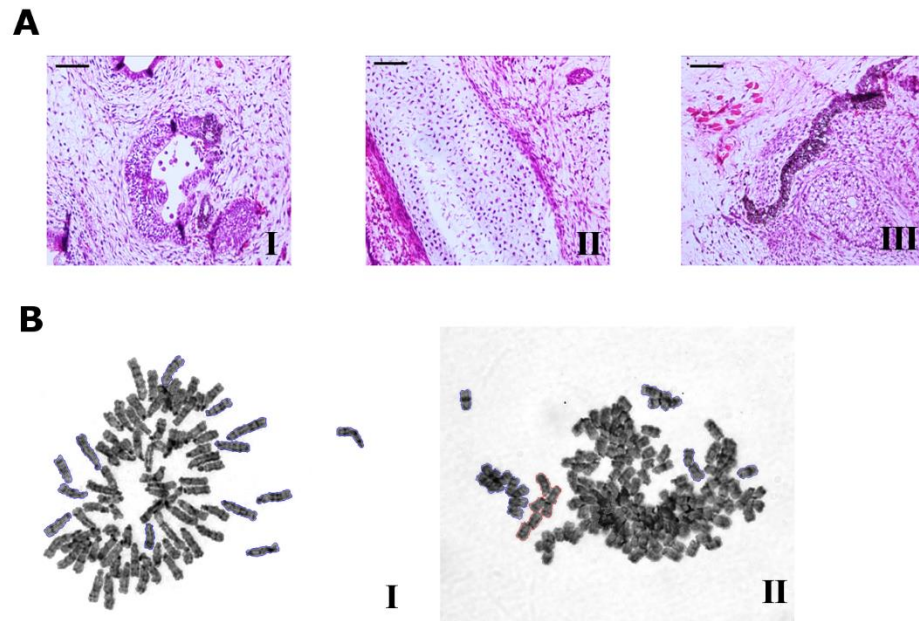


Figure 2-14. *In vivo* tumorigenicity and differentiation potential of typical human ESC line is not recapitulated by either L/F or 2iL cESCs.

(A) Representative hematoxylin and eosin stained sections of tumour derived from human ESC xenografts. Cell types and lineages represented include (I) villus gut epithelium (endoderm), (II) hyaline cartilage (mesoderm) and (III) pigmented epithelium (ectoderm). (B) Representative metaphase spreads of normal diploid (I) and abnormal polyploid (II) canine karyotypes.

culture by genetic drift. Metaphase spreads and Giemsa staining revealed detectable polyploid cell populations alongside karyotypically normal ($2n = 78 XY$) cESCs (Fig. 2-14B). Therefore, disruptions in cESC self-renewal long-term are associated with the emergence of karyotypic abnormalities in prolonged cESC culture.

2.4 Discussion

cESC lines with differing morphological and cell surface glycoproteins have been derived from canine preimplantation embryos (Vaags et al., 2009; Wilcox et al., 2009). However, heterogeneous features ascribed to these cESC cultures may be explained by the unique genetic backgrounds between individual embryo outgrowths. Previous cESC studies have limited the scope of investigation to core pluripotency-associated factors, rather than discriminatory markers of naïve versus primed pluripotency. Our data indicate that culture in 2iL enriches for a morphologically and molecularly distinct cESC population from originating L/F cESCs, which shares several features to other mammalian naïve PSCs. This naïve pluripotency-like phenotype was associated with elevated STAT3 phosphorylation, induction of several RNA transcripts characteristic of the mammalian epiblast and fewer epigenomic modifications associated with gene silencing. These findings provide the first evidence that partial repression of MEK1/2 and GSK3 β in the absence of exogenous FGF2 may support an earlier developmental state in cESCs.

After initial comparisons of the dog and human genome assembly revealed a high degree of genomic synteny (Ostrander and Wayne, 2005), the stem cell community was optimistic that cESC would exhibit greater similarity to hESC than mESC (Tecirlioglu and Trounson, 2007). In the absence of small molecule inhibitors, cESCs require exogenous FGF2 co-supplementation for *in vitro* proliferation (Vaags et al., 2009; Wilcox et al., 2009), which is reminiscent of primed mEpiSC/hESC. Conventional hESC lines are insensitive to LIF and refractory to nuclear reprogramming towards naïve-like pluripotency with 2i alone (Dahéron et al., 2004; Hanna et al., 2010). In contrast, mEpiSCs may be reverted to naïve pluripotent state in LIF-containing media and this process may be accelerated through the application of 2i (Adachi et al., 2018; Han et al., 2010; Onishi et al., 2012). In this respect, L/F cESCs more closely resemble the

developmental plasticity exhibited by mEpiSCs, which may be conferred to a subset of cESCs by pre-existing STAT3 signaling pathway activity. Accumulating evidence suggest that stabilization of naïve-like pluripotent state in primates requires a more comprehensive selection of inhibitors and growth factors (Gafni et al., 2013; Takashima et al., 2014; Theunissen et al., 2014; Ware et al., 2014). Hyperactivity of JAK/STAT3 signaling can drive reprogramming towards a naïve-like pluripotent state despite the presence of other antagonistic cues in both mice and humans (Chen et al., 2015; Van Oosten et al., 2012), lending support to a conserved role of STAT3 transcriptional activity in promoting a naïve pluripotency transcriptional network

Evolutionary variation to the wiring of pluripotency-associated transcription factors and their relationships to developmental signaling pathways may result in species-specific GRN memberships, hierarchical relationships, or characteristics of permissive niche microenvironments (Barakat et al., 2018; Glinsky, 2015; Kojima et al., 2017). We show that OCT4 and SOX2 are detected at similar levels in L/F and 2iL cESCs. Furthermore, we observe reciprocal changes in the abundance of NANOG and OTX2, which are expressed in the murine ICM/early epiblast or the late epiblast/anterior primitive streak, respectively (Acampora et al., 2012; Aizawa et al., 2004; Chambers et al., 2007). These findings indicate that changes to core pluripotency GRN topology in cESC during transitions between pluripotent states may share greater similarity to mESC/mEpiSC than human primed and naïve PSCs. With respect to the functional relevance of extrinsic factors promoting canine pluripotency, Luo *et al.* stipulated that LIF and FGF2 have anti-apoptotic and pro-proliferation roles in canine iPSC lines, respectively (Luo et al., 2011). In a follow up study, the same LIF and FGF2-dependent canine iPSC lines rely on paracrine Activin A signaling from MEF feeders (Luo and Cibelli, 2016). Conversely, L/F cESCs described in the present study appear to have adopted a self-renewal program largely unaided by Activin-SMAD2/3 signaling. We have not yet extended SB431542 treatments beyond a single passage of L/F cESCs to directly investigate the fundamental importance of ALK-SMAD2/3 signaling to long-term maintenance of primed-like cESCs. In our culture microenvironment, we provide exogenous ligands for the phosphoinositide 3 kinase-protein kinase B pathway (e.g. IGF, FGF2) that has been shown to modulate

SMAD2/3 signaling in hESC and in other cell types promote the cytosolic sequestration of SMAD2/3 (Conery et al., 2004; Remy et al., 2004; Singh et al., 2012).

Naïve and primed PSCs correspond to distinct spatiotemporal iterations of the developing embryo, and hence may be differentially responsive to lineage specifying cues in ways that reflect their *in vivo* approximate. BMP4 has a role in both naïve pluripotency maintenance and lineage restriction in the gastrulating embryo, the latter of which shares transcriptomic similarity to primed PSCs (Bernardo et al., 2011; Kojima et al., 2014; Ying et al., 2003). Induction of definitive mesoderm markers following BMP4 exposure in L/F cESCs but not in 2iL cESCs suggest the former is characteristic of precursors undergoing epithelial-to-mesenchymal transition. This response is consistent with the role of BMP4 in murine gastrulation in the formation primitive streak mesoderm (Winnier et al., 1995). We note that cell fate trajectories of BMP4-treated primed PSCs are highly contextual, and relative activities of the FGF or WNT signaling pathways may influence the predominant cell fate by crosstalk mechanisms (Bernardo et al., 2011; Bhushan et al., 2012). mEpiSCs share a transcriptome signature with the anterior primitive streak and appear to be poised for neural specification primed PSC (Iwafuchi-Doi et al., 2012; Kojima et al., 2014). Our L/F cESCs share a similar lineage bias towards neural lineages (Wilcox et al., 2011). We found that 2iL cESCs exhibit a less pronounced neural lineage bias under spontaneous differentiation conditions but not when differentiation is directed with Noggin. These findings indicate that 2iL cESC are likely not a direct precursor to the neural lineage and have a similar capacity for neural differentiation when appropriately specified.

2iL cESC colonies are induced over a prolonged time course (1-2 weeks), which is consistent with a selection or epigenetic reprogramming event rather than an adaptive response to a unique microenvironment. The difference in global DNA methylation between 2iL enriched cESCs compared to L/F cESCs is indicative of an epigenetic barrier that prevents the resetting of the most parental cESCs. Similar magnitudes of DNA demethylation are observed upon treatment of S/L mESC with 2i and has been mechanistically linked altered DNMT and TET enzyme activity (Hackett et al., 2013; Leitch et al., 2013). Consistent with the notion that 2iL cESCs adopt an earlier

developmental identity, we observed a decline in global H3K27me3. The H3K27me3 modification is a hallmark of polycomb repressive complex activity that establishes facultative heterochromatin during differentiation and the naïve to primed transition (Gifford et al., 2013; Tosolini et al., 2018). Histone H3 acetylation was maintained in 2iL culture compared to LIF-FGF2 cESCs, which may reflect generalized chromatin plasticity of the pluripotent state (Melcer et al., 2012; Meshorer et al., 2006). Further experimentation in genetically female cESC lines may shed light on the dynamics of X-chromosome inactivation in canine development. Interestingly, Whitworth *et al.* detected two active X-chromosomes in female canine iPSC lines and multipotent stromal cells, which may indicate species-specific regulation of X-chromosome activation status (Whitworth et al., 2014). Otherwise a lack of X-chromosome dosage compensation in canine iPSC-derived somatic cells could result from incomplete silencing of the six reprogramming transgenes (Whitworth et al., 2014).

Low clonogenicity related to slow growth kinetics and sensitivity to enzyme-induced apoptosis is generally understood as a property of primed PSCs (Hanna et al., 2010). Improvements in cloning efficiency with 2iL cESCs (~ 3%) are consistent to what other groups have reported in naïve porcine cell lines (~12%), but far below cloning efficiencies achieved in hESC and mESC lines (~40%) (Gafni et al., 2013; Gu et al., 2014). Furthermore, expansion of cESCs in 2iL did not grant teratoma-forming ability in immunodeficient mouse xenografts. Canine PSCs have had low success and poor reproducibility with these traditional *in vivo* assays of self-renewal and differentiation into mature lineages. The lack of any tumor mass following transplantation suggests that apoptosis or senescence within the *in vivo* niche may be a barrier to successful teratoma assay outcomes. Whereas the finite proliferation of 2iL cESCs is similar to what has been described for naïve ESC lines independent of ectopic transactors (Hanna et al., 2010) and may reflect the inability of the culture conditions to sustain the naïve transcriptional circuitry long-term.

In summary, the described work represents the first evidence for population-level metastability in canine PSCs and reveals an opportunity to alter pluripotent characteristics of cESCs using small-molecule kinase inhibitors. This study lends

additional support to a conserved role for 2iL in promoting a naïve-like pluripotent state in mammals. However, the 2iL culture medium appears to be unable to fully support the self-renewal of reset cESCs long term. Given the recent success of empirically consolidated kinase inhibitor combinations in primate ESCs, we suspect that subtle modifications to the 2iL culture system, alone or in combination with genetic modification, may support a stable naïve pluripotency phenotype. Although the growth kinetics and bioprocessing characteristics of cESC are suboptimal for applications in transplantation medicine, our results demonstrate that the binary L/F and 2iL cESC cultures can yield new insights into canine preimplantation development and conserved features of mammalian pluripotency.

2.5 References

- Acampora, D., Di Giovannantonio, L. G., & Simeone, A. (2012). Otx2 is an intrinsic determinant of the embryonic stem cell state and is required for transition to a stable epiblast stem cell condition. *Development*.
- Adachi, K., Kopp, W., Wu, G., Heising, S., Greber, B., Stehling, M., ... Schöler, H. R. (2018). Esrrb Unlocks Silenced Enhancers for Reprogramming to Naive Pluripotency. *Cell Stem Cell*.
- Aizawa, S., Takasaki, N., Matsuo, I., Kurokawa, D., Kimura-Yoshida, C., Nakayama, R., & Kiyonari, H. (2004). Regulation of Otx2 expression and its functions in mouse epiblast and anterior neuroectoderm. *Development*.
- Barakat, T. S., Halbritter, F., Zhang, M., Rendeiro, A. F., Perenthaler, E., Bock, C., & Chambers, I. (2018). Functional Dissection of the Enhancer Repertoire in Human Embryonic Stem Cells. *Cell Stem Cell*.
- Bernardo, A. S., Faial, T., Gardner, L., Niakan, K. K., Ortmann, D., Senner, C. E., ... Pedersen, R. A. (2011). BRACHYURY and CDX2 mediate BMP-induced differentiation of human and mouse pluripotent stem cells into embryonic and extraembryonic lineages. *Cell Stem Cell*.
- Betts, D. H., & Tobias, I. C. (2015). Canine pluripotent stem cells: Are they ready for clinical applications? *Frontiers in Veterinary Science*, 7(2): 41.
- Bhushan, R., Lehrach, H., Fauler, B., Adjaye, J., & Sudheer, S. (2012). FGF Inhibition Directs BMP4-Mediated Differentiation of Human Embryonic Stem Cells to Syncytiotrophoblast. *Stem Cells and Development*.

- Brons, I. G. M., Smithers, L. E., Trotter, M. W. B., Rugg-Gunn, P., Sun, B., Chuva de Sousa Lopes, S. M., ... Vallier, L. (2007). Derivation of pluripotent epiblast stem cells from mammalian embryos. *Nature*, 448(7150), 191–195.
- Chambers, I., Silva, J., Colby, D., Nichols, J., Nijmeijer, B., Robertson, M., ... Smith, A. (2007). Nanog safeguards pluripotency and mediates germline development. *Nature*.
- Chen, H., Aksoy, I., Gonnot, F., Osteil, P., Aubry, M., Hamela, C., ... Savatier, P. (2015). Reinforcement of STAT3 activity reprogrammes human embryonic stem cells to naive-like pluripotency. *Nature Communications*.
- Conery, A. R., Cao, Y., Thompson, E. A., Townsend, C. M., Ko, T. C., & Luo, K. (2004). Akt interacts directly with Smad3 to regulate the sensitivity to TGF- β -induced apoptosis. *Nature Cell Biology*.
- Dahéron, L., Opitz, S. L., Zaehres, H., Lensch, W. M., Andrews, P. W., Itskovitz-eldor, J., & Daley, Q. (2004). LIF/STAT3 signaling fails to maintain self-renewal of human embryonic Stem Cells. *Stem Cells*.
- Gafni, O. et al., Weinberger, L., Mansour, A. A., Manor, Y. S., Chomsky, E., Ben-Yosef, D., ... Hanna, J. H. (2013). Derivation of novel human ground state naive pluripotent stem cells. *Nature*, 504(7479), 282–6.
- Gifford, C. A., Ziller, M. J., Gu, H., Trapnell, C., Donaghey, J., Tsankov, A., ... Meissner, A. (2013). Transcriptional and epigenetic dynamics during specification of human embryonic stem cells. *Cell*.
- Glinsky, G. V. (2015). Transposable elements and DNA methylation create in embryonic stem cells human-specific regulatory sequences associated with distal enhancers and noncoding RNAs. *Genome Biology and Evolution*.
- Greber, B., Wu, G., Bernemann, C., Joo, J. Y., Han, D. W., Ko, K., ... Schöler, H. R. (2010). Conserved and Divergent Roles of FGF Signaling in Mouse Epiblast Stem Cells and Human Embryonic Stem Cells. *Cell Stem Cell*.
- Gu, Q., Hao, J., Hai, T., Wang, J., Jia, Y., Kong, Q., ... Zhou, Q. (2014). Efficient generation of mouse ESCs-like pig induced pluripotent stem cells. *Protein & Cell*, 5(5), 338–342.
- Hackett, J. A., Dietmann, S., Murakami, K., Down, T. A., Leitch, H. G., & Surani, M. A. (2013). Synergistic mechanisms of DNA demethylation during transition to ground-state pluripotency. *Stem Cell Reports*, 1(6), 518–531.
- Han, D. W., Tapia, N., Joo, J. Y., Greber, B., Araúzo-Bravo, M. J., Bernemann, C., ... Schöler, H. R. (2010). Epiblast stem cell subpopulations represent mouse embryos of distinct pregastrulation stages. *Cell*.

- Hanna, J., Cheng, A. W., Saha, K., Kim, J., Lengner, C. J., Soldner, F., ... Jaenisch, R. (2010). Human embryonic stem cells with biological and epigenetic characteristics similar to those of mouse ESCs. *Proceedings of the National Academy of Sciences*.
- Hanna, J., Markoulaki, S., Mitalipova, M., Cheng, A. W., Cassady, J. P., Staerk, J., ... Jaenisch, R. (2009). Metastable Pluripotent States in NOD-Mouse-Derived ESCs. *Cell Stem Cell*.
- Hatoya, S., Torii, R., Kondo, Y., Okuno, T., Kobayashi, K., Wijewardana, V., ... Inaba, T. (2006). Isolation and characterization of embryonic stem-like cells from canine blastocysts. *Molecular Reproduction and Development*, 73(3), 298–305.
- Hayashi, K., Lopes, S. M. C. de S., Tang, F., & Surani, M. A. (2008). Dynamic Equilibrium and Heterogeneity of Mouse Pluripotent Stem Cells with Distinct Functional and Epigenetic States. *Cell Stem Cell*.
- Hayes, B., Fagerlie, S. R., Ramakrishnan, A., Baran, S., Harkey, M., Graf, L., ... Torok-Storb, B. (2008). Derivation, Characterization, and In Vitro Differentiation of Canine Embryonic Stem Cells. *Stem Cells*, 26(2), 465–473.
- Iwafuchi-Doi, M., Matsuo, I., Tesar, P. J., Murakami, K., Niwa, H., Aruga, J., ... Kondoh, H. (2012). Transcriptional regulatory networks in epiblast cells and during anterior neural plate development as modeled in epiblast stem cells. *Development*.
- Koh, S., & Piedrahita, J. A. (2014). From “ES-like” cells to induced pluripotent stem cells: A historical perspective in domestic animals. *Theriogenology*.
- Koh, S., Thomas, R., Tsai, S., Bischoff, S., Lim, J.-H., Breen, M., ... Piedrahita, J. A. (2013). Growth Requirements and Chromosomal Instability of Induced Pluripotent Stem Cells Generated from Adult Canine Fibroblasts. *Stem Cells and Development*.
- Kojima, Y., Kaufman-Francis, K., Studdert, J. B., Steiner, K. A., Power, M. D., Loebel, D. A. F., ... Tam, P. P. L. (2014). The transcriptional and functional properties of mouse epiblast stem cells resemble the anterior primitive streak. *Cell Stem Cell*.
- Kojima, Y., Sasaki, K., Yokobayashi, S., Sakai, Y., Nakamura, T., Yabuta, Y., ... Saitou, M. (2017). Evolutionarily Distinctive Transcriptional and Signaling Programs Drive Human Germ Cell Lineage Specification from Pluripotent Stem Cells. *Cell Stem Cell*.
- Leitch, H. G., McEwen, K. R., Turp, A., Encheva, V., Carroll, T., Grabole, N., ... Hajkova, P. (2013). Naive pluripotency is associated with global DNA hypomethylation. *Nature Structural & Molecular Biology*, 20(3), 311–316.

- Luo, J., & Cibelli, J. B. (2016). Conserved Role of bFGF and a Divergent Role of LIF for Pluripotency Maintenance and Survival in Canine Pluripotent Stem Cells. *Stem Cells and Development*, 25(21), 1670–1680.
- Luo, J., Suhr, S. T. S. T., Chang, E. A. E. A., Wang, K., Ross, P. J. P. J., Nelson, L. L. L., ... Cibelli, J. B. J. B. (2011). Generation of leukemia inhibitory factor and basic fibroblast growth factor-dependent induced pluripotent stem cells from canine adult somatic cells. *Stem Cells and Development*, 20(10), 1669–1678.
- Melcer, S., Hezroni, H., Rand, E., Nissim-Rafinia, M., Skoultchi, A., Stewart, C. L., ... Meshorer, E. (2012). Histone modifications and lamin A regulate chromatin protein dynamics in early embryonic stem cell differentiation. *Nature Communications*.
- Meshorer, E., Yellajoshula, D., George, E., Scambler, P. J., Brown, D. T., & Misteli, T. (2006). Hyperdynamic plasticity of chromatin proteins in pluripotent embryonic stem cells. *Developmental Cell*.
- Nagashima, J. B., Sylvester, S. R., Nelson, J. L., Cheong, S. H., Mukai, C., Lambo, C., ... Travis, A. J. (2015). Live births from domestic dog (*Canis familiaris*) embryos produced by in vitro fertilization. *PLoS ONE*.
- Ohtsuka, S., & Niwa, H. (2015). The differential activation of intracellular signaling pathways confers the permissiveness of embryonic stem cell derivation from different mouse strains. *Development*.
- Onishi, K., Tonge, P. D., Nagy, A., & Zandstra, P. W. (2012). Microenvironment-mediated reversion of epiblast stem cells by reactivation of repressed JAK-STAT signaling. *Integrative Biology*.
- Ostrander, E. A., & Wayne, R. K. (2005). The canine genome. *Genome Research*, 15(12):1706-1716.
- Remy, I., Montmarquette, A., & Michnick, S. W. (2004). PKB/Akt modulates TGF- β signalling through a direct interaction with Smad3. *Nature Cell Biology*.
- Renton, J. P., Boyd, J. S., Eckersall, P. D., Ferguson, J. M., Harvey, M. J., Mullaney, J., & Perry, B. (1991). Ovulation, fertilization and early embryonic development in the bitch (*Canis familiaris*). *Journal of Reproduction and Fertility*, 93(1), 221–31.
- Reynaud, K., Fontbonne, A., Marseloo, N., Thoumire, S., Chebrou, M., Viaris de Lesegno, C., & Chastant-Maillard, S. (2005). In vivo meiotic resumption, fertilization and early embryonic development in the bitch. *Reproduction*.
- Reynaud, K., Fontbonne, A., Marseloo, N., Viaris de Lesegno, C., Saint-Dizier, M., & Chastant-Maillard, S. (2006). In vivo canine oocyte maturation, fertilization and early embryogenesis: A review. *Theriogenology*.

- Schneider, M. R., Braun, J., Adler, H., Wolf, E., Kienzle, B., & Kolb, H.-J. (2007). Canine Embryo-Derived Stem Cells-Toward Clinically Relevant Animal Models for Evaluating Efficacy and Safety of Cell Therapies. *Stem Cells*.
- Singh, A. M., Reynolds, D., Cliff, T., Ohtsuka, S., Mattheyses, A. L., Sun, Y., ... Dalton, S. (2012). Signaling network crosstalk in human pluripotent cells: A Smad2/3-regulated switch that controls the balance between self-renewal and differentiation. *Cell Stem Cell*.
- Takashima, Y., Guo, G., Loos, R., Nichols, J., Ficz, G., Krueger, F., ... Smith, A. (2014). Resetting Transcription Factor Control Circuitry toward Ground-State Pluripotency in Human. *Cell*, 158((6)),
- Tecirlioglu, R. T., & Trounson, A. O. (2007). Embryonic stem cells in companion animals (horses, dogs and cats): present status and future prospects. *Reproduction, Fertility, and Development*, 19(6), 740–7.
- Tesar, P. J., Chenoweth, J. G., Brook, F. A., Davies, T. J., Evans, E. P., Mack, D. L., ... McKay, R. D. G. (2007). New cell lines from mouse epiblast share defining features with human embryonic stem cells. *Nature*, 448(7150), 196–199.
- Theunissen, T. W., Powell, B. E., Wang, H., Mitalipova, M., Faddah, D. A., Reddy, J., ... Jaenisch, R. (2014). Systematic identification of culture conditions for induction and maintenance of naive human pluripotency. *Cell Stem Cell*.
- Tosolini, M., Brochard, V., Adenot, P., Chebrou, M., Grillo, G., Navia, V., ... Jouneau, A. (2018). Contrasting epigenetic states of heterochromatin in the different types of mouse pluripotent stem cells. *Scientific Reports*.
- Vaags, A. K., Rosic-Kablar, S., Gartley, C. J., Zheng, Y. Z., Chesney, A., Villagómez, D. A. F., ... Hough, M. R. (2009). Derivation and Characterization of Canine Embryonic Stem Cell Lines with In Vitro and In Vivo Differentiation Potential. *Stem Cells*, 27(2), 329–340.
- Vallier, L., Mendjan, S., Brown, S., Chng, Z., Teo, A., Smithers, L. E., ... Pedersen, R. A. (2009). Activin/Nodal signalling maintains pluripotency by controlling Nanog expression. *Development*.
- Van Oosten, A. L., Costa, Y., Smith, A., & Silva, J. C. R. (2012). JAK/STAT3 signalling is sufficient and dominant over antagonistic cues for the establishment of naive pluripotency. *Nature Communications*.
- Van Soom, A., Rijsselaere, T., & Filliers, M. (2014). Cats and dogs: Two neglected species in this era of embryo production in vitro? *Reproduction in Domestic Animals*.

- Ware, C. B., Nelson, A. M., Mecham, B., Hesson, J., Zhou, W., Jonlin, E. C., ... Ruohola-Baker, H. (2014). Derivation of naive human embryonic stem cells. *Proceedings of the National Academy of Sciences*, 111(12), 4484–4489.
- Whitworth, D. J., Ovchinnikov, D. a, Sun, J., Fortuna, P. R. J., & Wolvetang, E. J. (2014). Generation and characterization of leukemia inhibitory factor-dependent equine induced pluripotent stem cells from adult dermal fibroblasts. *Stem Cells and Development*, 23(13), 1515–23.
- Wilcox, J. T., Lai, J. K. Y. Y., Semple, E., Brisson, B. A., Gartley, C., Armstrong, J. N., & Betts, D. H. (2011). Synaptically-competent neurons derived from canine embryonic stem cells by lineage selection with EGF and noggin. *PLoS ONE*, 6(5), e19768.
- Wilcox, J. T., Semple, E., Gartley, C., Brisson, B. A., Perrault, S. D., Villagómez, D. A. F., ... Betts, D. H. (2009). Characterization of Canine Embryonic Stem Cell Lines Derived From Different Niche Microenvironments. *Stem Cells and Development*, 18(8), 1167–1178.
- Winnier, G., Blessing, M., Labosky, P. A., & Hogan, B. L. M. (1995). Bone morphogenetic protein-4 is required for mesoderm formation and patterning in the mouse. *Genes and Development*.
- Ying, Q. L., Nichols, J., Chambers, I., & Smith, A. (2003). BMP induction of Id proteins suppresses differentiation and sustains embryonic stem cell self-renewal in collaboration with STAT3. *Cell*.

Chapter 3

3 Pluripotent state influences metabolic activity and mitochondrial structure in canine embryonic stem cells

A version of this chapter has been published:

Tobias, I.C., Isaac, R.R., Dierolf, J.G., Khazaei, R., Cumming, R.C., and Betts, D.H. (2018). *Metabolic plasticity during transition to naïve-like pluripotency in canine embryo-derived stem cells*. *Stem Cell Research* 30, 22-33.

Reproduced here with permission from Elsevier publishers (Appendix B).

3.1 Introduction

Naïve and primed PSCs are metastable and occasionally interconvertible cell lines, which represent different temporal cellular compartments within the pre-implantation embryo (Brons et al., 2007; Nichols and Smith, 2009; Tesar et al., 2007). The naïve pluripotent state may be established directly from cells of the inner cell mass (ICM) or induced by pharmacological manipulation of primed PSCs, with or without the assistance of transgenes favouring naïve pluripotency (Bao et al., 2009; Guo et al., 2009; Nichols et al., 2009). The molecular and functional characteristics that distinguish naïve pluripotency are tolerance to partial repression of mitogen-activated protein kinase kinase (MEK) signaling and abrogation of T-cell factor 3 (TCF3) signaling (Meek et al., 2013; Wray et al., 2011; Zhou et al., 2015), global epigenomic de-repression (Ficz et al., 2013; Leitch et al., 2013), reactivation of the silent X-chromosome in female cells (Gafni et al., 2013; Ware et al., 2014), ease of clonogenic selection and contribution to embryonic lineages of pre-gastrulation embryos (Buecker et al., 2010; Gafni et al., 2013).

Both naïve and primed PSCs exhibit high rates of glycolysis in hyperoxic environments, resembling the aerobic glycolysis phenotype observed in certain transformed cells (Racker, 1972; Vander Heiden et al., 2009; Zhang et al., 2012a). The diversion of metabolic intermediates from complete mitochondrial oxidation supplies intermediates to anabolic pathways, while mitigating the production of reactive oxygen species (ROS) (Folmes et al., 2011; Panopoulos et al., 2012; Varum et al., 2009). This metabolic state differs from specialized post-natal cell types, which prioritize efficient adenosine triphosphate (ATP) synthesis by oxidative phosphorylation (OXPHOS) (Chung et al., 2007). Interestingly, naïve PSCs have greater rates of respiration despite housing less mature mitochondria compared to their primed counterparts (Sperber et al., 2015; Zhou et al., 2012). Mitochondrial function is restrained in primed PSCs by uncoupling the oxidation of glycolysis-derived pyruvate (Samudio et al., 2009; Zhou et al., 2012). Mitochondrial homeostasis and energy production may be linked to pluripotency and self-renewal via the metabolic sensor AMP-activated protein kinase (AMPK) (Liu Y et al., 2019). However, it remains unclear whether the AMPK pathway is differentially regulated in a pluripotent state-specific manner.

The existence of a *de facto* naïve pluripotent state in non-rodent species is controversial. However, naïve-like PSC lines have been characterized in various mammalian species including porcine (Nakano et al., 2013), rabbit (Osteil et al., 2013), equine (Whitworth et al., 2014) and bovine (Verma et al., 2013). Canine ESCs (cESCs) can be derived and expanded on mouse embryonic fibroblast (MEF) feeder layers in the presence of leukemia inhibitory factor and fibroblast growth factor 2 (L/F) (Tobias et al., 2013). These LIF-FGF2 dependent cESCs exhibit features of primed pluripotency such as sensitivity to enzymatic passaging regimes, expression of primed pluripotency markers (e.g. OTX2, FGF5) and a neural lineage bias in minimal media (Wilcox et al., 2011, 2009). In the previous chapter, I showed that dual inhibition of MEK and GSK3 β along with LIF (2iL) conditionally stabilizes cESCs in a pluripotent state that shares several properties with canonical naïve PSCs (Chapter 2). Interestingly, our 2iL cESCs show markedly slower *in vitro* growth compared to initiating LIF-FGF2 cESC populations (Tobias et al., 2016). Nevertheless, the fundamentals of pluripotent state progression appear to be conserved in placental mammals, making it a priority to define the divergent attributes and culture requirements of non-rodent equivalents to naïve and primed PSCs.

PSC metabolism is inherently flexible, permitting the maintenance of proliferation and differentiation capacity within a dynamic physicochemical environment (Harvey et al., 2016), but the persistence of suboptimal conditions would be expected to negatively impact PSC physiology. All canine ESC/iPSC lines established to date are maintained in media formulations previously optimized for the growth of human or mouse PSCs (Betts and Tobias, 2015). Furthermore, imprecise definition of the extrinsic requirements for canine PSC self-renewal may hinder the ability of these lines to proliferate extensively *in vitro* or demonstrate pluripotency *in vivo* through teratoma formation. The goal of this work is to assess mitochondrial function and the contribution of bioenergetic pathways to proliferation in the undifferentiated state for primed-like LIF-FGF2 cESCs and naïve-like 2iL cESC populations. We propose that different metabolic pathway activities support ATP generation and biomass accumulation necessary for proliferation of cESCs.

3.2 Materials and Methods

3.2.1 Feeder Layer and Embryonic Stem Cell Culture

MEF monolayer preparation and culture of cESCs were conducted as previously described (Tobias et al., 2016). Briefly, E12.5 DR4 MEFs were mitotically arrested and seeded at 1.5×10^4 cells/cm² for ESC co-culture. Canine ESC lines (BE5, IO3) derived at the Ontario Veterinary College from embryo explants (OVC.EX) (Wilcox et al., 2009) were seeded onto growth-arrested MEFs and cultured in base media: KnockOut DMEM/F12, 15% KnockOut Serum Replacement (KOSR), 1X GlutaMAX, 1X non-essential amino acids, 10 ng/mL recombinant insulin-like growth factor (R₃IGF1; Sigma Aldrich) and 0.1 mM 2-mercaptoethanol. Base medium was supplemented with 10 ng/mL human LIF and 4 ng/mL human FGF2 for maintenance of control L/F cESCs; or 10 ng/mL human LIF, 0.5 μ M MEK inhibitor PD0325901 and 3 μ M GSK3 β inhibitor CHIR99021 for establishment and culture of 2iL cESCs (Tobias et al., 2016). To deplete MEF contamination prior to experiments, cESCs were transferred to Geltrex-coated dishes and cultured with 70% MEF-conditioned medium balanced with non-conditioned base media. Control human ESC line HES-2 (Reubinoff et al., 2000) and murine ESC line R1 (Nagy et al., 1993) were adapted and maintained in base medium containing 15% KOSR for at least three passages prior to analyses to standardize nutrient availability (Zhang et al., 2016). Incubators were maintained at 37°C, 5% CO₂ and ambient oxygen. Unless otherwise stated, all cell culture reagents were obtained from Thermo Fisher Scientific (MA, USA). Inhibitors of metabolic enzymes were from Sigma Aldrich (MO, USA).

3.2.2 Oxygen Consumption Rate and Extracellular Acidification Rate

Cells were seeded onto Geltrex-coated XF_e24 Seahorse plates (Agilent Technologies) at 3×10^4 or 6×10^4 cells per well. Culture media were exchanged for unbuffered media supplemented with either 1 mM sodium pyruvate and 10 mM glucose (Mitochondrial assay); or 2 mM glutamine (Glycolysis assay) one hour before the assay. After basal metabolic readings were recorded, substrates and selective inhibitors were injected to achieve final concentrations of: glucose (2.5 mM), 4-(trifluoromethoxy) phenylhydrazone

(FCCP, 1 μ M), oligomycin (1 μ M), 2-deoxyglucose, (2-DG, 50 mM) antimycin A (2.5 μ M) and rotenone (2.5 μ M). Changes in oxygen consumption rate (OCR) and extracellular acidification rate (ECAR) in response to the addition of substrates/inhibitors were described as the mean change after injection compared with the average OCR or ECAR before the injection. The OCR and ECAR values were normalized to the total quantity of protein isolated from each well.

3.2.3 Protein Extraction, SDS-PAGE and Western Blotting

Cells were lysed in 100 μ L RIPA buffer (150 mM sodium chloride, 1% NP-40, 0.5% sodium deoxycholate, 0.1% sodium dodecyl sulfate, 50 mM Tris, pH 8.0) with a protease and phosphatase inhibitor cocktail (EMD Millipore) for 15 minutes on ice. Supernatant protein concentration was determined by DCTM Protein Assay (BIO-RAD Technologies). Protein lysates were resolved on 4-12% SDS-PAGE gels (Thermo Fisher Scientific), transferred onto Immobilon polyvinylidene difluoride membranes followed by incubation with 5% skim milk powder/TBS/0.1% Tween-20 for 1 hour. Antibodies used in the work are summarized in Table 3-1. After 16 hours of primary antibody incubation, membranes were incubated with HRP-coupled secondary antibodies for 1 hour at room temperature. Immune-reactive proteins were visualized by chemiluminescence on Molecular Imager[®] VersaDocTM System and Quantity One software (BIO-RAD Technologies). Densitometry was performed using ImageLab 3.0 software (BIO-RAD Technologies).

Table 3-1. Primary antibody information

Target Protein	Isotype Species	Application (Dilution)	Supplier (Catalog)
ACC1	Rabbit	WB (1:1000)	Cell Signaling (3662)
p-ACC (S79)	Rabbit	WB (1:1000)	Cell Signaling (3661)
AMPK α	Rabbit	WB (1:500)	Cell Signaling (2603)
p-AMPK α (T172)	Rabbit	WB (1:500)	Cell Signaling (2535)
ATP5A	Mouse	WB (1:1000)	Abcam (AB14748)
FASN	Mouse	WB (1:1000)	Santa Cruz (sc-48357)
GLUT1	Rabbit	WB (1:500)	Santa Cruz (sc-7903)
HXK2	Mouse	WB (1:2000)	Novus (NBP2-02272)
LDHA	Rabbit	WB (1:1000)	Cell Signaling (2012)
MIC60	Rabbit	WB (1:2000)	Novus (NB100-1919)
PDH (E1 α)	Mouse	WB (1:2000)	Abcam (AB110334)
p-PDH (S232)	Rabbit	WB (1:2000)	Millipore (AP1063)

PKM1	Rabbit	WB (1:1000)	Proteintech (15821-1AP)
PKM2	Rabbit	WB (1:1000)	Proteintech (15822-1AP)
PDHK1	Rabbit	WB (1:1000)	Enzo (ADI-KAP- PK112)
SDHB	Mouse	WB (1:1000)	Abcam (AB14745)
TOMM2	Rabbit	WB (1:1000)	Proteintech (11802-1AP)
UQCRC2	Mouse	WB (1:1000)	Abcam (AB14714)

3.2.4 Flow Cytometric Analysis of cESC-MEF Co-cultures

To discriminate cESCs from feeder cells, the plasma membrane of MEFs were stained with lipophilic dialkylcarbocyanine dyes (Nakayama et al., 1992) in either the green (SP-DiOC₁₈) or far red (Di-D) fluorescent spectrum. Adherent MEFs were stained with 5 µg/mL of Di-D or SP-DiOC₁₈ diluted in culture media for two hours at 37°C. MEFs were washed twice with PBS prior to seeding L/F or 2iL cESCs. Events were recorded using the Accuri C6 platform (BD Bioscience) using standard laser configuration, a flow rate of 35 µL/minute and the following optical filters: 533/30 (FL-1), 585/40 (FL-2), 670 LP (FL-3) and 675/25 (FL-4). Single colour or fluorescence minus one control samples containing an equivalent volume of diluent were included to set analyses gates and to threshold background autofluorescence. Briefly, the single-cell population was gated by pulse processing (pulse height vs. pulse area) to remove cell doublets and obvious debris. Markers were applied to FL-1A and FL-4A cytograms to exclude SP-DiOC₁₈ or Di-D stained MEFs from further interrogation. Average fluorescence intensity values from are presented as the geometric mean.

3.2.5 Chemifluorescence and Flow Cytometry

JC-1 green fluorescence reflects JC-1 monomers and the formation of J⁺-aggregates in the mitochondrial matrix leads to orange fluorescence. The dual-colour properties of JC-1 allows a ratiometric comparison of relative mitochondrial polarization states (Cossarizza et al., 1993; Smiley et al., 1991). Tetramethylrodamine methyl ester (TMRM) is a yellow-red fluorescent stain, which is highly sensitive to changes in the mitochondrial electrochemical gradient (Scaduto and Grotyohann, 1999). However, MitoTracker Green FM has been reported to stain mitochondria regardless of chemical ablation of the $\Delta\Psi_m$

(Buckman et al., 2001). For mitochondrial labelling, single live cells in suspension were adjusted to a density of approximately 1×10^6 cells/mL in flow staining buffer and incubated with 200 nM MitoTracker Green or 5 $\mu\text{g/mL}$ JC-1 for 30 minutes protected from light. Alternatively, single live cells were incubated with 150 nM TMRM for 15 minutes. 30,000 total events were recorded at a flow rate of 35 $\mu\text{L/minute}$. In JC-1 experiments, spectral compensation was performed by subtracting 12% of FL-1A from FL-2A. In TMRM experiments, spectral compensation was performed by subtracting 9% of FL-1A from FL-2A. Relative $\Delta\Psi\text{m}$ was calculated as geometric mean of FL-2A fluorescence intensity (for TMRM) or the ratio of FL2-A: FL1-A geometric mean fluorescence intensity (J^+ -aggregate: JC-1 monomer).

3.2.6 Chemifluorescence and Live Cell Imaging

Cells were stained for 1 hour with 1 μM Calcein Green AM and then 15 minutes with 25 nM TMRM diluted in Live Cell Imaging Solution (Thermo Fisher Scientific). Cells were imaged within a 5% CO_2 live cell imaging chamber mounted on the stage of a Leica DMI 6000B microscope. Digital images were captured with an Orca Flash camera (Hamamatsu Photonics) and Application Suite X software (Leica Microsystems). Exposure time, illumination intensity and experimental duration were minimized to preserve mitochondrial integrity and avoid artefactual changes in fluorescence intensity (Iannetti et al., 2016; Mitra and Lippincott-Schwartz, 2010). Brightness and contrast were standardized to unstained control samples and the equivalent imaging parameters were applied to all other images using ImageJ. Membrane potential was calculated as the change in fluorescence intensity of TMRM in redistribution (non-quenching) mode after FCCP-induced mitochondrial depolarization. Calcein fluorescence was recorded to control for plasma membrane integrity. Fluorescent intensity was monitored for five minutes to establish baseline values (set to 100%) and an additional fifteen minutes after treatment with 250 nM FCCP or vehicle (DMSO). The mean fluorescent intensity of cytoplasmic foci corresponding to mitochondria in cESCs was measured using ImageJ (National Institutes of Health, MD).

3.2.7 Mitochondrial and Genomic DNA Isolation and Quantitative PCR

Mitochondrial DNA (mtDNA) and genomic DNA were purified from cESC pellets using GenElute Mammalian Genomic DNA Miniprep Kit (Sigma Aldrich), according to manufacturer's instructions. Quality and quantity of DNA was determined through spectrometry using a NanoDrop ND-2000 (NanoDrop Technologies). Oligonucleotide primers targeting cytochrome oxidase II (MTCOII) were designed from published canine mtDNA sequences (Kim et al., 1998) using accession number U96639.2. Polycystin-1 (PKD1) was selected as a single copy genomic reference gene in the domestic dog (Dackowski et al., 2002). Primer sequences and amplicon sizes are summarized in Table 3-2. Specificity of each primer set was determined by gel electrophoresis, band excision and sequencing of the resultant amplicon using the Applied Biosystems 3730 DNA Analyzer (London Regional Genomics Center). Quantitative PCR was performed using 6 ng of template DNA and SensiFAST™ SYBR (Bioline Reagents, MA). Thermal cycling conditions included 2 minutes at 95°C followed by 39 cycles of 95°C for 5 seconds, 62°C for 10 seconds and 72°C for 20 seconds. Reaction data were corrected for individual primer amplification efficiencies, calculated from a standard dilution series. Relative transcript abundance was determined using CFX384 Real-time system on a C1000 Thermal Cycler (BIO-RAD Technologies) CFX software and calculated using $2^{-\Delta\Delta Ct}$ method.

Table 3-2. Custom oligonucleotide primer sequences.

Gene Identifier	Sequence (5' to 3')	Size (bp)
MTCO2	F – ATCGCTCTACCTTCCCTCCG R – ACAGTCCTGGTCGTATGGCT	349
PKD1	F – AGCTGCATAACTGGATCGACAAC R – ATGTAACGCATGGGGAACCG	128

3.2.8 Sample Preparation for Transmission Electron Microscopy

Briefly, cells were washed with PBS and fixed directly on the plate with a pre-warmed 1:1 mixture of media and Karnovsky's fixative (2% Paraformaldehyde, 2.5%

Glutaraldehyde, 0.1 M Sodium Cacodylate, pH 7.4) for 10 minutes. Cells were gently scraped into a 1.5 mL microcentrifuge tube and gently pelleted at a very low speed (200 RCF with no centrifuge braking). Cells were resuspended in pure Karnovsky's fixative (10-20X the pellet volume) for 15 minutes, then gently pelleted and resuspended in fresh Karnovsky's fixative. Primary fixation continued for 2 hours, then cells were washed four times in 0.1 M Sodium Cacodylate buffer, pH 7.4 for 5 minutes each. Samples were encapsulated 2% agarose, cut into 1 mm cubes using a razor and soaked for one hour in 0.5% Osmium Tetroxide in foil-wrapped glass tubes on crushed ice. Samples were rinsed three times in 0.1 M Cacodylate buffer for 10 minutes each, followed by another three washes in water for 40 minutes each. Samples were soaked for eight hours in a half-saturated Uranyl Acetate solution, and then rinsed six times in water for 30 minutes each. Agarose pieces were transferred through a graded series of acetone at: 20%, 50%, 70%, 95%, and finally three times at 100% for 15 minutes each. Samples were placed on a rotary mixer will be embedded with graded mixtures of Epon-Araldite resin and acetone at 1:2 overnight, 1:1 for eight hours, 2:1 overnight and finally pure resin for five hours. Molds of samples were prepared and baked at 60 °C for 96 hours. Ultra-thin sections (70 nm) were retrieved from cell-containing areas of the resin blocks and placed on 200 mesh nickel grids. Post-staining of grids was carried out with 2% Uranyl Acetate for 15 minutes and Reynold's Lead Citrate for 1 minute, rinsing with water between stains. Grids were air-dried and imaged within 48 hours.

3.2.9 Mitochondrial Morphometric Image Analysis

At least 60 images containing 18 distinct cells were taken from coded L/F and 2iL cESC samples using a Philips CM10 transmission electron microscope at 34,000X magnification for observation of 380 total mitochondria. Mitochondrial counts, dimensions and cristae orientation were assessed by blinded investigators using ImageJ. The aspect ratio was calculated as the ratio between the unit length of major and minor axes for mitochondrial ellipsoids. The cristae density was calculated from the cristae number normalized to calculated mitochondrial surface area. To evaluate the degree of cristae alignment within mitochondria, cristae angles were recorded to calculate the mean incident angle between cristae.

3.2.10 Metabolic Inhibitor Treatment and Cell Counting

20,000 cESCs were seeded into multiwell plates and total cell counts were performed every 24 hours for 4 days using a hemocytometer. For inhibitor treatments, cells adhered overnight in the absence of inhibitors and growth in the presence of inhibitors was scored after 48 hours. Data are presented as the fold change in total cell number relative to the initial cell number at the 0-hour time point. 2-deoxy-D-glucose (2-DG) and Rotenone (RTN) were diluted into culture media to final concentrations of 1.25 mM and 250 nM, respectively. Concentrations used in our assays were determined by single inhibitor dose-titrations to find the minimum concentration affecting cell proliferation.

3.2.11 Cellular ATP Detection Assay

L/F and 2iL cESCs were treated with 2-DG, RTN or vehicle and diluted to 100,000 cells/mL in cESC culture media. Cell suspensions were transferred to an opaque white 96-well microplate (10,000 cells/well) and ATP content was determined using the Luminescent ATP Detection Assay Kit (Abcam). Luminescence was quantified with the SpectroMax M5 (Molecular Devices, CA) instrument and ATP content (pM/cell) was interpolated from an eight-point standard curve.

3.2.12 Cell Death and Apoptosis Assay

The incidence of cell death and apoptosis during steady-state growth and inhibitor assays was assessed by measuring the percentage of 7-aminoactinomycin D (7-AAD)/Annexin-V positive cells. Briefly, single cells suspended in Annexin binding buffer (10 mM HEPES, 140 mM Sodium Chloride, 2.5 mM Calcium Chloride, pH 7.4) were stained with fluorescein isothiocyanate (FITC) Annexin-V conjugate (Thermo Fisher Scientific) for 20 minutes and 7-AAD Viability staining solution (eBioscience) for 5 minutes. 20,000 total events were recorded using an Accuri C6 flow cytometer (BD Biosciences). Spectral compensation was performed by subtracting 2% of FL1 from FL3 to adjust for minor FITC overlap into FL-3. Changes in cell viability was assessed as the mean proportion of Annexin-V-FITC⁻/7-AAD⁻ (viable), Annexin-V-FITC⁺/7-AAD⁻ (apoptotic) or Annexin-V-FITC⁺/7-AAD⁺ (dead) cells.

3.2.13 Statistical Analysis

Data were analyzed using R (version 3.2.3) by two-sample composite t-test or one-way analysis of variance (ANOVA) followed by Tukey's HSD multiple comparison method as appropriate. $P < 0.05$ was considered statistically significant. Data were visualized using GraphPad Prism 6 and presented as mean \pm standard error of the mean (SEM).

3.3 Results

3.3.1 Enhanced glucose oxidation and respiratory capacity in 2iL cESC

Glycolytic and oxidative metabolism in ESCs were assessed by measuring the extracellular acidification rate (ECAR) and oxygen consumption rate (OCR), respectively (Zhang et al., 2012b). To explore if activation of mitochondrial respiration is a feature conserved in naïve-like cESCs, we compared the metabolic rate measurements of BE5 cESCs maintained in L/F or 2iL, HES-2 human (h)ESCs and R1 murine (m)ESCs. OCR was monitored after cells were successively exposed to oligomycin (OLIGO), 4-(trifluoromethoxy)-phenylhydrazone (FCCP) and antimycin A/rotenone (Fig. 3-1A).

In the presence of glucose, both R1 mESCs ($P=1.03 \times 10^{-4}$) and 2iL cESCs ($P=0.025$) have greater OCR: ECAR ratio compared to primed-like L/F cESCs and hESCs (Fig. 3-1B). The respiration attributable to ATP-synthase activity did not differ between hESCs, LIF-FGF2 or 2iL cESCs ($P=0.25$) but was markedly greater in mESCs ($P=6.8 \times 10^{-6}$) (Fig. 3-1C). The fold change in OCR following FCCP-stimulated maximal respiration (a measure of mitochondrial spare capacity) is significantly elevated in 2iL cESCs ($P=1.40 \times 10^{-3}$) and R1 mESCs ($P=7.2 \times 10^{-6}$) in comparison to primed human ESCs and L/F cESCs (Fig. 3-1D). However, rate measurements correlating to basal oxygen consumption ($P=0.024$), ATP synthase-linked respiration and mitochondrial spare capacity ($P=0.013$) in 2iL cESCs all remain below naïve mESCs.

To assess if enhanced 2iL cESC respiration is reproducible in a different genetic background, we examined OCR responses to chemical manipulation of mitochondrial function in IO3 cESCs (Fig. 3-2A). Like BE5 cESCs, we observed a statistically

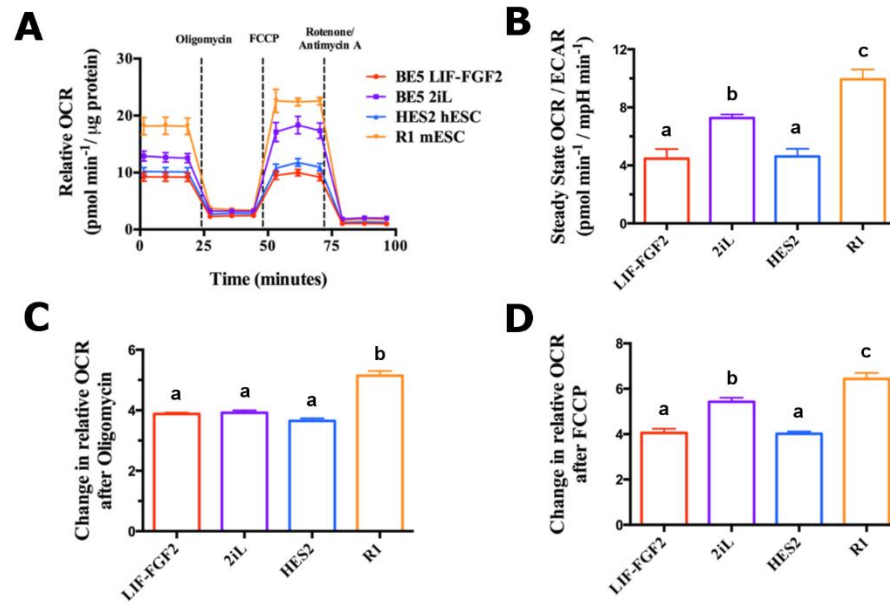


Figure 3-1. Culture in 2iL enhances glucose oxidation and respiratory capacity of BE5 cESCs.

(A) Oxygen consumption rate (OCR) tracing of BE5 LIF-FGF2 cESCs, BE5 2iL cESCs, HES-2 hESCs and R1 mESCs. Addition of oligomycin reduces OCR and reflects respiration independent of oxidative phosphorylation. Addition of FCCP stimulates electron transport chain activity and maximal OCR. Addition of Antimycin A/Rotenone (mitochondrial chain complex inhibitors) shows OCR independent of mitochondrial metabolism. (B) Basal OCR with respect to ECAR in glucose-containing media (C) Relative decreases in OCR after oligomycin injection. (D) Relative increases in OCR after FCCP injection. Rate measurements were normalized to total protein quantified by Lowry assay. Bars represent standard error of the mean (SEM), $n = 5$. Means followed by the same letter are not significantly different, $P < 0.05$.

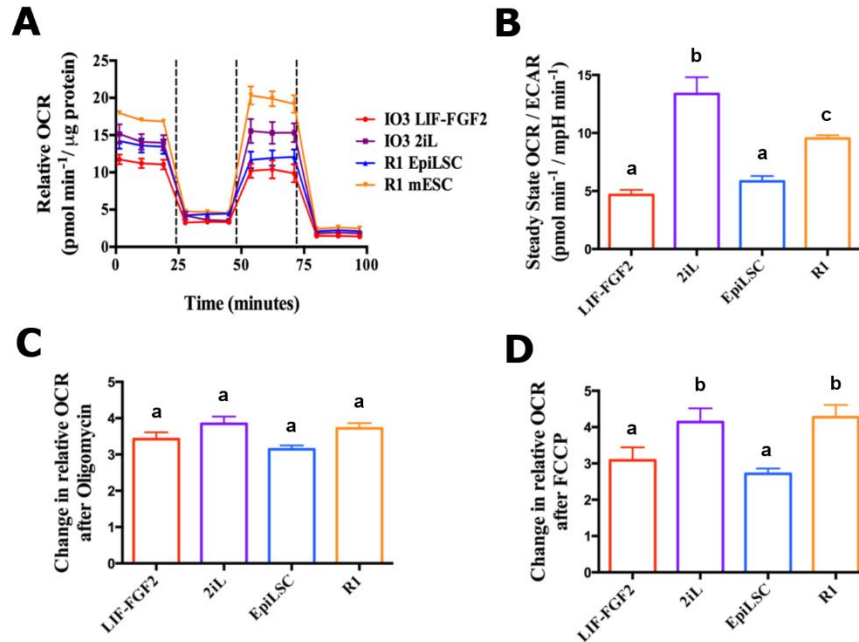


Figure 3-2. 2iL-induced respiration is reproducible in IO3 cESC line.

(A) Oxygen consumption rate tracing of IO3 LIF-FGF2 cESCs, IO3 2iL cESCs, R1-derived epiblast-like stem cells and R1 mESCs. (B) Basal OCR with respect to ECAR in glucose-containing media (C) Relative decreases in OCR after oligomycin injection. (D) Relative increases in OCR after FCCP injection. Rate measurements were normalized to total protein quantified by Lowry assay. Bars represent standard error of the mean (SEM), $n = 5$. Means followed by the same letter are not significantly different, $P < 0.05$.

significant increase in basal OCR: ECAR ratio ($P=1.94 \times 10^{-5}$) and mitochondrial spare capacity ($P=0.042$), but not ATP-coupled respiration ($P=0.30$) in IO3 2iL cESCs compared to L/F cESCs (Fig. 3-2B-D).

3.3.2 Altered mitochondrial ultrastructure but not mitochondrial biomass in 2iL cESC

We next sought to quantify mitochondrial content to determine if altered mitochondrial biomass contributed to cESC metabolic function. Lipophilic dialkylcarbocyanine dyes were applied to co-cultured MEFs to discriminate cESC-specific signals by flow cytometry (Fig. 3-3A-B). The geometric mean of MitoTracker Green FM fluorescence intensity was significantly lower in the 2iL cESC population (Fig. 3-3C-D, $P=4.40 \times 10^{-3}$). Whereas, the geometric mean of forward scatter (FSC) intensity, an estimate of cell size, was not different between L/F and 2iL cESCs (Fig. 3-3E-F, $P=0.97$). Therefore, it is unlikely that altered cell volume contributed to the observed change in MitoTracker Green FM accumulation in cESCs. We probed cESC lysates for TOMM20, an integral component of the outer mitochondrial membrane (Rassow and Pfanner, 2000), as a surrogate measure of mitochondrial content. TOMM20 abundance was not different in 2iL cESCs compared to originating L/F cESCs (Fig. 3-4A, $P=0.21$). Similarly, we observed no change in the relative mitochondrial DNA (mtDNA) quantity between L/F and 2iL cESCs (Fig. 3-4B, $P=0.53$). The level of Mitofilin (MIC60), an inner mitochondrial membrane protein associated with tubular cristae formation (Hessenberger et al., 2017), was significantly reduced in 2iL cESCs compared to L/F cESCs (Fig. 3-4C, $P=9.0 \times 10^{-4}$).

Alterations to 2iL cESC mitochondrial ultrastructure may affect MitoTracker Green FM accumulation despite indications that overall mitochondrial biomass are unchanged. Using transmission electron microscopy, we observed that mitochondria of both L/F and 2iL cESCs were typically arranged in perinuclear clusters (Fig. 3-5A). Furthermore, the internal structure of L/F and 2iL mitochondria exhibited several contrast features selected for detailed morphometric analysis (Fig. 3-5B-C). Mitochondria visualized in L/F cESCs tended to have lower overall abundance and larger surface area compared to mitochondria within 2iL cESCs, but these metrics were not considered statistically

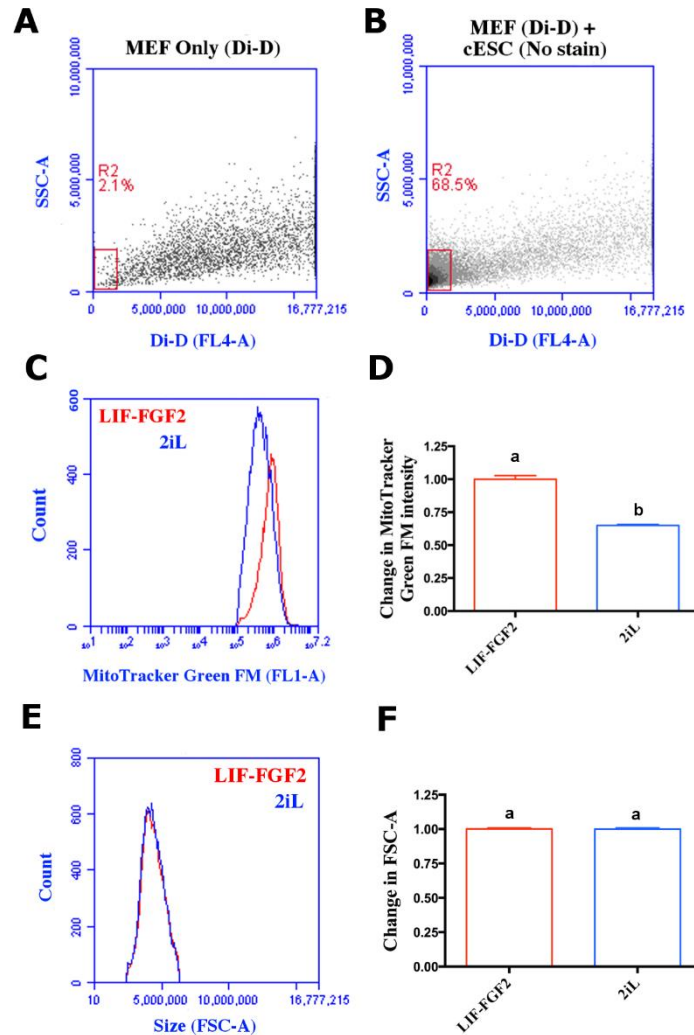


Figure 3-3. 2iL cESCs show lower MitoTracker Green FM accumulation independent of cell size.

Representative inclusion gating of (A) Di-D labelled MEFs and (B) unstained cESCs in co-culture on SSC-A vs. FL4-A cytograms to exclude contaminating MEFs from flow cytometric analysis. (C) Overlay FL1-A histogram and (D) quantification of geometric mean MitoTracker Green FM intensity as an estimate of mitochondrial mass in singularized L/F and 2iL cESCs. (E) Overlay histogram of forward light scatter area (FSC-A) and (F) quantification of change in FSC-A as an estimate of relative L/F or 2iL cESC size. Bars represent standard error of the mean (SEM), $n = 3$. Means followed by the same letter are not significantly different, $P < 0.05$.

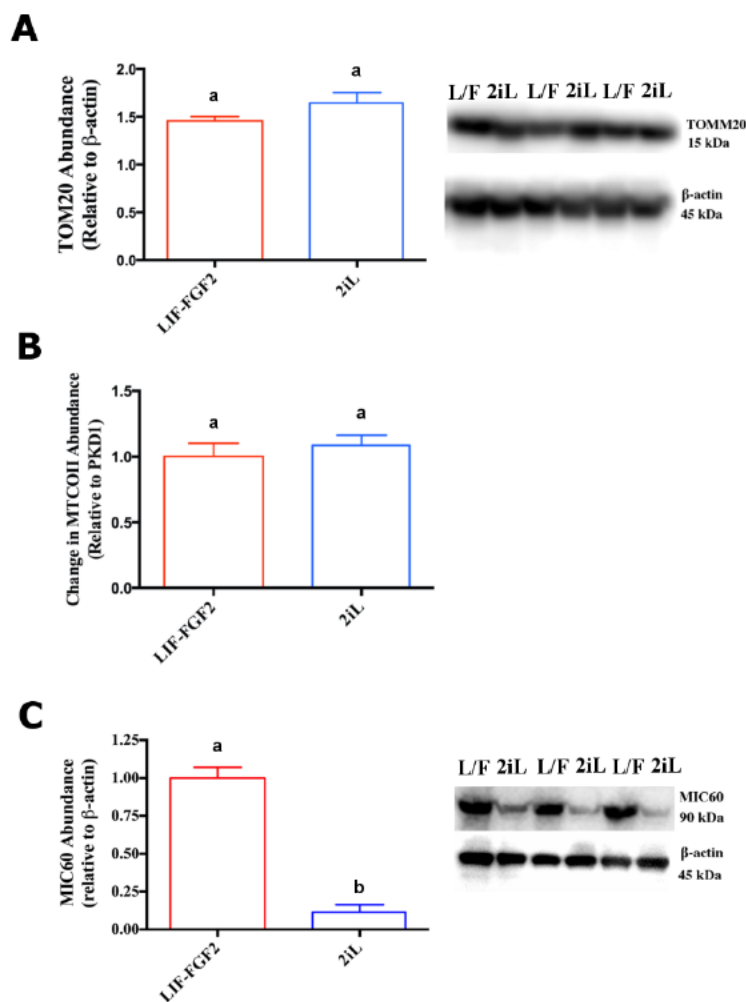


Figure 3-4. 2iL cESCs exhibit a selective decrease in the inner mitochondrial membrane protein MIC60.

(A) Representative western blot membrane image and protein quantification by densitometry for translocase of outer mitochondrial membrane 20 (TOMM20). (B) Ratiometric estimation of relative mitochondrial DNA abundance by quantitative PCR amplification of mitochondrially encoded cytochrome oxidase 2 (MTCOII) and nuclear single copy gene polycystic kidney disease 1 (PKD1). (C) Representative western blot membrane image and protein quantification by densitometry for Mitofilin (MIC60). Bars represent standard error of the mean, $n = 3$. Means followed by the same letter are not significantly different, $P < 0.05$.

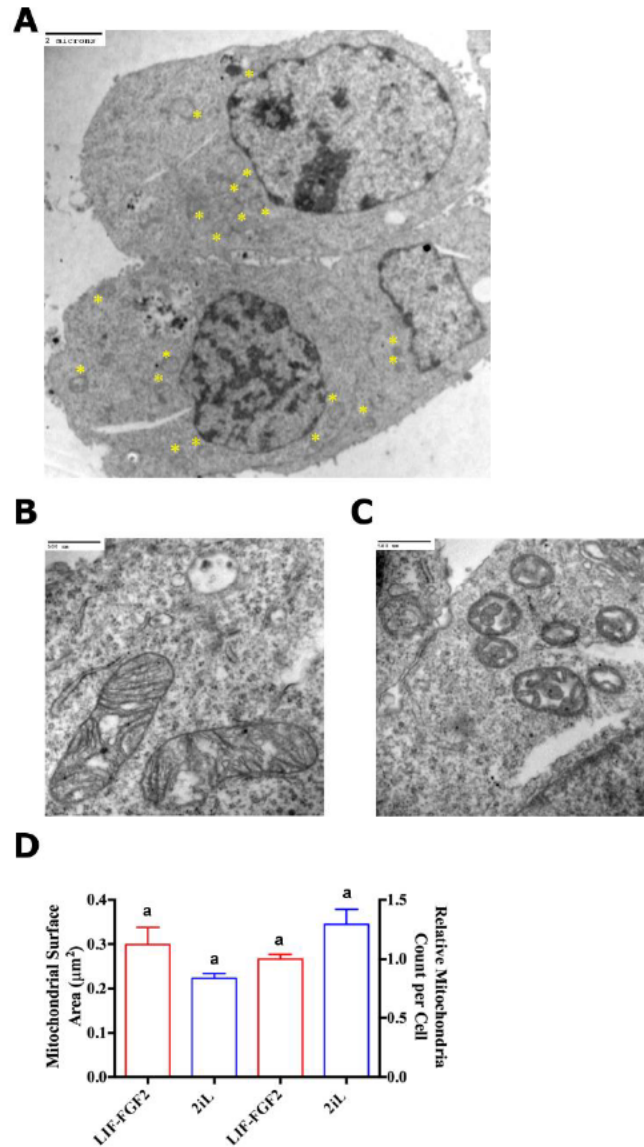


Figure 3-5. L/F and 2iL cESCs harbor structurally distinct mitochondria but do not differ in mitochondrial biomass.

(A). Transmission electron micrograph at 5,800X magnification of mitochondrial within cESCs. Yellow asterisks “*” denote a mitochondrion. Scale bar unit length is 2 μm. Transmission electron micrograph at 34,000X magnification of mitochondrial within (B) L/F cESCs and (C) 2iL cESCs. Scale bar unit length is 500 nm. (D) Quantification of mitochondrial surface area and relative mitochondrial abundance in L/F and 2iL cESCs. Bars represent standard error of the mean, n = 3. Means followed by the same letter are not significantly different, P < 0.05.

significant (Fig. 3-5D, $P=0.1403$ and $P=0.1866$). 2iL cESCs contained shorter and more rounded mitochondria with respect to mean aspect ratio compared to mitochondria within L/F cESCs (Fig. 3-6A, $P=0.003$). Mitochondria from L/F and 2iL cESCs exhibit a similar density of cristae membranes (Fig. 3-6B, $P=0.861$). Interestingly, the mitochondria in 2iL cESCs exhibited poorer pairwise alignment of crista membranes (i.e. 0° represents parallel membrane orientation), with a mean incident cristae angle of 58.02° compared to 38.07° in L/F cESCs (Fig. 3-6C, $P=0.019$).

3.3.3 Increased mitochondrial membrane potential and ATP level in 2iL cESC

Cellular ATP production is regulated by mitochondrial membrane potential ($\Delta\Psi_m$), which is established by electron transport and the coincident transport of protons to the intermembrane space (Ehrenberg et al., 1988; Kamo et al., 1979). We assessed mitochondrial polarization state using the $\Delta\Psi_m$ -sensitive dyes tetramethylrhodamine, methyl ester (TMRM) and JC-1 to explore the relationship between mitochondrial respiration and proton-motive force in cESCs.

Contrary to the anticipated result, quantification of cells stained with JC-1 (Fig. 3-7A, $P=4.60 \times 10^{-3}$) or TMRM (Fig. 3-7B, $P=1.30 \times 10^{-3}$) by flow cytometry showed significant reductions in the relative $\Delta\Psi_m$ of 2iL cESCs compared to those expanded in L/F. However, quantification of fluorescent intensity per cell may not be a reliable comparison if ultrastructural changes in mitochondria affect probe uptake and retention kinetics between L/F and 2iL cESCs. Rather than performing a static comparison between whole cell mitochondrial polarization states, we sought to quantify the dynamic re-distribution of TMRM upon selective depolarization of $\Delta\Psi_m$ by live cell fluorescent microscopy (Fig. 3-7C). 2iL cESCs exhibited a significantly greater decrease in TMRM fluorescence intensity following FCCP-mediated depolarization compared to L/F cESCs (Fig. 3-7D, $P=0.0106$). Calcein Green AM fluorescence intensity was maintained after FCCP treatment (Fig. 3-8), suggesting that viability or plasma membrane integrity do not confound TMRM re-distribution.

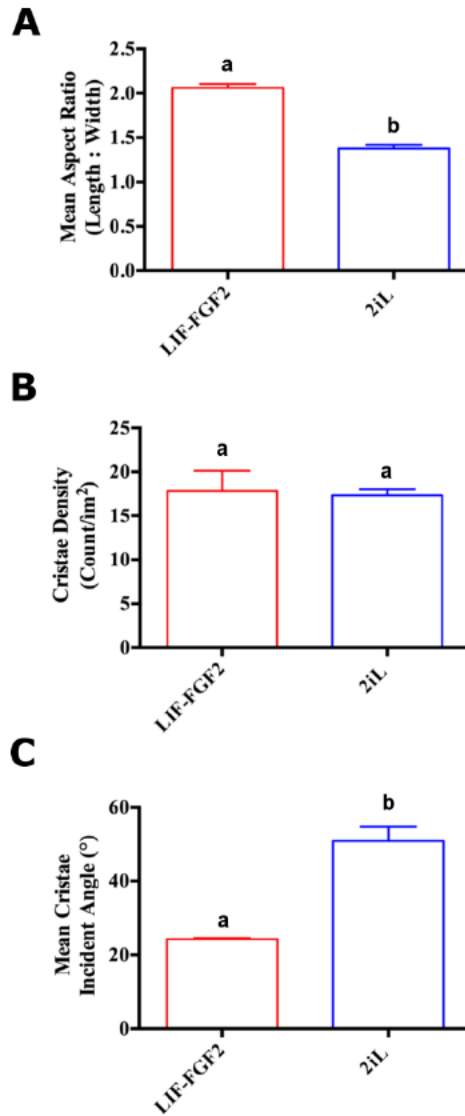


Figure 3-6. Remodeling of mitochondrial ultrastructure in 2iL cESC.

Over 150 mitochondria from at least 18 different cells per cESC population were observed for morphometric analysis by blinded investigators (A) Calculation of the mean aspect ratio (major axis length: minor axis length) of mitochondria. (B) Quantification of the mean cristae density estimated as the cristae number normalized to surface area. (C) Calculation of the mean incident angle between cristae. Bars represent standard error of the mean, $n = 3$. Means followed by the same letter are not significantly different, $P < 0.05$.

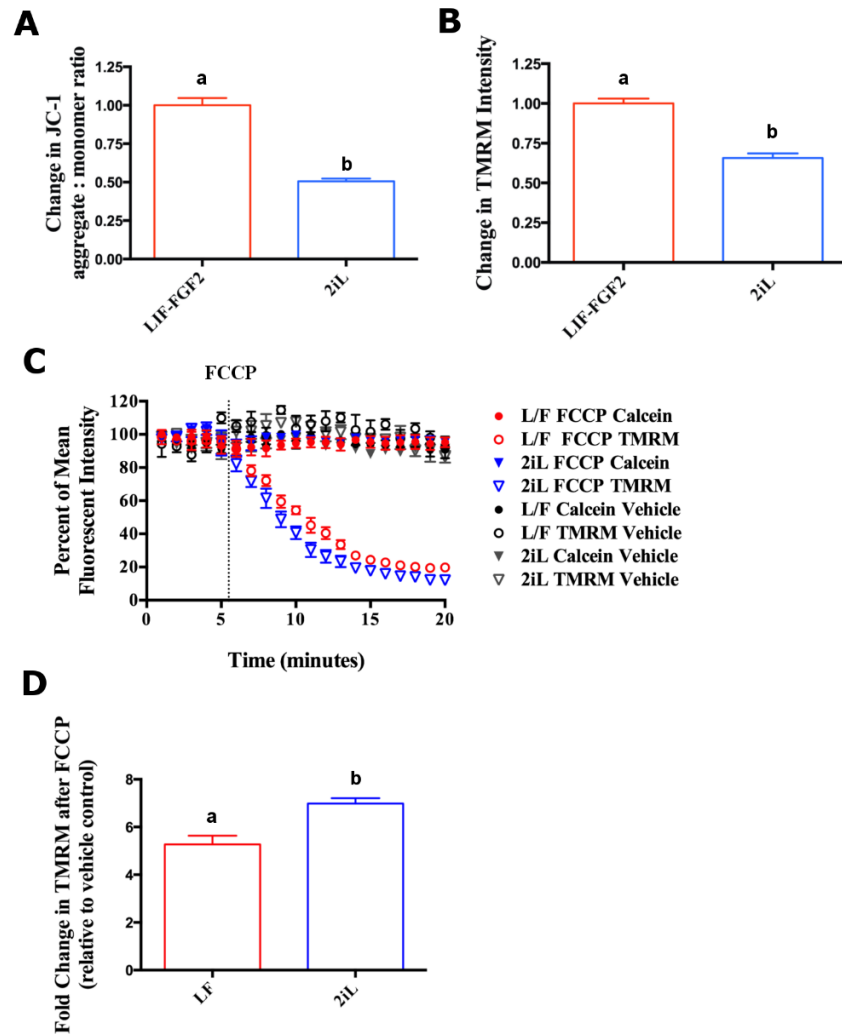


Figure 3-7. Dynamic redistribution but not static accumulation of mitochondrial polarization-sensitive dyes correlates with respiratory activity in cESCs.

(A) Geometric mean J-aggregate intensity to JC-1 monomer intensity ratio (FL2-A : FL1-A) in singularized L/F and 2iL cESCs. (B) Geometric mean tetramethylrhodamine, methyl ester (TMRM) fluorescence intensity (FL2-A) in singularized L/F and 2iL cESCs. (C) Time course of TMRM mean fluorescence intensity before (baseline) and after selective depolarization FCCP. Calcein Green AM mean fluorescence intensity was also recorded as an indicator of plasma membrane integrity. (D) Magnitude of FCCP-mediated reduction in TMRM staining in redistribution conditions. Bars represent standard error of the mean, $n = 4-6$. Means followed by the same letter are not significantly different, $P < 0.05$.

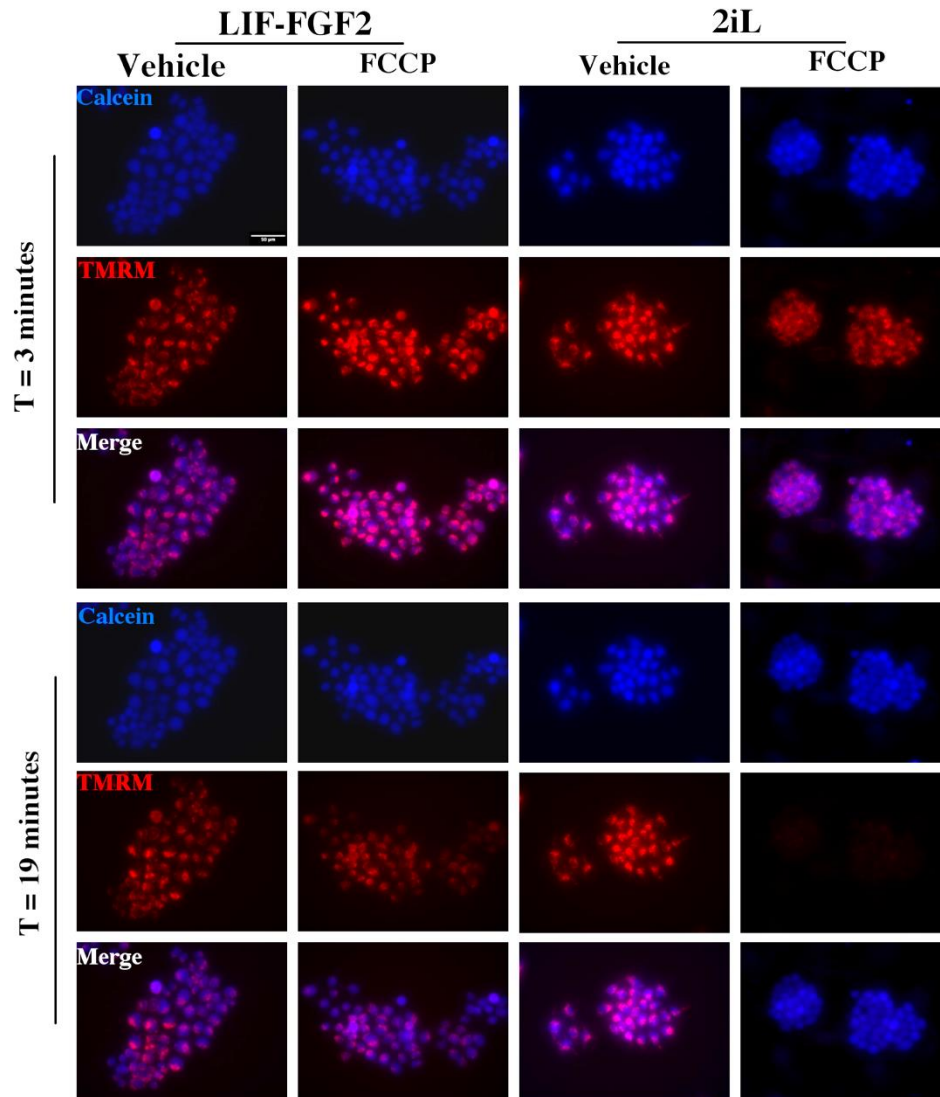


Figure 3-8. Selective decrease in mitochondrial but not cytosolic staining with FCCP treatment.

L/F and 2iL cESCs were monitored for TMRM (red) or Calcein Green AM (blue) fluorescence for a duration of 20 minutes. Initial readings establish baseline fluorescence intensity (0-5 minutes) and afterwards the change in fluorescence intensity after FCCP (250 nM) or vehicle treatment (6-20 minutes) was monitored. Representative micrographs are shown, and scale bar unit length is 50 μm .

We next investigated the abundance of mitochondrial chain complex subunits by immunoblot analysis. 2iL cESCs exhibited a significant increase ($P=1.5 \times 10^{-3}$) in succinate dehydrogenase iron sulfur subunit B (SDHB; complex II) and lower ($P=0.026$) F1-ATP synthase subunit 5 alpha (ATP5A; complex V) (Fig. 3-9A-C) abundance compared to L/F cESCs. Ubiquinol-cytochrome c reductase core protein 2 (UQCRC2; complex III) did not significantly differ between L/F and 2iL cESCs (Fig. 3-9D, $P=0.53$). Furthermore, steady-state ATP levels were greater in 2iL cESCs compared to L/F cESCs (Fig. 3-10A, $P=1.0 \times 10^{-5}$). This result is corroborated by enhanced phosphorylation of AMP-activated protein kinase (AMPK) at Thr172 (Fig. 3-10B-C, $P=0.044$) as well as increased Ser79 phosphorylation of acetyl-CoA carboxylase (ACC1), a canonical AMPK target enzyme, in L/F cESCs compared to 2iL cESCs (Fig. 3-10D, $P=0.020$). Reliable signals could not be obtained for antibodies directed against human cytochrome C oxidase 2 (MTCOX2; complex IV) and NADH: ubiquinone oxidoreductase subunit B8 (NDUFB8; complex I) due to poor amino acid conservation in the canine homologs (<85% similarity by blastp algorithm).

3.3.4 Differentiation regulation of pyruvate metabolizing enzymes is associated with altered lipid accumulation

Multiple enzymes responsible for pyruvate flux into the TCA cycle are differentially regulated in naïve versus primed PSC populations (Zhang et al., 2011; Zhou et al., 2012). Therefore, we assessed the levels of proteins involved in pyruvate handling by immunoblot analysis. L/F cESCs exhibited increased levels of lactate dehydrogenase isoform A (LDHA), a key enzyme in maintaining high glycolytic flux, compared to 2iL cESCs (Fig. 3-11A-B, $P=0.01$). Whereas levels of M2 isoform of pyruvate kinase (PKM2), an isoenzyme associated with elevated aerobic glycolysis in transformed cells, exhibited similar levels in L/F and 2iL cESCs (Fig. 3-11C, $P=0.65$). However, the M1 isoform of pyruvate kinase (PKM1), which is suggested to promote mitochondrial pyruvate oxidation (Taniguchi et al., 2016), was significantly enriched in 2iL cESCs (Fig. 3-11D, $P=0.013$). Surprisingly, levels of pyruvate dehydrogenase (PDH) kinase 1 (Fig. 3-11E-F, $P=0.045$) and the ratio phosphorylated PDH to total PDH (Fig. 3-11G, $P=7.0 \times 10^{-3}$) were both elevated in 2iL cESCs.

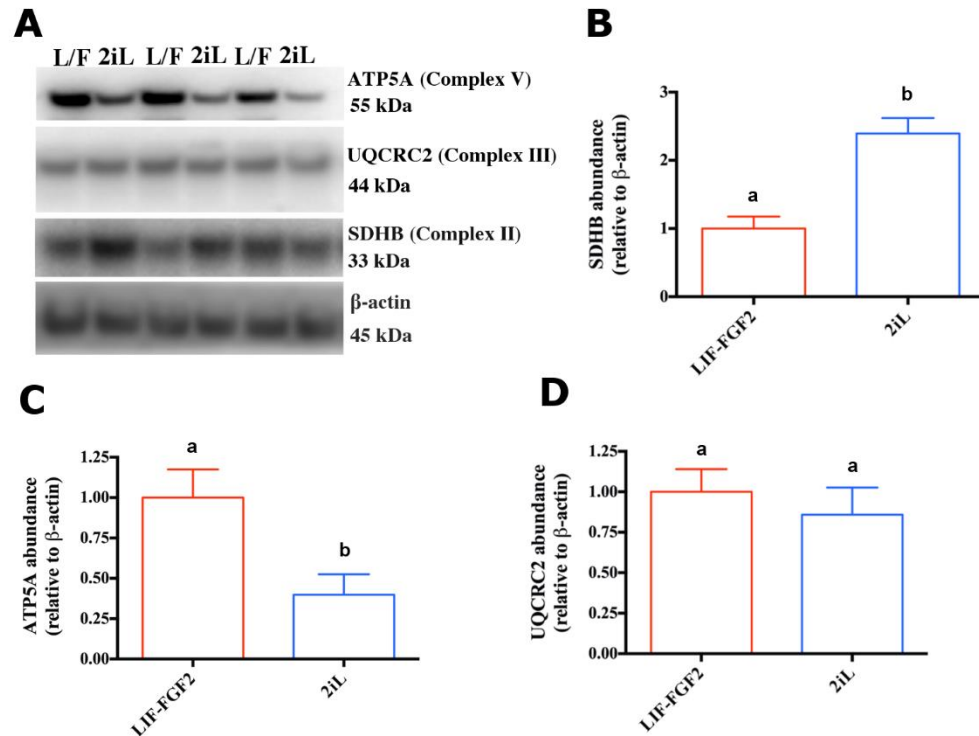


Figure 3-9. Altered respiratory chain complex subunit abundances between L/F and 2iL cESCs.

Representative western blot membrane images of L/F and 2iL cESC whole lysates probed for F1 ATP synthase alpha subunit (ATP5A), succinate dehydrogenase beta (SDHB), ubiquinol-cytochrome c reductase core protein 2 (UQCRC2) and reference protein beta-actin. Densitometric quantification of protein levels for (B) SDHB, (C) ATP5A, and (D) UQCRC2. Means are normalized to internal standard beta-actin and expressed as relative ratios to L/F cESC samples. Bars represent standard error of the mean, $n = 4$. Means followed by the same letter are not significantly different, $P < 0.05$.

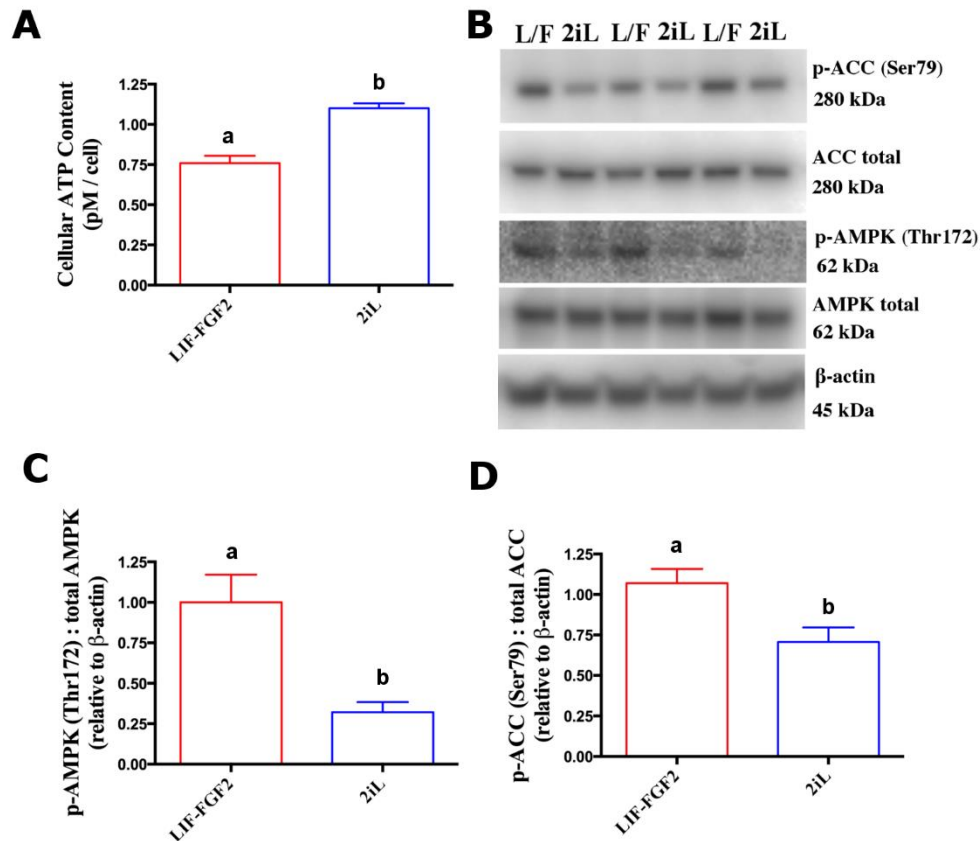


Figure 3-10. 2iL cESCs display elevated ATP content and AMPK signaling.

(A). Calculation of cellular ATP by interpolating standard curve values in a luminescent microplate assay and normalized to cell number. (B) Representative western blot membrane image for phosphorylated and total AMP-activated protein kinase (AMPK) or acetyl-CoA carboxylase (ACC). Protein quantification by densitometry for (C) AMPK phosphorylation (D) ACC phosphorylation. Means are normalized to internal standard beta-actin and expressed as relative ratios to L/F cESC samples. Bars represent standard error of the mean (SEM), n= 4-7. Means followed by the same letter are not significantly different, $P < 0.05$.

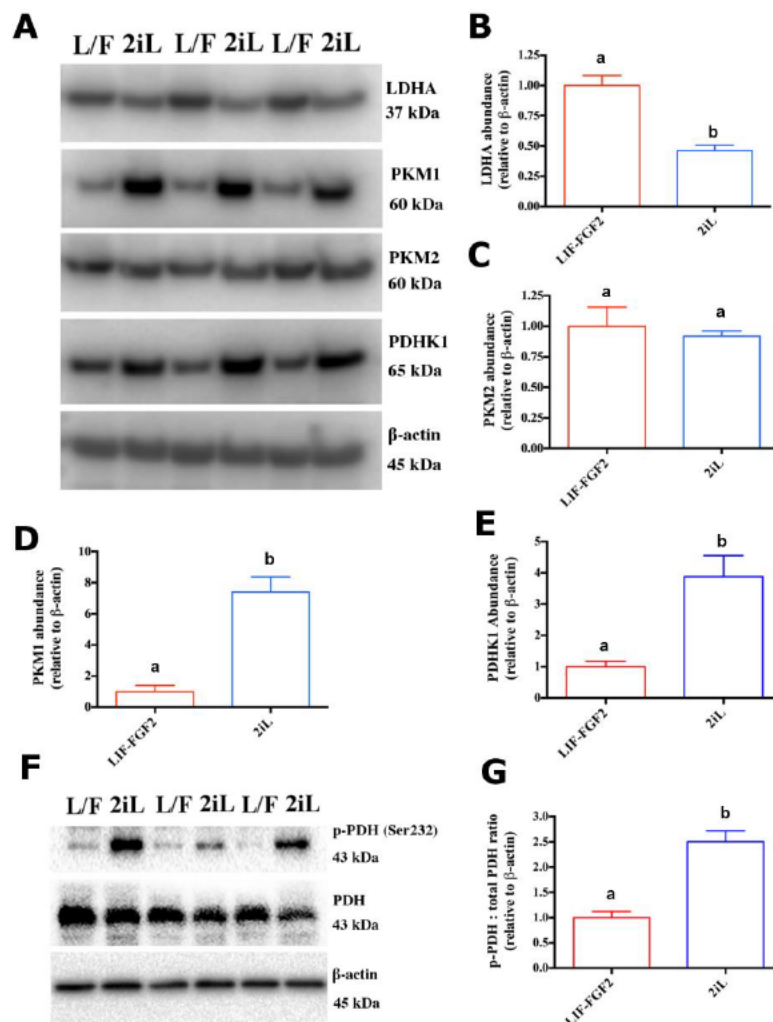


Figure 3-11. Differential regulation of pyruvate metabolizing enzymes between L/F and 2iL cESCs.

(A) Representative western blot membrane images probed for lactate dehydrogenase isoform A (LDHA), pyruvate kinase M2 isoform (PKM2) and pyruvate kinase M1 isoform (PKM1). Protein quantification by densitometry for (B) LDHA, (C) PKM2, (D) PKM1 and (E) PDHK1. (F) Representative western blot membrane images probed for pyruvate dehydrogenase kinase 1 (PDHK1), total pyruvate dehydrogenase (PDH) and phosphorylated (Ser232) PDH (p-PDH). (G) Protein quantification by densitometry for PDH phosphorylation. Means are normalized to internal standard beta-actin and expressed as relative ratios to L/F cESC samples. Bars represent standard error of the mean (SEM), $n = 3$. Means followed by the same letter are not significantly different, $P < 0.05$.

Incomplete oxidation of glucose may favour the redirection of intermediate metabolites towards anabolic processes, such as lipogenesis (Tohyama et al., 2016). We therefore investigated the level of neutral lipids within L/F and 2iL cESCs using Nile Red. Flow cytometric analysis revealed greater mean fluorescence intensity associated with neutral lipids in L/F cESCs compared to 2iL cESCs (Fig. 3-12A-B, $P=3.0 \times 10^{-4}$). Nile Red fluorescence attributable to polar lipids, such as phospholipids, did not significantly differ between L/F and 2iL cESCs (Fig. 3-12C, $P=0.78$). Indeed, fatty acid synthase (FASN), a key enzyme in *de novo* lipogenesis, was significantly more abundant in L/F cESC than 2iL cESC protein lysates (Fig. 3-12D, $P=0.015$).

3.3.5 HXK2 level and glycolytic capacity are correlated among mammalian ESC lines

To examine glycolytic activity in PSC lines, ECAR was monitored after the sequential addition of glucose, oligomycin and 2-deoxy-D-glucose (2-DG) (Fig. 3-13A). ECAR measurements in the absence of glucose, or after 2-DG exposure, did not differ between all lines tested, implying that non-glycolytic acidification mechanisms did not substantially contribute to ECAR observations. Glucose-induced ECAR (i.e. glycolytic acidification) in L/F cESCs were equivalent to those recorded from naïve-like R1 mESCs or 2iL cESCs ($P=0.88$) and lower than HES2 hESCs ($P=0.046$) (Fig. 3-13B).

Oligomycin-stimulated ECAR (i.e. maximum glycolytic capacity) was equivalent between L/F and 2iL cESCs ($P=0.98$), but significantly lower than R1 mESC ($P=6.3 \times 10^{-3}$) and HES2 hESC lines ($P=9.25 \times 10^{-3}$) (Fig. 3-13C). However, the quotient of oligomycin and glucose stimulated ECAR (i.e. glycolytic reserve capacity) was augmented in 2iL cESCs ($P=0.017$), HES2 hESCs ($P=4.59 \times 10^{-3}$) and R1 mESCs ($P=1.0 \times 10^{-7}$) compared to LIF-FGF2 cESCs (Fig. 3-13D). Interestingly, L/F cESCs, 2iL cESCs, HES2 hESC and R1 mESC did not show any difference in constitutive glucose uniporter GLUT1 quantity (Fig. 3-14A, $F=0.20456$, $P=0.89$). However, rate-limiting glycolytic enzyme Hexokinase-2 (HXK2) (Bissonnette et al., 1996) differed among ESC populations (Fig. 3-14B, $F=11.38$, $P=3.0 \times 10^{-4}$). HXK2 level was significantly greater in HES2 ($P=3.02 \times 10^{-2}$) and R1 ($P=2.0 \times 10^{-4}$) compared to L/F cESCs, which exhibited similar HXK2 levels to 2iL cESCs ($P=0.68$).

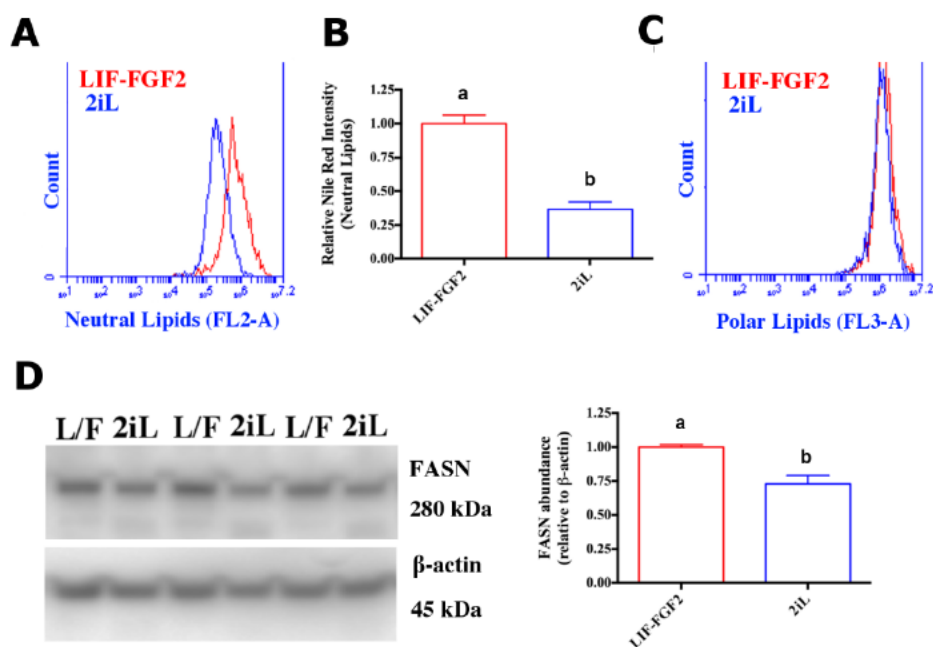


Figure 3-12. Altered lipogenic properties between L/F and 2iL cESCs.

(A) Overlay FL2-A (neutral lipids) histogram of Nile Red staining intensity in singularized L/F or 2iL cESCs. (B) Flow cytometric analysis of MEF-depleted cESCs of geometric mean fluorescence intensity associated with neutral lipid stores. (C) Overlay FL3-A (polar lipids) histogram of Nile Red staining intensity of singularized L/F or 2iL cESCs. (D) Representative western blot membrane images of fatty acid synthase (FASN) and reference protein beta-actin. (E) Protein quantification by densitometry for FASN. Bars represent standard error of the mean (SEM), $n = 4$. Means followed by the same letter are not significantly different, $P < 0.05$.

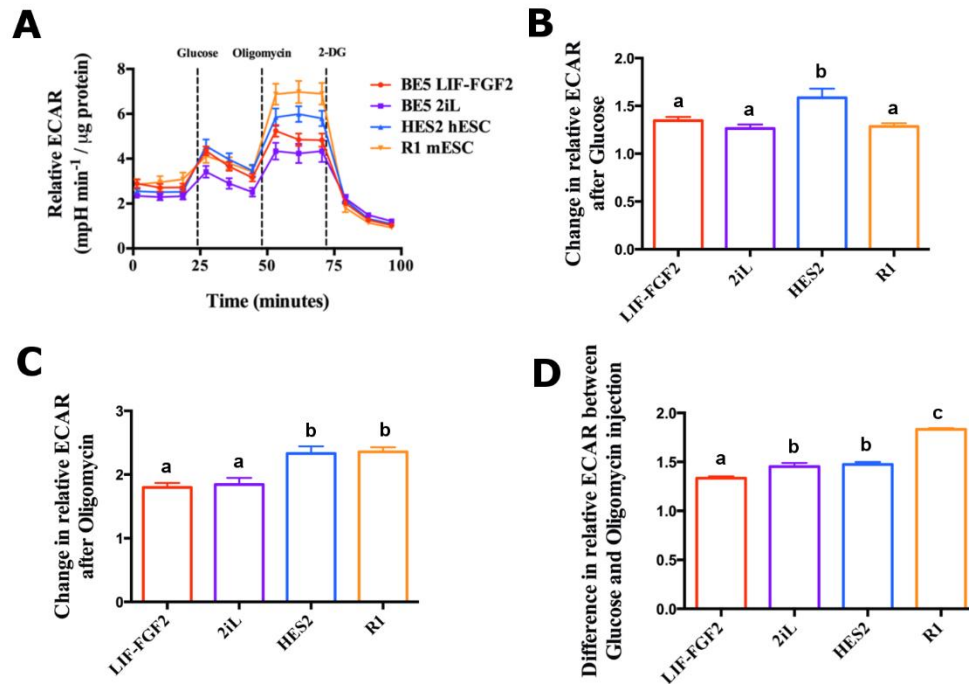


Figure 3-13. Both L/F and 2iL cESC exhibit lower glycolytic capacities than human or mouse ESC.

(A) Extracellular acidification rate tracing of LIF-FGF2 cESCs, 2iL cESCs, HES-2 hESCs and R1 mESCs measured by Seahorse extracellular flux analyzer. Addition of glucose to cells equilibrated in glucose-free media establishes the basal glycolytic rate. Addition of oligomycin stimulates glycolytic flux in response to a deficiency in mitochondrial ATP production resulting in maximum ECAR. The difference between baseline ECAR and rate measurements after injection of 2-DG is non-glycolytic acidification. (B) Relative changes in ECAR after glucose injection. (C) Relative changes in ECAR after oligomycin injection. (D) Difference between oligomycin and glucose stimulated ECAR. Rate measurements were normalized to total protein quantified by Lowry assay. Bars represent standard error of the mean (SEM), $n = 5$. Means followed by the same letter are no significantly different, $P < 0.05$.

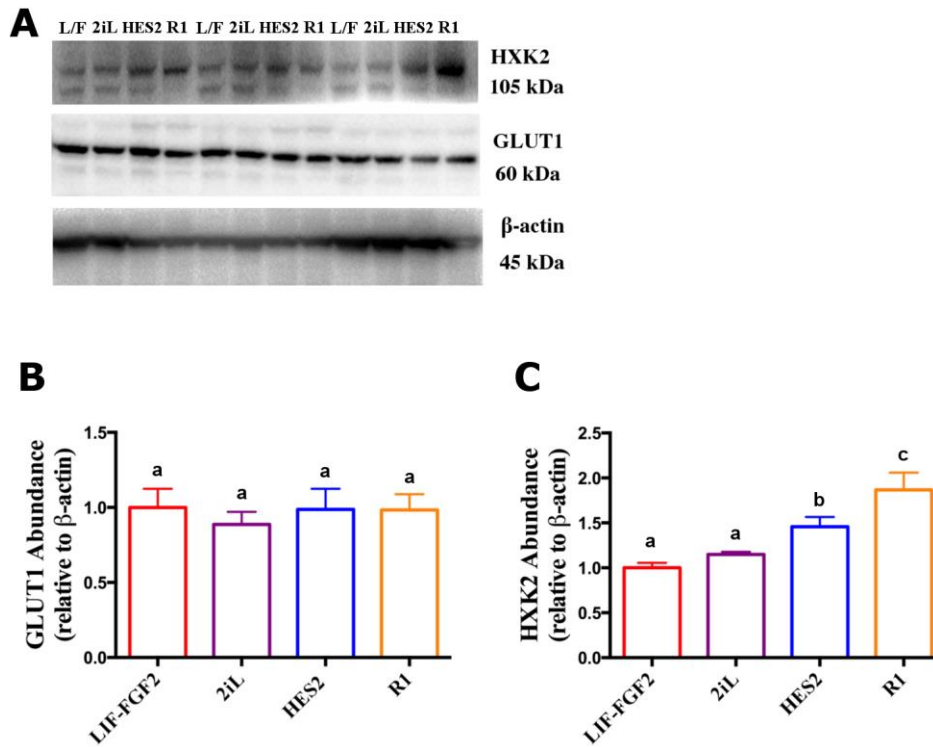


Figure 3-14. Both L/F and 2iL cESCs exhibit lower HXK2 abundance compared to human or murine ESC.

(A) Representative western blot membrane image of hexokinase 2 (HXK2), constitutive glucose uniporter (GLUT1) and reference protein beta-actin in L/F cESC, 2iL cESC, HES2 hESC and R1 mESC. Protein quantification by densitometry for (B) GLUT1 and (C) HXK2. Bars represent standard error of the mean (SEM), $n = 3$. Means followed by the same letter are not significantly different, $P < 0.05$.

3.3.6 Bioenergetic pathway inhibition differentially affects L/F and 2iL cESCs

We used inhibitors of the electron transport chain (ETC) and glycolysis to dissect the contributions of these metabolic pathways to acute L/F and 2iL cESC proliferation. Given that 2iL cESCs have greater respiratory and glycolytic reserve capacities than L/F cESCs, we posited that 2iL cESC expansion would be less sensitive to bioenergetic pathway antagonism. Expansion of L/F cESCs was impaired by 2-DG, a competitive inhibitor of HXK (Fig. 3-15A, $P=2.24 \times 10^{-3}$), without altering the proportion of live cells (Fig. 3-16B, $P=0.58$). In contrast, the mitochondrial complex I inhibitor RTN did not alter L/F cESC proliferation (Fig. 3-15A, $P=0.67$) or viability (Fig. 3-15B, $P=0.89$). 2iL cESC expansion was unaffected by the presence 2-DG (Fig. 3-15C, $P=0.92$), however, RTN exposure decreased acute proliferation 2iL cESC expansion (Fig. 3-15C, $P=6.30 \times 10^{-3}$) without a change in cell viability (Fig. 3-15D, $P=0.67$).

Exposure of L/F cESCs to 2-DG and RTN during steady-state growth did not significantly affect the ATP content (Fig. 3-16A, $F=3.185$, $P=0.065$). Whereas, ATP levels within 2iL cESCs were sensitive to the presence of partial blockade of bioenergetic pathways (Fig. 3-16B, $F=61.439$, $P=9.08 \times 10^{-9}$). Interestingly, treatment of 2iL cESCs with RTN ($P=1.0 \times 10^{-7}$), but not with 2-DG ($P=0.93$), significantly decreased ATP concentrations. No significant changes in the proportion of apoptotic or dead cells were detected in either cESC population for the duration of 2-DG exposure (Fig. 3-17A-C, $P=0.84$ & $P=0.20$) or RTN treatment (Fig. 3-17D-F, $P=0.80$ and $P=0.74$).

3.4 Discussion

Our data indicate that 2iL-enriched cESCs display enhanced mitochondrial respiration, increased mitochondrial intermembrane potential, remodeling of mitochondrial ultrastructure, and changes in the abundance of enzymes involved in pyruvate handling, electron transport and lipid synthesis. Pluripotent state-associated changes in cESC metabolic pathway activity and enzyme abundance have a functionally relevant impact on cESC ATP synthesis and proliferation. Our study provides the first evidence for suboptimal glycolytic flux in cESCs lines as well as extensive remodeling of the cristae

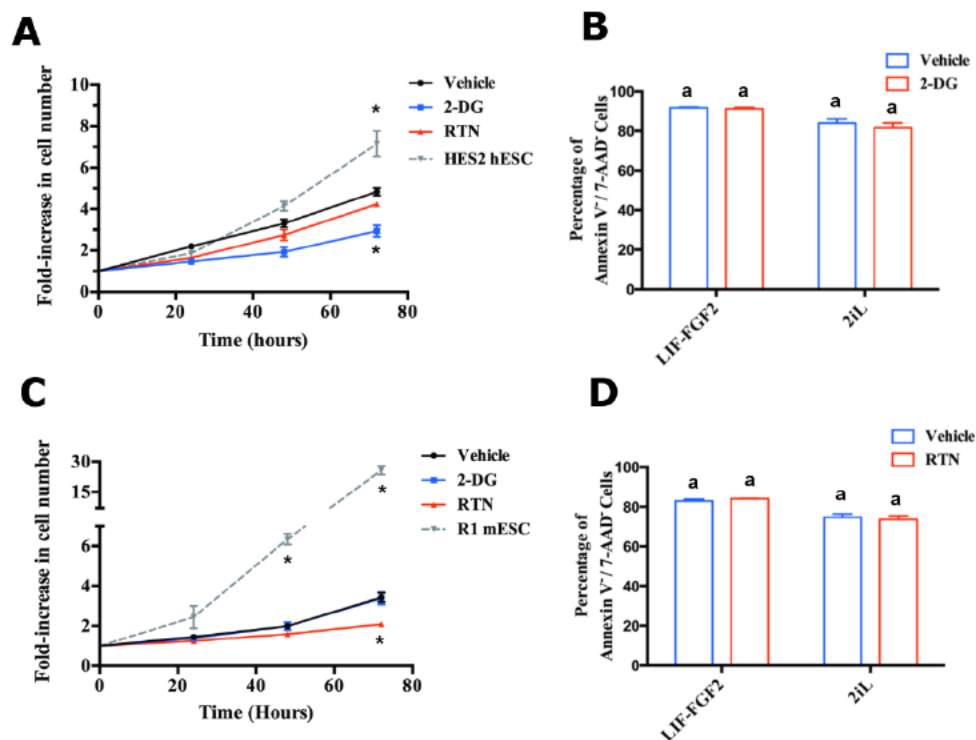


Figure 3-15. Different chemical inhibitors of bioenergetics influence the acute expansion of L/F or 2iL cESCs.

L/F cESC (A) proliferation assay and (B) viability assay in the presence or absence 2-deoxy-D-glucose (2-DG) or rotenone (RTN). 2iL cESC (C) proliferation assay and (D) viability assay in the presence of 2-DG or RTN at the same concentration. Cells were seeded in the absence of any inhibitors, counted each day and expressed relative to the initial cell number and compared to vehicle treated control cESCs. Viability was assessed by the percentage of Annexin V⁻/7-AAD⁻ cESCs following exposure to 2-DG or RTN. Dashed line represents doubling time of primed PSC control HES-2 hESC (in A) or naïve PSC control R1 mESC (in C). Bars represent standard error of the mean (SEM) n = 3-6. Means followed by the same letter are not significantly different, P < 0.05. Data points annotated with asterisks are significantly different from vehicle-treated cESC populations at the equivalent time point, P < 0.05.

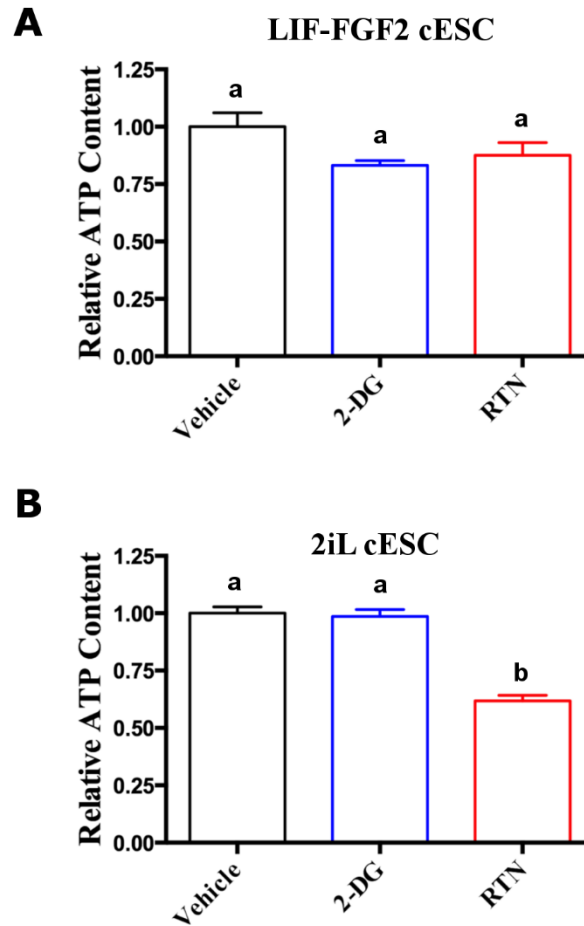


Figure 3-16. Selective metabolic pathway inhibition affects ATP level of 2iL cESCs but not L/F cESCs.

Quantification of cellular ATP level in (A) L/F cESCs or (B) 2iL cESCs following acute exposure to 2-deoxy-D-glucose (2-DG) or rotenone (RTN). Bars represent standard error of the mean (SEM) $n = 5$. Means followed by the same letter are not significantly different, $P < 0.05$.

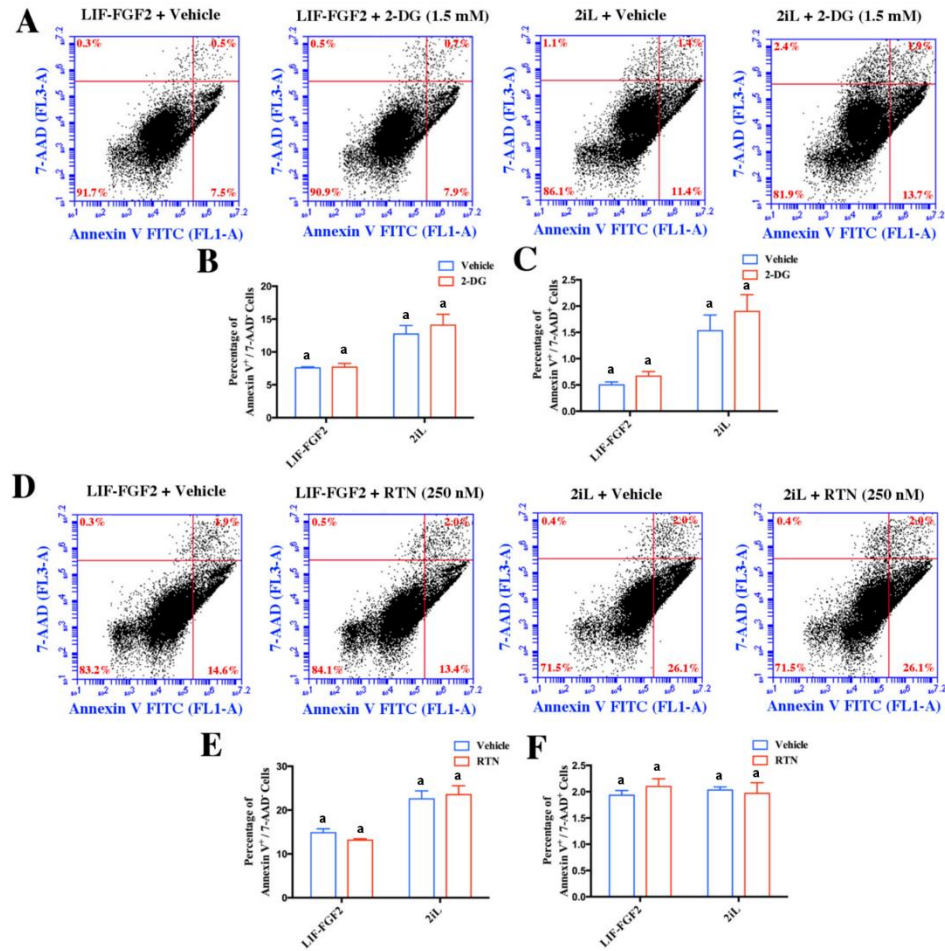


Figure 3-17. Titrated metabolic pathway inhibitors do not increase apoptotic or dead cESCs.

(A) Representative dotplots of Annexin V-FITC and 7-aminoactinomycin D (7-AAD) stained cESCs treated with 2-deoxyglucose (2-DG) or vehicle. Quantification of (B) apoptotic and (C) dead cells following treatment with 2-DG or vehicle. (D) Representative dotplots of Annexin V-FITC and 7-AAD stained cESCs treated with rotenone (RTN) or vehicle. Quantification of (E) apoptotic and (F) dead cells following treatment with RTN or vehicle. Bars represent standard error of the mean (SEM) $n = 3$. Means followed by the same letter are not significantly different, $P < 0.05$.

membranes associated with a metabolic switch towards mitochondrial metabolism with naïve-like pluripotency induction.

We found that 2iL subculture enriches for a cESC population with greater respiratory spare capacity and a preference for mitochondrial glucose oxidation under steady-state conditions compared to L/F cESCs. Augmented cellular respiration has also been reported upon induction of naïve-like hESCs (Takashima et al., 2014) and may represent a conserved attribute of naïve pluripotency in placental mammals. We found that elevated respiratory capacity 2iL cESCs is not associated with any difference in overall mitochondrial biomass with respect to L/F cESCs. However, 2iL cESCs predominantly contain smaller, rounded mitochondria that morphologically similar to those within mouse ESC and chemically induced naïve-like human ESC (Sperber et al., 2015; Zhou et al., 2012). We investigated glycolytic enzymes upstream of mitochondrial substrate provision and identified increased levels PKM isoform 1 and a lower LDH isoform A level in 2iL cESCs. These observations are suggestive of increased mitochondrial pyruvate and NADH availability at the expense of LDH-mediated NAD^+ regeneration (Fantin et al., 2006). Elevated phosphorylation of PDH would be expected to limit pyruvate conversion to acetyl-CoA in 2iL cESCs, implicating reductive carboxylation of pyruvate as an alternative mechanism of TCA cycle replenishment. As a plausible consequence of greater pyruvate oxidation, fewer metabolic intermediates may be available for anabolic pathways such as *de novo* lipogenesis (Tohyama et al., 2016). We found that L/F cESCs exhibited greater FASN abundance and accumulated more intracellular neutral lipids than 2iL cESCs.

In contrast to previous reports that mitochondria within naïve-like ESCs are qualitatively cristae-poor (Ware et al., 2014; Zhou et al., 2012), we observed that mitochondrial cristae density is preserved in 2iL cESCs. Furthermore, we quantified previously unrecognized changes to the degree of cristae organization between different states of pluripotency *in vitro*. 2iL cESCs contained mitochondria with disorganized cristae that project along the periphery of the organelle rather than assuming a lamellar, axis-spanning orientation. The arch-like inner mitochondrial membranes within 2iL cESCs are similar to those described in early preimplantation embryos (Baharvand and Matthaiei, 2003; Sathanathan and

Trounson, 2000), suggesting that immature mitochondrial morphology is not an artifact of *in vitro* culture. Altered cristae architecture is associated with changes to the abundance of Mitofilin/MIC60, a component of the mitochondrial contact site and cristae organizing system (Hessenberger et al., 2017). We also observed, but did not directly quantify, the widening of cristae, particularly at the tips and the cristae junctions. Conceivably, lower abundance of catalytic ATP synthase subunits in 2iL cESCs could limit the pool of oligomerized ATP synthase complexes, which induce membrane curvature and restrict the circumference of cristae rims and tips (Davies et al., 2012). Structural changes to the cristae inflate the intracristal space, increasing the diffusion distance needed to traverse the outer mitochondrial membrane and plausibly function as a proton or ROS reservoir (Plecitá-Hlavatá and Ježek, 2016).

The transition from OXPHOS to aerobic glycolysis in human and mouse ESCs is accompanied by coordinated changes in mitochondrial chain complex subunit expression (Zhou et al., 2012), electron transport chain (ETC) activity and ATP synthesis by OXPHOS. However, reconfiguration of membrane composition or chain complex stoichiometry can have a less obvious influence on mitochondrial function through the formation of supercomplexes that channel substrates and electron carriers (Dudek et al., 2013; Lapuente-Brun et al., 2013). We identified an enrichment of SDHB subunit (i.e. complex II) and a reduction of ATP5A subunit (i.e. complex V). The observed changes in respiratory chain subunits implicate both altered OXPHOS kinetics or efficiency and expedited conversion of succinate to fumarate in the TCA cycle. Our data also suggest that increased cellular ATP level may promote global changes in 2iL cESCs through retrograde signaling via the energy-sensing AMPK pathway (Herzig and Shaw, 2018), or speculatively ATP-dependent chromatin remodeling enzymes (Zhang et al., 2018).

We find that L/F cESCs do not exhibit the mitochondrial reserve capacity to oxidize pyruvate thereby rendering L/F cESCs dependent on glycolysis for *in vitro* growth. Indeed, inhibition of electron transport had no effect on the acute expansion of L/F cESC, whereas blockade of glycolysis was observed to reduce L/F cESC proliferation independent of ATP. This is consistent with respirometry experiments with hESCs (Sperber et al., 2015) and reports that ETC activity is dispensable for maintenance of

primed pluripotency (Varum et al., 2009). In contrast, 2iL cESCs showed both elevated respiratory and glycolytic reserve capacity and were tolerant to partial inhibition of glycolysis by 2-DG, implicating that divergent metabolic programs support proliferation in L/F and 2iL cESCs with regards to glucose utilization. Comparative experiments including hESC/mEpiLC, mESC, L/F and 2iL cESC lines indicate that glycolytic capacity is not influenced by pluripotent state. However, there appears to be a canine-specific reduction in glycolytic capacity that coincides with prolonged population doubling intervals observed cESC lines. Glucose uptake and metabolism are typically co-regulated by transcriptional programs controlling cell growth and proliferation (e.g. MYC), however we observe a selective decrease in HXK2 in cESCs compared to mESC or hESC (Dang et al., 2008). Indeed, several tumor-suppressor pathways involving micro-RNA species or autophagic clearance have been implicated in selective HXK2 repression (Jiao et al., 2018; Liu et al., 2017; Peschiaroli et al., 2013).

Enhanced glycolytic reserve capacity observed in oxidative 2iL cESCs suggests a degree metabolic pathway flexibility that resembles the ‘bivalent’ metabolic responses observed with naïve R1 mESCs than primed HES-2 hESCs. However, 2iL cESC proliferation and ATP generation was sensitive to RTN exposure, which is dissimilar to experiments performed in naïve mESC (Vlaski-Lafarge et al., 2019). Lower ATP content of RTN-treated 2iL cESCs could signify that glycolysis alone cannot meet the bioenergetic demand for steady state growth of 2iL cESCs. Conversely, RTN treatment may be associated with ROS production (Li et al., 2003) and indirectly affecting cellular ATP through retrograde ROS signaling mechanisms. We have not yet followed up on the potential contributions of redox-sensitive retrograde signaling pathways such as nuclear respiratory factor (NRF), p53 and p21 that are understood to influence the cell cycle and mitochondrial metabolism (Chandel et al., 2000; Khacho et al., 2016; Passos et al., 2010).

The described work represents the first evidence of suboptimal glycolytic flux in cESCs lines as well as extensive remodeling of the cristae membranes associated with a metabolic switch towards mitochondrial metabolism with naïve-like pluripotency induction in the dog. Our data demonstrate that L/F cESCs exhibit a preferentially glycolytic and anabolic phenotype. Whereas 2iL cESCs acquire both glycolytic and

respiratory reserve capacities but remain less bioenergetic and metabolically flexible than naïve mESC. This study lends additional support to the notion that cellular metabolism is a conserved discriminatory readout of pluripotent states in placental mammals. However, species-specific attributes appear to constrain glycolytic flux in cESCs and metabolic bivalency achievable through a 2iL-supported naïve pluripotent state.

3.5 References

- Baharvand, H., & Matthaei, K. I. (2003). The ultrastructure of mouse embryonic stem cells. *Reproductive Biomedicine Online*, 7(3), 330–335.
- Bao, S., Tang, F., Li, X., Hayashi, K., Gillich, A., Lao, K., & Surani, M. A. (2009). Epigenetic reversion of post-implantation epiblast to pluripotent embryonic stem cells. *Nature*, 461(7268), 1292–1295.
- Betts, D. H., & Tobias, I. C. (2015). Canine Pluripotent Stem Cells: Are They Ready for Clinical Applications? *Frontiers in Veterinary Science*, 2, 41.
- Bissonnette, P., Gagné, H., Blais, A., Berteloot, A. (1996). 2-Deoxyglucose transport and metabolism in Caco-2 cells. *The American Journal of Physiology*, 270(1 Pt 1), G153-62.
- Brons, I. G. M., Smithers, L. E., Trotter, M. W. B., Rugg-Gunn, P., Sun, B., Chuva de Sousa Lopes, S. M., ... Vallier, L. (2007). Derivation of pluripotent epiblast stem cells from mammalian embryos. *Nature*, 448(7150), 191–195.
- Buckman, J. F., Hernandez, H., Kress, G. J., Votyakova, T. V., Pal, S., & Reynolds, I. J. (2001). MitoTracker labeling in primary neuronal and astrocytic cultures: Influence of mitochondrial membrane potential and oxidants. *Journal of Neuroscience Methods*, 104(2), 165–176.
- Buecker, C., Chen, H. H., Polo, J. M., Daheron, L., Bu, L., Barakat, T. S., ... Geijsen, N. (2010). A murine ESC-like state facilitates transgenesis and homologous recombination in human pluripotent stem cells. *Cell Stem Cell*, 6(6), 535–546.
- Carbognin, E., Betto, R. M., Soriano, M. E., Smith, A. G., & Martello, G. (2016). Stat3 promotes mitochondrial transcription and oxidative respiration during maintenance and induction of naïve pluripotency. *The EMBO Journal*, 35(6), 618–34.
- Chandel, N. S., Vander Heiden, M. G., Thompson, C. B., & Schumacker, P. T. (2000). Redox regulation of p53 during hypoxia. *Oncogene*.
- Chung, S., Dzeja, P. P., Faustino, R. S., Perez-Terzic, C., Behfar, A., & Terzic, A. (2007). Mitochondrial oxidative metabolism is required for the cardiac

differentiation of stem cells. *Nature Clinical Practice Cardiovascular Medicine*, 4, S60–S67.

- Cossarizza, A., Baccaranicontri, M., Kalashnikova, G., & Franceschi, C. (1993). A New Method for the Cytofluorometric Analysis of Mitochondrial Membrane Potential Using the J-Aggregate Forming Lipophilic Cation 5,5',6,6'-Tetrachloro-1,1',3,3'-tetraethylbenzimidazolcarbocyanine Iodide (JC-1). *Biochemical and Biophysical Research Communications*, 197(1), 40–45.
- Dackowski, W. R., Luderer, H. F., Manavalan, P., Bukanov, N. O., Russo, R. J., Roberts, B. L., ... Ibraghimov-Beskrovnaya, O. (2002). Canine PKD1 is a single-copy gene: genomic organization and comparative analysis. *Genomics*, 80(1), 105–112.
- Dang, C. V., Kim, J. W., Gao, P., & Yustein, J. (2008). The interplay between MYC and HIF in cancer. *Nature Reviews Cancer*.
- Davies, K. M., Anselmi, C., Wittig, I., Faraldo-Gomez, J. D., & Kuhlbrandt, W. (2012). Structure of the yeast F1Fo-ATP synthase dimer and its role in shaping the mitochondrial cristae. *Proceedings of the National Academy of Sciences*, 109(34), 13602–13607.
- Dudek, J., Cheng, I. F., Balleininger, M., Vaz, F. M., Streckfuss-Bömeke, K., Hübscher, D., ... Guan, K. (2013). Cardiolipin deficiency affects respiratory chain function and organization in an induced pluripotent stem cell model of Barth syndrome. *Stem Cell Research*, 11(2), 806–819.
- Ehrenberg, B., Montana, V., Wei, M. D., Wuskell, J. P., & Loew, L. M. (1988). Membrane potential can be determined in individual cells from the nernstian distribution of cationic dyes. *Biophysical Journal*, 53(5), 785–94.
- Fantin, V. R., St-Pierre, J., & Leder, P. (2006). Attenuation of LDH-A expression uncovers a link between glycolysis, mitochondrial physiology, and tumor maintenance. *Cancer Cell*, 9(6), 425–434.
- Ficz, G., Hore, T. A., Santos, F., Lee, H. J., Dean, W., Arand, J., ... Reik, W. (2013). FGF Signaling Inhibition in ESCs Drives Rapid Genome-wide Demethylation to the Epigenetic Ground State of Pluripotency. *Cell Stem Cell* (Vol. 13).
- Floryk, D., & Houštek, J. (1999). Tetramethyl rhodamine methyl ester (TMRM) is suitable for cytofluorometric measurements of mitochondrial membrane potential in cells treated with digitonin. *Bioscience Reports*, 19(1), 27–34.
- Folmes, C. D. L., Nelson, T. J., Martinez-Fernandez, A., Arrell, D. K., Lindor, J. Z., Dzeja, P. P., ... Terzic, A. (2011). Somatic Oxidative Bioenergetics Transitions into Pluripotency-Dependent Glycolysis to Facilitate Nuclear Reprogramming. *Cell Metabolism*, 14(2), 264–271.

- Gafni, O. et al., Weinberger, L., Mansour, A. A., Manor, Y. S., Chomsky, E., Ben-Yosef, D., ... Hanna, J. H. (2013). Derivation of novel human ground state naive pluripotent stem cells. *Nature*, 504(7479), 282–6.
- Guo, G. G., Yang, J., Nichols, J., Hall, J. S., Eyres, I., Mansfield, W., ... Mansfield, W. (2009). Klf4 reverts developmentally programmed restriction of ground state pluripotency. *Development*, 136(7), 1063–9.
- Harvey, A. J., Rathjen, J., Yu, L. J., & Gardner, D. K. (2016). Oxygen modulates human embryonic stem cell metabolism in the absence of changes in self-renewal. *Reproduction, Fertility and Development*, 28(4), 446–458.
- Herzig, S., & Shaw, R. J. (2018). AMPK: Guardian of metabolism and mitochondrial homeostasis, *Nature Reviews Molecular Cell Biology* 19, 121–135.
- Hessenberger, M., Zerbes, R. M., Rampelt, H., Kunz, S., Xavier, A. H., Purfürst, B., ... Daumke, O. (2017). Regulated membrane remodeling by Mic60 controls formation of mitochondrial crista junctions. *Nature Communications*, 8, 152-158.
- Iannetti, E. F., Smeitink, J. A. M., Beyrath, J., Willems, P. H. G. M., & Koopman, W. J. H. (2016). Multiplexed high-content analysis of mitochondrial morphofunction using live-cell microscopy. *Nature Protocols*, 11(9), 1693–1710.
- Jiao, L., Zhang, H. L., Li, D. D., Yang, K. L., Tang, J., Li, X., ... Zhu, X. F. (2018). Regulation of glycolytic metabolism by autophagy in liver cancer involves selective autophagic degradation of HK2 (hexokinase 2). *Autophagy*. 14(4), 671-684
- Kamo, N., Muratsugu, M., Hongoh, R., & Kobatake, Y. (1979). Membrane potential of mitochondria measured with an electrode sensitive to tetraphenyl phosphonium and relationship between proton electrochemical potential and phosphorylation potential in steady state. *The Journal of Membrane Biology*, 49(2), 105–21.
- Khacho, M., Clark, A., Svoboda, D. S., Azzi, J., MacLaurin, J. G., Meghaizel, C., ... Slack, R. S. (2016). Mitochondrial Dynamics Impacts Stem Cell Identity and Fate Decisions by Regulating a Nuclear Transcriptional Program. *Cell Stem Cell*.
- Kim, K. S., Lee, S. E., Jeong, H. W., & Ha, J. H. (1998). The complete nucleotide sequence of the domestic dog (*Canis familiaris*) mitochondrial genome. *Molecular Phylogenetics and Evolution*, 10(2), 210–220.
- Lapiente-Brun, E., Moreno-Loshuertos, R., Acin-Perez, R., Latorre-Pellicer, A., Colas, C., Balsa, E., ... Enriquez, J. A. (2013). Supercomplex Assembly Determines Electron Flux in the Mitochondrial Electron Transport Chain. *Science*, 340(6140), 1567–1570.

- Leitch, H. G., McEwen, K. R., Turp, A., Encheva, V., Carroll, T., Grabole, N., ... Hajkova, P. (2013). Naive pluripotency is associated with global DNA hypomethylation. *Nature Structural & Molecular Biology*, 20(3), 311–316.
- Li, N., Ragheb, K., Lawler, G., Sturgis, J., Rajwa, B., Melendez, J. A., & Robinson, J. P. (2003). Mitochondrial complex I inhibitor rotenone induces apoptosis through enhancing mitochondrial reactive oxygen species production. *The Journal of Biological Chemistry*, 278(10), 8516–25.
- Liu, H., Liu, N., Cheng, Y., Jin, W., Zhang, P., Wang, X., ... Tu, Y. (2017). Hexokinase 2 (HK2), the tumor promoter in glioma, is downregulated by miR-218/Bmi1 pathway. *PLoS ONE*.
- Liu, Y., & Yamashita J.K. (2019). AMPK activators contribute to maintain naïve pluripotency in mouse embryonic stem cells. *Biochem Biophys Res Commun*.
- Meek, S., Wei, J., Sutherland, L., Nilges, B., Buehr, M., Tomlinson, S. R., ... Burdon, T. (2013). Tuning of β -catenin activity is required to stabilize self-renewal of rat embryonic stem cells. *Stem Cells*, 31(10), 2104–2115.
- Mitra, K., & Lippincott-Schwartz, J. (2010). Analysis of mitochondrial dynamics and functions using imaging approaches. *Current Protocols in Cell Biology*, Chapter 4, Unit 4.25.1-21.
- Nagy, A., Rossant, J., Nagy, R., Abramow-Newerly, W., & Roder, J. C. (1993). Derivation of completely cell culture-derived mice from early-passage embryonic stem cells. *Proceedings of the National Academy of Sciences*, 90(18), 8424–8.
- Nakano, K., Watanabe, M., Matsunari, H., Matsuda, T., Honda, K., Maehara, M., ... Nagashima, H. (2013). Generating Porcine Chimeras Using Inner Cell Mass Cells and Parthenogenetic Preimplantation Embryos. *PLoS ONE*, 8(4), e61900.
- Nakayama, T., Ueda, Y., Yamada, H., Shores, E. W., Singer, A., & June, C. H. (1992). In vivo calcium elevations in thymocytes with T cell receptors that are specific for self ligands. *Science*, 257(5066), 96–99.
- Nichols, J., Silva, J., Roode, M., & Smith, A. (2009). Suppression of Erk signalling promotes ground state pluripotency in the mouse embryo. *Development*, 136(19), 3215–22.
- Nichols, J., & Smith, A. (2009). Naive and Primed Pluripotent States. *Cell Stem Cell*, 4(6), 487–492.
- Osteil, P., Tapponnier, Y., Markossian, S., Godet, M., Schmaltz-Panneau, B., & Jouneau, L. (2013). Induced pluripotent stem cells derived from rabbits exhibit some characteristics of naïve pluripotency. *Biology Open*, 2(6), 613–28.

- Panopoulos, A. D., Yanes, O., Ruiz, S., Kida, Y. S., Diep, D., Tautenhahn, R., ... Belmonte, J. C. I. (2012). The metabolome of induced pluripotent stem cells reveals metabolic changes occurring in somatic cell reprogramming. *Cell Research*, 22(1), 168–177.
- Passos, J. F., Nelson, G., Wang, C., Richter, T., Simillion, C., Proctor, C. J., ... Von Zglinicki, T. (2010). Feedback between p21 and reactive oxygen production is necessary for cell senescence. *Molecular Systems Biology*.
- Perry, S. W., Norman, J. P., Barbieri, J., Brown, E. B., & Gelbard, H. A. (2011). Mitochondrial membrane potential probes and the proton gradient: A practical usage guide. *BioTechniques*.
- Peschiaroli, A., Giacobbe, A., Formosa, A., Markert, E. K., Bongiorno-Borbone, L., Levine, A. J., ... Melino, G. (2013). MiR-143 regulates hexokinase 2 expression in cancer cells. *Oncogene*.
- Plecitá-Hlavatá, L., & Ježek, P. (2016). Integration of superoxide formation and cristae morphology for mitochondrial redox signaling. *International Journal of Biochemistry and Cell Biology*.
- Racker, E. (1972). Bioenergetics and the problem of tumor growth. *American Scientist*, 60(1), 56–63.
- Rassow, J., & Pfanner, N. (2000). The protein import machinery of the mitochondrial membranes. *Traffic*, 1(6), 457–464.
- Reubinoff, B. E., Pera, M. F., Fong, C.-Y. Y., Trounson, A., Bongso, A., Reubinoff, B. E., ... Bongso, A. (2000). Embryonic stem cell lines from human blastocysts: Somatic differentiation in vitro. *Nature Biotechnology*, 18(4), 399–404.
- Samudio, I., Fiegl, M., & Andreeff, M. (2009). Mitochondrial Uncoupling and the Warburg Effect: Molecular Basis for the Reprogramming of Cancer Cell Metabolism. *Cancer Research*, 69(6), 2163–2166.
- Sathanathan, A. H., & Trounson, A. O. (2000). Mitochondrial morphology during preimplantational human embryogenesis. *Human Reproduction*, 15(2), 148–159.
- Scaduto, R. C., & Grotyohann, L. W. (1999). Measurement of mitochondrial membrane potential using fluorescent rhodamine derivatives. *Biophysical Journal*, 76(1 Pt 1), 469–77.
- Smiley, S. T., Reers, M., Mottola-Hartshorn, C., Lin, M., Chen, A., Smith, T. W., ... Chen, L. B. (1991). Intracellular heterogeneity in mitochondrial membrane potentials revealed by a J-aggregate-forming lipophilic cation JC-1. *Proceedings of the National Academy of Sciences of the United States of America*, 88(9), 3671–3675.

- Sperber, H., Mathieu, J., Wang, Y., Ferreccio, A., Hesson, J., Xu, Z., ... Ruohola-Baker, H. (2015). The metabolome regulates the epigenetic landscape during naive-to-primed human embryonic stem cell transition. *Nature Cell Biology*, 17(12), 1523–1535.
- Takashima, Y., Guo, G., Loos, R., Nichols, J., Ficuz, G., Krueger, F., ... Smith, A. (2014). Resetting Transcription Factor Control Circuitry toward Ground-State Pluripotency in Human. *Cell*, 158((6)), 1254–69.
- Taniguchi, K., Sakai, M., Sugito, N., Kuranaga, Y., Kumazaki, M., Shinohara, H., ... Akao, Y. (2016). PKM1 is involved in resistance to anti-cancer drugs. *Biochemical and Biophysical Research Communications*, 473(1), 174–180.
- Tesar, P. J., Chenoweth, J. G., Brook, F. A., Davies, T. J., Evans, E. P., Mack, D. L., ... McKay, R. D. G. (2007). New cell lines from mouse epiblast share defining features with human embryonic stem cells. *Nature*, 448(7150), 196–199.
- Tobias, I. C., Brooks, C. R., Teichroeb, J. H., & Betts, D. H. (2013). Derivation and culture of canine embryonic stem cells. *Methods in Molecular Biology* (Vol. 1074).
- Tobias, I. C., Brooks, C. R., Teichroeb, J. H., Villagómez, D. A., Hess, D. A., Séguin, C. A., & Betts, D. H. (2016). Small-Molecule Induction of Canine Embryonic Stem Cells Toward Naïve Pluripotency. *Stem Cells and Development*, 25(16).
- Tohyama, S., Fujita, J., Hishiki, T., Matsuura, T., Hattori, F., Ohno, R., ... Fukuda, K. (2016). Glutamine Oxidation Is Indispensable for Survival of Human Pluripotent Stem Cells. *Cell Metabolism*, 23(4), 663–674.
- Vander Heiden, M. G., Cantley, L. C., Thompson, C. B., Heiden, M. G. Vander, Cantley, L. C., & Thompson, C. B. (2009). Understanding the warburg effect: The metabolic requirements of cell proliferation. *Science*, 324(5930), 1029–33.
- Varum, S., Momčilović, O., Castro, C., Ben-Yehudah, A., Ramalho-Santos, J., & Navara, C. S. (2009). Enhancement of human embryonic stem cell pluripotency through inhibition of the mitochondrial respiratory chain. *Stem Cell Research*, 3(2), 142–156.
- Verma, V., Huang, B., Kallingappa, P. K., & Oback, B. (2013). Dual Kinase Inhibition Promotes Pluripotency in Finite Bovine Embryonic Cell Lines. *Stem Cells and Development*, 22(11), 1728–1742.
- Vlaski-Lafarge, M., Loncaric, D., Perez, L., Labat, V., Debeissat, C., Brunet de la Grange, P., ... Bœuf, H. (2019). Bioenergetic Changes Underline Plasticity of Murine Embryonic Stem Cells. *Stem Cells*.

- Ware, C. B., Nelson, A. M., Mecham, B., Hesson, J., Zhou, W., Jonlin, E. C., ... Ruohola-Baker, H. (2014). Derivation of naive human embryonic stem cells. *Proceedings of the National Academy of Sciences*, 111(12), 4484–4489.
- Whitworth, D. J., Ovchinnikov, D. a, Sun, J., Fortuna, P. R. J., & Wolvetang, E. J. (2014). Generation and characterization of leukemia inhibitory factor-dependent equine induced pluripotent stem cells from adult dermal fibroblasts. *Stem Cells and Development*, 23(13), 1515–23.
- Wilcox, J. T., Lai, J. K. Y. Y., Semple, E., Brisson, B. A., Gartley, C., Armstrong, J. N., & Betts, D. H. (2011). Synaptically-competent neurons derived from canine embryonic stem cells by lineage selection with EGF and noggin. *PLoS ONE*, 6(5), e19768.
- Wilcox, J. T., Semple, E., Gartley, C., Brisson, B. A., Perrault, S. D., Villagómez, D. A. F., ... Betts, D. H. (2009). Characterization of Canine Embryonic Stem Cell Lines Derived From Different Niche Microenvironments. *Stem Cells and Development*, 18(8), 1167–1178.
- Wray, J., Kalkan, T., Gomez-Lopez, S., Eckardt, D., Cook, A., Kemler, R., & Smith, A. (2011). Inhibition of glycogen synthase kinase-3 alleviates Tcf3 repression of the pluripotency network and increases embryonic stem cell resistance to differentiation. *Nature Cell Biology*, 13(7), 838–845.
- Zhang, H., Badur, M. G., Divakaruni, A. S., Parker, S. J., Jäger, C., Hiller, K., ... Metallo, C. M. (2016). Distinct Metabolic States Can Support Self-Renewal and Lipogenesis in Human Pluripotent Stem Cells under Different Culture Conditions. *Cell Reports*, 16(6), 1536–47.
- Zhang, J., Khvorostov, I., Hong, J. S., Oktay, Y., Vergnes, L., Nuebel, E., ... Teitell, M. A. (2011). UCP2 regulates energy metabolism and differentiation potential of human pluripotent stem cells. *The EMBO Journal*, 30(24), 4860–4873.
- Zhang, J., Nuebel, E., Daley, G. Q., Koehler, C. M., & Teitell, M. A. (2012). Metabolic Regulation in Pluripotent Stem Cells during Reprogramming and Self-Renewal. *Cell Stem Cell*, 11(5), 589–595.
- Zhang, J., Nuebel, E., Wisidagama, D. R. R., Setoguchi, K., Hong, J. S., Van Horn, C. M., ... Teitell, M. A. (2012). Measuring energy metabolism in cultured cells, including human pluripotent stem cells and differentiated cells. *Nature Protocols*, 7(6), 1068–1085.
- Zhang, Y., Cui, P., Li, Y., Feng, G., Tong, M., Guo, L., ... Zhou, Q. (2018). Mitochondrially produced ATP affects stem cell pluripotency via Act16a-mediated histone acetylation. *FASEB Journal*.
- Zhou, W., Choi, M., Margineantu, D., Margaretha, L., Hesson, J., Cavanaugh, C., ... Ruohola-Baker, H. (2012). HIF1 α induced switch from bivalent to exclusively

glycolytic metabolism during ESC-to-EpiSC/hESC transition. *The EMBO Journal*, 31(9), 2103–2116.

Zhou, X., Contreras-Trujillo, H., & Ying, Q.-L. (2015). New insights into the conserved mechanism of pluripotency maintenance. *Current Opinion in Genetics & Development*, 34, 1–9.

Chapter 4

4 Bioactive metabolite supplementation promotes mesenchymal-to-epithelial transition in early canine reprogramming

4.1 Introduction

Domestic dogs are susceptible to a spectrum of inherited and acquired diseases with analogy to humans (Ostrander et al., 2000; Sutter and Ostrander, 2004). Exposure to environmental mutagens during human-canine coexistence (Backer et al., 2008) as well as similarities in immune system anatomy and development (Storb and Thomas, 1985) have likely contributed to these shared pathologies. Approximately 94% of the canine genome is syntenic to the human assembly and considered conserved ancestral sequence (Lindblad-Toh et al., 2005; Ostrander and Wayne, 2005). Modeling the effect of disease-associated loci in a variety of cell types has been made feasible by the ectopic expression of a defined set of factors to generate induced pluripotent stem cells (iPSCs) (Takahashi and Yamanaka, 2006). However, the routine use of canine iPSCs has been limited by protocol inconsistency (Betts and Tobias, 2015), low number of clonal iPSC lines established (Chow et al., 2017; Luo et al., 2011) and a lack of quantitative evidence of long-term self-renewal. Despite a high degree of synteny through evolution, studies of several putative canine iPSC lines have revealed unique features compared to human iPSC including the requirement of LIF/STAT3 signaling for prolonged self-renewal (Chow et al., 2017; Koh et al., 2013; Luo et al., 2011).

Global analyses of epigenetic modifications in reprogramming intermediates suggest that progress towards a pluripotent state is constrained by repressive modifications on chromatin (Apostolou and Hochedlinger, 2013; De Carvalho et al., 2010). Focal DNA demethylation during iPSC generation and maintenance of hypomethylated chromatin in pluripotent cells are mediated by the ten-eleven translocation (TET) family of methylcytosine dioxygenase (Bagci and Fisher, 2013; Wu and Zhang, 2017). TET enzymes mediate active-active and active-passive mechanisms of DNA demethylation, through the oxidation of 5-methylcytosine (5-mC) into a variety of cytosine substituents

that may be recognized by base-excision repair machinery (He et al., 2011; Ito et al., 2011). Functional genomics and computational modelling of iPSC derivation indicate that engagement of reprogramming transactors with previously silent regulatory sequences facilitates local epigenetic remodeling and elevated transcriptional output at critical pluripotency regulators (Koche et al., 2011; Soufi et al., 2012). Recently, it was demonstrated that TET recruitment and active demethylation at pluripotency-associated enhancers and promoters, occurs prior to chromatin opening and stable transcriptional activation (Sardina et al., 2018).

The density of CpG islands (CGIs) is the highest in the domestic canine genome assembly among completely sequenced placental mammals, despite no genome-wide difference in the parameters used to define CGIs (Han et al., 2008). Mammalian genomes contain subgroups of high CpG (HCP), intermediate CpG (ICP) and low CpG promoters (LCP), each with a distinct relationship between DNA methylation and transcriptional activity (Meissner et al., 2008). HCPs contain at least one *de facto* CGI (Fouse et al., 2008) and are generally not transcriptionally active when methylated (Antequera et al., 1990; Deaton and Bird, 2011; Weber et al., 2007). TET binding is elevated at CpG-rich sequences such as CGIs, owing to its CXXC domain (Williams et al., 2011; Xu et al., 2011). TET enzymes lacking the CXXC domain exhibit similar genomic localization, albeit with lower enrichment, suggesting that protein-protein interactions also contribute to TET recruitment (Zhang et al., 2016). 5-hydroxymethylcytosine (5-hmC), a stable product of TET-catalysis (Bachman et al., 2014), is critical to the maintenance of active cis-regulatory modules (CRMs). The demethylated state of pluripotency-associated enhancers and promoters are dependent on TET because these regions gain the greatest *de novo* methylation in TET1-3 triple knockout mESCs (Lu et al., 2014). At least one competent TET paralog is required for successful acquisition of pluripotency by somatic cell reprogramming (Hu et al., 2014).

Reprogramming canine fibroblasts with integrating vectors is reported to be highly protracted process (30-40 days) (Koh and Piedrahita, 2015), and the molecular events during canine reprogramming have not been characterized or time-resolved. An understanding of the bottlenecks in canine somatic cell reprogramming is vital to increase

the probability of successful reprogramming and map the molecular events in canine pluripotency acquisition. The temporary use of small molecules to enhance the endogenous DNA demethylation machinery is a promising strategy to improve the efficiency and kinetics of reprogramming in challenging cell populations. Kinetics are critical for non-integrating gene delivery systems, such as Sendai virus (SeV) vectors, with a limited timeframe for cells to achieve transgene-independence.

Several physiological metabolites have been demonstrated to regulate TET abundance, catalytic activity or recruitment including alpha-ketoglutarate, L-ascorbic acid (Vitamin C) and retinoic acid (a derivative of Vitamin A) (Blaschke et al., 2013; Carey et al., 2014; Hore et al., 2016; Yin et al., 2013). TET enzymes have affinity for CpG-rich sequences that are frequent in a canine genome, as well as other regulatory elements when recruited by pluripotency transcription factors in a reprogramming context. It is conceivable that TET proteins might have an important role in active DNA demethylation, or otherwise enable more permissive histone modifications by indirect cross-talk mechanisms, at endogenous DNA- and chromatin-binding pluripotency regulators in the uniquely CpG island-rich canine genome. However, the soluble factors controlling TET abundance and activity in a somatic nuclear environment, and how they could be leveraged in reprogramming canine cells has yet to be explored.

Taking advantage of the efficient, non-integrating CytoTune SeV gene-delivery system, which is designed as self-limiting and non-transmissible (Ban et al., 2011; Fusaki et al., 2009), we investigated whether modifiers of DNA methylation could promote early canine de-differentiation. We highlight that initiation of canine fetal fibroblast reprogramming features a mesenchymal-to-epithelial transition within the first week, which is bolstered by physiological metabolites that enhance TET-mediated 5-hmC generation.

4.2 Materials and Methods

4.2.1 Genomic Sequence Retrieval and Processing

Genomic sequence and gene features were retrieved from the Ensembl genome browser (Release 92) using the biomaRt/Bioconductor package. The 5'-flanking sequences of 1-1-

1 orthologous genes from the canine (CanFam3.1), human (GRCh38.p12) and mouse (GRCm38.p6) genomic assemblies were accessed using biomaRt (Drost and Paszkowski, 2017). For hierarchical cluster analysis, the common orthologs of three additional Eutherian species were included: rabbit (OryCun2.0), porcine (Sscrofa11.1) and bovine (UMD3.1). See Table 4-1 for specific details regarding the retrieval of differentially expressed gene sets accessed in this work. Our analysis included regions 2 kilobases upstream and 500 bases downstream of each transcription start site, as defined by track RefSeq genes (O’Leary et al., 2016). Retrieved sequences with large gaps (ambiguous bases [N] > 250) were excluded from further analyses, whereas smaller gaps were accounted for in DNA string length calculations.

Table 4-1. Summary of conserved reprogramming-associated gene products.

Study Information	Data Accessed	Resultant Gene List
Mouse Fibroblast Reprogramming (Nefzger et al., 2017)	Accessed list of highly correlated genes (fibroblast versus neutrophil/keratinocyte) with correlation coefficient cut-off of 0.9 and a minimum of 4-fold change	POU5F1, PRDM14, DNMT3B, TET1, SALL4, EZH2, NANOG, DPPA4, SOX2, JARID2, LIN28A, OTX2, NR5A2, NR0B1, ZFP42, TRIM71, TET2, FOXH1, WDR5, MYBL2, KDM2B.
Human Fibroblast Reprogramming (Tanaka et al., 2015)	Accessed list of Type III/ESC genes (Table S3). Identified by factor loadings in principle components.	

4.2.2 Identification of CpG Islands and Calculation of CpG Sequence Metrics

Promoter sequence bioinformatics were performed using applications from the European Molecular Biology Open Software Suite (EMBOSS 6.6.0) (Rice et al., 2000). Putative CGIs were revealed with the “newcpgreport” EMBOSS tool, using the default application parameters. Promoters were further characterized as High CpG Promoters (HCP), Intermediate CpG Promoters (ICP) or Low CpG Promoters (LCP) according to established criteria (Fouse et al., 2008; Weber et al., 2007): Briefly, HCP must contain at minimum a 500-bp window where fractional GC-content is greater than 0.55 and CpGobs/CpGexp ratio is greater than 0.6; whereas ICP include any regions falling

between LCP and HCP; finally LCP must lack a CpG rich 500 bp window but exhibit a CpG_{obs}/CpG_{exp} ratio is >0.4.

We identified and scored focal CpG-rich regions using the “newcpgseek” EMBOSS tool, which computes a running sum of clustered CpG dinucleotides from all positions in the sequence. Additionally, for each retrieved promoter the whole sequence CpG_{obs}/CpG_{exp} ratio was calculated:

$$CpG\ Ratio = \frac{(Count_{CpG} \times Length_{bp})}{(Count_C \times Count_G)}$$

4.2.3 Sequence Alignment and Motif Discovery

In the obtained promoters, pairwise alignment and identification of conserved non-coding sequence was performed using mVISTA (<http://genome.lbl.gov/vista/index.shtml>).

Position weight matrices were accessed from the JASPAR 2018 database. Transcription factor binding motif discovery was performed with “jaspSCAN” EMBOSS tool using the default parameters. Consensus motifs were visualized as a sequence logo graphic (<http://weblogo.threeplusone.com/>).

4.2.4 Primary Cell Culture

Primary canine adult dermal fibroblast was purchased from National Institute of General Medical Science Repository (Coriell Institute, Camden, NJ). Additionally, canine fetal fibroblasts amendable to somatic cell nuclear transfer-mediated reprogramming (Jeong et al., 2012) were a gift from Dr. Jeong Yeon-Woo of Sooam Biotech Research Foundation (Seoul, South Korea). Somatic cells maintained in DMEM high glucose supplemented with 10% FBS, 2 mM GlutaMax, 1X non-essential amino acids and 0.5 mM 2-mercaptoethanol.

4.2.5 Somatic Cell Reprogramming

Two days prior to transduction, canine fibroblasts were seeded at 5×10^4 cells/well of a six-well plate. Using the CytoTune 2.0 Reprogramming Kit, Sendai viral vectors (SeV)

encoding human KOS (KLF4/OCT4/SOX2), c-MYC and KLF4 were added to individual wells containing 2×10^5 cells according to manufacturer's protocol with some modifications. The KOS and c-MYC SeV vectors were applied at a multiplicity of infection (MOI) of 6, based on transduction efficiencies achieved using CytoTune emGFP reporter (Thermo Fisher Scientific). The KLF4-SeV vector MOI was increased from 3 to 5 to improve the transcriptional output of the reprogramming vectors (personal communication with Thermo Fisher Scientific).

Two days post-infection (DPI), fibroblast medium was supplemented with either 0.1 nM Retinoic Acid/100 μ M Ascorbic Acid (RA/AA) or an equivalent volume of diluent (vehicle). Treatments were applied with daily medium exchanges for four days. At 6 DPI, the transduced cells were bulk passaged and transferred (3×10^4 cells) to 10 cm culture dishes containing $2 \times 10^4/\text{cm}^2$ γ -irradiated CF1 strain MEFs (Applied Stem Cell). For analysis of 6 DPI intermediates, 0.8×10^6 cells were pelleted, submerged in 300 μ L RNAlater (Sigma Aldrich) and stored at -80°C until nucleic acid extraction. Presumptive canine iPSCs were maintained in basal medium containing Knockout DMEM/F12, 20% KSR (Tobias et al., 2016; Yoshida et al., 2009) or DMEM with 10% FBS. Co-cultures of transduced canine fibroblasts and arrested MEFs were monitored for epithelialization and the emergence of primary colonies. For clonal isolation (10-20 DPI), primary colonies were mechanically isolated with a pipet tip and transferred into a Geltrex- and MEF-coated 48-well plate.

4.2.6 Reverse Transcription and Quantitative PCR

Total RNA from cultured cells was isolated using PureLink RNA kit (Thermo Fisher) and quantified using a NanoDrop spectrophotometer. 500 ng of total RNA was treated with RQ1 DNase (Promega) and used to synthesize cDNA using the Superscript III Reverse Transcription kit (Thermo Fisher) with 1.25 μ M each of oligo dT and random hexamers. Aliquots of cDNA were diluted 1:20 in nuclease-free water for use as template in qPCR reaction mixtures containing: 5 μ L SensiFast SYBR (BioLine Reagents), 1 μ L primer mixture (500 nm final), 2 μ L nuclease-free water and 2 μ L template. PCR assays were run on using the CFX384 Real-Time System (BIO-RAD). Thermal cycling conditions included 2 minutes at 95°C followed by 39 cycles of 95°C for 15 seconds and

60°C for 30 seconds. Annealing temperatures were optimized for the amplification of a single product of expected size, excised and sequenced at the London Regional Genomics Center (Robarts Research Institute, ON) to confirm specificity. All custom primer sequences and amplicon sizes can be found in Table 4-2. Reaction data were corrected for individual primer amplification efficiencies, calculated from a standard dilution series. The expression ratio for genes of interest were normalized to two reference genes (TBP and RPS5) and calculated using the $2^{-\Delta\Delta C_t}$ method.

Table 4-2. Custom oligonucleotide primer sequences.

Gene Identifier	Sequence (5' to 3')	Amplicon Size
TET1	F – CCAGTTAACCCGACCTGTCC R – CGGCCGAGAGCCATTAGAAA	124
TET2	F – AGCACATTGGTATGCACCCT R – TGTCGGCATGTCTTGACTGG	224
TET3	F – GCCCCCTACTCAGGAAATGA R – GGTAGAAAAAGGGCTCTCGGG	223
CDH1	F – AGGCTAACGTCGAAATCGCT R – GAGGATGACCTCAAACGGGG	236
CDH2	F – ACGGACCCAAACAGCAATGA R – ACAGACACAGTTGCCGTTGA	155
DSP	F – AATCCTCTGGCCGTAGACCT R – CCTGACGCATCGTTTTTCAGC	175
KRT19	F – AGCTCACCATGCAGAACCTC R – GACGGGCATTGTCAATCTGC	237
SMAD2	F – AAGTGGTGTGAGAAAGCGGT R – GGCCGTGTGTATCCCACTGA	187
SNAI2	F – GAACTGGACACGCACACAGT R – CACACGGTAATGGGGCTGTA	116
VIM	F – TTCAGAGAGAGGAAGCCGAGA R – AGGTCAGGCTTGGAACATCC	214
TBP	F – GAGCTCTGGGATCGTGCCGC R – TCAGTGCAGTGGTTCCGGGGC	167
RPS5	F – TCACTGGTGAGAACCCCT R – CCTGATTCACACGGCGTAG	141

4.2.7 Targeted Bisulfite PCR

Genomic DNA (gDNA) from cultured cells was isolated using GenElute Mammalian Genomic DNA Miniprep kit (Sigma Aldrich). Genomic DNA was eluted in 30 μ L of

sterile TE buffer pH 8.0 and determine concentration using NanoDrop 2000 spectroscopy (Thermo Fisher Scientific). Bisulfite modification and purification was performed using the EZ DNA Methylation Gold kit (Zymo Research) with 400 ng of gDNA. Eluted bisulfite-converted DNA was used immediately for PCR using Platinum Taq Polymerase and primer pairs designed to target the 5'-flanking sequences close to the transcriptional start site of canine OCT4 and NANOG (Luo et al., 2011). See Table 4-3 for primer sequences and amplicon sizes. To account for stochastic amplification, three parallel 25 μ L reactions for each template and primer combination were performed, pooled and re-aliquoted for future steps. Nested re-PCR was performed with 3 μ L of the resultant bisulfite-PCR reaction mixture. PCR amplifications used variations of the following thermal cycling protocol: 3 minutes at 94°C; 35 cycles of 94°C for 20 seconds, 59-64°C gradient for 15 seconds, 72°C for 15 seconds; 72°C for 5 minutes final extension. In nested re-PCR reactions a touchdown annealing range of 70-64°C was added before amplification cycles.

Table 4-3. NANOG and OCT4 primer sequences for bisulfite PCR.

Primer Set	Sequence (5' to 3')	Amplicon Size
NANOG_OUT	F – GTATTTTGGATTTTAAAGGATGGA R – AAAACCTCCACATATAAAAAATAAA	359
NANOG_IN	F – TAGAAATATTTAATTGTGGGGTT R – CATATAAAAAATAAAAAAAAAACAAAAT	312
OCT4_OUT	F – AGGTTAGTGGGTGGGATTGG R – CCTTAAAACAACAACCCCACTC	362
OCT4_IN	F – AGGTGTTGAGTAGTTTTTAGGAGA R – ACTCCACCTAAAATCCACAATA	314

4.2.8 Clone Sequencing and Methylation Analysis

Fresh PCR amplicons were ligated into pCR2.1 vectors and transformed into TOP10 competent *E. coli* using TA cloning kit (Thermo Fisher). Bacteria were plated onto LB agar with ampicillin and streaked with X-gal. No more than 10 white bacterial colonies were picked for each biological replicate and transferred into 3-mL of LB medium with antibiotic. Clones were grown for 16 hours in a 37°C bacterial incubator. The plasmid DNA were purified with Presto Mini Plasmid kit (Frogga Bio) and sequenced with 3730

DNA Analyzer System (Applied Biosciences) using M13 forward and reverse primers (London Regional Genomics Centre, Robarts Research Institute). Base calls, quality trimming, vector clipping and contig assembly was performed using the pre-Gap and Gap4 tools (Staden Package) (Staden, 1996). To determine accurate methylation patterns on target regions, at least 18 total processed clone sequences were aligned to the reference genomic sequence using methVisual R/Bioconductor package (Bioconductor release 3.6) (Zackay and Steinhoff, 2010). Alignment and quality control functions were used to compute bisulfite conversion rate and percentage sequence identity. The methylation state for each CpG site was exported from the quality-checked aligned sample sequences. For each acceptable clone, we adjusted cytosine methylation level to the bisulfite conversion rate (Bis_{con}):

$$\text{Adjusted Cytosine Methylation Level} = \frac{(C_{meth}/Bis_{con})}{C_{total}}$$

4.2.9 DNA Enzyme-linked Immunosorbant Assay (ELISA)

Genomic DNA was isolated as described above (see Section 2.4), aliquoted and diluted to 10 ng/ μ L. Global 5-methylcytosine or 5-hydroxymethylcytosine level were assessed from 100 ng of total gDNA using 5-mC DNA ELISA Kit or Quest 5-hmC DNA ELISA Kit (Zymo Research), according to the manufacturers' recommendations. Briefly, percent 5-mC or 5-hmC was interpolated from a five-point standard curve and adjusted based on the CpG dinucleotide density of the reference genome assembly for the species under investigation.

4.2.10 RT² Profiler PCR Array Analysis

Total RNA from cultured cells was isolated using PureLink RNA kit (Thermo Fisher) and quantified using a NanoDrop spectrophotometer. Genomic DNA digestion was performed using the RNase-free DNase Set (Qiagen). For the RT² Profiler PCR array, 400 ng of RNA was reverse transcribed to cDNA using the RT² First Strand Kit (Qiagen). Quantitative PCR was performed using the Canine Epithelial-Mesenchymal Transcription RT² Profiler PCR Array (Qiagen) according to manufacturer's guidelines. Data generated

from the PCR Array was analyzed as expression ratios using five reference genes (ACTB, B2M, GAPDH, HPRT1, RPLP1) and calculated using the $2^{-\Delta\Delta C_t}$ method. Differentially expressed transcripts targets were validated using custom oligonucleotide primers and qPCR analysis (see section 4.2.6).

4.2.11 Statistical Analysis

Experiments were not randomized, and the investigators were not blinded to allocation during experiments and outcome assessment. No statistical method was used to predetermine sample size. Sample sizes specific to each figure are denoted in figure legends. A p-value < 0.05 was considered significant. When two groups were compared, an unpaired t-test or, if assumptions of normality and equal variance were violated, a Wilcoxon rank sum test was performed. For multiple group comparisons, either one-way analyses of variance (ANOVA) or the non-parametric Welch's ANOVA was applied. A two-way ANOVA was performed in instances of two grouping variables. Where significance existed for a grouping factor, Tukey or Games-Howell post-hoc methods were carried out to determine differences between groups. Permutation tests were applied to determine if promoter class assignments and CpG richness scores are independent. For correlation analyses, the linear association was assessed using Spearman's rho statistic. All statistical analyses and plotting were carried out using R 3.5.0 statistical computing environment.

4.3 Results

4.3.1 A subset of reprogramming-associated orthologues is CpG-rich in the canine genome assembly.

We first sought to assess the conservation of CpG-rich sequences and CGIs, which are targets of cytosine modification enzymes, in the promoter sequences of shared orthologous genes between canine, human and mouse. To this end, we compiled a gene set from the intersection of differentially expressed genes between day 0 of reprogramming and the iPSC state in humans and mice (Nefzger et al., 2017; Tanaka et al., 2015). The gene set filtered based on Gene Ontology terms "DNA binding" or "Chromatin binding" and limited to those with a RefSeq annotated canine ortholog.

STRING protein association network construction showed the resultant gene set form two interconnected clusters of conventional pluripotency transcription factors (e.g. NANOG, ZFP42) and epigenetic modifying enzymes (e.g. JARID2, DNMT3B) (Fig. 4-1A). Peripheral components of the set consist of general regulators of proliferation with complex contributions to reprogramming (e.g. MYBL2, TRIM71) (Chang et al., 2012; Ward et al., 2018).

The promoter class assignments in 22 qualifying regions associated with reprogramming are distinct from the class allocations in 40 randomly selected background loci filtered based on gene Ontology Terms “DNA binding” (GO:0003677) or “Chromatin binding” (GO:0003682) ($P = 0.039$, Permutation Test). We observe marginally greater numbers of HCPs in the canine promoter set, however this distribution of promoter classes was not significantly different from human or mouse (Fig. 4-1B, $P = 0.587$ & $P = 0.575$, Permutation Test). It remained plausible that canine promoter sequences are more CpG-rich but fall below the threshold of CGIs. We performed pairwise comparisons between CpG richness scores from each species, using permutational percentile tests which account for subsets of promoter sequences contributing to data asymmetry within groups (Mangiafico, 2015). The median was not significantly different among canine-human ($P = 0.156$), canine-mouse ($P = 0.08$) or mouse-human ($P = 1$) pairs. However, the 75th percentile was significantly different between canine and mouse ($P = 0.038$), but not canine-human ($P = 0.107$) or human-mouse ($P = 0.526$) pairs (Fig. 4-1C).

To determine if the CpG sequence features among canine promoters diverge from other placental mammals (human, mouse, rabbit, porcine, bovine), we assessed paired association of whole promoter CpG ratio. Hierarchical cluster analysis of species grouped canine with murine promoter sets away from a porcine, human, bovine and rabbit cluster (Fig. 4-2). This analysis also highlighted that, among the mammalian promoters collected, canine sequences exhibit the greatest dissimilarity aside from rabbit. Whereas, clustering of promoters revealed four groups: 1) high CpG ratio in all species (SOX2,

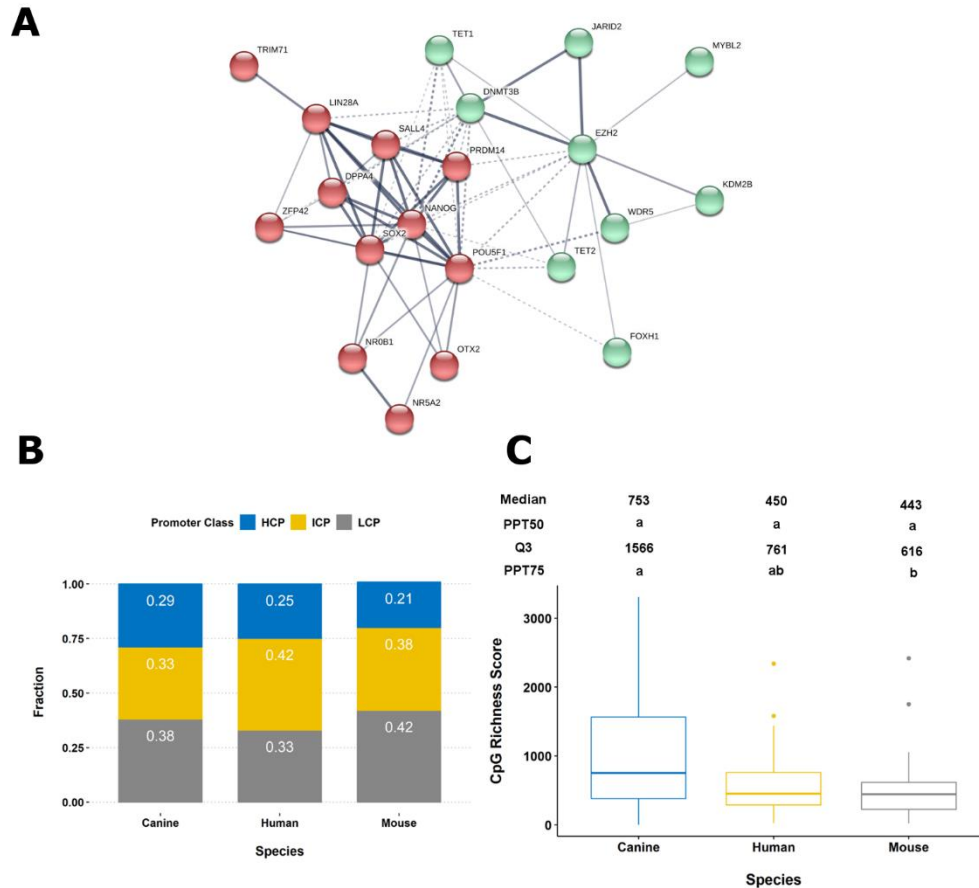


Figure 4-1. Class assignments and CpG-rich sequence score among promoters of genes associated with somatic cell reprogramming.

(A) STRING network visualization of putative protein-protein interactions between common differentially expressed genes in human and mouse reprogramming time course transcriptome experiments. K-means clustering ($k=2$) of networks demarcates DNA-binding and chromatin modifying enzymes. (B) Proportion of sequences assigned to high CpG promoter (HCP), intermediate CpG promoter (ICP) and low CpG promoter (LCP) classifications. (C) CpG richness score of promoter sequences from canine, human and mouse genome assemblies. Permutational percentile tests (PPT) were used to determine if the distribution of samples were significantly different between species at different quartiles (median = PPT50, Q3/upper quartile = PPT75). The indicated quartiles of sample distributions that are followed by the same letter are not significantly different.

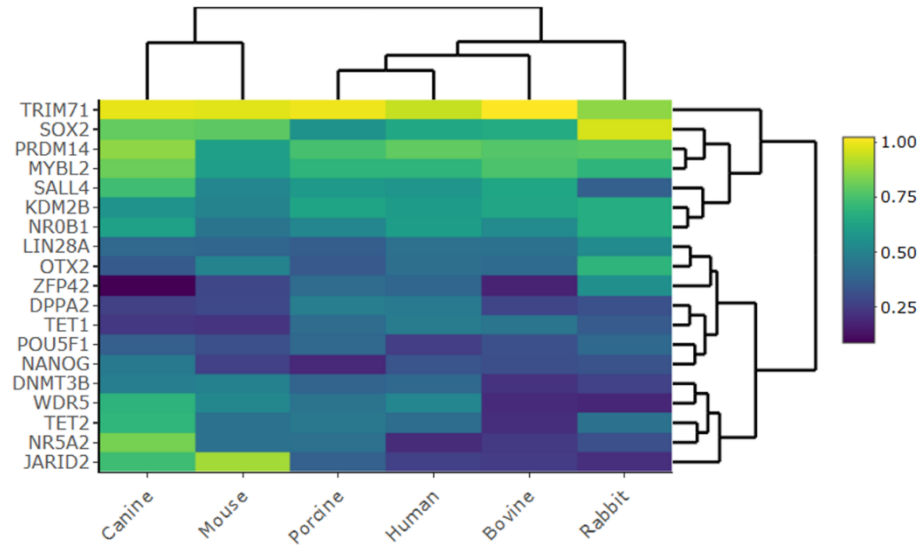


Figure 4-2. A subset of promoters associated with reprogramming is exclusively CpG-rich in the canine genome.

Comparison of CpG ratio by hierarchical cluster analysis between collected promoters from different mammalian superorders: Euarchontoglires (Human, Mouse, Rabbit) and Laurasiatheria (Canine, Porcine, Bovine). A CpG ratio approaching 0 indicates few cytosine and guanine bases are arranged in CpG dinucleotides, whereas a CpG ratio approaching 1 indicates that more cytosine and guanine bases are found in a CpG context than expected by randomization. Dendrograms represent Euclidean distance.

PRDM14), 2) high CpG ratio in rabbit (OTX2, ZFP42), 3) low CpG ratio in all species (NANOG, POU5F1) and 4) high CpG ratio in dog (TET2, NR5A2, JARID2). Pairwise association analysis revealed that canine promoter sets are significantly correlated with other species, except rabbit ($\rho=0.314$, $P=0.241$) and human ($\rho=0.499$, $P=0.054$). Collectively, these results suggest that the promoters of genes involved in mammalian iPSC generation are not enriched for CGIs in dogs, however a subset of canine promoters are composed of more CpG-rich compared to the murine promoter set.

4.3.2 OCT4 and NANOG promoters are methylated in canine fibroblasts and partially reprogrammed cells

Manipulation of genomic DNA methylation is an effective means of increasing the probability of complete reprogramming, but only when applied at the appropriate point in the workflow (Mikkelsen et al., 2008). Indeed, we observe that global DNA demethylation is significantly reduced in canine adult fibroblast (cAF) after four ($P=0.015$) or seven (Fig. 4-3A, $P=0.024$) days of exposure to 5- μ M 5azaC. We established three partially reprogrammed cell lines, cPR-L6, cPR-D7 and cPR-F9, in our attempt to reprogram adult dermal fibroblast with CytoTune 2.0 Sendai reprogramming vectors and transient DNMT inhibition. They produce heterogeneous cultures consisting of colonies with compact centres consisting of cells positive for SSEA4, a marker of cESCs, surrounded by cells with bipolar morphology (Fig. 4-3B). RT-qPCR analyses show incomplete expression of the triad of core pluripotency markers in cPR clones (Fig. 4-3C).

To investigate the extent of pluripotency gene silencing in cPR cells and parental fibroblasts compared to pluripotent cESCs we assessed the methylation status of regions within the canine NANOG or POU5F1/OCT4 promoter. Differing methylation profiles are evident in the OCT4 promoter region (Fig. 4-4A) and the NANOG promoter region (Fig. 4-4B) between cDF, cPR and cESCs. Methylation of the POU5F1 promoter region is lower in cESC compared to cDF ($P=0.032$), but not cPR (Fig 4-4C, $P=0.082$). Methylation of the NANOG promoter region is lower in cESC compared to both cDF ($P=1.25 \times 10^{-3}$) and cPR ($P=6.36 \times 10^{-4}$) (Fig. 4-4D). In summary, DNMT inhibition elicits global DNA demethylation in cDF but is limited as a reprogramming supplement

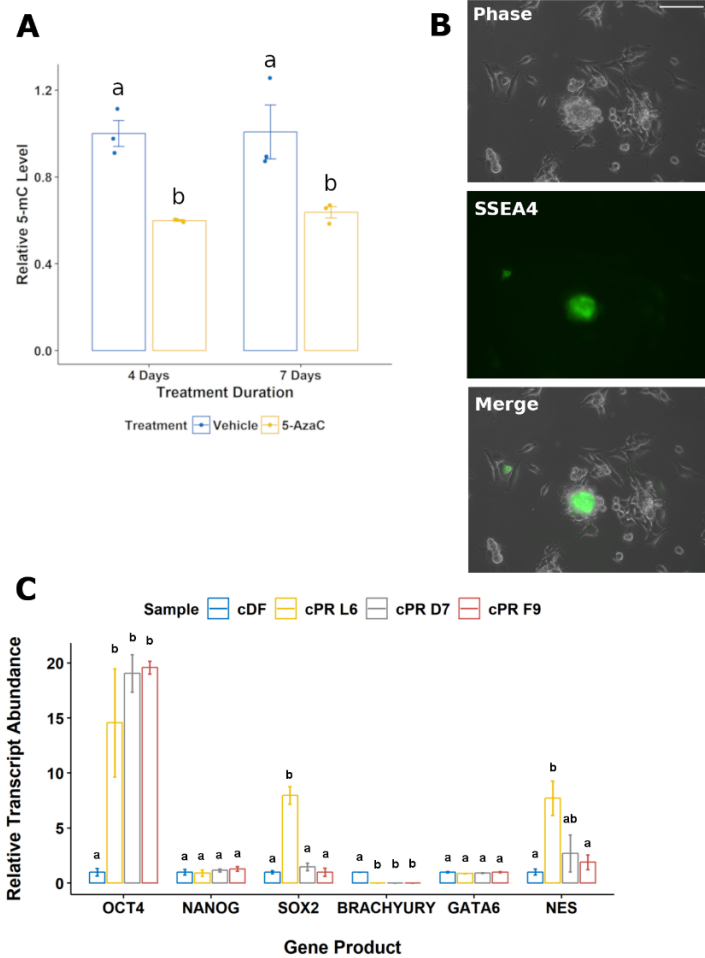


Figure 4-3. Canine dermal fibroblasts exposed transiently to 5-azacytidine (5-AzaC) generate partially reprogrammed cell lines.

(A) 5-mC level in canine dermal fibroblasts exposed to 5- μ M 5-azacytidine (5-AzaC), a DNMT inhibitor, for four or seven days. (B) Representative phase-contrast and direct immunofluorescence image for stage-specific embryonic antigen 4 (SSEA4) antibody stain of a partially reprogrammed clonal cell population (cPR-L6). (C) Transcript abundance of core pluripotency factors (OCT4, SOX2, NANOG) and tri-lineage markers (BRACHYURY, GATA6, NESTIN) in partially reprogrammed cell lines and parental fibroblast (cDF). Transcript levels are normalized to internal reference gene TATA-binding protein (TBP) and expressed as relative ratios to cDF samples. Bars represent standard error of the mean, $n = 3$. Means followed by the same letter are not significantly different, $P < 0.05$.

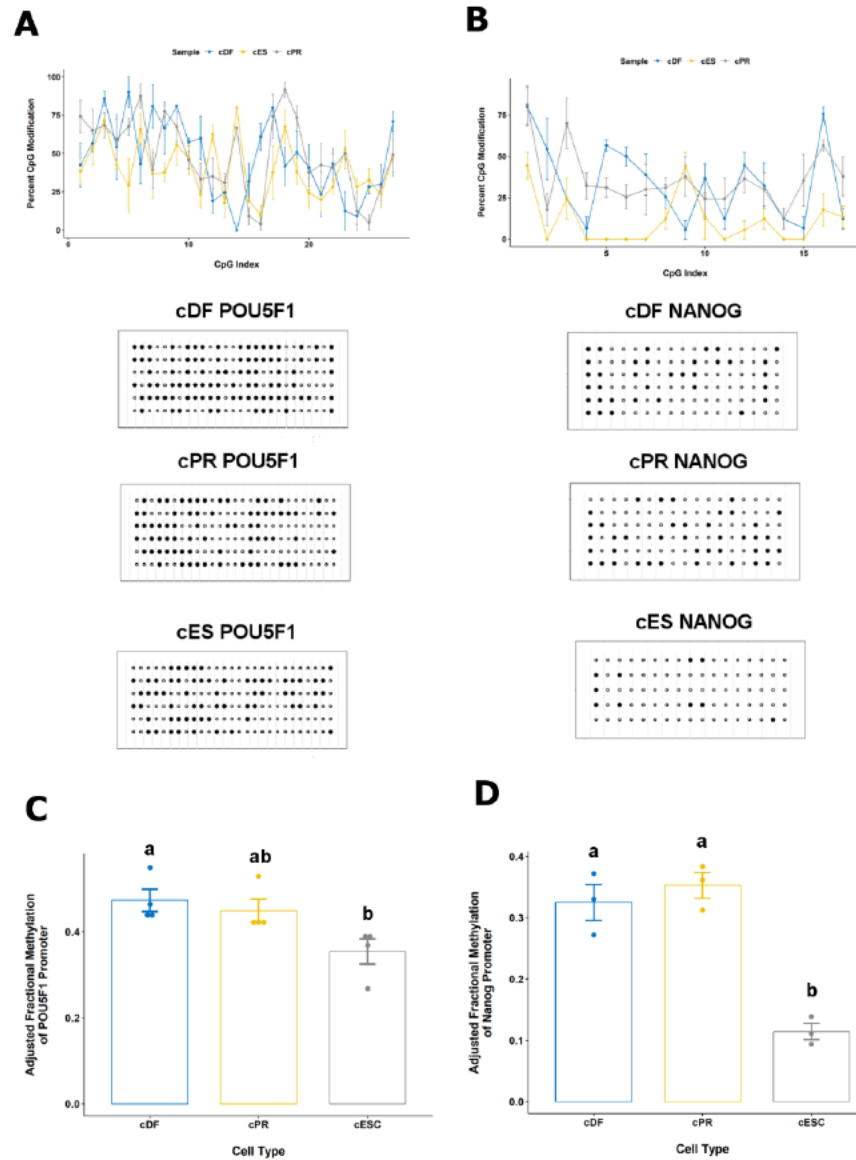


Figure 4-4. Incomplete demethylation of the NANOG promoter in canine partially reprogrammed cells.

Mean frequency of CpG methylation by position (CpG Index) for promoter fragments at canine (A) POU5F1/OCT4 and (B) NANOG. Associated lollipop plots depict unmethylated (open circle) and methylated (filled circle) CpG dinucleotides in seven representative technical replicates. Mean adjusted methylation frequency for whole promoter fragments at canine (C) POU5F1/OCT4 and (D) NANOG loci. Bars represent standard error of the mean (SEM), $n = 4$. Means followed by the same letter are not significantly different, $P < 0.05$.

in canines because only partially reprogrammed clones with methylated NANOG promoters could be attained.

4.3.3 5-hmC level varies among species and cell type

TET activity is thought to have a conserved role in a variety nuclear reprogramming systems by facilitating conversion of methylcytosine (5-mC) to 5-hydroxymethylcytosine (5-hmC) (Gao et al., 2013; Hill et al., 2014). To determine if the degree of global cytosine methylation (catalyzed by DNMTs) or cytosine hydroxymethylation (catalyzed by TET) differs among mammalian somatic genomes, we performed a comparative analysis of 5-mC and 5-hmC level in primary fibroblasts from canine, human and mouse. Total genome methylation was significantly lower in canine fibroblasts, compared to human neonatal BJ1 fibroblasts (Fig. 4-5A, $P = 3.67 \times 10^{-2}$) or embryonic fibroblast from CF1 mice (Fig. 4-5A, $P = 2.60 \times 10^{-3}$). The degree of cytosine hydroxymethylation was significantly greater in murine fibroblasts compared to human fibroblasts and canine fibroblasts (Fig. 4-5B, $P = 3.7 \times 10^{-6}$ & $P = 1.0 \times 10^{-7}$). Furthermore, 5-hmC level was also greater in human fibroblasts compared to canine fibroblasts. (Fig. 4-5B, $P = 6.83 \times 10^{-3}$). We compared canine adult (cAF) and fetal fibroblasts (cFF) to discern the impact of donor tissue maturity on global cytosine modification level. Basal 5-mC and 5-hmC were not significantly different between cFF and cAF (Fig. 4-5C-D, $P = 0.22$). Both fibroblast cell populations exhibit lower 5-hmC compared to pluripotent cESCs ($P < 1 \times 10^{-7}$) and transitional cPR cells (Fig. 4-5C-D, $P < 1 \times 10^{-7}$). These results suggest that steady-state cytosine modification levels, particularly 5-hmC, are detectably influenced by covariates such as the species and age of the donor tissue and may impact the ability of a given cell population to generate iPSCs.

4.3.4 Identification of L-ascorbic acid and retinoic acid concentrations that increase TET activity

Before proceeding to a modified reprogramming study, we sought to profile pan-TET activity and TET paralog expression in canine somatic cells upon exposure to combinations of RA and AA at levels used for iPSC generation. In murine and human ESCs or reprogramming cells, TET2 expression is responsive to a conserved retinoic

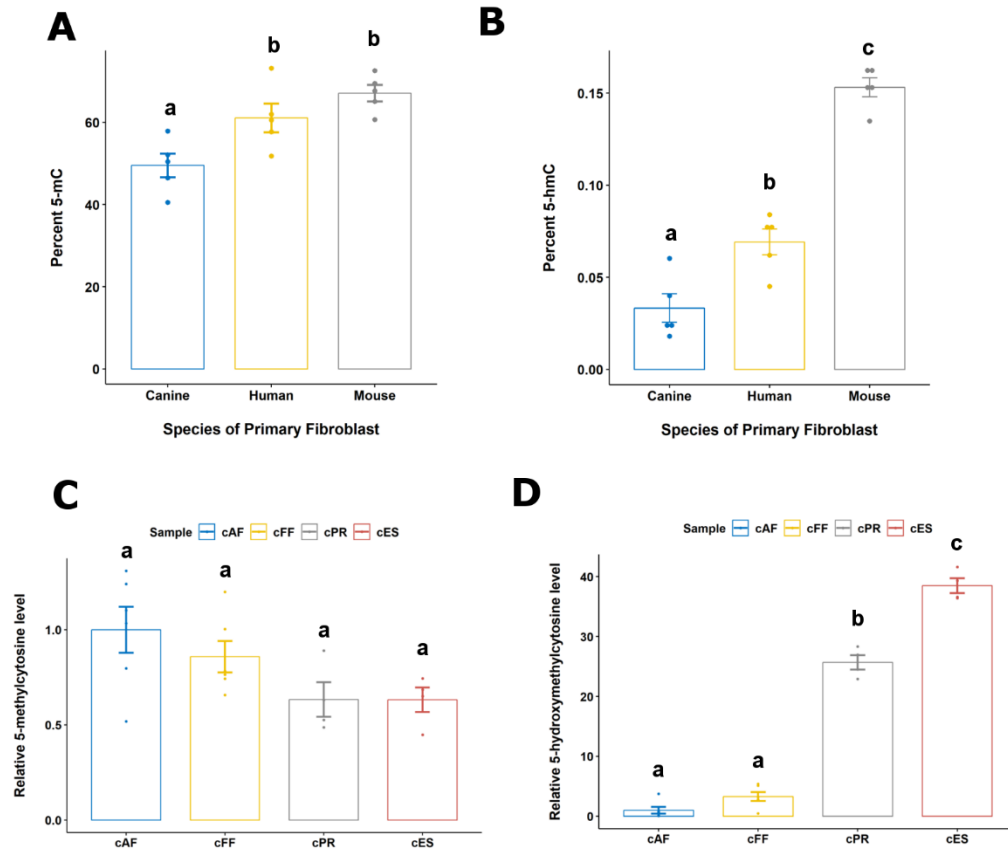


Figure 4-5. 5-hydroxymethylcytosine level varies with species and cell type.

(A) Percent 5-methylcytosine (5-mC) in cultures of primary fibroblast derived from canine, human and mouse. (B) Percent 5-hydroxymethylcytosine (5-hmC) in cultures of primary fibroblast derived from canine, human and mouse. (C) Relative 5-mC level levels in canine adult fibroblast (cAF), canine fetal fibroblast (cFF), canine partially reprogrammed (cPR) and canine embryonic stem (cES) cells. (D) Relative 5-hmC level in cAF, cFF, cPR and cES cells. The percentage of each modified base is corrected for the CpG dinucleotide density for each specific genome assembly. Bars represent standard error of the mean (SEM), $n = 4-5$. Means followed by the same letter are not significantly different, $P < 0.05$.

acid (RA) signaling element, distinct from the enzyme cofactor function of L-ascorbic acid (AA) (Hore et al., 2016). Using the ratio of genome-wide 5-hmC to 5-mC as an index of the overall catalytic output of TET enzymes (Ficz et al., 2011), we observed both AA (Fig. 4-6A, $F = 4.08$, $P = 2.83 \times 10^{-2}$) and RA (Fig. 4-6A, $F = 6.73$, $P = 4.26 \times 10^{-3}$) have a significant independent influence on 5-hmC:5-mC ratio. Only the combinations of 100 μM AA (Fig. 4-6A, $P = 0.033$) and 0.1 nM or 1 nM RA (Fig. 4-6A, $P = 0.035$) significantly elevated 5-hmC:5-mC ratio compared to vehicle controls.

Analysis of endogenous TET expression levels revealed basal levels of TET transcript in canine fibroblast ranging from 0.57% of reference gene expression for TET1, 8.30% for TET2 and 1.58% for TET3 transcripts. Interestingly, exposure of canine fibroblast to various RA concentrations did not alter TET paralog expression (Fig. 4-6B - 4-6D). Significant changes in cTET1 (Fig. 4-6B, $P = 0.0171$) and cTET3 (Fig. 4-6D, $P = 6.29 \times 10^{-3}$) abundance were only detected in 250 μM AA compared to vehicle control. The observation that cTET paralog expression is not sensitive to RA in canine fibroblast may indicate that the reprogramming OKSM factors are required co-factors. Indeed, we have identified a putative OCT4:SOX2 composite motif upstream of cTET1 and a partial OCT4 motif upstream of cTET2 in conserved non-coding sequence (Fig. 4-6E).

4.3.5 Physiological oxygen changes the influence of metabolites on TET activity

Physiological oxygen tensions (i.e. $< 5\% \text{ O}_2$) have been shown to improve iPSC derivation efficiency (Yoshida et al., 2009) and increased TET paralog expression in cultured cells and embryos (Mariani et al., 2014; Skiles et al., 2018). We next sought determine whether cTET transcript abundance and catalytic output are similarly responsive to AA, a pleiotropic molecule with donor antioxidant activity (Du et al., 2012), when cultured in a 5% oxygen environment. We observe relative 5-hmC levels approximately 1.4-fold higher than at atmospheric oxygen cultures. Surprisingly, in a physiological oxygen condition, neither AA (Fig. 4-7A, $F = 0.30$, $P = 0.74$) nor RA (Fig. 4-7A, $F = 0.74$, $P = 0.57$) significantly alter the 5-hmC:5-mC ratio compared to vehicle controls. We find that all cTET paralogs are generally more abundant (between 1.3 and 2.5-fold) in 5% oxygen

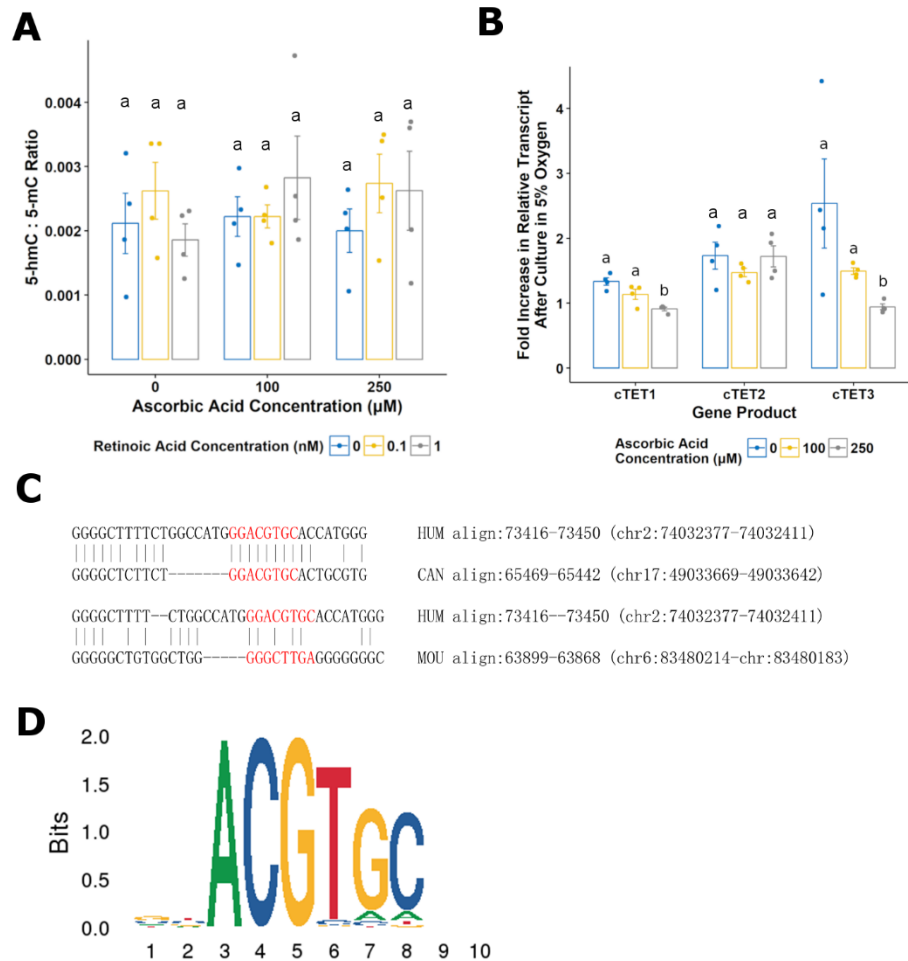


Figure 4-7. L-ascorbic acid suppresses hypoxia-mediated induction of cTET1 and cTET3.

(A) 5-hmC:5-mC ratio in canine dermal fibroblasts cultured in a 5% physiological oxygen environment and exposed to various concentrations ascorbic acid (AA) and/or retinoic acid (RA). Each data point is calculated from paired aliquots from the same purified gDNA sample and analyzed by separate ELISA assay kits. (B) Relative transcript abundances for cTET1, cTET2 and cTET3 in canine dermal fibroblasts cultured in physiological 5% oxygen and exposed to various concentrations of AA. (C) Pairwise alignment of canine, human and mouse TET3 promoter with partially conserved HIF-1 motif. (D) Weighted sequence motif logo for HIF-1. Bars represent standard error of the mean (SEM), $n = 4$. Means followed by the same letter are not significantly different, $P < 0.05$.

without culture media supplements. (Fig. 4-7B). This hypoxia-mediated induction of cTET1 and cTET3 transcripts is abrogated in the presence of AA at 250 μ M (Fig. 4-7B, $P = 2.16 \times 10^{-3}$ & $P = 0.018$). The notion that TETs may be a target of the hypoxic response is supported by the presence of a partially conserved HIF1 motif in the cTET3 locus (Fig. 4-7C-D). In summary a negative regulatory effect of AA on the cTET1 and cTET3 hypoxic response may obscure the role of AA and RA in regulating 5-hmC and 5-mC content in canine fibroblasts.

4.3.6 L-ascorbic acid and retinoic acid promote focal epithelialization during early canine reprogramming

The KOS, KLF4 and c-MYC SeV vectors were applied at a multiplicity of infection (MOI) of 5 or 6, based on transduction efficiencies achieved using control emGFP control SeV reporter (Fig. 4-8A-B). Increased levels of reprogramming factor expression have been shown to improve reprogramming in refractory mouse lacking NANOG (Carter et al., 2014; Schwarz et al., 2014). Further, inadequate KLF4 expression has been shown to pause the reprogramming process independent of the remaining Yamanaka transactors (Nishimura et al., 2014). Low passage canine fetal fibroblast (cFF at p1) cells were selected as the donor cell population. Throughout the first 48 hours after viral transduction, we observed slightly greater levels of cytotoxicity in SeV-transduced cFFs versus non-transduced control cells (~8% vs. ~20%, visual record) (Fig. 4-9A). After 24 hours of treatment with AA/RA or vehicle, transduced cFFs enter a hyperproliferative state and reach confluency. Transduced cFFs treated with AA/RA exhibited small clusters with epithelial character by 4 DPI which increased in size and frequency by 5 DPI (Fig. 4-9B). Interestingly, we observe that AA/RA-treated cells form more primary colonies upon re-seeding onto MEF feeders (Fig. 4-9C, $P = 0.029$).

We next examined the abundance of transcripts associated with mesenchymal-to-epithelial transition (MET) in 6 DPI reprogramming intermediates by qPCR array. Pairwise correlation analysis and clustering revealed that targeted expression profiles of biological replicates were highly similar ($\rho > 0.94$), suggesting that merging data across arrays was robust to batch effects (Fig. 4-10A). This analysis also highlighted that AA/RA treated intermediates were more dissimilar to non-transduced cFF cells by the

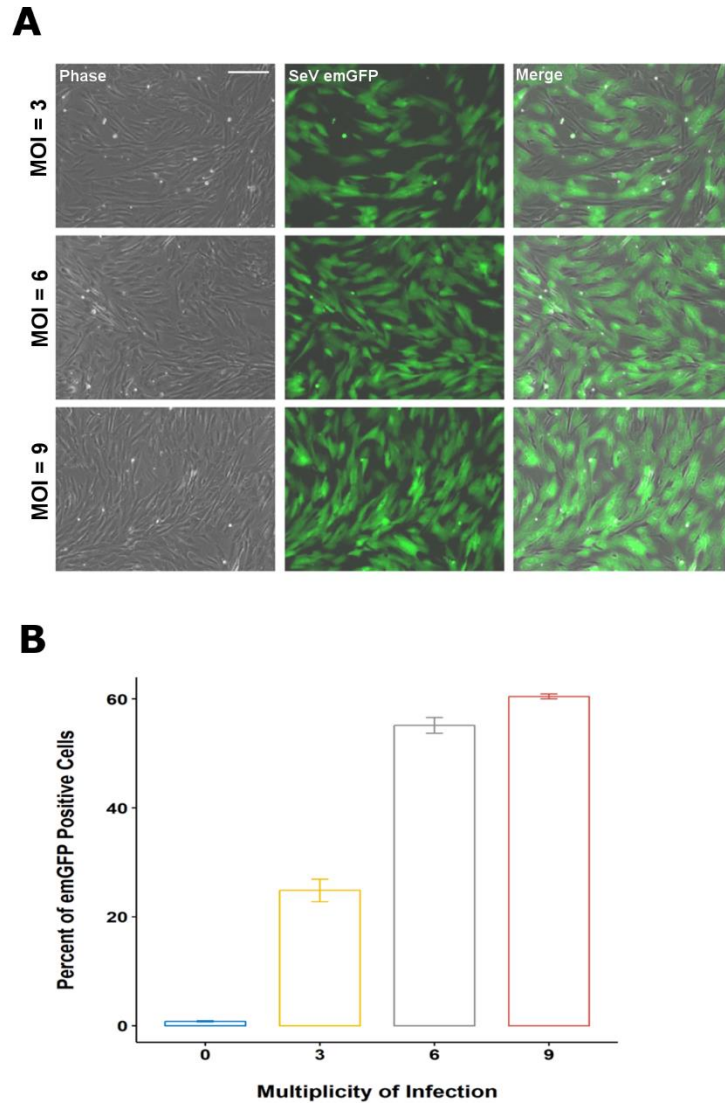


Figure 4-8. Optimization of multiplicity of infection (MOI) in canine fibroblast using Sendai emGFP control vector.

(A) Representative phase-contrast and fluorescent micrographs of canine dermal fibroblast transduced with emGFP control Sendai vector at various multiplicity of infection (MOI). Scale bar unit length is 125 μ m. (B) Summarization of the mean percent emGFP-positive cells at each MOI. Bars represent standard error of the mean (SEM), n = 2.

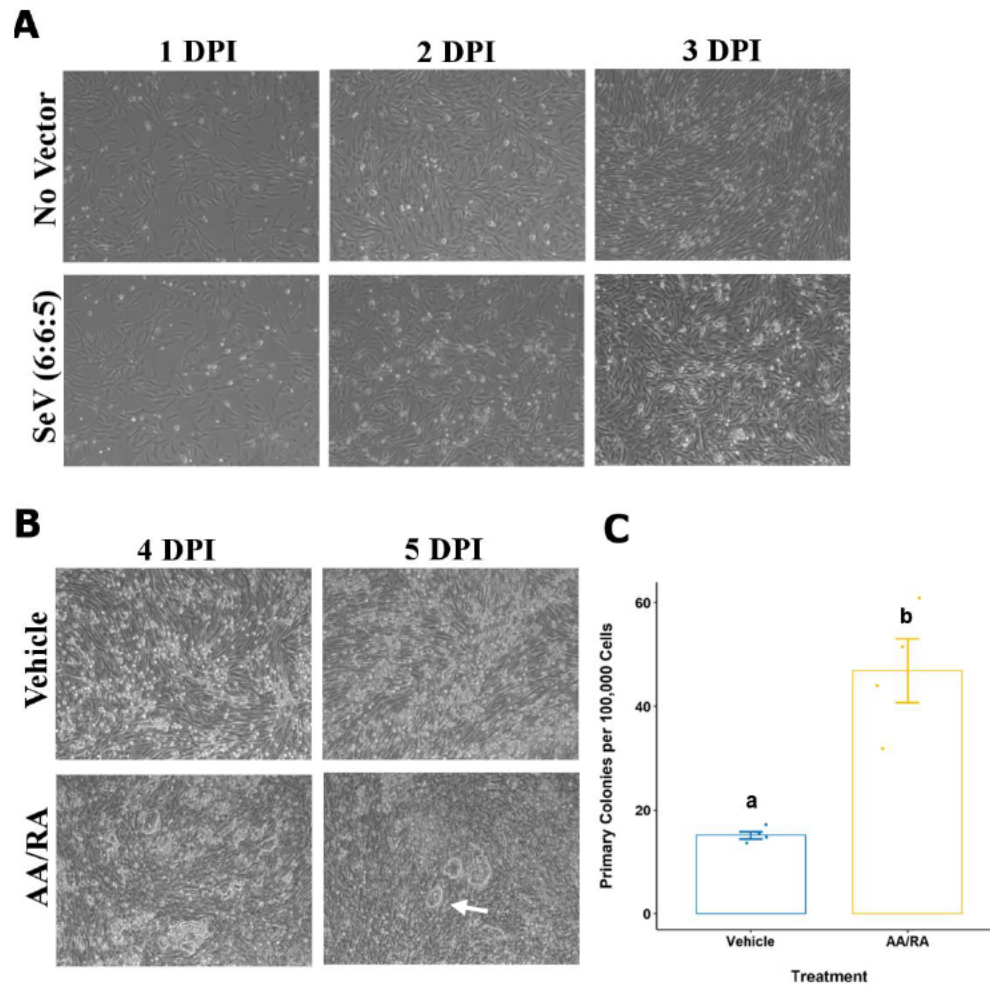


Figure 4-9. L-ascorbic acid and retinoic acid promote focal epithelialization and primary colony formation in early canine reprogramming.

(A) Representative phase-contrast micrographs of density-matched canine fetal fibroblast in steady-state culture (No Vector) or transduced with CytoTune-iPS 2.0 Sendai Reprogramming Kit (SeV 6:6:5) for the first three days post-infection (DPI). (B) Representative phase-contrast micrographs of transduced cFF treated with L-ascorbic acid and retinoic acid (AA/RA) or an equivalent volume of diluent (Vehicle). Scale bar unit length is 100 μ m. White arrows indicate epithelialized clusters. (C) Summarization of the of primary colony counts (per 100,000 transduced cells) performed four days after re-seeding on feeder cells (10 DPI). Bars represent standard error of the mean (SEM), $n = 3$. Means followed by the same letter are not significantly different, $P < 0.05$.

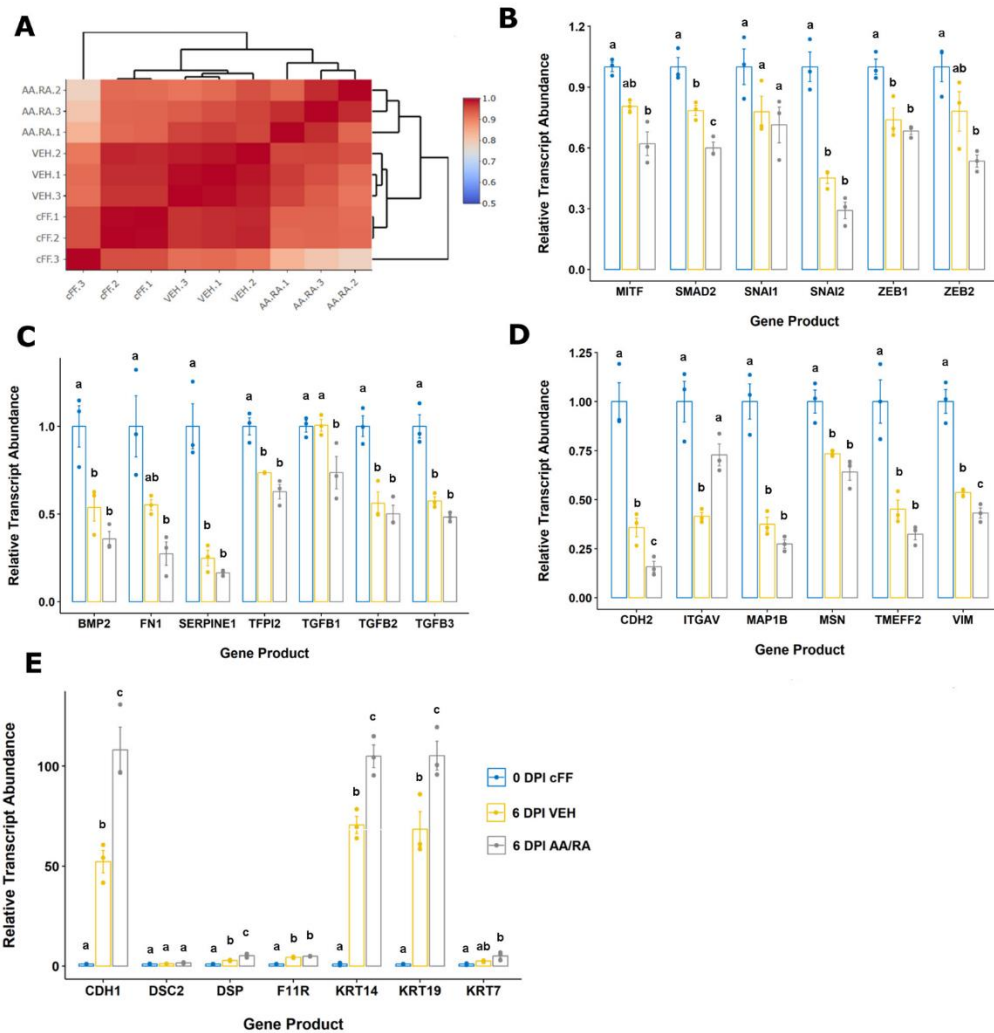


Figure 4-10. L-ascorbic acid and retinoic acid enhance a transcriptional response resembling mesenchymal-to-epithelial transition.

(A) Density matrix of Pearson correlation coefficients of transcript panel abundances in each sample. (B) Relative abundances of transcripts associated with DNA binding proteins. (C) Relative abundances of transcripts associated with secreted ligands or extracellular matrix components. (D) Relative abundances of transcripts associated with the cytoskeleton or cell adhesion that are down-regulated at 6 DPI. (E) Relative abundances of transcripts associated with the cytoskeleton or cell adhesion that are up-regulated at 6 DPI. Bars represent standard error of the mean (SEM), $n = 3$. Means followed by the same letter are not significantly different, $P < 0.05$.

Euclidean distance than vehicle-treated intermediates at 6 DPI. The transcripts of several DNA-binding proteins involved in the repression of epithelial gene expression were downregulated in 6 DPI samples (e.g. *SNAI2*, *ZEB1*) (Fig. 4-10B, $P < 8.63 \times 10^{-3}$). Furthermore, *SMAD2* transcript was significantly decreased in AA/RA intermediates compared to vehicle control (Fig. 4-10B, $P = 1.08 \times 10^{-2}$). Similarly, 6 DPI intermediates exhibited a lower abundance of several mesenchyme-associated transcripts with known signaling or structural role in the extracellular space (e.g. *FN1*, *BMP2*, *SERPINE1*) compared to parental cFF cells (Fig. 4-10C, $P < 1.99 \times 10^{-2}$). Among different TGF β isoforms, only TGF β 1 was significantly decreased in AA/RA intermediates relative to vehicle control (Fig. 4-10C, $P = 4.28 \times 10^{-2}$). Strikingly, several transcripts related to cytoskeletal (e.g. *MSN*, *MAP1B*, *KRT7*) and plasma membrane (e.g. *F11R*, *TMEFF2*) components were differentially abundant in reprogramming intermediates compared to donor cFF cells. (Fig. 4-10D-E, $P < 1.30 \times 10^{-2}$). Notably, characteristic mesodermal markers *CDH2* ($P = 4.51 \times 10^{-2}$) and *VIM* ($P = 3.55 \times 10^{-2}$) are significantly lower in AA/RA-treated intermediates (Fig. 4-10D). Whereas, epithelial hallmark transcripts *CDH1* ($P = 2.31 \times 10^{-3}$), *DSP* ($P = 6.54 \times 10^{-3}$), *KRT14* ($P = 2.43 \times 10^{-3}$) and *KRT19* ($P = 1.72 \times 10^{-2}$) were significantly elevated in reprogramming intermediates exposed to AA/RA (Fig. 4-10D). Custom oligonucleotides were designed to validate several differentially abundant transcripts relevant to MET (Fig 4-11A-B).

Defining the culture conditions that support self-renewal of pluripotent cells from dogs remains a challenge. We and others have expanded cESC (Tobias et al., 2016) and ciPSC (Luo et al., 2011; Nishimura et al., 2013) in Knockout Serum Replacement (KOSR)-containing medium optimized for hESC. In the previous chapter, I demonstrated that cESCs cultured in this medium exhibit deficiencies in the glycolysis pathway compared to human or mouse ESCs (Chapter 3). To propagate presumptive ciPSCs, we attempted single- and bulk-colony passaging techniques in different medium and growth factor combinations (Fig. 4-12A). We found that cESC-like culture conditions containing KOSR could not mature canine iPSC-like cells (Fig. 4-12B). Conversely, standard DMEM with 10% FBS media was more effective at stabilizing early reprogramming intermediates, which was accentuated with exogenous LIF supplementation (Fig. 4-12C).

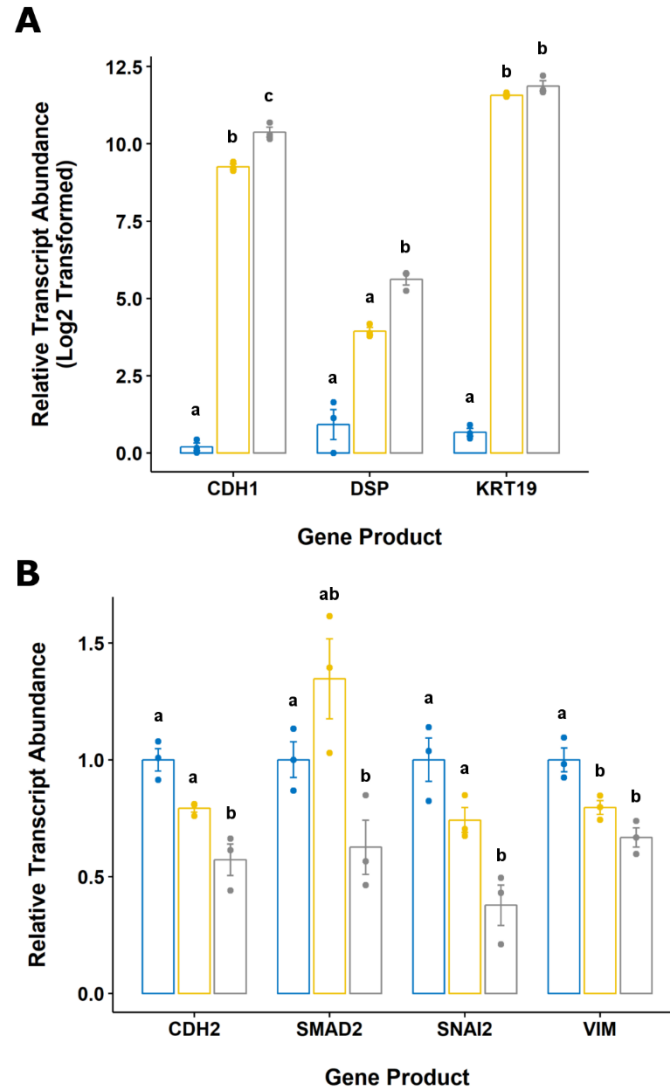


Figure 4-11. Validation of differentially abundant mesenchymal and epithelial transcripts using custom oligonucleotide primers.

(A) Relative abundances of transcripts associated epithelial cell types quantified by reverse-transcription qPCR. (B) Relative abundances of transcripts associated with mesenchymal cell types quantified by reverse-transcription qPCR. Bars represent standard error of the mean (SEM), $n = 3$. Means followed by the same letter are not significantly different, $P < 0.05$.

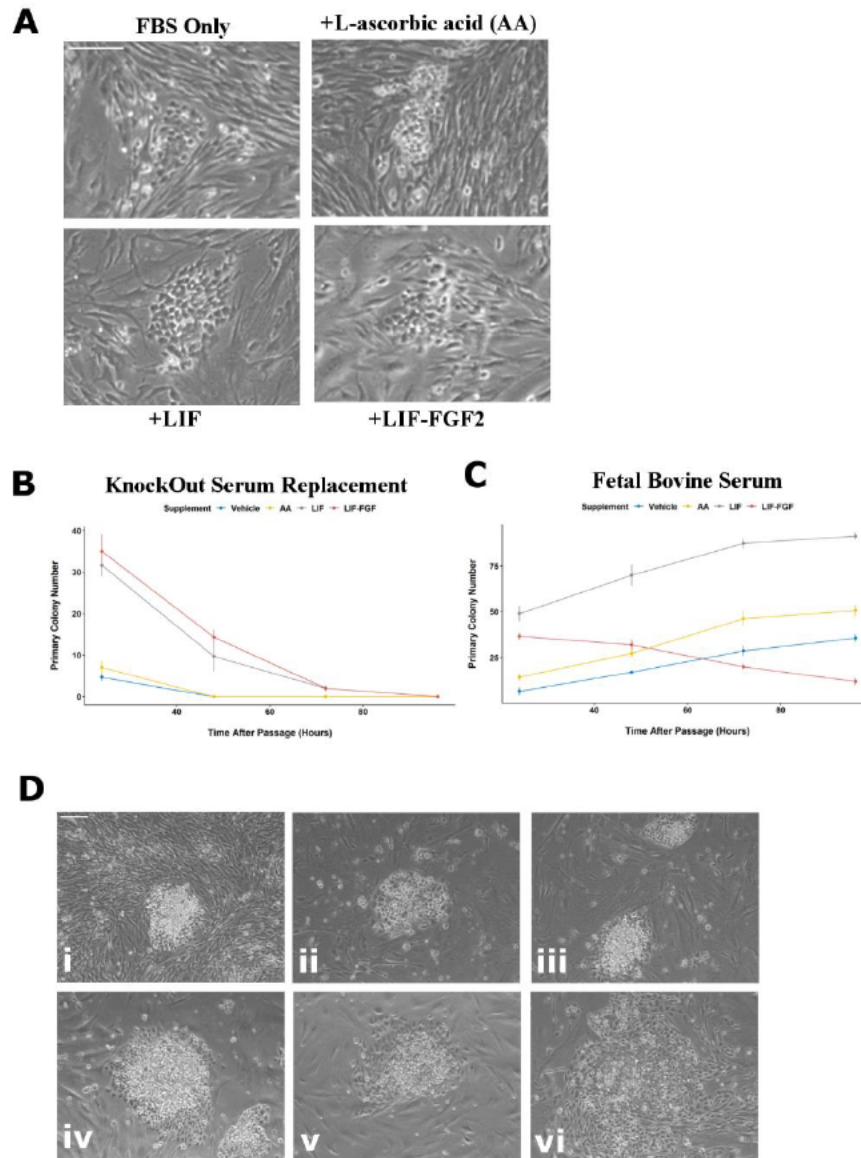


Figure 4-12. Presumptive canine iPSCs are temporarily supported in media containing fetal bovine serum and LIF supplementation.

A) Representative phase-contrast micrographs of primary colonies emerging after passage of transduced cDF (9 days post infection (DPI)) in medium containing fetal bovine serum (FBS). Summarization of raw counts of primary colonies emerging in the first four days after passaging transduced cFF (7-10 DPI) in medium containing (B) Knockout Serum Replacement (KOSR) or (C) FBS. (D) Representative phase-contrast micrograph of a serially pick-passaged primary colony on (I)10 DPI, (II) 14 DPI, (III) 18 DPI, (IV) 22 DPI, (V) 26 DPI, and (VI) 30 DPI. Scale bar unit length is 100 μ m.

However, within three-to-four passages, presumptive ciPSCs progressively lost compact border morphology and gradually formed monolayer structures with radial asymmetry (Fig. 4-12D). These results suggest that LIF supplementation supports the emergence of early reprogramming intermediates, but insufficient to propagate maturing canine iPSCs long-term.

4.4 Discussion

It is currently unknown if canine reprogramming mirrors the trajectory of human or mouse cells towards the iPSC state. Previous studies have focused on the molecular characteristics and differentiation potential of a limited number of putative iPSC clones derived from a single reprogramming experiment (Luo and Cibelli, 2016). To develop a reproducible system to derive and maintain canine iPSCs, it is essential to identify the most obstructive mechanisms to the reprogramming of canine cells by forced expression of transcription factors. We found that global 5-hmC level varies among primary fibroblast cultures from different species commonly used for reprogramming experiments. Gene expression and epigenetic assays indicate that partially reprogrammed cells exhibit limited pluripotency factor expression, methylation of the NANOG promoter and lower 5-hmC levels compared to canine ESC lines. Our study also indicates that a transcriptional response resembling MET occurs within the first week of canine reprogramming. Morphological and transcriptional indicators of MET can be facilitated using bioactive metabolites, which modulate 5-hmC accumulation in canine fibroblasts independent of changes in TET paralog expression.

During iPSC generation thousands of loci gain or lose methylation (Polo et al., 2012) as reprogramming factors direct active demethylation (Sardina et al., 2018) and outcompete the somatic gene regulatory network allowing *de novo* methylation of lineage-associated genes (Schwarz et al., 2018). Ultimately, genome-wide methylation in the established pluripotent cells is estimated to be similar to somatic cells unless small molecular inhibitors or activators are added to drive further epigenome erasure (Ficz et al., 2013; Leitch et al., 2013). We have previously demonstrated that small molecule inhibitors of MEK1/2 and GSK3 enrich for a population of cESCs with lower global 5-mC levels (Tobias et al., 2016) and noted a previously recognized over-representation of CGIs in

the canine genome assembly (Han et al., 2008). In addition to prompting targeted chromatin remodeling, TET enzymes help to maintain the hypomethylated state of high CpG density regions (Williams et al., 2011; Wu et al., 2011). Previous enrichment analyses of canine-human homologous genes focused on subsets of loci with a CGI present only in the human assembly (Han and Zhao, 2009). Due to a lack of a formal gene ontology term affiliated with somatic cell reprogramming, we derived a gene list from time-course transcriptome experiments in human and murine cells. Our sequence analyses showed that there were no differences in the number of canine promoters with a unique CGI among conserved reprogramming genes, but a subset of promoters (~20%) consisted of uniquely CpG-rich sequence in the canine genome. A valuable extension of this investigation would include collecting CpG-related sequence features from regions associated with cis-regulatory modules, particularly distal regulatory elements predicted from clustered pluripotency transcription factor motifs.

Higher reprogramming efficiencies between somatic cell types positively correlate with the number hypermethylated tissue-specific genes shared with pluripotent ESCs (Barrero et al., 2012). Furthermore, embryonic and fetal cell populations are often more efficiently reprogrammed, occasionally with fewer ectopic transactors, compared to differentiated adult cells (Hansel et al., 2014; Kleger et al., 2012). We found no differences in the fraction of 5-mC among total genome CpG dinucleotides between adult or fetal canine fibroblasts, partially reprogrammed cells or ES cells. However, 5-hmC level was associated with cES and cPR cells considered to be more plastic populations than somatic fibroblasts. Interestingly, canine fibroblasts appear to be deficient in 5-hmC compared to human and mouse fibroblasts. This may be due, in part to lower global levels of 5-mC substrate available for oxidation, a species-dependent or time-dependent consequence of adaptation to culture (Nestor et al., 2015).

Comparisons of time-resolved data from the reprogramming of different cell types and/or species have identified context specific trajectories and barriers to acquired pluripotency (Fu et al., 2018; Nefzger et al., 2017). We observed incomplete demethylation of the NANOG promoter region, and as a plausible consequence endogenous NANOG transcripts are not upregulated in partially reprogrammed clones. Limited epigenetic

remodeling and endogenous pluripotency gene re-activation is also evident in porcine reprogramming (Choi et al., 2016), another Laurasiatherian species. We found that endogenous POU5F1 expression in cPR lines does not correlate well with the methylation status of the -394 to -88 region targeted in this study. One possibility is that cytosine residues with gene regulatory activity are present elsewhere in the canine POU5F1 promoter. POU5F1 expression in cPR lines suggest that POU5F1 re-expression dynamics resemble the human reprogramming time course, wherein POU5F1 is reversibly re-expressed during MET, as opposed to during the later maturation phase in murine reprogramming (Brambrink et al., 2008; Teshigawara et al., 2016).

To date, canine reprogramming studies have only applied small molecule inhibitors to facilitate reprogramming (Betts and Tobias, 2015). In our hands, transient exposure to DNMT inhibitor 5-azaC did not noticeably impact the initiation canine reprogramming but enabled the stabilization of partially reprogrammed cell populations. Prolonged disruption of DNMT is not desirable due to the potential to activate retrotransposons and induce genome instability (Eden et al., 2003; Walsh et al., 1998). Analysis of cells apparently trapped in partially reprogrammed states have provided useful information on reprogramming obstacles, notably in the maturing iPSCs (Mikkelsen et al., 2008). However, the continued emergence of partially reprogrammed cells has diminishing value and may confound molecular analyses by misidentification with cells undergoing productive reprogramming.

Experimental manipulations that increase TET abundance or catalytic activity promotes 5-methylcytosine removal and iPSC generation in both human and murine cells (Costa et al., 2013; Doege et al., 2012; Gao et al., 2013). L-ascorbic acid directly interacts with the TET catalytic domain as a cofactor (Blaschke et al., 2013; Yin et al., 2013) and enhances Fe (II) recycling (Hore et al., 2016) to elevate methylcytosine dioxygenase activity. Whereas, retinoic acid may synergistically increase TET action via nuclear receptor complex-dependent functions such as: up-regulation of TET2/TET3 expression (Hore et al., 2016) and focal recruitment of TET1/2 and base-excision repair machinery (Hassan et al., 2017). Interestingly, retinoid ligands appear to have TET-independent mechanisms to regulate early human and mouse reprogramming via retinoic acid receptor-gamma

(RARG) and binding partner NR5A2 (also known as LRH1) (Wang et al., 2011). As the reactions catalyzed by TET enzymes are dependent on molecular oxygen, it is not surprising that physiological levels of extracellular oxygen promote TET activity (Burr et al., 2018). In the present study, we observed an antagonistic effect of L-ascorbic acid on the expression of TET1 and TET3 in a 5% oxygen environment. Our result resembles the ability of L-ascorbic acid to suppress the HIF-1 transcriptional response in cancer cells by stimulating the activity of HIF-degrading prolyl hydroxylase enzymes (Kuiper and Vissers, 2014).

The first phase of cell reprogramming is initiation, which encompasses several of transgene-dependent events including hyper-proliferation and loss of somatic identity (Stadtfield et al., 2008). The specific cellular and molecular events that define the initiation phase is dependent on cell type (Nefzger et al., 2017) and in fibroblast is highlighted by MET (Li et al., 2010; Samavarchi-Tehrani et al., 2010). In our single-infection reprogramming system, we observed altered expression of a variety of growth factors, adhesion molecules, cytoskeletal components and transcriptional regulators on day six, which is consistent with the process of MET. Interestingly, exposure to AA/RA enhanced several previously established aspects of MET including a switch from neuronal-type to epithelial-type cadherin expression (Araki et al., 2011) and the induction of keratin gene expression (Kagawa et al., 2019). Clusters epithelial-like cells are observed as early as four days post infection, but only in AA/RA treated reprogramming intermediates. Surprisingly, the apparent timing of the initiation phase in canine cells in our reprogramming system bears stronger resemblance to mouse reprogramming than human reprogramming (Høffding and Hyttel, 2015; Teshigawara et al., 2016). We note that other reprogramming vector systems may yield results that differ from our observations because the trajectory of cell states towards pluripotency and overall kinetics of iPSC generation are influenced by the reprogramming system utilized (Chantzoura et al., 2015). Our strategy to stabilize maturing canine iPSC intermediates in culture media used for routine culture of canine ESC and putative iPSC was unsuccessful beyond days 26-30 of reprogramming. Fundamental questions remain outstanding regarding the trophic requirements and regulatory processes that achieve a transgene-independent pluripotent state in the dog.

Our study represents the first investigation to identify phase-specific hurdles to canine induced pluripotency. We identified several promoter regions controlling canine genes involved in pluripotency regulation with distinctively CpG-rich sequence. Our examination of early canine reprogramming suggests that MET initiates four-to-six days after canine fibroblast infection, which is consistent with the kinetics of murine reprogramming systems. The notion that the over-representation of clustered CpG dinucleotides in the dog may influence the redistribution of DNA methylation during canine reprogramming warrants further investigation by untargeted, genome-wide approaches. This study also lends support to an evolutionarily conserved TET regulatory mechanism controlling the MET program, which has broader implications in the areas of developmental and cancer biology.

4.5 References

- Antequera, F., Boyes, J., & Bird, A. (1990). High levels of De Novo methylation and altered chromatin structure at CpG islands in cell lines. *Cell*, 62(3), 503–514.
- Apostolou, E., & Hochedlinger, K. (2013). Chromatin dynamics during cellular reprogramming. *Nature*. 502(7472), 462-71.
- Araki, K., Shimura, T., Suzuki, H., Tsutsumi, S., Wada, W., Yajima, T., ... Kuwano, H. (2011). E/N-cadherin switch mediates cancer progression via TGF- β -induced epithelial-to-mesenchymal transition in extrahepatic cholangiocarcinoma. *British Journal of Cancer*.
- Bachman, M., Uribe-Lewis, S., Yang, X., Williams, M., Murrell, A., & Balasubramanian, S. (2014). 5-Hydroxymethylcytosine is a predominantly stable DNA modification. *Nature Chemistry*, 6(12), 1049–1055.
- Backer, L. C., Coss, A. M., Flanders, W. D., & Reif, J. S. (2008). Exposure To Drinking Water Disinfection By-Products and Bladder Cancer in Dogs. *Journal of the American Veterinary Medical Association (JAVMA)*, 232, 1663–1668.
- Bagci, H., & Fisher, A. G. (2013). Dna demethylation in pluripotency and reprogramming: The role of Tet proteins and cell division. *Cell Stem Cell*.
- Ban, H., Nishishita, N., Fusaki, N., Tabata, T., Saeki, K., Shikamura, M., ... Nishikawa, S.-I. (2011). Efficient generation of transgene-free human induced pluripotent stem cells (iPSCs) by temperature-sensitive Sendai virus vectors. *Proceedings of the National Academy of Sciences of the United States of America*.
- Barrero, M. J., Berdasco, M., Paramonov, I., Bilic, J., Vitaloni, M., Esteller, M., &

- Belmonte, J. C. I. (2012). DNA hypermethylation in somatic cells correlates with higher reprogramming efficiency. *Stem Cells*.
- Betts, D. H., & Tobias, I. C. (2015). Canine pluripotent stem cells: Are they ready for clinical applications? *Frontiers in Veterinary Science*, 7(2), 41.
- Blaschke, K., Ebata, K. T., Karimi, M. M., Zepeda-Martínez, J. A., Goyal, P., Mahapatra, S., ... Ramalho-Santos, M. (2013). Vitamin C induces Tet-dependent DNA demethylation and a blastocyst-like state in ES cells. *Nature*, 500(7461), 222–226.
- Brambrink, T., Foreman, R., Welstead, G. G., Lengner, C. J., Wernig, M., Suh, H., & Jaenisch, R. (2008). Sequential Expression of Pluripotency Markers during Direct Reprogramming of Mouse Somatic Cells. *Cell Stem Cell*.
- Burr, S., Caldwell, A., Chong, M., Beretta, M., Metcalf, S., Hancock, M., ... Brewer, A. C. (2018). Oxygen gradients can determine epigenetic asymmetry and cellular differentiation via differential regulation of Tet activity in embryonic stem cells. *Nucleic Acids Research*.
- Carey, B. W., Finley, L. W. S., Cross, J. R., Allis, C. D., & Thompson, C. B. (2014). Intracellular α -ketoglutarate maintains the pluripotency of embryonic stem cells. *Nature*, 518(7539), 413–416.
- Carter, A. C., Davis-Dusenbery, B. N., Koszka, K., Ichida, J. K., & Eggan, K. (2014). Nanog-independent reprogramming to iPSCs with canonical factors. *Stem Cell Reports*.
- Chang, H. M., Martinez, N. J., Thornton, J. E., Hagan, J. P., Nguyen, K. D., & Gregory, R. I. (2012). Trim71 cooperates with microRNAs to repress Cdkn1a expression and promote embryonic stem cell proliferation. *Nature Communications*.
- Chantzoura, E., Skylaki, S., Menendez, S., Kim, S. Il, Johnsson, A., Linnarsson, S., ... Kaji, K. (2015). Reprogramming Roadblocks Are System Dependent. *Stem Cell Reports*.
- Choi, K. H., Park, J. K., Son, D., Hwang, J. Y., Lee, D. K., Ka, H., ... Lee, C. K. (2016). Reactivation of endogenous genes and epigenetic remodeling are barriers for generating transgene-free induced pluripotent stem cells in Pig. *PLoS ONE*.
- Chow, L., Johnson, V., Regan, D., Wheat, W., Webb, S., Koch, P., & Dow, S. (2017). Safety and immune regulatory properties of canine induced pluripotent stem cell-derived mesenchymal stem cells. *Stem Cell Research*, 25, 221–232.
- Costa, Y., Ding, J., Theunissen, T. W., Faiola, F., Hore, T. A., Shliaha, P. V., ... Wang, J. (2013). NANOG-dependent function of TET1 and TET2 in establishment of pluripotency. *Nature*, 495(7441), 370–374.
- De Carvalho, D. D., You, J. S., & Jones, P. A. (2010). DNA methylation and cellular

reprogramming. *Trends in Cell Biology*.

- Deaton, A. M., & Bird, A. (2011). CpG islands and the regulation of transcription. *Genes & Development*.
- Doerge, C. A., Inoue, K., Yamashita, T., Rhee, D. B., Travis, S., Fujita, R., ... Abeliovich, A. (2012). Early-stage epigenetic modification during somatic cell reprogramming by Parp1 and Tet2. *Nature*.
- Drost, H. G., & Paszkowski, J. (2017). Biomart: Genomic data retrieval with R. *Bioinformatics*.
- Du, J., Cullen, J. J., & Buettner, G. R. (2012). Ascorbic acid: Chemistry, biology and the treatment of cancer. *Biochimica et Biophysica Acta (BBA) - Reviews on Cancer*.
- Eden, A., Gaudet, F., Waghmare, A., & Jaenisch, R. (2003). Chromosomal instability and tumors promoted by DNA hypomethylation. *Science*.
- Ficz, G., Branco, M. R., Seisenberger, S., Santos, F., Krueger, F., Hore, T. A., ... Reik, W. (2011). Dynamic regulation of 5-hydroxymethylcytosine in mouse ES cells and during differentiation. *Nature*.
- Ficz, G., Hore, T. A., Santos, F., Lee, H. J., Dean, W., Arand, J., ... Reik, W. (2013). FGF Signaling Inhibition in ESCs Drives Rapid Genome-wide Demethylation to the Epigenetic Ground State of Pluripotency. *Cell Stem Cell* (Vol. 13).
- Fouse, S. D., Shen, Y., Pellegrini, M., Cole, S., Meissner, A., Van Neste, L., ... Fan, G. (2008). Promoter CpG Methylation Contributes to ES Cell Gene Regulation in Parallel with Oct4/Nanog, PcG Complex, and Histone H3 K4/K27 Trimethylation. *Cell Stem Cell*.
- Fu, K., Chronis, C., Soufi, A., Bonora, G., Edwards, M., Smale, S. T., ... Pellegrini, M. (2018). Comparison of reprogramming factor targets reveals both species-specific and conserved mechanisms in early iPSC reprogramming. *BMC Genomics*, 19(1), 956.
- Fusaki, N., Ban, H., Nishiyama, A., Saeki, K., & Hasegawa, M. (2009). Efficient induction of transgene-free human pluripotent stem cells using a vector based on Sendai virus, an RNA virus that does not integrate into the host genome. *Proc. Jpn. Acad., Ser. B*.
- Gao, Y., Chen, J., Li, K., Wu, T., Huang, B., Liu, W., ... Gao, S. (2013). Replacement of Oct4 by Tet1 during iPSC induction reveals an important role of DNA methylation and hydroxymethylation in reprogramming. *Cell Stem Cell*, 12(4), 453–469.
- Han, L., Su, B., Li, W. H., & Zhao, Z. (2008). CpG island density and its correlations with genomic features in mammalian genomes. *Genome Biology*, 9(5).

- Han, L., & Zhao, Z. (2009). Contrast features of CpG islands in the promoter and other regions in the dog genome. *Genomics*, 94(2), 117–124.
- Hansel, M. C., Gramignoli, R., Blake, W., Davila, J., Skvorak, K., Dorko, K., ... Strom, S. C. (2014). Increased reprogramming of human fetal hepatocytes compared with adult hepatocytes in feeder-free conditions. *Cell Transplantation*.
- Hassan, H. M., Kolendowski, B., Isovici, M., Bose, K., Dranse, H. J., Sampaio, A. V., ... Torchia, J. (2017). Regulation of Active DNA Demethylation through RAR-Mediated Recruitment of a TET/TDG Complex. *Cell Reports*, 19(8), 1685–1697.
- He, Y. F., Li, B. Z., Li, Z., Liu, P., Wang, Y., Tang, Q., ... Xu, G. L. (2011). Tet-mediated formation of 5-carboxylcytosine and its excision by TDG in mammalian DNA. *Science*, 333(6047), 1303–1307.
- Hill, P. W. S., Amouroux, R., & Hajkova, P. (2014). DNA demethylation, Tet proteins and 5-hydroxymethylcytosine in epigenetic reprogramming: An emerging complex story. *Genomics*.
- Høffding, M. K., & Hyttel, P. (2015). Ultrastructural visualization of the Mesenchymal-to-Epithelial Transition during reprogramming of human fibroblasts to induced pluripotent stem cells. *Stem Cell Research*, 14(1), 39–53.
- Hore, T. A., von Meyenn, F., Ravichandran, M., Bachman, M., Ficz, G., Oxley, D., ... Reik, W. (2016). Retinol and ascorbate drive erasure of epigenetic memory and enhance reprogramming to naïve pluripotency by complementary mechanisms. *Proceedings of the National Academy of Sciences*, 113(43), 12202–12207.
- Hu, X., Zhang, L., Mao, S. Q., Li, Z., Chen, J., Zhang, R. R., ... Xu, G. L. (2014). Tet and TDG mediate DNA demethylation essential for mesenchymal-to-epithelial transition in somatic cell reprogramming. *Cell Stem Cell*, 14(4), 512–522.
- Ito, S., Shen, L., Dai, Q., Wu, S. C., Collins, L. B., Swenberg, J. A., ... Zhang, Y. (2011). Tet proteins can convert 5-methylcytosine to 5-formylcytosine and 5-carboxylcytosine. *Science*, 333(6047), 1300–1303.
- Jeong, Y. W., Lee, G.-S., Kim, J. J., Park, S. W., Ko, K. H., Kang, M., ... Hwang, W. S. (2012). Establishment of a canine model of human type 2 diabetes mellitus by overexpressing phosphoenolpyruvate carboxykinase. *International Journal of Molecular Medicine*.
- Kagawa, H., Shimamoto, R., Kim, S.-I., Ocegüera-Yanez, F., Yamamoto, T., Schroeder, T., & Woltjen, K. (2019). OVOL1 Influences the Determination and Expansion of iPSC Reprogramming Intermediates. *Stem Cell Reports*.
- Kleger, A., Mahaddalkar, P. U., Katz, S. F., Lechel, A., Joo, J. Y., Loya, K., ... Rudolph, K. L. (2012). Increased reprogramming capacity of mouse liver progenitor cells, compared with differentiated liver cells, requires the BAF complex.

Gastroenterology.

- Koche, R. P., Smith, Z. D., Adli, M., Gu, H., Ku, M., Gnirke, A., ... Meissner, A. (2011). Reprogramming factor expression initiates widespread targeted chromatin remodeling. *Cell Stem Cell*
- Koh, S., & Piedrahita, J. A. (2015). Generation of Induced Pluripotent Stem Cells (iPSCs) from Adult Canine Fibroblasts. *Methods in Molecular Biology*, 1330, 69–78.
- Koh, S., Thomas, R., Tsai, S., Bischoff, S., Lim, J.-H., Breen, M., ... Piedrahita, J. A. (2013). Growth Requirements and Chromosomal Instability of Induced Pluripotent Stem Cells Generated from Adult Canine Fibroblasts. *Stem Cells and Development*.
- Kuiper, C., & Vissers, M. C. M. (2014). Ascorbate as a Co-Factor for Fe- and 2-Oxoglutarate Dependent Dioxygenases: Physiological Activity in Tumor Growth and Progression. *Frontiers in Oncology*.
- Leitch, H. G., McEwen, K. R., Turp, A., Encheva, V., Carroll, T., Grabole, N., ... Hajkova, P. (2013). Naive pluripotency is associated with global DNA hypomethylation. *Nature Structural & Molecular Biology*, 20(3), 311–316.
- Li, R., Liang, J., Ni, S., Zhou, T., Qing, X., Li, H., ... Pei, D. (2010). A mesenchymal-to-epithelial transition initiates and is required for the nuclear reprogramming of mouse fibroblasts. *Cell Stem Cell*.
- Lindblad-Toh, K., Wade, C. M., Mikkelsen, T. S., Karlsson, E. K., Jaffe, D. B., Kamal, M., ... Lander, E. S. (2005). Genome sequence, comparative analysis and haplotype structure of the domestic dog. *Nature*, 438(7069), 803–819.
- Lu, F., Liu, Y., Jiang, L., Yamaguchi, S., & Zhang, Y. (2014). Role of Tet proteins in enhancer activity and telomere elongation. *Genes and Development*, 28(19), 2103–2119.
- Luo, J., & Cibelli, J. B. (2016). Conserved Role of bFGF and a Divergent Role of LIF for Pluripotency Maintenance and Survival in Canine Pluripotent Stem Cells. *Stem Cells and Development*, 25(21), 1670–1680.
- Luo, J., Suhr, S. T., Chang, E. A., Wang, K., Ross, P. J., Nelson, L., ... Cibelli, J. B. (2011). Generation of leukemia inhibitory factor and basic fibroblast growth factor-dependent induced pluripotent stem cells from canine adult somatic cells. *Stem Cells and Development*, 20(10).
- Mangiafico, S. S. (2015). *An R Companion for the Handbook of Biological Statistics*. New Brunswick, NJ: Rutgers Cooperative Extension. Retrieved from <http://rcompanion.org/documents/RCompanionBioStatistics.pdf>

- Mariani, C. J., Vasanthakumar, A., Madzo, J., Yesilkamal, A., Bhagat, T., Yu, Y., ... Godley, L. A. (2014). TET1-mediated hydroxymethylation facilitates hypoxic gene induction in neuroblastoma. *Cell Reports*.
- Meissner, A., Mikkelsen, T. S., Gu, H., Wernig, M., Hanna, J., Sivachenko, A., ... Lander, E. S. (2008). Genome-scale DNA methylation maps of pluripotent and differentiated cells. *Nature*.
- Mikkelsen, T. S., Hanna, J., Zhang, X., Ku, M., Wernig, M., Schorderet, P., ... Meissner, A. (2008). Dissecting direct reprogramming through integrative genomic analysis. *Nature*.
- Nefzger, C. M., Rossello, F. J., Chen, J., Liu, X., Knaupp, A. S., Firas, J., ... Polo, J. M. (2017). Cell Type of Origin Dictates the Route to Pluripotency. *Cell Reports*.
- Nestor, C. E., Ottaviano, R., Reinhardt, D., Cruickshanks, H. A., Mjoseng, H. K., McPherson, R. C., ... Meehan, R. R. (2015). Rapid reprogramming of epigenetic and transcriptional profiles in mammalian culture systems. *Genome Biology*.
- Nishimura, K., Kato, T., Chen, C., Oinam, L., Shiomitsu, E., Ayakawa, D., ... Hisatake, K. (2014). Manipulation of KLF4 expression generates iPSCs paused at successive stages of reprogramming. *Stem Cell Reports*.
- Nishimura, T., Hatoya, S., Kanegi, R., Sugiura, K., Wijewardana, V., Kuwamura, M., ... Inaba, T. (2013). Generation of Functional Platelets from Canine Induced Pluripotent Stem Cells. *Stem Cells and Development*.
- O'Leary, N. A., Wright, M. W., Brister, J. R., Ciufu, S., Haddad, D., McVeigh, R., ... Pruitt, K. D. (2016). Reference sequence (RefSeq) database at NCBI: Current status, taxonomic expansion, and functional annotation. *Nucleic Acids Research*.
- Ostrander, E. A., Galibert, F., & Patterson, D. F. (2000). Canine genetics comes of age. *Trends in Genetics*. 16(3), 117-124.
- Ostrander, E. A., & Wayne, R. K. (2005). The canine genome. *Genome Research*. 15(12), 1706-1716
- Polo, J. M., Anderssen, E., Walsh, R. M., Schwarz, B. A., Nefzger, C. M., Lim, S. M., ... Hochedlinger, K. (2012). A molecular roadmap of reprogramming somatic cells into iPS cells. *Cell*, 151(7), 1617–1632.
- Rice, P., Longden, L., & Bleasby, A. (2000). EMBOSS: The European Molecular Biology Open Software Suite. *Trends in Genetics*.
- Samavarchi-Tehrani, P., Golipour, A., David, L., Sung, H. K., Beyer, T. A., Datti, A., ... Wrana, J. L. (2010). Functional genomics reveals a BMP-Driven mesenchymal-to-Epithelial transition in the initiation of somatic cell reprogramming. *Cell Stem Cell*.

- Sardina, J. L., Collombet, S., Tian, T. V., Gómez, A., Di Stefano, B., Berenguer, C., ... Graf, T. (2018). Transcription Factors Drive Tet2-Mediated Enhancer Demethylation to Reprogram Cell Fate. *Cell Stem Cell*.
- Schwarz, B. A., Bar-Nur, O., Silva, J. C. R., & Hochedlinger, K. (2014). Nanog is dispensable for the generation of induced pluripotent stem cells. *Current Biology*.
- Schwarz, B. A., Cetinbas, M., Clement, K., Walsh, R. M., Cheloufi, S., Gu, H., ... Hochedlinger, K. (2018). Prospective Isolation of Poised iPSC Intermediates Reveals Principles of Cellular Reprogramming. *Cell Stem Cell*.
- Skiles, W. M., Kester, A., Pryor, J. H., Westhusin, M. E., Golding, M. C., & Long, C. R. (2018). Oxygen-induced alterations in the expression of chromatin modifying enzymes and the transcriptional regulation of imprinted genes. *Gene Expression Patterns*. 28, 1–11.
- Soufi, A., Donahue, G., & Zaret, K. S. (2012). Facilitators and impediments of the pluripotency reprogramming factors' initial engagement with the genome. *Cell*.
- Staden, R. (1996). The staden sequence analysis package. *Molecular Biotechnology*. 5(3), 233-241
- Stadtfield, M., Maherali, N., Breault, D. T., & Hochedlinger, K. (2008). Defining Molecular Cornerstones during Fibroblast to iPS Cell Reprogramming in Mouse. *Cell Stem Cell*.
- Storb, R., & Thomas, E. D. (1985). Graft-versus-Host Disease in Dog and Man: The Seattle Experience. *Immunological Reviews*, 88(1), 215–238.
- Sutter, N. B., & Ostrander, E. A. (2004). Dog star rising: The canine genetic system. *Nature Reviews Genetics*. 5(12), 900-910
- Takahashi, K., & Yamanaka, S. (2006). Induction of Pluripotent Stem Cells from Mouse Embryonic and Adult Fibroblast Cultures by Defined Factors. *Cell*, 126(4), 663–676.
- Tanaka, Y., Hysolli, E., Su, J., Xiang, Y., Kim, K. Y., Zhong, M., ... Park, I. H. (2015). Transcriptome Signature and Regulation in Human Somatic Cell Reprogramming. *Stem Cell Reports*.
- Teshigawara, R., Hirano, K., Nagata, S., Ainscough, J., & Tada, T. (2016). OCT4 activity during conversion of human intermediately reprogrammed stem cells to iPSCs through mesenchymal-epithelial transition. *Development*.
- Tobias, I. C., Brooks, C. R., Teichroeb, J. H., Villagómez, D. A., Hess, D. A., Séguin, C. A., & Betts, D. H. (2016). Small-Molecule Induction of Canine Embryonic Stem Cells Toward Naïve Pluripotency. *Stem Cells and Development*, 25(16).

- Tobias, I. C., Isaac, R. R., Dierolf, J. G., Khazaee, R., Cumming, R. C., & Betts, D. H. (2018). Metabolic plasticity during transition to naïve-like pluripotency in canine embryo-derived stem cells. *Stem Cell Research*, 30.
- Walsh, C. P., Chaillet, J. R., & Bestor, T. H. (1998). Transcription of IAP endogenous retroviruses is constrained by cytosine methylation. *Nature Genetics*. 20(2), 116-117
- Wang, W., Yang, J., Liu, H., Lu, D., Chen, X., Zenonos, Z., ... Liu, P. (2011). Rapid and efficient reprogramming of somatic cells to induced pluripotent stem cells by retinoic acid receptor gamma and liver receptor homolog 1. *Proceedings of the National Academy of Sciences*.
- Ward, C., Volpe, G., Cauchy, P., Ptasinska, A., Almaghrabi, R., Blakemore, D., ... García, P. (2018). Fine-Tuning Mybl2 Is Required for Proper Mesenchymal-to-Epithelial Transition during Somatic Reprogramming. *Cell Reports*.
- Weber, M., Hellmann, I., Stadler, M. B., Ramos, L., Pääbo, S., Rebhan, M., & Schübeler, D. (2007). Distribution, silencing potential and evolutionary impact of promoter DNA methylation in the human genome. *Nature Genetics*.
- Williams, K., Christensen, J., Pedersen, M. T., Johansen, J. V., Cloos, P. A. C., Rappsilber, J., & Helin, K. (2011). TET1 and hydroxymethylcytosine in transcription and DNA methylation fidelity. *Nature*.
- Wu, H., D'Alessio, A. C., Ito, S., Xia, K., Wang, Z., Cui, K., ... Zhang, Y. (2011). Dual functions of Tet1 in transcriptional regulation in mouse embryonic stem cells. *Nature*.
- Wu, X., & Zhang, Y. (2017). TET-mediated active DNA demethylation: Mechanism, function and beyond. *Nature Reviews Genetics*. 18(9), 517-534
- Xu, Y., Wu, F., Tan, L., Kong, L., Xiong, L., Deng, J., ... Shi, Y. G. (2011). Genome-wide Regulation of 5hmC, 5mC, and Gene Expression by Tet1 Hydroxylase in Mouse Embryonic Stem Cells. *Molecular Cell*.
- Yin, R., Mao, S. Q., Zhao, B., Chong, Z., Yang, Y., Zhao, C., ... Wang, H. (2013). Ascorbic acid enhances tet-mediated 5-methylcytosine oxidation and promotes DNA demethylation in mammals. *Journal of the American Chemical Society*, 135(28), 10396–10403.
- Yoshida, Y., Takahashi, K., Okita, K., Ichisaka, T., & Yamanaka, S. (2009). Hypoxia Enhances the Generation of Induced Pluripotent Stem Cells. *Cell Stem Cell*.
- Zackay, A., & Steinhoff, C. (2010). MethVisual - Visualization and exploratory statistical analysis of DNA methylation profiles from bisulfite sequencing. *BMC Research Notes*.

Zhang, W., Xia, W., Wang, Q., Towers, A. J., Chen, J., Gao, R., ... Xie, W. (2016). Isoform Switch of TET1 Regulates DNA Demethylation and Mouse Development. *Molecular Cell*.

Chapter 5

5 General Discussion and Conclusions

5.1 Discussion and Significance of Research

It has long been understood that manipulation of developmental signaling pathways can influence lineage specification from the pluripotent state. A recent extension of this paradigm suggest manipulations to the culture environment can affect the range of characteristics and differentiation potential of plastic mammalian cell populations. In this plateau model, developmental trajectories can be halted by specific extrinsic signals in a lineage-primed pluripotent state. Under distinct environmental constraints, this progression can even be reversed to stabilize an earlier developmental state on a nearby plateau representing a closely-related cell population. In mammals, two discrete pluripotency plateaus appear to be obtainable, known as naïve and primed, through direct embryonic derivation or reprogramming technologies with developmentally appropriate stimuli from culture environments. Direct reprogramming of somatic cells to either pluripotent state requires ectopic TF overexpression and/or modulation of epigenome modifying enzymes to override the somatic nucleus. In pluripotent stem cells derived from large mammals, such as domestic dogs, there is little consensus regarding the exogenous requirements for the acquisition or maintenance of stable pluripotency. Variation among permissive culture environments may be confounded by the co-existence of multiple canine pluripotent states with exclusive input requirements and discrete cellular and molecular characteristics.

The overall hypothesis of my thesis is that *the culture environment can promote nuclear and metabolic reprogramming of canine cell lines towards a more primitive state of pluripotency*. The main findings of this thesis that support my hypothesis and advance this knowledge are:

1. Manipulation of FGF-ERK and WNT- β -catenin signaling pathways enriched for a unique cESC population with ultrastructural, transcriptional and epigenetic similarity to the naïve pluripotent state.

2. Maintenance of cESCs in discrete culture environments are dependent on different metabolic pathways for *in vitro* proliferation.
3. Combinatorial exposure to metabolites that influence cell signaling and epigenetics facilitate the early de-differentiation of canine somatic cells.

With my thesis work, I have advanced our understanding of the extrinsic requirements and potential intrinsic mediators for the induction and maintenance of phenotypically distinct cESC. Furthermore, we illustrated the utility of metabolite supplementation targeting epigenetic remodeling processes during de-differentiation to facilitate phase-specific progression towards a reprogrammed pluripotent state. Taken together, these investigations establish a developmental context for cESCs that is dependent on complex interactions between gene regulatory mechanisms, metabolic activities and the microenvironment (Figure 5-1).

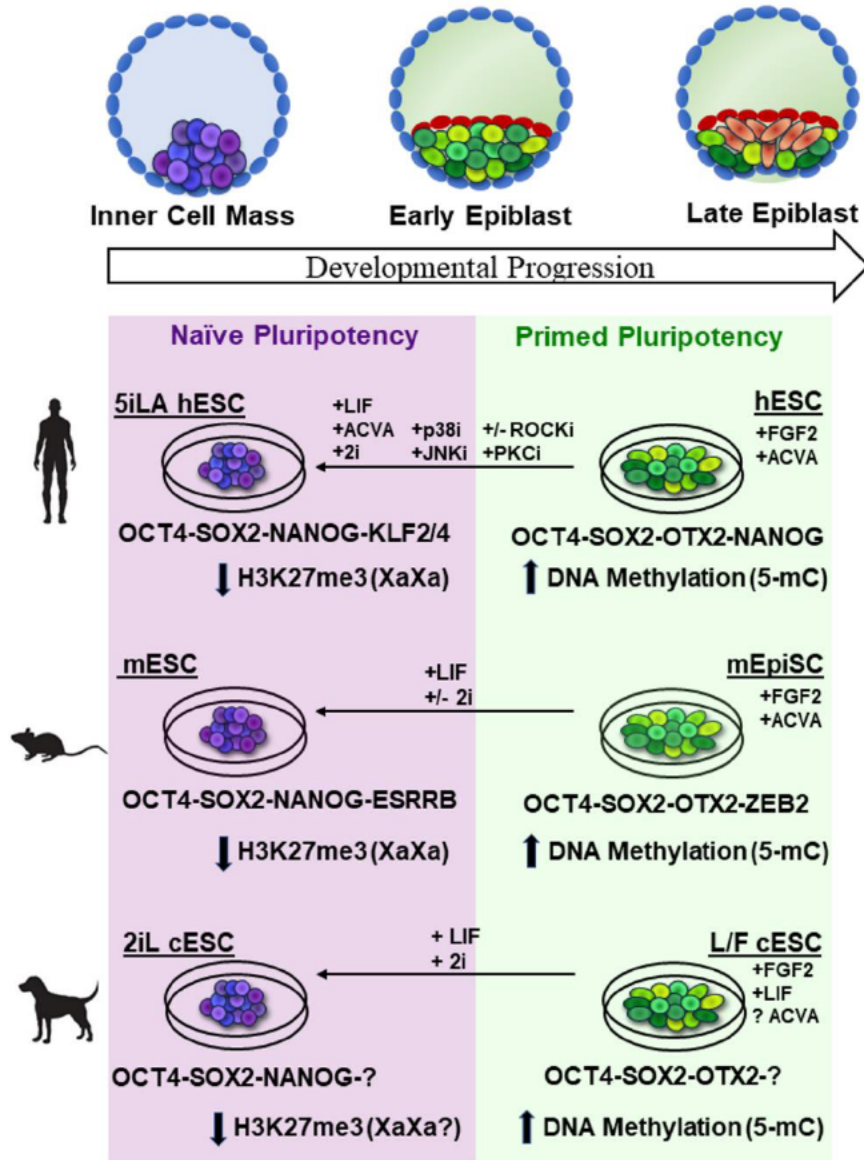


Figure 5-1. Conserved and divergent features of pluripotent state progression in canines.

Pluripotent cells reside in transient and discrete embryonic compartments in mammals known as the inner cell mass, early epiblast and late (peri-gastrulation) epiblast. The epiblast adopts a flattened disc-shape (depicted here) in humans and dogs as opposed to the egg cylinder of rodents. NANOG and OTX2 appear to be conserved transcriptional regulators of mammalian naïve and primed pluripotent states, respectively. Although X-chromosome activation status is still unclear, both H3K27me3 and 5-mC are depleted in canine naïve-like pluripotency.

5.1.1 Pluripotent state-specific signaling and metabolic pathways support cESC maintenance

Extracellular signals cooperate with transcriptional regulatory machinery to organize epigenetic features critical to multi-lineage plasticity and to minimize the loss of pluripotent attributes through rapid symmetrical cell divisions. Despite greater than a dozen derivation and characterization studies of canine embryo-derived or reprogramming factor-induced PSCs (Menon et al., 2019), the similarity of canine ESC/iPSC to pluripotent state phenotypes described in rodents and primates remain unexplored.

I propose a model in which blastocyst-derived canine pluripotent stem cells maintained in LIF and FGF2 (L/F) represent a metastable lineage-primed state of pluripotency from which a developmentally immature subpopulation may be enriched with selective disruption of developmental signaling pathways. Application of small molecule inhibitors of GSK3 β and MEK signaling with LIF supplementation (2iL) support a pluripotent cell population with transcriptional, epigenetic and differentiation tendencies suggestive of an earlier developmental identity (Chapter 2). The discrete pluripotent cell populations supported by L/F or 2iL exhibit morphologically and functionally distinct mitochondria, that alter metabolic pathway prioritization for anabolism and ATP generation (Chapter 3) (Figure 5-2).

LIF and FGF2-dependent canine ESCs/iPSCs spontaneously differentiate *in vitro* in the absence of exogenous LIF (Koh et al., 2013; Vaags et al., 2009; Wilcox et al., 2009). We show that pre-existing LIF-STAT3 signaling activity in L/F cESCs is enhanced with the induction and culture of naïve-like cESCs in 2iL (Chapter 2). The induction of STAT3 signaling is consistent with an evolutionarily conserved role in the establishment and maintenance of naïve pluripotency among rodents, primates and ungulates (Chen et al., 2015; Meng et al., 2015; Van Oosten et al., 2012; Wu et al., 2019). We also observe that 2iL cESCs have elevated respiratory capacities compared to L/F cESCs (Chapter 3). During primed-to-naïve pluripotency resetting in mice, STAT3 has been shown to directly promote respiration by activation of mtDNA transcription (Carbognin et al., 2016). Reprogramming of mEpiSC to mESC by LIF-STAT3 signaling is halted by

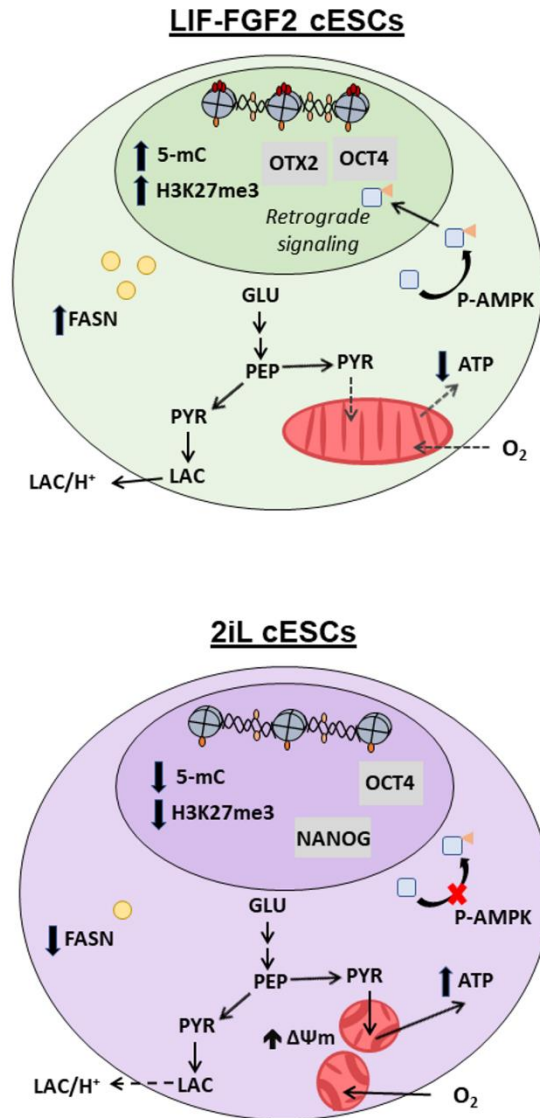


Figure 5-2. Different metabolic pathway activities support proliferation of canine ESCs approximating primed and naïve pluripotency.

Conversion of LIF-FGF2 (L/F) cESCs to a naïve-like pluripotent state in 2iL medium is associated with enhanced mitochondrial respiration and membrane potential ($\Delta\Psi_m$). Incomplete oxidation of glucose in L/F cESCs is accompanied by lower ATP production and elevated neutral lipid accumulation. Remodeling of mitochondrial ultrastructure in 2iL cESCs includes shorter mitochondria and disorganized cristae. Elevated mitochondrial activity in 2iL cESCs may have a widespread influence on cellular processes by altering retrograde AMPK signaling. Abbreviations: Glucose (GLU), Phosphoenolpyruvate (PEP), pyruvate (PYR), lactate (LAC), fatty acid synthase (FASN).

respiratory complex I inhibitor rotenone, implying that electron transport chain activity is important for rewiring the pluripotency GRN (Carbognin et al., 2016). There is some evidence that 2i has a complementary function to LIF by suppressing PGC-1 α expression to maintain the structural immaturity of mitochondria (Mahato et al., 2014). We qualitatively observed the broadening of cristae outlets and tips and detected significant decreases in MIC60 and assembled F1 ATP synthase subunits (Chapter 3). A similar mitochondrial morphology is apparent in 2i mESC compared to S/L controls, suggesting that 2i may directly affect cristae remodeling in naïve PSC (Mahato et al., 2014).

Activin/Nodal-SMAD2 signaling is believed to have an evolutionarily conserved role in mEpiSC/hESC coordinating the primed pluripotency GRN and reducing paracrine BMP signaling that drives lineage specification (Bertero et al., 2015; Sakaki-Yumoto et al., 2013; Senft et al., 2018). We found no difference in SMAD2 phosphorylation between L/F and 2iL cESCs indicating that this pathway is not likely to oppose the stabilization of naïve or primed pluripotency in canines (Chapter 2). We noted that Activin receptor type 2B (ACVR2B) transcript abundance is down-regulated in 2iL cESCs, which implies that 2iL cESCs may be less sensitized to TGF β ligands (Chapter 2). Additionally, phospho-SMAD2 level was not significantly different between ALK inhibitor SB431542 treatment and steady-state L/F cESC culture suggesting low basal SMAD2 signaling may be supported by alternative signaling cascades (Chapter 2). A comparison of independently derived metastable porcine iPSC lines with distinct culture requirements (+LIF; +FGF2; +LIF+FGF2) demonstrated that OCT4 and NANOG expression and self-renewal is improved with Activin A exposure (Yang et al., 2017). Furthermore, exogenous Activin A was recently shown to replace FGF2 signaling and induce NANOG expression in LIF and FGF2-dependent canine iPSCs (Luo and Cibelli, 2016). Taken together, these studies indicate that a more stable primed pluripotent state may be obtained through an evolutionarily conserved Activin-SMAD2/3-NANOG axis.

5.1.2 Intracellular signaling pathways may link bioenergetics to self-renewal and tumorigenicity of cESCs

Quantification of cESC proliferative rates during steady-state growth indicated that culture conditions may be suboptimal, and that cell metabolism is influenced by the

pluripotent state (Chapter 2). These observations were confirmed with quantifiably lower glycolytic capacities and HXK2 abundances in cESCs compared to hESC and mESC cultures, despite culture in controlled nutritional environments (Chapter 3). Furthermore, 2iL cESCs exhibit greater spare respiratory and glycolytic reserve capacities than L/F cESCs (Chapter 3). These observations raise fundamental questions regarding the regulation of glycolysis and proliferation in ESCs derived from dogs. It should be noted that indirect measurements of glycolytic and mitochondrial activities were used in this work. A direct analysis of metabolic flux and dissection of metabolic pathway dynamics could be achieved through stable isotope-assisted metabolomics.

Glycolytic flux in PSC and embryos are regulated at the level of glucose uptake by GLUT transporters as well as glycolytic enzyme abundances or activities. Constitutive transporter GLUT1 is expressed in both hESC and mESC, correlates with glucose uptake and mediates hypoxic adaptation of PSC to anaerobic glycolysis following HIF stabilization (Forristal et al., 2013; Wu et al., 2017). While we found no difference in the abundance of GLUT1 (Chapter 3), we cannot formally rule out differential rates of glucose consumption underlying significantly different glycolytic capacities between cESCs and hESCs or mESCs. We did not investigate the contribution of GLUT3, which is developmentally regulated and shows high correspondence with OCT4 expression (Carayannopoulos et al., 2014; Christensen et al., 2015). Recently, blunted glycolytic rates in iPSC lines derived from aged donors was associated with elevated ROS and depleted of TCA cycle phenotype that was rescued by GLUT3 overexpression (Zhang et al., 2017). Manipulation of glycolytic flux in cESCs may be required to mitigate the incidence of spontaneous differentiation, improve scalable culture as well as promote *in vivo* survival and proliferation following xenotransplantation assays.

Gene regulatory networks controlled by OCT4 and C-MYC/N-MYC promote high glycolytic flux in both mESC and hESC by regulating glycolytic enzyme expressions including HXK2, LDHA and PKM2 (Cliff et al., 2017; Gu et al., 2016; Kim et al., 2015). C-MYC/N-MYC double knockout studies indicate that growth-arrested mESCs remain functionally pluripotent (Scognamiglio et al., 2016). Therefore, regulators of cell growth, metabolism and pluripotency are strongly interconnected in PSC but disruption of

intracellular signaling networks can functionally uncouple pluripotency and self-renewal. In the present work, we did not observe any difference in the abundances of core pluripotency factor OCT4 or the level of HXK2 or PKM2 between L/F and 2iL cESCs (Chapters 2 and 3). However, we found decreased HXK2 in both L/F and 2iL cESCs compared to hESC or mESC (Chapter 3). The low proliferation rate in cESC cultures bears a striking resemblance to a novel “paused” pluripotent state induced in mESC by inhibition of mechanistic target of rapamycin (mTOR) (Bulut-Karslioglu et al., 2016). Notably, progression through the cell cycle is slower in paused pluripotency without appreciable apoptosis or differentiation (Bulut-Karslioglu et al., 2016). Inhibition of mTOR promotes autophagy and suppresses global transcriptional and translational output, all of which characterize paused pluripotent cells (Bulut-Karslioglu et al., 2016; Sotthibundhu et al., 2016). Interestingly, selective HXK2 degradation by chaperone-mediated autophagy is an anti-cancer mechanism employed by non-transformed cells (Jiao et al., 2018; Xia et al., 2015).

Several lines of evidence suggest that cESCs in L/F or 2iL conditions may represent a similarly idle pluripotent phenotype where glycolytic capacity is blunted by hyperactive autophagy. In addition to mTOR, autophagy may be initiated in mammalian cells by liver kinase B1 (LKB1)-AMPK signaling (Kim et al., 2011). We found that increased mitochondrial respiration and ATP level in 2iL cESCs was associated with a decrease AMPK activity compared to L/F cESC (Chapter 3). These observations provoke questions regarding the roles of nutrient and energy sensing pathways in regulating autophagy and related catabolic pathways (e.g. mitophagy) in pluripotency maintenance and self-renewal. Future investigations should also attempt to disentangle the contributions of regulated degradation versus fission-fusion homeostasis to mitochondrial networks in pluripotent state transitions and lineage restriction.

PSC normally maintain low expression of p21 and exclude p53 from the nucleus to rapidly progress through G1/S or G2/M cell cycle checkpoints (Calder et al., 2013; Suvorova et al., 2016; Zhang et al., 2014). Unsurprising, mammalian PSC traditionally do not exhibit contact inhibition *in vitro* and possess high tumorigenic potential in immunocompromised hosts (Ben-David and Benvenisty, 2011). Observations that LIF

and FGF2-dependent cESC lines derived in an independent laboratory generate teratomas have not been replicated (Vaags et al., 2009). We showed that cESC transplantation from either L/F or 2iL conditions do not readily yield tumors compared to hESCs that generate mature teratomas (Chapter 2). Cell intrinsic factors that contribute to low tumorigenicity of cESCs may resemble some combination of sensitivity to apoptosis, low competitive fitness and/or poor transcriptional activation of proto-oncogenic GRNs. Transcriptional networks centered around C-MYC/N-MYC typically show considerable overlap between steady-state PSCs and cancer cells, which is largely related to a shared role in transcriptional amplification (Kim et al., 2010; Lin et al., 2012). There are also species-specific drivers of tumorigenicity in PSCs such as embryonic ras-like gene (Eras). Eras constitutively activates the PI3K-mTOR signaling pathway to augment the proliferation and tumorigenicity of mESC but does not contribute to tumorigenic potential of primate ESC (Takahashi et al., 2003; Tanaka et al., 2009; Yu and Cui, 2016).

5.2 Future Studies: Purification and analysis of canine reprogramming intermediate cells

Somatic cell reprogramming is a multi-step process that requires phase-specific epigenomic remodeling and transcriptional activity for productive transitions towards pluripotency. Initiation of reprogramming in fibroblast populations is characterized by silencing the somatic GRN that de-represses epithelial gene expression (Li et al., 2010; Samavarchi-Tehrani et al., 2010). Productively reprogramming cells undergo mesenchymal-to-epithelial transition (MET) characterized by the induction of gene products that form epithelial tight junctions (Høffding and Hyttel, 2015; Shook and Keller, 2003). Dose-optimization of the combination of L-ascorbic acid and retinoic acid can reproducibly induce the accumulation of oxidized products of methylated DNA catalyzed by the TET dioxygenase family enzymes (Chapter 4). Combined and transient (2-6 DPI) metabolite treatment correlates positively with a MET transcriptional response and increased frequency of reprogramming progression to the maturation phase (Chapter 4). However, exogenous growth factor/cytokine supplementation alone was not suitable to stabilize canine reprogramming intermediates (Chapter 4).

Pluripotency maturation is the greatest obstacle to successful reprogramming because it depends on the rare and probabilistic activation of previously silent genomic regions. Reactivation of pluripotency-associated loci during iPSC maturation is reversible and sustained transcriptional output is dependent on the recruitment of chromatin modifying enzymes to important CRMs (Teshigawara et al., 2016). The ability of a given region to recruit histone or DNA modifying enzymes that support or oppose reprogramming is partly dependent on the composition of the local genomic sequence (Behera et al., 2018; Carcamo-Orive et al., 2017). We have assessed the conservation of CpG-sequence richness among 1:1:1 orthologues that are differentially expressed during primate and rodent reprogramming. A subset of promoters with substantial gains in CpG-sequence richness were identified as potentially unique to the canine genome assembly (Chapter 4). These sequence features are distinct from other Laurasiatherian mammals (e.g. pig, cow) and therefore are more likely to be a consequence of canid evolution (Chapter 4). It is tempting to speculate that localized gains in CpG-richness would increase the affinity and grant regulatory control to specific enzyme classes containing CpG DNA binding domains (e.g. CXXC, MDB) domains such as DNMTs, TETs and components of polycomb group repressive complexes (Du Q et al., 2015; Risner et al., 2013). However, we are limited in the scope of this investigation to shared orthologues selected from genome-wide sequencing experiments from a different clade of placental mammals. Future studies should prioritize unbiased identification of genes predictive of the establishment and maintenance of different canine pluripotent states. In this regard, a comparative transcriptomic approach between dissected canine preimplantation embryos (e.g. embryonic ICM or epiblast) as well as cESC cultures approximating different pluripotent states would identify both divergent and conserved molecular determinants of canine pluripotency (Bernardo et al., 2018).

Complicating the study of iPSC maturation is high biological variation caused by non-hierarchical gene activation and clonal dominance effects (Kuno et al., 2018; Tanabe et al., 2013). To address this challenge, strategies are required to enrich for cells exhibiting early pluripotency characteristics. The inclusion of additional transactors such as LIN28 and NANOG alongside O-K-S-M has been shown to increase reprogramming efficiency or overcome age-related cellular senescence in donor cells (Lapasset et al., 2011; Liao et

al., 2008). It is believed that LIN28 and NANOG function independent of cell division kinetics by co-targeting pluripotency-associated CRMs and facilitating both combinatorial and cooperative TF binding to stably reactivate endogenous pluripotency loci (Hanna et al., 2009). Although, this approach increases the probability of reprogramming intermediates reaching the maturation phase, it does not guarantee deterministic reprogramming. Hence, biological heterogeneity would be expected to persist and confound the identification of endogenous gene sets and processes important for the completion of iPSC maturation.

MET-associated transcriptional response in early canine reprogramming implicates several gene products localized to the cell surface. Sorting and enrichment of cell populations based on epithelial or mesenchymal surface markers using FACS will deconvolute the heterogeneity among the mixture of productively reprogramming canine cell populations and alternative cell fates. Intermediate subpopulations undergoing a productive reprogramming trajectory have been successfully isolated by monitoring the loss of somatic surface markers and concomitant gain of epithelial surface markers (Nefzger et al., 2015; Polo et al., 2012). This approach will allow us to dissect the pathways and processes active in productively reprogramming versus refractory cell populations (Fig. 5-3).

To this end, I have validated canine-reactive antibodies against glycoprotein epitopes characteristic of mesenchymal cell types. Canine fibroblast populations are immunoreactive to mesenchymal surface markers such as the CD90/THY1 and CD44/ECMR-III (Fig. 5-4A). These antigens are uniformly present (>98%) on fibroblast cultures, but only CD90/THY1 is absent from control epithelial cell line MDCK-II and hence apparently specific to the mesenchymal state (Fig. 5-4B). In contrast, the epithelial adhesion protein CD324/CDH1 level is elevated in MDCK-II compared to fibroblasts (Fig. 5-4B). CD324/CDH1 was significantly induced by AA/RA treatment at 6 DPI by reverse transcription qPCR using commercial and custom oligonucleotide primers (Chapter 4). I predict that CD90/THY1 and CD324/CDH1 will serve as selectable markers to discriminate between epithelial and mesenchymal cells, among the heterogeneous intermediates in early canine reprogramming for detailed molecular analyses.

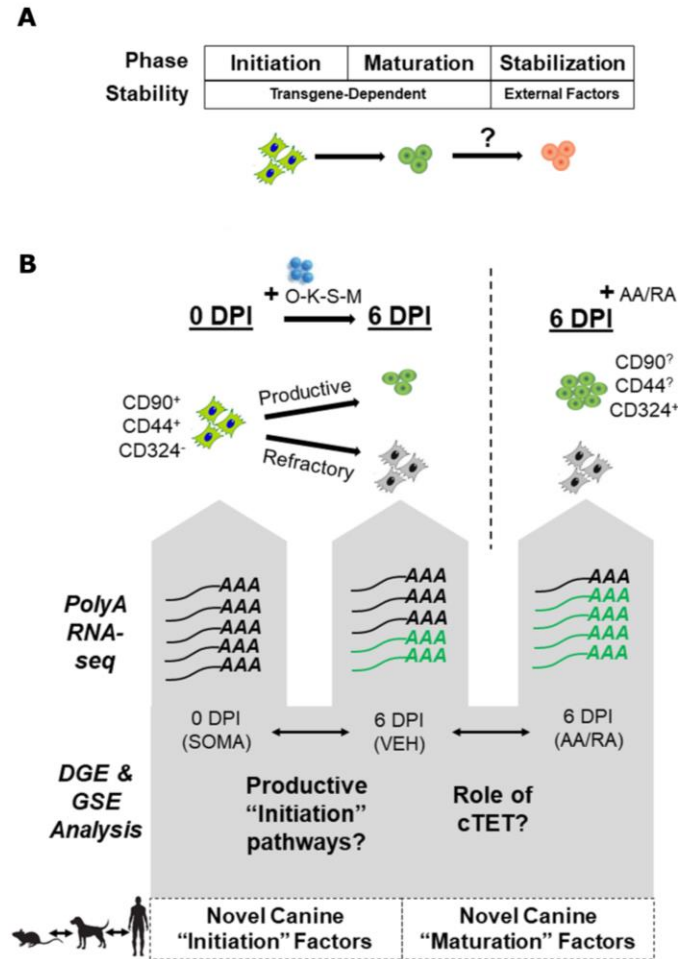


Figure 5-3. Strategy to investigate conserved and divergent reprogramming mechanisms in the dog.

(A) Initiation and maturation phases of reprogramming are reversible and dependent on reprogramming factor expression. Stabilization of induced pluripotency relies on currently unknown extrinsic signals that are distinct from those involved in pluripotency maintenance. (B) Putative canine-reactive antibodies for mesenchymal (e.g. CD44/ECMR-III, CD90/THY1) or epithelial (e.g. CD324/CDH1) glycoprotein antigens may be applied to enrich for productively reprogramming intermediate cells that have undergone mesenchymal-to-epithelial transition. Comparison of productive and refractory reprogramming intermediates will identify gene products and processes important to canine reprogramming. Interspecies differences may be elucidated by comparing these datasets to publicly available human and mouse reprogramming studies at matched reprogramming timepoints.

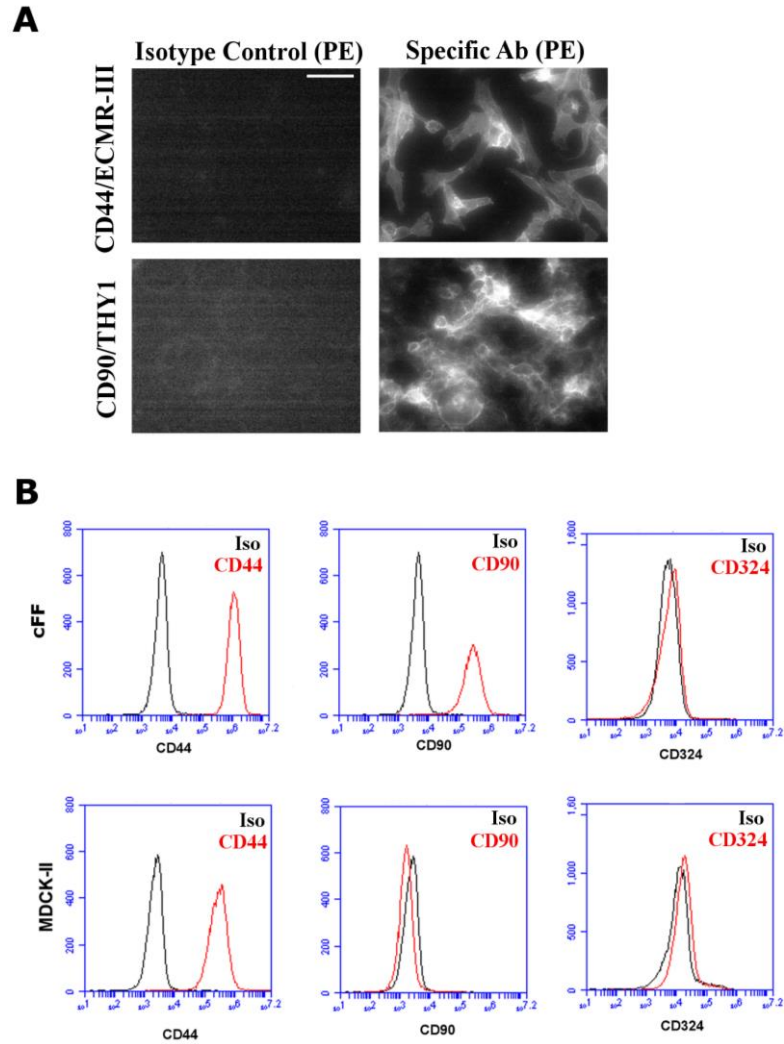


Figure 5-4. Validation of canine-reactive surface markers to discriminate mesenchymal or epithelial canine cells.

Representative direct immunofluorescence images in canine fetal fibroblast for extracellular matrix receptor III (CD44/ECMR-III) and thymus cell antigen (CD90/THY1). Scale bar unit length is 50 μm . (B) Representative overlay histograms of canine fetal fibroblast (cFF) and Madin Darby Canine Kidney (MDCK-II) epithelial cell line stained with CD44, CD90 or epithelial cadherin (CDH1/CD324).

5.3 Summary

Pluripotency and self-renewal are widely presumed to be conserved features of the inner cell mass and epiblast of mammalian embryos. Environmental stimuli change dynamically during early development and so these distinct pluripotent cell populations rely on variations of core gene regulatory mechanisms and metabolic activities. This ensures that pluripotent cells are to undergo robust symmetric self-renewal, while remaining poised for embryonic lineage specification. Evolutionary divergence in reproductive physiology and early developmental progression lead to species-specific pluripotent cell attributes, which will also likely alter the molecular roadmaps to an induced pluripotent state. My discovery that cESC may adopt molecularly distinct phenotypes with metabolic requirements mirroring primed and naïve pluripotent states advances the knowledge of conserved pluripotent state regulators. In summary, this thesis expands on the influence of the culture environment on phenotypic plasticity exhibited by cESCs and canine reprogramming intermediates.

5.4 References

- Behera, V., Evans, P., Face, C. J., Hamagami, N., Sankaranarayanan, L., Keller, C. A., ... Blobel, G. A. (2018). Exploiting genetic variation to uncover rules of transcription factor binding and chromatin accessibility. *Nature Communications*.
- Ben-David, U., & Benvenisty, N. (2011). The tumorigenicity of human embryonic and induced pluripotent stem cells. *Nature Reviews Cancer*.
- Bernardo, A. S., Jouneau, A., Marks, H., Kensche, P., Kobolak, J., Freude, K., ... Dinnyes, A. (2018). Mammalian embryo comparison identifies novel pluripotency genes associated with the naïve or primed state. *Biology Open*.
- Bertero, A., Madrigal, P., Galli, A., Hubner, N. C., Moreno, I., Burks, D., ... Vallier, L. (2015). Activin/Nodal signaling and NANOG orchestrate human embryonic stem cell fate decisions by controlling the H3K4me3 chromatin mark. *Genes and Development*.
- Bulut-Karslioglu, A., Biechele, S., Jin, H., MacRae, T. A., Hejna, M., Gertsenstein, M., ... Ramalho-Santos, M. (2016). Inhibition of mTOR induces a paused pluripotent state. *Nature*.

- Calder, A., Roth-Albin, I., Bhatia, S., Pilquill, C., Lee, J. H., Bhatia, M., ... Draper, J. S. (2013). Lengthened G1 Phase Indicates Differentiation Status in Human Embryonic Stem Cells. *Stem Cells and Development*, 22(2), 279–295.
- Carayannopoulos, M. O., Xiong, F., Jensen, P., Rios-Galdamez, Y., Huang, H., Lin, S., & Devaskar, S. U. (2014). GLUT3 gene expression is critical for embryonic growth, brain development and survival. *Molecular Genetics and Metabolism*.
- Carbognin, E., Betto, R. M., Soriano, M. E., Smith, A. G., & Martello, G. (2016). Stat3 promotes mitochondrial transcription and oxidative respiration during maintenance and induction of naive pluripotency. *The EMBO Journal*, 35(6), 618–34.
- Carcamo-Orive, I., Hoffman, G. E., Cundiff, P., Beckmann, N. D., D'Souza, S. L., Knowles, J. W., ... Lemischka, I. (2017). Analysis of Transcriptional Variability in a Large Human iPSC Library Reveals Genetic and Non-genetic Determinants of Heterogeneity. *Cell Stem Cell*.
- Chen, H., Aksoy, I., Gonnot, F., Osteil, P., Aubry, M., Hamela, C., ... Savatier, P. (2015). Reinforcement of STAT3 activity reprogrammes human embryonic stem cells to naive-like pluripotency. *Nature Communications*.
- Christensen, D. R., Calder, P. C., & Houghton, F. D. (2015). GLUT3 and PKM2 regulate OCT4 expression and support the hypoxic culture of human embryonic stem cells. *Scientific Reports*.
- Cliff, T. S., Wu, T., Boward, B. R., Glushka, J. N., Prestegaard, J. H., Dalton, S., ... Glushka, J. N. (2017). MYC Controls Human Pluripotent Stem Cell Fate MYC Controls Human Pluripotent Stem Cell Fate. *Cell Stem Cell*, 21(4), 1–15.
- Du, Q., Luu, P. L., Stirzaker, C., & Clark, S. J. (2015). Methyl-CpG-binding domain proteins: Readers of the epigenome. *Epigenomics*.
- Forristal, C. E., Christensen, D. R., Chinnery, F. E., Petruzzelli, R., Parry, K. L., Sanchez-Elsner, T., & Houghton, F. D. (2013). Environmental Oxygen Tension Regulates the Energy Metabolism and Self-Renewal of Human Embryonic Stem Cells. *PLoS ONE*.
- Gu, W., Gaeta, X., Sahakyan, A., Chan, A. B., Hong, C. S., Kim, R., ... Christofk, H. R. (2016). Glycolytic Metabolism Plays a Functional Role in Regulating Human Pluripotent Stem Cell State. *Cell Stem Cell*.
- Hanna, J., Saha, K., Pando, B., Van Zon, J., Lengner, C. J., Creighton, M. P., ... Jaenisch, R. (2009). Direct cell reprogramming is a stochastic process amenable to acceleration. *Nature*.

- Høffding, M. K., & Hyttel, P. (2015). Ultrastructural visualization of the Mesenchymal-to-Epithelial Transition during reprogramming of human fibroblasts to induced pluripotent stem cells. *Stem Cell Research*, 14(1), 39–53.
- Jiao, L., Zhang, H. L., Li, D. D., Yang, K. L., Tang, J., Li, X., ... Zhu, X. F. (2018). Regulation of glycolytic metabolism by autophagy in liver cancer involves selective autophagic degradation of HK2 (hexokinase 2). *Autophagy*.
- Kim, H., Jang, H., Kim, T. W., Kang, B. H., Lee, S. E., Jeon, Y. K., ... Youn, H. D. (2015). Core Pluripotency Factors Directly Regulate Metabolism in Embryonic Stem Cell to Maintain Pluripotency. *Stem Cells*.
- Kim, J., Woo, A. J., Chu, J., Snow, J. W., Fujiwara, Y., Kim, C. G., ... Orkin, S. H. (2010). A Myc Network Accounts for Similarities between Embryonic Stem and Cancer Cell Transcription Programs. *Cell*.
- Kim, J., Kundu, M., Viollet, B., & Guan K.L. (2011). AMPK and mTOR regulate autophagy through direct phosphorylation of Ulk1. *Nat Cell Biol*.
- Koh, S., Thomas, R., Tsai, S., Bischoff, S., Lim, J.-H., Breen, M., ... Piedrahita, J. A. (2013). Growth Requirements and Chromosomal Instability of Induced Pluripotent Stem Cells Generated from Adult Canine Fibroblasts. *Stem Cells and Development*.
- Kuno, A., Nishimura, K., & Takahashi, S. (2018). Time-course transcriptome analysis of human cellular reprogramming from multiple cell types reveals the drastic change occurs between the mid phase and the late phase. *BMC Genomics*.
- Lapasset, L., Milhavet, O., Prieur, A., Besnard, E., Babled, A., Ät-Hamou, N., ... Lemaitre, J. M. (2011). Rejuvenating senescent and centenarian human cells by reprogramming through the pluripotent state. *Genes and Development*.
- Li, R., Liang, J., Ni, S., Zhou, T., Qing, X., Li, H., ... Pei, D. (2010). A mesenchymal-to-Epithelial transition initiates and is required for the nuclear reprogramming of mouse fibroblasts. *Cell Stem Cell*.
- Liao, J., Wu, Z., Wang, Y., Cheng, L., Cui, C., Gao, Y., ... Xiao, L. (2008). Enhanced efficiency of generating induced pluripotent stem (iPS) cells from human somatic cells by a combination of six transcription factors. *Cell Research*.
- Lin, C. Y., Lovén, J., Rahl, P. B., Paranal, R. M., Burge, C. B., Bradner, J. E., ... Young, R. A. (2012). Transcriptional amplification in tumor cells with elevated c-Myc. *Cell*.
- Luo, J., & Cibelli, J. B. (2016). Conserved Role of bFGF and a Divergent Role of LIF for Pluripotency Maintenance and Survival in Canine Pluripotent Stem Cells. *Stem Cells and Development*, 25(21), 1670–1680.

- Mahato, B., Home, P., Rajendran, G., Paul, A., Saha, B., Ganguly, A., ... Paul, S. (2014). Regulation of mitochondrial function and cellular energy metabolism by protein kinase C- λ 1: a novel mode of balancing pluripotency. *Stem Cells* (Dayton, Ohio), 32(11), 2880–92.
- Meng, F., Oback, B., Turner, P., Forrester-Gauntlett, B., & Henderson, H. (2015). Signal Inhibition Reveals JAK/STAT3 Pathway as Critical for Bovine Inner Cell Mass Development1. *Biology of Reproduction*.
- Menon, D. V., Patel, D., Joshi, C. G., & Kumar, A. (2019). The road less travelled: The efficacy of canine pluripotent stem cells. *Experimental Cell Research*.
- Nefzger, C. M., Alaei, S., & Polo, J. M. (2015). Isolation of reprogramming intermediates during generation of induced pluripotent stem cells from mouse embryonic fibroblasts. In *Methods in Molecular Biology*.
- Polo, J. M., Anderssen, E., Walsh, R. M., Schwarz, B. A., Nefzger, C. M., Lim, S. M., ... Hochedlinger, K. (2012). A molecular roadmap of reprogramming somatic cells into iPS cells. *Cell*, 151(7), 1617–1632.
- Risner, L. E., Kuntimaddi, A., Lokken, A. A., Achille, N. J., Birch, N. W., Schoenfelt, K., ... Zeleznik-Le, N. J. (2013). Functional specificity of CpG DNA-binding CXXC domains in mixed lineage leukemia. *Journal of Biological Chemistry*.
- Sakaki-Yumoto, M., Liu, J., Ramalho-Santos, M., Yoshida, N., & Derynck, R. (2013). Smad2 Is essential for maintenance of the human and mouse primed pluripotent stem cell state. *Journal of Biological Chemistry*.
- Samavarchi-Tehrani, P., Golipour, A., David, L., Sung, H. K., Beyer, T. A., Datti, A., ... Wrana, J. L. (2010). Functional genomics reveals a BMP-Driven mesenchymal-to-Epithelial transition in the initiation of somatic cell reprogramming. *Cell Stem Cell*.
- Scognamiglio, R., Cabezas-Wallscheid, N., Thier, M. C. C., Altamura, S., Reyes, A., Prendergast, Á. M. M., ... Trumpp, A. (2016). Myc Depletion Induces a Pluripotent Dormant State Mimicking Diapause. *Cell*, 164(4), 668–680.
- Senft, A. D., Costello, I., King, H. W., Mould, A. W., Bikoff, E. K., & Robertson, E. J. (2018). Combinatorial Smad2/3 Activities Downstream of Nodal Signaling Maintain Embryonic/Extra-Embryonic Cell Identities during Lineage Priming. *Cell Reports*.
- Shook, D., & Keller, R. (2003). Mechanisms, mechanics and function of epithelial-mesenchymal transitions in early development. *Mechanisms of Development*.
- Sotthibundhu, A., McDonagh, K., Von Kriegsheim, A., Garcia-Munoz, A., Klawiter, A., Thompson, K., ... Shen, S. (2016). Rapamycin regulates autophagy and cell adhesion in induced pluripotent stem cells. *Stem Cell Research and Therapy*.

- Suvorova, I. I., Grigorash, B. B., Chuykin, I. A., Pospelova, T. V., & Pospelov, V. A. (2016). G1 checkpoint is compromised in mouse ESCs due to functional uncoupling of p53-p21waf1 signaling. *Cell Cycle*.
- Takahashi, K., Mitsui, K., & Yamanaka, S. (2003). Role of ERas in promoting tumour-like properties in mouse embryonic stem cells. *Nature*.
- Tanabe, K., Yamanaka, S., Narita, M., Takahashi, K., & Nakamura, M. (2013). Maturation, not initiation, is the major roadblock during reprogramming toward pluripotency from human fibroblasts. *Proceedings of the National Academy of Sciences*.
- Tanaka, Y., Ikeda, T., Kishi, Y., Masuda, S., Shibata, H., Takeuchi, K., ... Hanazono, Y. (2009). ERas is expressed in primate embryonic stem cells but not related to tumorigenesis. *Cell Transplantation*.
- Teshigawara, R., Hirano, K., Nagata, S., Ainscough, J., & Tada, T. (2016). OCT4 activity during conversion of human intermediately reprogrammed stem cells to iPSCs through mesenchymal-epithelial transition. *Development*.
- Vaags, A. K., Rosic-Kablar, S., Gartley, C. J., Zheng, Y. Z., Chesney, A., Villagómez, D. A. F., ... Hough, M. R. (2009). Derivation and Characterization of Canine Embryonic Stem Cell Lines with In Vitro and In Vivo Differentiation Potential. *Stem Cells*, 27(2), 329–340.
- Van Oosten, A. L., Costa, Y., Smith, A., & Silva, J. C. R. (2012). JAK/STAT3 signalling is sufficient and dominant over antagonistic cues for the establishment of naive pluripotency. *Nature Communications*.
- Wilcox, J. T., Semple, E., Gartley, C., Brisson, B. A., Perrault, S. D., Villagómez, D. A. F., ... Betts, D. H. (2009). Characterization of Canine Embryonic Stem Cell Lines Derived From Different Niche Microenvironments. *Stem Cells and Development*, 18(8), 1167–1178.
- Wu, H., Song, C., Zhang, J., Zhao, J., Fu, B., Mao, T., & Zhang, Y. (2017). Melatonin-mediated upregulation of GLUT1 blocks exit from pluripotency by increasing the uptake of oxidized Vitamin C in mouse embryonic stem cells. *FASEB Journal*.
- Wu, R., Liu, Y., Zhao, Y., Bi, Z., Yao, Y., Liu, Q., ... Wang, X. (2019). m6A methylation controls pluripotency of porcine induced pluripotent stem cells by targeting SOCS3/JAK2/STAT3 pathway in a YTHDF1/YTHDF2-orchestrated manner. *Cell Death & Disease*, 10(3), 171.
- Xia, H. guang, Najafov, A., Geng, J., Galan-Acosta, L., Han, X., Guo, Y., ... Vakifahmetoglu-Norberg, H. (2015). Degradation of HK2 by chaperone-mediated autophagy promotes metabolic catastrophe and cell death. *Journal of Cell Biology*.

- Yang, F., Wang, N., Wang, Y., Yu, T., & Wang, H. (2017). Activin-SMAD signaling is required for maintenance of porcine iPS cell self-renewal through upregulation of NANOG and OCT4 expression. *Journal of Cellular Physiology*.
- Yu, J. S. L., & Cui, W. (2016). Proliferation, survival and metabolism: the role of PI3K/AKT/mTOR signalling in pluripotency and cell fate determination. *Development*.
- Zhang, C., Skamagki, M., Liu, Z., Ananthanarayanan, A., Zhao, R., Li, H., & Kim, K. (2017). Biological Significance of the Suppression of Oxidative Phosphorylation in Induced Pluripotent Stem Cells. *Cell Reports*.
- Zhang, Z. N., Chung, S. K., Xu, Z., & Xu, Y. (2014). Oct4 maintains the pluripotency of human embryonic stem cells by inactivating p53 through sirt1-mediated deacetylation. *Stem Cells*.

Appendix A: Materials and Methods for cell surface marker validation

Immunolabeling for Fluorescence Microscopy

For fluorescence microscopy, cells were stained for 1 hour with CD44-PE (1:100) or CD90-PE (1:50) diluted in a 3% BSA staining solution. Table A-1 contains primary antibody information. Cells were imaged on the stage of a Leica DMI 6000B microscope. Digital images were captured with an Orca Flash camera (Hamamatsu Photonics) and Application Suite X software (Leica Microsystems). Brightness and contrast were standardized to isotype stained samples and the equivalent imaging parameters were applied to all other images using ImageJ (National Institutes of Health, MD).

Table 0-1. Primary antibody information for flow cytometry.

Antibody	Fluorochrome	Supplier (Catalog)
Anti-CD44 (IM7)	PE	Thermo Fisher (12-0441-82)
Anti-CD90 (YKIX337.217)	PE	Thermo Fisher (12-5900-42)
Anti-CD324 (DECMA-1)	FITC	Thermo Fisher (14-3249-82)
Rat IgG Isotype Control	PE	Thermo Fisher (12-4031-82)
Rat IgG Isotype Control	FITC	Thermo Fisher (11-4321-80)

Immunolabeling for Flow Cytometry

For flow cytometry, cells were collected by a cell scraper after treating with enzyme-free cell dissociation buffer containing EDTA for 5 min at 37 °C, and was treated TrypLE enzyme for 6 minutes at 37 °C. Single live cells in suspension were filtered through a 70- μ m strainer adjusted to a density of approximately 1×10^6 cells/mL in staining buffer (1% bovine serum albumin, 0.075% Sodium Azide) and incubated with CD90-PE (1:50) or CD44-PE (1:100) and CD324 (1:25) for 1 hour protected from light. Cells were washed twice with staining buffer, transferred to a polystyrene tube and stained with 7-AAD reagent to exclude dead cells. Events were recorded using the Accuri C6 platform (BD Bioscience) using standard laser configuration, a flow rate of 35 μ L/minute and the following optical filters: 533/30 (FL-1), 585/40 (FL-2), 670 LP (FL-3) and 675/25 (FL-

4). Single colour or fluorescence minus one control samples containing an equivalent volume of diluent were included to set analyses gates and to threshold background autofluorescence. Briefly, the single-cell population was isolated by pulse processing (pulse height vs. pulse area) for further interrogation. Samples stained with the appropriate isotype control were used to determine non-specific antibody binding.

Appendix B: Copyright Approval

Dear Ian:

Copyright permission is granted for use of your article published in STEM CELLS AND DEVELOPMENT, 25/16, 2016, in your thesis. Please give proper credit to the journal and to the publisher: Mary Ann Liebert, Inc., New Rochelle, NY".

Kind regards,

Karen Ballen
Manager, Reprints, Permissions and Open Access

From: [REDACTED]
Sent: Friday, March 08, 2019 4:47 PM
To: Ballen, Karen [REDACTED]
Subject: LiebertPub Website Customer Question

LiebertPub Website Customer Question

Name - Ian Tobias
Position - PhD Candidate
Department - Physiology and Pharmacology
Institution/Affiliation - Western University
Address - 1151 Richmond Street +
City - London
State - ONTARIO
Country/Province - CANADA
Zip - N6A3K7
Email - [REDACTED]
Phone - [REDACTED]
Fax -
Regarding - Reprints and permissions
For Publication - Stem Cells and Development



RightsLink®

[Home](#)
[Create Account](#)
[Help](#)


Title: Metabolic plasticity during transition to naive-like pluripotency in canine embryo-derived stem cells

Author: I.C. Tobias,R.R. Isaac,J.G. Dierolf,R. Khazaei,R.C. Cumming,D.H. Betts

Publication: Stem Cell Research

Publisher: Elsevier

Date: July 2018

© 2018 The Author(s). Published by Elsevier B.V.

[LOGIN](#)

If you're a [copyright.com](#) user, you can login to RightsLink using your copyright.com credentials. Already a [RightsLink](#) user or want to [learn more?](#)

Please note that, as the author of this Elsevier article, you retain the right to include it in a thesis or dissertation, provided it is not published commercially. Permission is not required, but please ensure that you reference the journal as the original source. For more information on this and on your other retained rights, please visit: <https://www.elsevier.com/about/our-business/policies/copyright#Author-rights>

Appendix C: Animal Use Protocol Approval



AUP Number: 2018-033

PI Name: Betta, Dean

AUP Title: NSG mouse for assessing in vivo differentiation capacity of putative pluripotent stem cell lines*

Approval Date: 06/01/2018

Official Notice of Animal Care Committee (ACC) Approval:

Your new Animal Use Protocol (AUP) 2018-033:1 - entitled "NSG mouse for assessing in vivo differentiation capacity of putative pluripotent stem cell lines*" has been APPROVED by the Animal Care Committee of the University Council on Animal Care. This approval, although valid for up to four years, is subject to annual Protocol Renewal.

Prior to commencing animal work, please review your AUP with your research team to ensure full understanding by everyone listed within this AUP.

As per your declaration within this approved AUP, you are obligated to ensure that:

- 1) Animals used in this research project will be cared for in alignment with:
 - a) Western's Senate MAPs 7.12, 7.10, and 7.15
http://www.uwo.ca/arts/sci/policies_procedures/research.html
 - b) University Council on Animal Care Policies and related Animal Care Committee procedures
http://www.uwo.ca/research/services/animalethics/animal_care_and_use_policies.htm
- 2) As per UCAC's Animal Use Protocols Policy:
 - a) this AUP accurately represents intended animal use;
 - b) external approvals associated with this AUP (including permits and scientific/departmental peer approvals, are complete and accurate;
 - c) any divergence from this AUP will not be undertaken until the related Protocol Modification is approved by the ACC; and
 - d) AUP form submissions - Annual Protocol Renewals and Full AUP Renewals - will be submitted and attended to within timeframes outlined by the ACC.
http://www.uwo.ca/research/services/animalethics/animal_use_protocols.html
- 3) As per MAP 7.10 all individuals listed within this AUP as having any hands-on animal contact will
 - a) be made familiar with and have direct access to this AUP;
 - b) complete all required CCAC mandatory training (training@uwo.ca); and
 - c) be overseen by me to ensure appropriate care and use of animals.
- 4) As per MAP 7.15,
 - a) Practice will align with approved AUP elements;
 - b) Unrestricted access to all animal areas will be given to ACVS Veterinarians and ACC Leaders;
 - c) UCAC policies and related ACC procedures will be followed, including but not limited to:
 - i) Research Animal Procurement
 - ii) Animal Care and Use Records
 - iii) Sick Animal Response
 - iv) Continuing Care Visits
- 5) As per institutional OHS policies, all individuals listed within this AUP who will be using or potentially exposed to hazardous materials will have completed in advance the appropriate institutional OHS training, facility-level training, and reviewed related (MSDS Sheets, <http://www.uwo.ca/training/required/index.html>

Submitted by: Copeman, Laura
on behalf of the Animal Care Committee
University Council on Animal Care

The University of Western Ontario
Animal Care Committee / University Council on Animal Care
London, Ontario Canada N6A 3C1
519-661-2111 x 88792 Fax 519-661-2028
aupc@uwo.ca <http://www.uwo.ca/research/services/animalethics/index.html>

Appendix D: Curriculum Vitae

Name: Ian Tobias

Post-secondary Education and Degrees: Western University
London, Ontario, Canada
2009-2013 B.MSc.

The University of Western Ontario
London, Ontario, Canada
2013-2019 Ph.D.

Honours and Awards: Natural Sciences and Engineering Research Council (NSERC)
Masters Postgraduate Scholarship
2013-2014

Natural Sciences and Engineering Research Council (NSERC)
Masters Canada Graduate Scholarship
2014-2015

Ontario Graduate Scholarship
2015-2016

Hari and Gudrun Sharma Award
2016

Natural Sciences and Engineering Research Council (NSERC)
Doctoral Canada Graduate Scholarship
2016-2018

Gordon J. Mogenson Award
2018

Related Work Experience Teaching Assistant
Western University
2013-2018

Publications:

Betts DH and Tobias IC (2015). Canine pluripotent stem cells: Are they ready for clinical applications? *Frontiers in Veterinary Science*. 2: 41

Tobias IC, Teichroeb JH, Brooks CR, Villagomez D, Hess DA, Séguin CA and Betts DH (2016). Small molecule induction of canine embryonic stem cells towards naïve pluripotency. *Stem Cells and Development*. 25(16): 1208-1222

Tobias IC, Dierolf JD, Isaac RR, Khazaei R, Cumming RC and Betts DH (2018). Metabolic plasticity following conversion to naïve-like pluripotency in canine embryo-derived stem cells. *Stem Cell Research* 30: 22-33

Tobias IC, Khazaei and Betts DH (2018). Analysis of mitochondrial dimensions and cristae architecture in pluripotent stem cells using transmission electron microscopy. *Current Protocols in Stem Cell Biology*.